

แผนที่พิบัติภัยแผ่นดินไหวบริเวณภาคใต้ของประเทศไทย



นายจินดา สุทธิวานิช

ศูนย์วิทยทรัพยากร จุฬาลงกรณ์มหาวิทยาลัย

วิทยานิพนธ์นี้เป็นส่วนหนึ่งของการศึกษาตามหลักสูตรปริญญาวิทยาศาสตรดุษฎีบัณฑิต

สาขาวิชาธรณีวิทยา ภาควิชาธรณีวิทยา

คณะวิทยาศาสตร์ จุฬาลงกรณ์มหาวิทยาลัย

ปีการศึกษา 2553

ลิขสิทธิ์ของจุฬาลงกรณ์มหาวิทยาลัย

SEISMIC HAZARD MAP OF SOUTHERN THAILAND



Mr.Chinda Sutiwanich

ศูนย์วิทยทรัพยากร
จุฬาลงกรณ์มหาวิทยาลัย

A Dissertation Submitted in Partial Fulfillment of the Requirements

for the Degree of Doctor of Philosophy Program in Geology

Department of Geology

Faculty of Science


Chulalongkorn University

Academic Year 2010

Copyright of Chulalongkorn University


Thesis Title SEISMIC HAZARD MAP OF SOUTHERN THAILAND
By Mr. Chinda Sutiwanich
Field of Study Geology
Thesis Advisor Associate Professor Punya Charusiri, Ph.D.
Thesis Co-advisor Thanu Harnpattanapanich, Ph.D.


Accepted by the Faculty of Science, Chulalongkorn University in Partial
Fulfillment of the Requirements for the Doctoral Degree

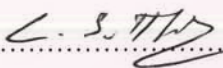
.....Dean of the Faculty of Science
(Professor Supot Hannongbua, Dr.rer.nat.)

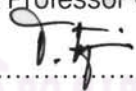
THESIS COMMITTEE

..... Chairman
(Assistant Professor Sombat Yumuang, Ph.D.)


.....Thesis Advisor
(Associate Professor Punya Charusiri, Ph.D.)

.....Thesis Co-advisor
(Thanu Harnpattanapanich, Ph.D.)

.....Examiner
(Assistant Professor Chakkaphan Sutthirat, Ph.D.)

.....Examiner
(Thanop Thitimakorn, Ph.D.)

..... Examiner
(Assistant Professor Anat Ruangrassamee, Ph.D.)

.....External Examiner
(Passakorn Pananont, Ph.D.)

จินดา สุทธิวานิช : แผนที่พิบัติภัยแผ่นดินไหวบริเวณภาคใต้ของประเทศไทย (SEISMIC HAZARD MAP OF SOUTHERN THAILAND) อ. ที่ปรึกษาวิทยานิพนธ์หลัก : รศ.ดร. ปัญญา จารุศิริ, อ. ที่ปรึกษาวิทยานิพนธ์ร่วม : ดร. ธนุ หาญพัฒน์พานิชย์, 295 หน้า.

งานวิจัยนี้มุ่งเน้นการตรวจสอบแผ่นดินไหวบรรพกาลของรอยเลื่อนคลองมะรุ่ยและรอยเลื่อนระนอง โดยมีวัตถุประสงค์เพื่อจัดทำแผนที่พิบัติภัยแผ่นดินไหวในพื้นที่ภาคใต้ประเทศไทย ผลการศึกษาโสรสัมผัส การศึกษาในสนาม และการหาอายุของรอยเลื่อน พบว่ารอยเลื่อนคลองมะรุ่ยและรอยเลื่อนระนองเคยทำให้เกิดแผ่นดินไหวขนาดใหญ่สุด 6.6 และ 6.2 เมื่อ 2,000 และ 9,000 ปีผ่านมาแล้ว ตามลำดับ รอยเลื่อนคลองมะรุ่ยมีคาบอุบัติซ้ำ 2,200 ปี และอัตราการเคลื่อนตัว 0.08-0.5 มิลลิเมตรต่อปี และรอยเลื่อนระนองมีคาบอุบัติซ้ำ 8,300 ปี และอัตราการเคลื่อนตัว 0.04-0.17 มิลลิเมตรต่อปี การวิเคราะห์พิบัติภัยแผ่นดินไหวได้พิจารณาแหล่งกำเนิดแผ่นดินไหวทั้งที่อยู่ในพื้นที่ภาคใต้ประเทศไทยและพื้นที่ใกล้เคียง รวมทั้งเขตแผ่นเปลือกโลกมุดตัวสุมาตรา-อันดามันเป็นแหล่งกำเนิดแผ่นดินไหวด้วย นอกจากนี้ยังได้รวบรวมและวิเคราะห์ลักษณะและพฤติกรรมของแต่ละแหล่งกำเนิดแผ่นดินไหว จากข้อมูลในการศึกษาครั้งนี้ ผสมกับการศึกษาอื่นๆ และข้อมูลแผ่นดินไหวที่ตรวจวัดด้วยเครื่องมือในปัจจุบัน การวิเคราะห์พิบัติภัยแผ่นดินไหวได้ใช้วิธีความน่าจะเป็นและ Logic Tree ช่วยในการวิเคราะห์แผนที่พิบัติภัยแผ่นดินไหวที่ได้ประกอบด้วยแผนที่แสดงค่าความเร่งของพื้นดินในแนวราบสูงสุด (PGA) และค่าความเร่งสเปกตรัม ที่คาบเวลา 0.2, 0.3 และ 1 วินาที ในรอบ 500, 1000, 2,500 และ 10,000 ปี หรือที่มีโอกาสเกิดเกินค่าความเร่งที่กำหนด 10% 5% 2% และ 0.5% ในรอบ 50 ปี ผลการศึกษาพบว่าพื้นที่ที่อยู่ตามแนวรอยเลื่อนคลองมะรุ่ย ซึ่งอยู่ในเขต อ.เมือง พนม และวิภาวดี(สุราษฎร์ธานี) ทัพปุด (พังงา) ปลายพระยา (กระบี่) เป็นบริเวณที่มีแรงสั่นสะเทือนมากกว่าพื้นที่อื่นๆ โดยมีค่าความเร่งเฉลี่ยสูงสุดในรอบ 500-10,000 ปี ระหว่าง 0.28-0.52g สำหรับความเร่งสเปกตรัมค่ามากที่สุดเกิดที่คาบเวลา 0.2 วินาที ในรอบ 500-10,000 ปี และมีค่า 0.52-0.8g ส่วนพื้นที่ภาคใต้ล่างสุด คือ จ.ยะลา จ.ปัตตานี และจ.นราธิวาส เป็นพื้นที่ที่แรงสั่นสะเทือนน้อยที่สุด โดยสรุปข้อมูลที่ได้จากแผนที่พิบัติภัยแผ่นดินไหวนี้ใช้เป็นแนวทางในการวิเคราะห์ความมั่นคงของโครงสร้างที่อยู่บนชั้นหิน เช่น สะพาน อาคาร และสิ่งก่อสร้างขนาดใหญ่ เช่น ฝายและเขื่อน อนึ่งการศึกษานี้เป็นเพียงเบื้องต้น หากมีข้อมูลอายุและอัตราการเคลื่อนตัวของรอยเลื่อนเพิ่มมากขึ้นจะทำให้แผนที่มีรายละเอียดและความถูกต้องมากขึ้น

ภาควิชา.....ธรณีวิทยา... ลายมือชื่อนิสิต.....
 สาขาวิชา ...ธรณีวิทยา.... ลายมือชื่อ อ.ที่ปรึกษาวิทยานิพนธ์หลัก
 ปีการศึกษา...2553..... ลายมือชื่อ อ.ที่ปรึกษาวิทยานิพนธ์ร่วม.....

4973810023: MAJOR GEOLOGY

KEYWORDS : RECURRENCE INTERVAL/ SLIP RATE / SEISMIC HAZARD MAP / SOUTHERN THAILAND

CHINDA SUTIWANICH : SEISMIC HAZARD MAP OF SOUTHERN THAILAND
 ADVISOR : ASSOC. PROF. PUNYA CHARUSIRI, Ph.D., CO-ADVISOR : THANU HARNPATTANAPANICH, Ph.D., 295 pp.

This research concentrates on the re-evaluation of the paleo-earthquake activities of the Khlong Marui Fault (KMF) and Ranong Fault (RNF) with an aim to establish of seismic hazard maps of southern Thailand. Based on the results of satellite image interpretation, field investigation and geochronological analyses, the KMF and RNF produced the maximum paleo-magnitudes of M_w 6.6 and M_w 6.2 at 2,000 and 9,000 years ago, respectively. The KMF has the mean recurrence interval of 2,200 years and the slip rates of 0.1-0.5 mm/yr whereas the RNF has the mean recurrence interval of 8,300 years and the slip rates of 0.04-0.17 mm/yr. The seismic sources include the line and area sources in southern Thailand and nearby region including the Sumatra-Andaman subduction zone. The probability seismic hazard analysis and the logic tree approach were applied. The hazard maps consist of maps showing mean peak ground accelerations and spectral accelerations at 0.2, 0.3, and 1.0 seconds with a 10%, 5%, 2% and 0.5% probability of exceedance in 50-year hazard levels for rock site condition. The results reveal that the highest hazard areas are in districts of Muang, Phanom, and Viphavadi (Surat Thani), Thap Put (Phang Nga), Plai Phraya (Krabi). The lowest hazard areas are in the southernmost part of Thailand (Yala, Pattani and Narathiwat). The maximum values of the mean peak ground acceleration for the 500–10,000 yr return period are 0.28g-0.52g and the maximum spectral accelerations at 0.2 seconds for the same return period are 0.52-0.8 g. These seismic hazard maps are useful as a guideline for future design of buildings, bridges and high hazard structures as dams for rock sites to resist earthquake forces. This preliminary result will be more helpful and accurate if the more detailed dating data, and horizontal ground acceleration results can be synthesized.

Department : Geology

Student's Signature

Field of Study : Geology

Advisor's Signature

Academic Year : 2010

Co-advisor's Signature

Chinda Sutiwanich
Punya Charusiri
Thanu Harnpattanapanich

ACKNOWLEDGEMENTS

First and foremost, the author wish to express my sincere and profound gratitude to my dissertation advisor Associate Professor Dr.Punya Charusiri, Department of Geology, Faculty of Science, Chulalongkorn University for his valuable advice, guidance, suggestion, encouragement and recommendation through the study of the dissertation. Special acknowledgements are also made to Dr.Thanu Harnpattanapanich, my co-advisor, Panya Consultants Co., Ltd., for his teaching and advice the methodology of seismic hazard analysis. The author also wish to express my deep sense of gratitude to Assistant Professor Dr.Sombat Yumuang, Assistant Professor Dr.Chakkaphan Sutthirat, Dr.Thanob Thitimakorn, Assistant Professor Dr. Anat Ruangrassamee, and Dr.Passakorn Pananont who served as the member of the dissertation committee. The author would like to thank Dr.Santi Pailoplee and Mrs. Teerarat Pailoplee for all their valuable assistance in completing my dissertation.

Thanks and appreciations are also expressed to the Department of Geology, Faculty of Science, Chulalongkorn University for providing all facilities, the Royal Irrigation Department for allowing me to disclose paleosesimic data of the Khlong Marui fault zone, and Panya Consultant Co., Ltd. for logistical support.

Last but not least the author would like to thanks everyone, whom the author do not mentioned here, that has direct and indirect assistance for performance and completion of my dissertation. Finally, yet importantly, the author would like to express my heartfelt thanks to my beloved family for their understanding, endless patience and encouragement.

CONTENTS

	Page
ABSTRACT (THAI).....	iv
ABSTRACT (ENGLISH).....	v
ACKNOWLEDGEMENTS.....	vi
CONTENTS.....	vii
LIST OF TABLES.....	x
LIST OF FIGURES.....	xi
CHAPTER I INTRODUCTION.....	1
1.1 General Background.....	1
1.2 Objectives.....	6
1.3 Scopes.....	6
1.4 Study Area.....	8
CHAPTER II LITERATURE REVIEW.....	9
2.1 Seismic Hazard Analysis Methodology.....	9
2.1.1 Deterministic Seismic Hazard Analysis (DSHA).....	9
2.1.2 Probabilistic Seismic Hazard Analysis (PSHA).....	11
2.2 Seismotectonic Setting and Tectonic History.....	13
2.3 Earthquake Data.....	19
2.3.1 Pre-instrumental Seismicity.....	20
2.3.2 Instrumental Seismicity.....	20
2.4 Earthquake Sources.....	24
2.4.1 Fault Sources.....	25
2.4.2 Area Sources.....	32
2.5 Attenuation Relationships.....	32
2.6 Previous Paleoseismic Investigation.....	35
2.7 Previous Seismic Hazard Map of Thailand.....	37
CHAPTER III APPROACH AND METHODOLOGY.....	54
3.1 Approach.....	54

	Page
6.2.1 Comparison between with and without KMF Areal Source...	170
6.2.2 Seismogenic Depth and Fault Plane Inclination.....	172
6.2.3 Effect of b-value on Calculated Ground Motion.....	172
6.3 Effect of Attenuation Relationships on Ground Motion.....	174
6.4 Usefulness of Hazard Curves.....	176
6.5 Earthquake Source Contribution.....	177
CHAPTER VII CONCLUSION AND RECOMMENDATION.....	184
7.1 Conclusion.....	184
7.2 Recommendation.....	186
REFERENCE	187
APPENDICES	202
APPENDIX A CONSTANT VALUES OF ATTENUATION RELATION...	203
APPENDIX B CRISIS 2007 VERSION 1.1.....	209
APPENDIX C THERMOLUMINESCENCE (TL) DATING RESULTS.....	222
APPENDIX D RID'S TRENCH LOGS.....	229
APPENDIX E MARTEL'S LECTURE NOTE ON RECURRENCE AND PROBABILITY (2002).....	244
APPENDIX F HAZARD CURVES.....	256
BIOGRAPHY	295

LIST OF TABLES

	Page
Table 4.1 Table 4.1 Results of TL-age dating in this study.....	86
Table 4.2 Summary the slip rate of the KMF zone.....	107
Table 4.3 Summary the slip rate of the RNF zone.....	112
Table 5.1 KMF zone mode.....	119
Table 5.2 RNF zone model.....	123
Table 5.3 TNF model.....	125
Table 5.4 KYF and TVF models.....	127
Table 5.5 TPF model.....	132
Table 5.6 Megathrust of Sumatra-Andaman subduction zone and Ratchaprapha reservoir.....	134
Table 5.7 Earthquake catalog completeness and number of events used in recurrence for southern Thailand and adjacent areas.....	140
Table 5.8 Earthquake catalog completeness and number of events used in recurrence for the Sumatra-Andaman subduction zone.....	141
Table 5.9 Earthquake catalog completeness and number of events used in recurrence for western Thailand.....	143
Table 5.10 Mean peak ground accelerations and the spectral acceleration at 0.2, 0.3, and 1.0 seconds with a 10%, 5%, 2% and 0.5% probability of exceedance in 50-year hazard levels (500, 1,000, 2,500, and 10,000 years) for rock site condition at each province in southern Thailand.....	166
Table 6.1 Ground acceleration at the site with longitude of 98.82 ⁰ E and latitude of 9.21 ⁰ N contributed by with and without KMF areal source.....	171
Table 6.2 Effect of b-value on the acceleration.....	174

LIST OF FIGURES

	Page
Figure 1.1 Plate tectonic map of Southeast Asia consisting of Eurasian, Indo-Australian, Philippines Sea and Pacific plate (Metcalfe, 2009).....	1
Figure 1.2 Simplified geological map of Thailand showing the distribution of rocks of various ages, and major sutures/fault systems (Charusiri et al., 2002).....	3
Figure 1.3 Map of Thailand and nearby region showing movement rates of Thailand territory before the occurrence of M_w 9.1 earthquake at the Sumatra Island on December 26, 2004 (Phromthong et al., 2005).....	4
Figure 1.4 Map showing co-seismic displacement of Thailand and neighboring countries during the occurrence of M_w 9.1 earthquake at the Sumatra Island on December 26, 2004 (Vigny et al., 2005).....	5
Figure 1.5 Map of Thailand showing the area to be established a seismic hazard map.....	8
Figure 2.1 Four steps of the deterministic seismic hazard analysis based on Kramer (1996) (www.nibs.org).....	11
Figure 2.2 Four steps of the probabilistic seismic hazard analysis based on Kramer (1996) (www.nibs.org).....	12
Figure 2.3 Tectonic map of Southeast Asia (www.gsabulletin.gsapubs.org).....	14
Figure 2.4 Seismotectonic map of Thailand (Santoso, 1982).....	15
Figure 2.5 Regional seismic source zones of Thailand and nearby region and earthquake epicenters recorded during 1910-1979 (Nutalaya et al., 1985).....	16
Figure 2.6 Seismotectonic zone map of Thailand (WCFS, 1996).....	17
Figure 2.7 Seismotectonic province in Thailand (Charusiri et al., 2000).....	18
Figure 2.8 Seismotectonic zones in Southeast Asia (Charusiri et al., 2005).....	19
Figure 2.9 A map of southern Thailand showing epicenters recoded between 14 January 2005 and 30 June 2005 (Duerrast, 2007).....	21

	Page
Figure 2.10 Earthquakes were detected in the southern Thailand and Myanma during the years 2006-2008.....	23
Figure 2.11 Fault Map of Thailand comprising 13 fault zones (Chuaviroch, 1991).....	25
Figure 2.12 A map showing 22 active faults in Thailand (Hinthong, 1997).....	27
Figure 2.13 Seismically active belt map showing three groups of 17 faults as active, potentially active and tentatively active faults (Charusiri et al., 2002).....	28
Figure 2.14 Active fault map in Thailand (www.dmr.go.th).....	30
Figure 2.15 Active faults in the southern Thailand and Myanma (Wong, 2005).....	31
Figure 2.16 Map of shallow-depth earthquake source zones for southeast Asia (Petersen et al., 2007).....	33
Figure 2.17 Seismic risk map for the return period of 100 years of Southeast Asia (a) maximum acceleration map in gal (b) maximum velocity map in kine (Hattori, 1980).....	37
Figure 2.18 Ground acceleration map for (a) 36 years corresponding to 86% and (b) 74 years corresponding to 63% probabilities (Santoso, 1981).....	38
Figure 2.19 Maximum earthquake intensity map for Thailand and adjacent areas (Nutalaya et al., 1985).....	39
Figure 2.20 Peak ground acceleration map with the return period of (a) 90 years or 20% probability of exceedance and (b) 13 years or 80% probability of exceedance of Thailand and nearby region (Shrestha, 1986).....	40
Figure 2.21 Peak ground acceleration map of Thailand (Lukkunaprasit and Kuhatasanadeekul (1993).....	41

	Page
Figure 2.22 (a) Small seismic source blocks and their centers assumed to be seismic source points (b) Peak ground acceleration and seismic zoning map of Thailand with 10% probability of exceedance in 50 years based on Uniform Building Code 1991 Map (Lisantonno, 1994, Warnitchai and Lisantonno, 1997, Warnitchai, 1998).....	43
Figure 2.23 Seismic hazard zoned map of Thailand (Charusiri et al., 1997).....	44
Figure 2.24 Seismic intensity map of Thailand (DMR, 2005).....	45
Figure 2.25 Probabilistic seismic hazard maps for Southeast Asia showing the PGA with (a) 10% and (b) 2% probability of exceedance in 50-year return period for the rock site condition (Petersen et al., 2007).....	47
Figure 2.26 Probabilistic seismic hazard maps for Southeast Asia showing 1-Hz spectral acceleration with (a) 10% and (b) 2% probability of exceedance in 50-year return period for the rock site condition (Petersen et al., 2007).....	48
Figure 2.27 Probabilistic seismic hazard maps for Southeast Asia showing 5-Hz spectral acceleration with (a) 10% and (b) 2% probability of exceedance in 50-year return period for the rock site condition (Petersen et al., 2007).....	49
Figure 2.28 Possible maximum acceleration map of Thailand and adjacent areas computed by the deterministic method (Pailoplee, 2009).....	50
Figure 2.29 The peak ground acceleration maps with (a) 2% and (b) 10% probability of exceedance in 50 years as well as (c) 2% and (d) 10% probability of exceedance in 100 years (Pailoplee, 2009).....	52
Figure 2.30 Probability seismic hazard map of Thailand and nearby region (a) 10% probability of exceedance in 50 years (b) 2% probability of exceedance in 50 years (Palasri and Ruangrassamee, 2010).....	53
Figure 3.1 Flow chart showing steps of work in this study.....	55

	Page
Figure 3.2	Typical earthquake recurrence curves and discretized occurrence rates (US Army Corps of Engineers, 1999)..... 64
Figure 3.3	Graphs plotted between the annual rate of exceedance and magnitude for the characteristic earthquake-recurrence model (black line) and for the truncated exponential earthquake-recurrence model (dashed line) (Convertito et al., 2006)..... 66
Figure 3.4	Example of the logic tree applied for the probabilistic analysis of earthquake ground shaking along the Wasatch Front, Utah (Youngs et al., 1987)..... 73
Figure 3.5	Location map showing calculated 224 sites (black circles) for PSHA in this study..... 78
Figure 3.6	An example hazard curve showing the mean peak ground accelerations for 10%, 5%, 2% and 0.5% probabilities of exceedance in 50 years at the specified site..... 80
Figure 4.1	Major and minor faults in the KMF zone newly interpreted from the DEM image in this study. Major fault segments are : 1 = Takua Thung fault, 2 = Khlong Marui fault, 3 = Thap Put fault, 4 = Phanom fault, 5 = Ao Luk fault, 6 = Plai Phraya fault, 7 = Khao Phanom fault, 8 = Khian Sa fault, 9 = Ban Naderm fault..... 82
Figure 4.2	Major and minor faults in the northern Ranong fault zone newly interpreted from the DEM image in this study..... 83
Figure 4.3	Major and minor faults in the southern RNF zone newly interpreted from the DEM image in this study..... 84
Figure 4.4	Photographs show (a) faults (pointed by yellow arrows) cutting through Units A, B and D and absence of Unit C (b) faults (pointed by yellow arrows) cutting through Units D, E and F2 and a block of Unit E embedded in Unit F2..... 88
Figure 4.5	Fault (pointed by yellow arrows) cutting through Unit A, and Unit B..... 89

	Page	
Figure 4.6	Fault (pointed by yellow arrows) with the orientation of N12°W72°E extending from the bed rock Unit A and ending at the laterite Unit C at the station 54-57 m of the exposure no.1.....	91
Figure 4.7	The fracture (pointed by yellow arrows) appears in the bed rock Unit A and continues up to the laterite Unit C. Its orientation is N45°E34°NW. Close up photograph in a white rectangle (left figure) is illustrated in the right figure.....	91
Figure 4.8	Faults (pointed by yellow arrows) were observed. They cut the bed rock Unit A, weathered bed rock Unit B and the laterite Unit C. In the white rectangle (left figure), close up photograph is shown in the right figure.....	92
Figure 4.9	Excavation wall at site no.5 at Ban Bangsai, Phang Nga province showing faults, pointed by yellow arrows, cutting from the bed rock Unit A to the laterite Unit B.....	93
Figure 4.10	Trench wall of site no.6 showing faults (pointed by yellow arrows) passing from the bed rock Unit A up to the laterite Unit C.....	95
Figure 4.11	Fractures (pointed by yellow arrows) cutting through the laterite Unit B.....	96
Figure 4.12	Fissure occurs in Units C, D and G.....	98
Figure 4.13	Folded and faulted charcoal layer, orientation of a black pencil indicating fault direction, the right photograph is a close-up charcoal picture.....	98
Figure 4.14	(a) Faults and fractures (pointed by yellow arrows) in Unit C, D, G and H, (b) Silt lump of the Unit M embedded in laterite Unit G.....	99
Figure 4.15	Fault (pointed by yellow arrows) passing through laterite Unit B.....	100
Figure 4.16	Slit lump impregnated in the lateritic layer and the completely weathered rock, the right photograph is a close up silt lump picture at stations 36-37 m.....	101
Figure 4.17	Space-time diagram of the KMF zone, southern Thailand.....	104
Figure 4.18	Space-time diagram of the RNF zone, southern Thailand.....	110
Figure 4.19	Probability of large earthquakes produced by the KMF.....	113

	Page
Figure 4.20 Probability of the KMF's great earthquake occurrence in any year from the year 2009 based on the normally-distributed recurrence approach.....	114
Figure 4.21 Probability of the KMF's great earthquake occurrence in any year from the year 2009 based on the randomly-distributed approach.....	114
Figure 5.1 Seismicity sources in southern Thailand and adjacent areas, KMF = Khlong Marui fault, RNF = Ranong fault, TNF = Tenasserim fault, KYF = Kungyauangale fault, TVF = Tavoy fault, and TPF = Three Pagoda fault.....	116
Figure 5.2 Logic tree for the KMF.....	118
Figure 5.3 Logic tree for the RNF.....	122
Figure 5.4 Logic tree of the TNF.....	126
Figure 5.5 Logic tree of the KYF.....	128
Figure 5.6 Logic tree for the TVF.....	130
Figure 5.7 Logic tree for the TPF.....	131
Figure 5.8 Logic tree for the Sumatra-Andaman megathrust earthquake.....	135
Figure 5.9 Logic tree for the Ratchaprapha RTS.....	137
Figure 5.10 Map of epicenters for the period of 1964-2008, data obtained from the Thai Meteorological Department.....	138
Figure 5.11 Map showing epicenters of earthquakes used in the calculation of crustal earthquake recurrence (modified from Wong, 2005).....	139
Figure 5.12 Earthquake recurrence for southern Thailand and adjacent areas.....	140
Figure 5.13 Earthquake recurrence for the Sumatra-Andaman subduction zone.....	142
Figure 5.14 Earthquake recurrence for western Thailand.....	143
Figure 5.15 Location map showing 224 sites (black circles) performed the PSHA.....	145

	Page
Figure 5.16 Mean peak horizontal acceleration hazard curve contributed from various seismic sources at the site with longitude of 98.82°E and latitude of 9.59°N	147
Figure 5.17 Mean peak ground accelerations for 10%, 5%, 2% and 0.5% probabilities of exceedance in 50 years at the site with longitude of 98.82°E and latitude of 9.59°N	148
Figure 5.18 Seismic hazard map showing mean peak horizontal acceleration with 10% probability of exceedance in 50 years or for 500 years for the rock site condition in southern Thailand.....	150
Figure 5.19 Seismic hazard map showing mean peak horizontal acceleration with 5% probability of exceedance in 50 years or for 1,000 years for the rock site condition in southern Thailand.....	151
Figure 5.20 Seismic hazard map showing mean peak horizontal acceleration with 2% probability of exceedance in 50 years or for 2,500 years for the rock site condition in southern Thailand.....	152
Figure 5.21 Seismic hazard map showing mean peak horizontal acceleration with 0.5% probability of exceedance in 50 years or for 10,000 years for the rock site condition in southern Thailand.....	153
Figure 5.22 Seismic hazard map showing mean 0.2 sec horizontal spectral acceleration with 10% probability of exceedance in 50 years or for 500 years for the rock site condition in southern Thailand.....	154
Figure 5.23 Seismic hazard map showing mean 0.2 sec horizontal spectral acceleration with 5% probability of exceedance in 50 years or for 1,000 years for the rock site condition in southern Thailand.....	155
Figure 5.24 Seismic hazard map showing mean 0.2 sec horizontal spectral acceleration with 2% probability of exceedance in 50 years or for 2,500 years for the rock site condition in southern Thailand.....	156
Figure 5.25 Seismic hazard map showing mean 0.2 sec horizontal spectral acceleration with 0.5% probability of exceedance in 50 years or for 10,000 years for the rock site condition in southern Thailand.....	157

	Page
Figure 5.26 Seismic hazard map showing mean 0.3 sec horizontal spectral acceleration with 10% probability of exceedance in 50 years or for 500 years for the rock site condition in southern Thailand.....	158
Figure 5.27 Seismic hazard map showing mean 0.3 sec horizontal spectral acceleration with 5% probability of exceedance in 50 years or for 1,000 years for the rock site condition in southern Thailand.....	159
Figure 5.28 Seismic hazard map showing mean 0.3 sec horizontal spectral acceleration with 2% probability of exceedance in 50 years or for 2,500 years for the rock site condition in southern Thailand.....	160
Figure 5.29 Seismic hazard map showing mean 0.3 sec horizontal spectral acceleration with 0.5% probability of exceedance in 50 years or for 10,000 years for the rock site condition in southern Thailand.....	161
Figure 5.30 Seismic hazard map showing mean 1.0 sec horizontal spectral acceleration with 10% probability of exceedance in 50 years or for 500 years for the rock site condition in southern Thailand.....	162
Figure 5.31 Seismic hazard map showing mean 1.0 sec horizontal spectral acceleration with 5% probability of exceedance in 50 years or for 1,000 years for the rock site condition in southern Thailand.....	163
Figure 5.32 Seismic hazard map showing mean 1.0 sec horizontal spectral acceleration with 2% probability of exceedance in 50 years or for 2,500 years for the rock site condition in southern Thailand.....	164
Figure 5.33 Seismic hazard map showing mean 1.0 sec horizontal spectral acceleration with 0.5% probability of exceedance in 50 years or for 10,000 years for the rock site condition in southern Thailand.....	165
Figure 6.1 Hazard curve at longitude of 98.82 ⁰ E and latitude of 9.21 ⁰ N contributed by with and without KMF areal source.....	171
Figure 6.2 Hazard curve showing the influence of b-value on the ground motion.....	173
Figure 6.3 Peak horizontal acceleration-attenuation relationships for the magnitude M_w5	175

	Page
Figure 6.4 Peak horizontal acceleration-attenuation relationships for the magnitude M_w 7.....	176
Figure 6.5 Seismic intensity map of the earthquake occurred in the Gulf of Thailand nearby Prachuab Khirikhun province on 28 September 2006 (Department of Mineral Resources, 2006).....	178
Figure 6.6 Seismic intensity map of the earthquake occurred in the Gulf of Thailand nearby Prachuab Khirikhun province on 8 October 2006 (Department of Mineral Resources, 2006).....	179
Figure 6.7 Seismic intensity map of the earthquake occurred at Plai Phraya district, Krabi province on 4 May 2008 investigated by this study.....	180
Figure 6.8 Hazard curves for mean peak horizontal acceleration at the site with longitude of $99.81^{\circ}E$ and latitude of $11.85^{\circ}N$ at Prachaub Khirikhun province.....	181
Figure 6.9 Hazard curves for mean peak horizontal acceleration at the site with longitude of $98.82^{\circ}E$ and latitude of $8.55^{\circ}N$ at Prai Phraya district of Krabi province.....	182
Figure 6.10 Hazard curves for mean peak horizontal acceleration at the site with longitude of $98.16^{\circ}E$ and latitude of $7.89^{\circ}N$ on the west of Phuket Island.....	183

CHAPTER I

INTRODUCTION

1.1 General Background

The neotectonics of Thailand appear to be related to the interaction between the Indo-Australian, Eurasian, Philippine and Pacific plates combining with the opening of the Andaman Sea (Suensilpong, 1981, Polachan, 1988, Metcalfe, 2009) as shown in

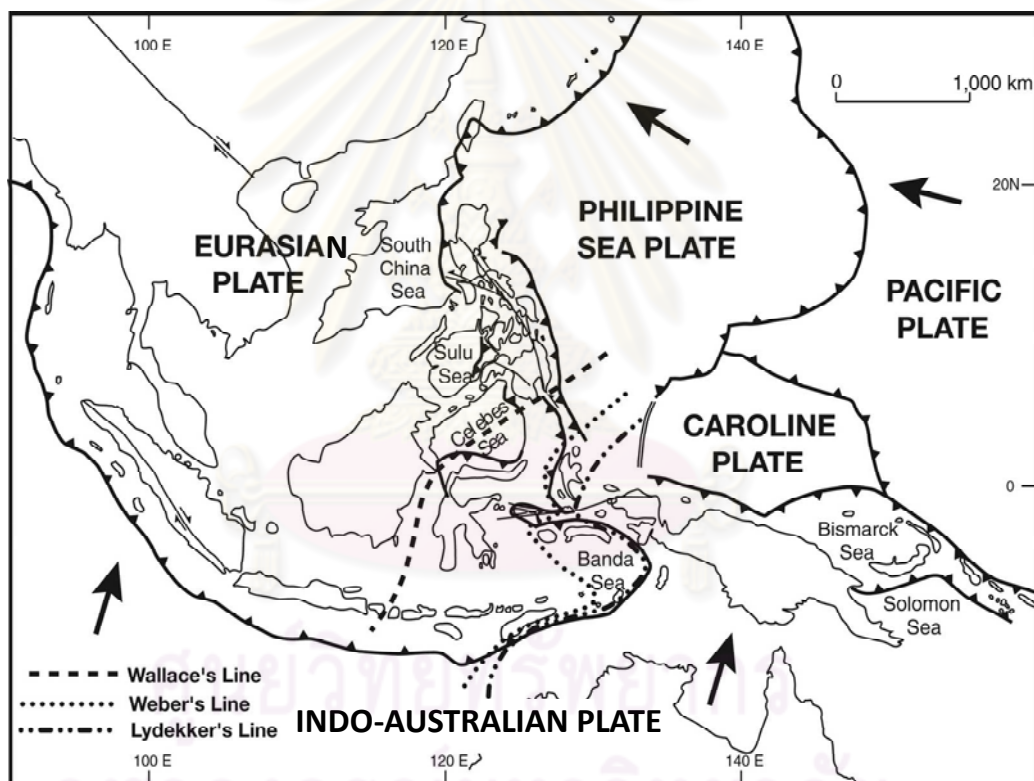


Figure 1.1 Plate tectonic map of Southeast Asia consisting of Eurasia, India-Australia, Philippine Sea, and Pacific plates (Metcalfe, 2009).

Figure 1.1. Due to the little relative motion between the Indian and Australian plates, they are considered to be an Indo-Australian plate. Thailand is situated within the Eurasian plate which is surrounded by the convergent margins, namely the Andaman subduction zone in the west, Sunda and Java trenches in the south and Philippine

trench in the east. The present tectonic regime in Thailand is transtension, i.e. extension along the north-south faults, right-lateral slip on northwest-striking faults and left-lateral slip on northeast-striking faults. The southern part of Thailand extends southward from the Three Pagodas fault zone in Kanchanaburi province to the Malaysian border. It consists mainly of Carboniferous to Jurassic meta-sedimentary bedrocks intruded by Late Paleozoic to Mesozoic igneous rocks as shown in Figure 1.2. The basement has been extensively faulted and folded with the orientation of predominant geologic structures in the northeast-southwest direction. The inferred strike-slip faults in southern Thailand –Ranong fault (RNF) and Khlong Marui fault (KMF)— did not show a large movement after 30 Ma (Morely, 2001). Based on the GPS data, there is no motion of the southern Thailand relative to the remainder of the country (Iwakuni et al., 2004), or the whole Thailand moves to the east with an equal rate of 3-4 cm per year as shown in Figure 1.3 (Phromthong et al., 2005, 2006). Before 2004, it was believed that southern Thailand is a tectonic stability region. There have been no identified surface faults associated with natural earthquakes in southern Thailand. However, many researchers reported that the RNF and KMF in the Thai Peninsula are potentially active (Natalaya, 1985, Chuavirot, 1991, Hinthong, 1995, DMR, 2002). After the occurrence of two large earthquakes with a magnitude of M_w 9.0 to 9.3 (USGS, 2005a, Park et al., 2005, Stein and Okal, 2005, Bilham, 2005, Ishii et al., 2005) on 26 December 2004 and M_w 8.6 (USGS, 2005b) on 28 March 2005 at the northwest of Sumatra Island, there are a number of small earthquakes recorded in Thai Peninsular (Duerrast et al., 2007) and differential movement of Thai territory observed from the GPS as shown in Figure 1.4 (Simons et al., 2005, Vigny et al., 2005, Phromthong et al., 2005, 2006). It can be concluded that Thai Peninsular is not tectonic stable territory.

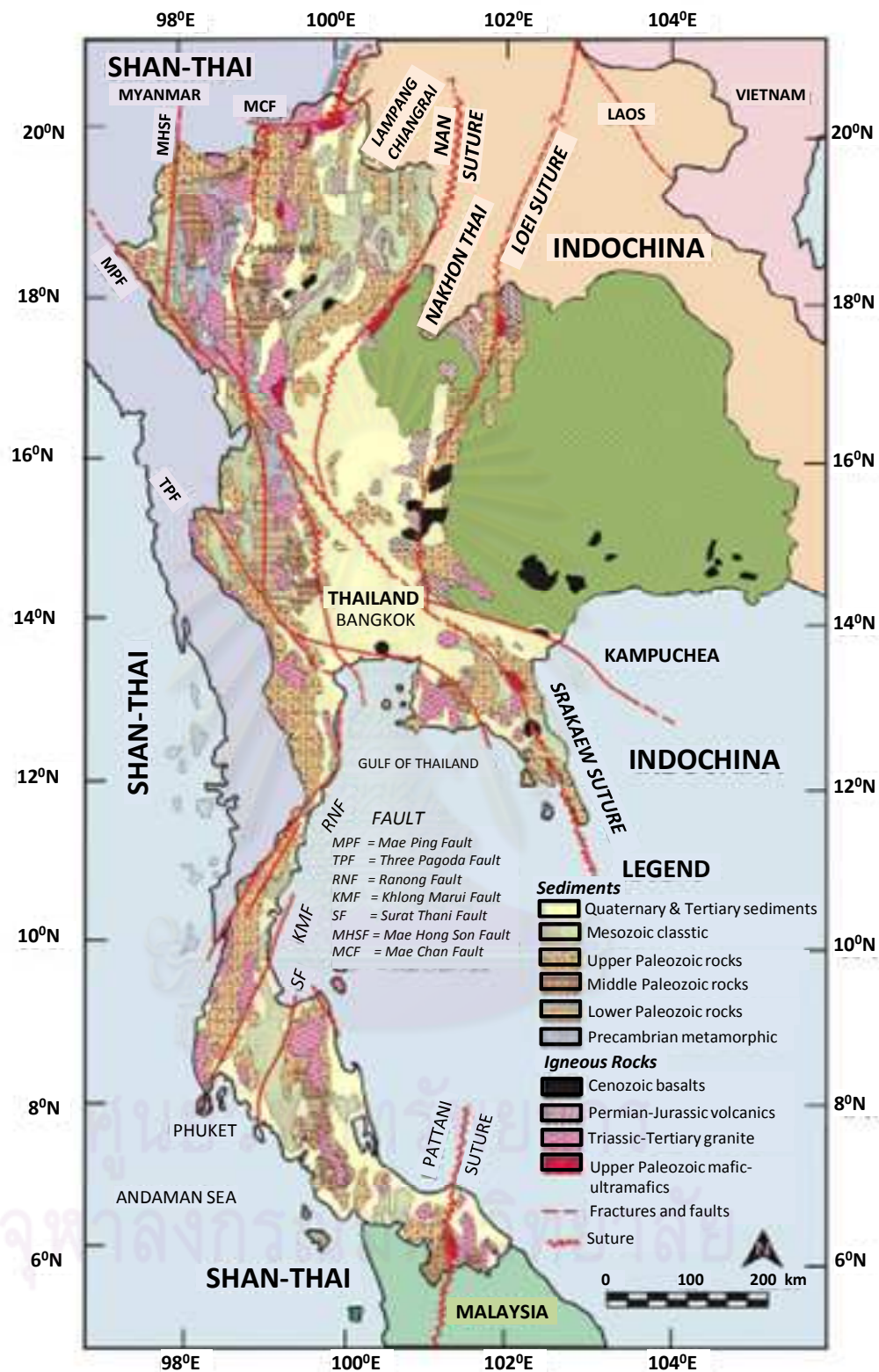


Figure 1.2 Simplified geological map of Thailand showing the distribution of rocks of various ages, and major sutures/fault systems (Charusiri et al., 2002).

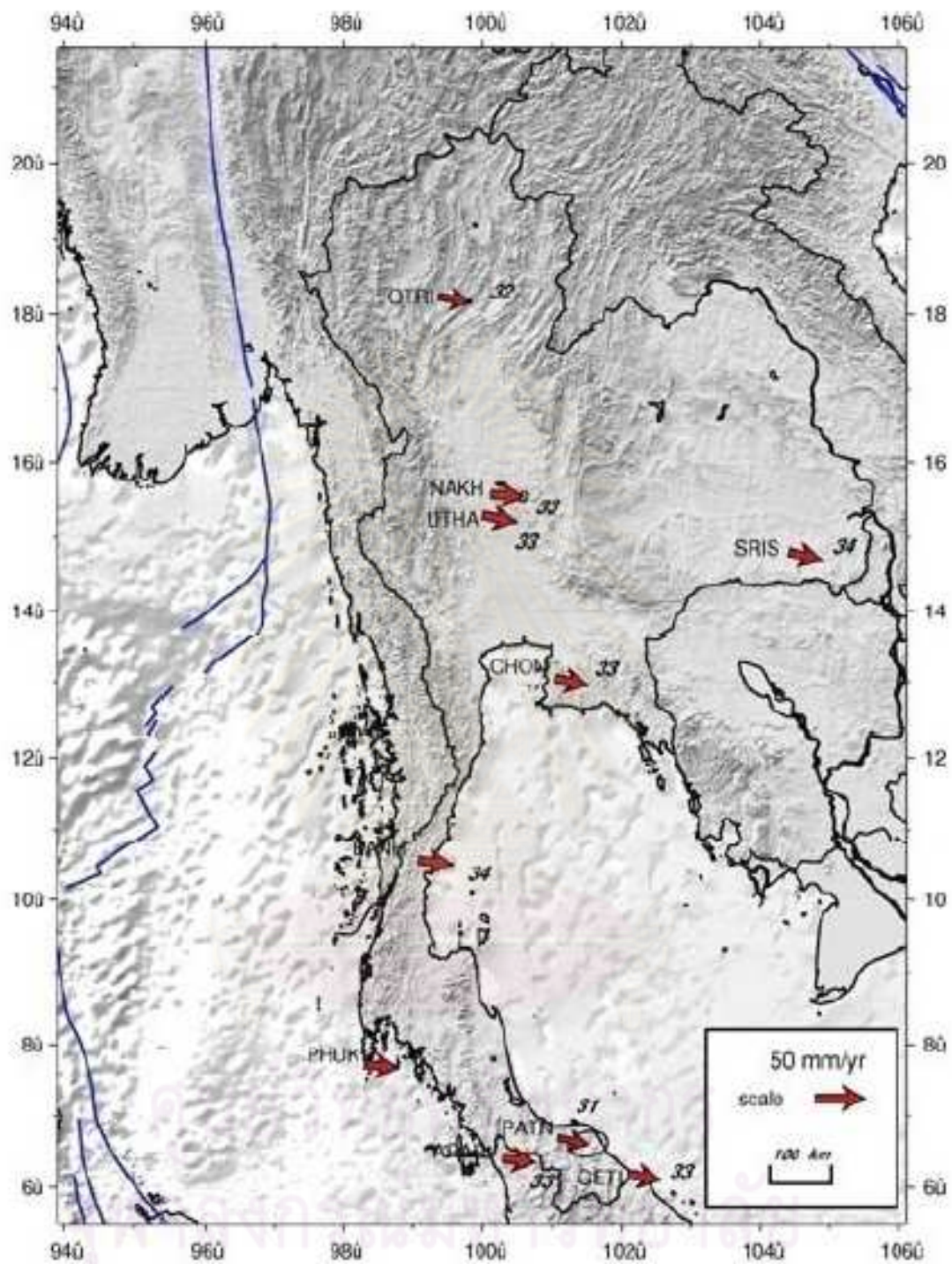


Figure 1.3 Map of Thailand and nearby region showing movement rates of Thailand territory before the occurrence of M_w 9.1 earthquake at the Sumatra Island on December 26, 2004 (Phromthong et al., 2005).

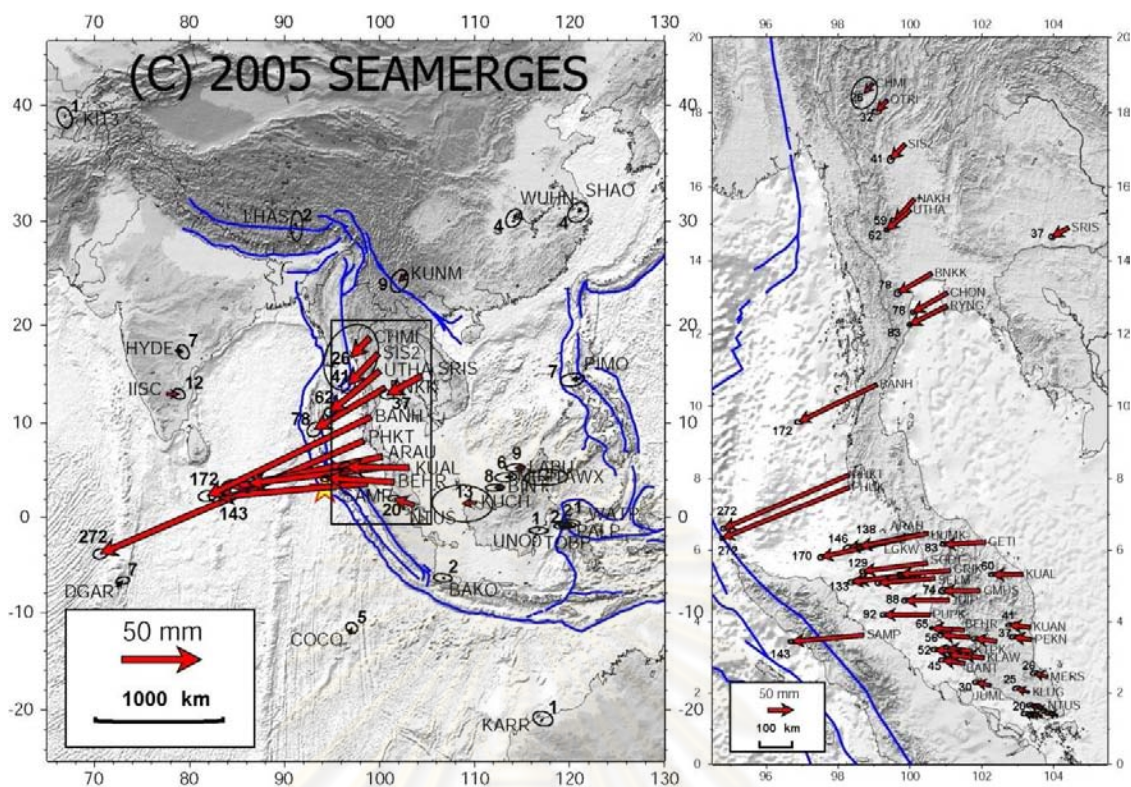


Figure 1.4 Map showing co-seismic displacement of Thailand and neighboring countries during the occurrence of M_w 9.1 earthquake at the Sumatra Island on December 26, 2004 (Vigny et al., 2005).

Based on earthquake data prior to the occurrence of the 2004 great Sumatra-Andaman earthquake and unavailable detailed information of potential active faults, most Thailand's seismicity hazard maps show that the southern peninsular Thailand is a low ground shaking region (Shrestha, 1986, Lukkunaprasit and Kuhatasanadeekul, 1993, Lisantono, 1994, Warnitchai and Lisantono, 1997, Charusiri et al., 1997, Warnitchai, 1998). Moreover, all of the maps were prepared with peak ground acceleration for 500 and 2,500 years corresponding to 10% and 2% probability of exceedance of 50 years. Due to many changes on the characteristics and activities of the seismic sources causing the ground shaking in southern Thailand, as well as for reliability and extensive uses of the seismic hazard maps of southern Thailand, this research performs satellite

image interpretation, field investigation and re-evaluation of fault activities, especially along the KMF and RNF,, and construct the maps displaying not only peak ground acceleration for 500 and 2,500 years corresponding to 10% and 2% probabilities of exceedance in 50 years but also those for 1,000 and 10,000 years corresponding to 5% and 0.5% probabilities of exceedance in 50 years as well as spectral acceleration at 0.2, 0.3, and 1.0 seconds for 500, 1,000, 2,500 and 10,000 years corresponding to 10%, 5%, 2% and 0.5% probabilities of exceedance in 50 years.

1.2 Objectives

The objective of this research is to establish seismic hazard maps of southern Thailand with peak ground acceleration and spectral acceleration at 0.2, 0.3, and 1.0 seconds for 500, 1,000, 2,500 and 10,000 years corresponding to 10%, 5%, 2% and 0.5% probabilities of exceedance in 50 years.

1.3 Scopes

All previous seismic hazard maps of southern Thailand are just a part of the seismic hazard map of Thailand and adjacent areas. Researchers did not concentrate sufficiently the seismic sources influencing the ground shaking in the Thai peninsular. They paid attention mostly to the sources that there are instrumentally-recorded earthquakes (Hattori, 1980; Santoso, 1982; Shrestha, 1987; Lukkunaprasit and Kuhatasanadeekul, 1993; Lisantono, 1994; Warnitchai and Lisantono, 1997; Warnitchai, 1998; Palasri, 2006). In this research, the seismic sources both in the southern part of Thailand and nearby region within 200 km (ICOLD, 1989) from southern Thailand are included in the seismic hazard analysis. Especially, the active seismic sources, based on the paleoseismic studies resulted from this study and others, that were not accounted as the sources in any studies are included in the analysis. These sources consist of Tenessarim fault (TNF), Tavoy fault (TVF) and Kunguangale fault (KYF) in Myanmar, Three Pagoda fault (TPF) in western Thailand, RNF and KMF in southern

Thailand, Ratchaprapha Dam's reservoir-triggered seismicity in Surat Thani province, the KMF's area source in the eastern part of the main alignment of the KMF. Even though the latest versions of the seismic hazard maps of Thailand and nearby region (Petersen et al., 2007, Pailoplee, 2009) include the KMF and RNF as the seismic sources but they considered incorrectly both faults are inactive with the long return period and low slip rate. This research also applies a logic tree approach to reduce the uncertainties of attenuation relationships, recurrence models, and parameters of seismic sources such as seismogenic crustal thickness, fault segmentation and maximum magnitudes whereas the others did excluded this approach. Four attenuation relationships are selected from western North America where seismotectonic characteristics and geological condition are similar to Thailand (WCFS, 1996, RID, 2005, Wong et al., 2006, Harnpattanapanich, 2010). They are equally weighted in the hazard analysis. The other researchers adopted only one relationship in the analysis without consideration of the seismotectonic characteristics of the regions where the attenuation relationships were originated. Some researchers choose an attenuation relationship that fits to few strong ground motion data in Thailand with the source-to-site distance over the upper constraint of that attenuation model. Moreover, the seismic hazard maps for southern Thailand derived from this study do not show only the peak ground acceleration with 2% and 10% probability of exceedance in 50 years as illustrated in previous seismic hazard maps of Thailand but also the peak ground acceleration with 0.5% and 5% probability of exceedance in 50 years. The last two types of hazard maps with the return period of 2,500 and 10,000 years are useful as a guideline for the design of high hazard structures resisting the earthquake such as dams (USCOLD, 1998, Charles et al., 1991). Additionally, the hazard maps herein have the advantage of being more application to other buildings with low frequency or long period of shaking as shown by the hazard map for 0.2-, 0.3- and 1.0-second spectral acceleration with 10%, 5%, 2% and 0.5% probabilities of exceedance in 50 years.

1.4 Study Area

The area to be depicted as acceleration hazard maps is located in southern Thailand from Ratchaburi Province southward to Yala Province as shown in Figure 1.5. Not only seismicity sources situated within southern Thailand but also those located in a 200-km distance from southern Thailand (ICOLD, 1989) are redefined and included in the analysis. Additionally, the Sumatra-Andaman subduction zone located in the west of the study area approximately more than 700 km is also considered in the study.

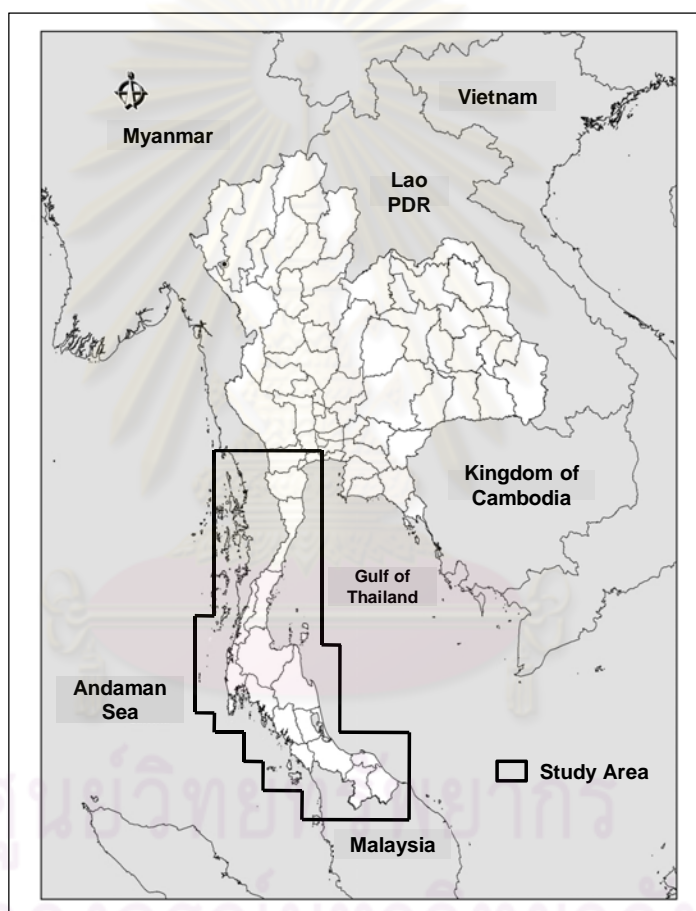


Figure 1.5 Map of Thailand showing the area to be established a seismic hazard map.

CHAPTER II

LITERATURE REVIEW

2.1 Seismic Hazard Analysis Methodology

Usually, when engineer would like to construct buildings in seismic zones, the seismic hazard maps will be used to find out how much the earthquake ground shaking to be included in the building design. Nowadays, many people have been confused the meaning between seismic risk and seismic hazard. Seismic hazard is results of expected earthquake ground motion at any point on the earth. Seismic risk is potential economic, social and environmental consequences of earthquake hazard events that may occur in a specified period of time.

Seismic hazard analysis is the method to estimate quantitatively earthquake ground motion at a particular site. Seismic hazards can be analyzed deterministically when a particular earthquake scenario is assumed, or probabilistically in which uncertainties in earthquake size, location, and time of occurrence are explicitly considered (Kramer, 1996). Concepts of both deterministic and probabilistic seismic hazard analyses can be summarized as below.

2.1.1 Deterministic Seismic Hazard Analysis (DSHA)

Deterministic seismic hazard analysis has to be carried out by using geological and seismic historical data to identify earthquake sources of which the strongest earthquake may be produced regardless of time (Krinitzsky, 1995). The largest earthquake of each source is called Maximum Credible Earthquake (MCE) that appears possible along identified faults under presently known or presumed activity (USCOLD, 1998).

Consequently, it may cause the most severe damage to the considered site. The method of the deterministic seismic hazard analysis is simple procedure and can be divided into 4 steps (Reiter, 1990, Kramer, 1996) as follows (Figure 2.1):

1. Identification and characterization of all seismic sources that could produce significant ground shaking at the considered site. Characterization of sources is identification of source location, geometry, orientation and earthquake potential. The seismic sources can be classified as: (1) point source, constant source-site distance, such as volcanoes, short fault (2) linear or line source, one parameter controls distance, shallow depth, such as long fault, (3) areal source, two geometric parameter control distance, constant depth crustal source, and (4) volumetric source, three parameters control distance.
2. Selection of a shortest distance between the earthquake source and considered site. The distance may be shown as an epicentral distance or hypocentral distance. It will be dependent upon the measured distance included in attenuation relationships that are adopted in the following step.
3. Selection of the controlling earthquake that generates the most ground motion at the site. Normally, the controlling earthquake expresses in terms of magnitude and distance to the site. The maximum credible earthquake (MCE) and shortest distance to the site of each source will be selected to be included in ground motion calculation at the site in a next step.
4. Computation of the ground motion at the site produced by the controlling earthquake by using selected attenuation relations. Ground motion can be illustrated in terms of peak ground acceleration, peak ground velocity, and response spectrum ordinates

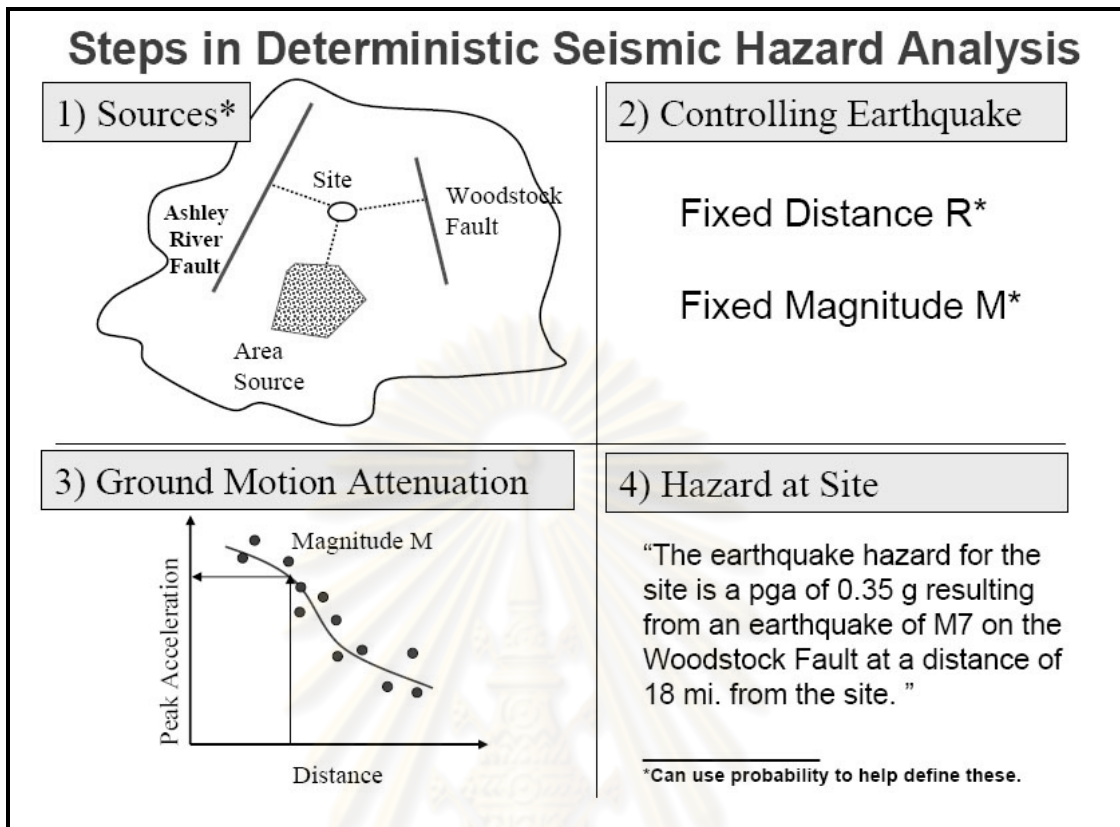


Figure 2.1 Four steps of the deterministic seismic hazard analysis based on Kramer (1996) (www.nibs.org).

2.1.2 Probabilistic Seismic Hazard Analysis (PSHA)

The probability seismic hazard analysis is firstly developed by Cornell (1968). Uncertainties excluded in the deterministic analysis such as the size, location, and recurrence rate of earthquakes will be identified, quantified and combined in the probabilistic seismic hazard analysis in order to provide more complete picture of the seismic hazard. Four steps of the probabilistic seismic hazard analysis each of which express somewhat similarly to the steps of the DSHA method are shown in Figure 2.2. Each step of the PSHA can be explained as below:

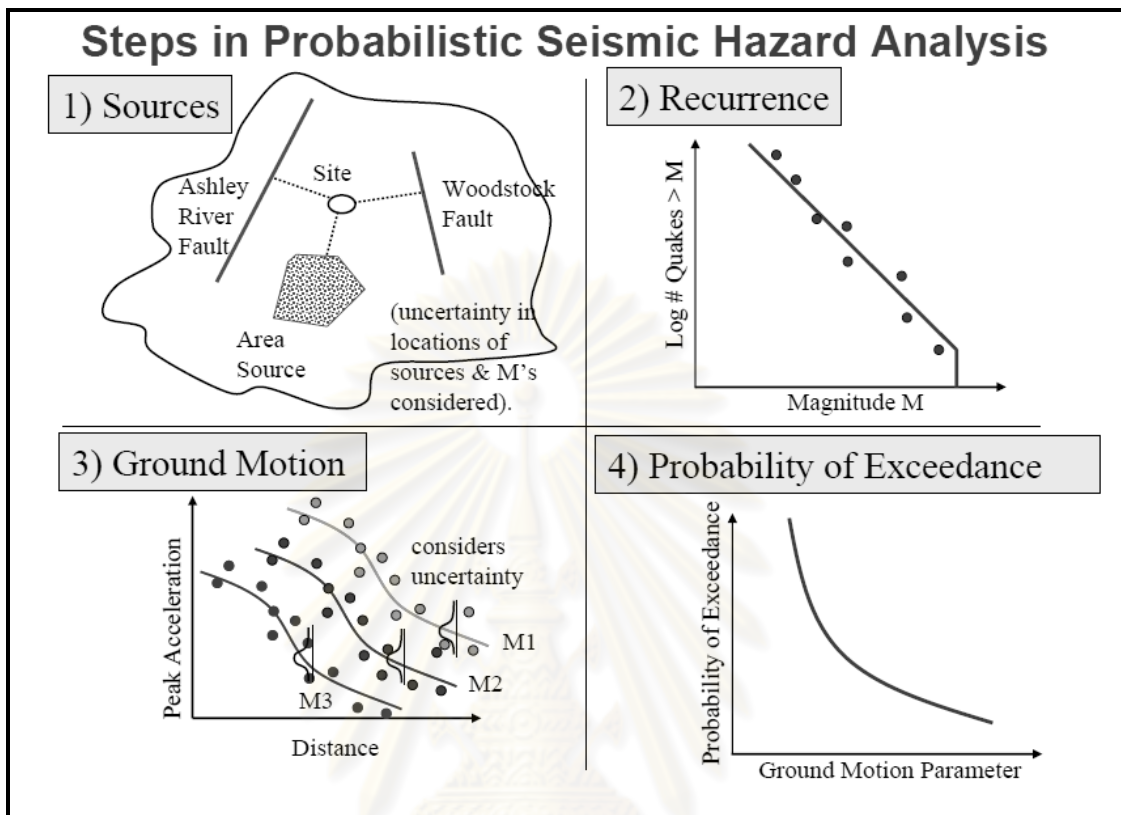


Figure 2.2 Four steps of the probabilistic seismic hazard analysis based on Kramer (1996) (www.nibs.org).

1. Similar to the first step of the DSHA procedure, identification and characterization of all earthquake sources that can affect the ground shaking at the site. The difference of both procedures is that the PSHA has to characterize the probability distribution of the potential rupture location within the sources. In general practice, the earthquake occurrence is always specified to distribute uniformly within the sources. Combined with the source geometry, the

earthquake distribution will provide probability distribution of the source-to-site distance.

2. Characterization of temporal distribution of earthquake recurrence. The recurrence rate, which is an average rate of some earthquake magnitude will be exceeded, will be established for each source.
3. Computation of ground motion. The ground motion at the site produced from any earthquake magnitude at any point within each source will be computed with the use of the attenuation relationships. The uncertainty of the attenuation models is also included in the PSHA procedure.
4. Determination of probability of exceedance. The ground motion parameters with probability of exceedance for specified year will be obtained from uncertainties of earthquake location, earthquake magnitude, and attenuation models.

2.2 Seismotectonic Setting and Tectonic History

The present tectonics of Thailand appear to be related to the interaction between three major plates, namely the Indo-Australian, Eurasian, West Pacific plates combining with the opening of the Andaman Sea as shown in Figure 2.3. Thailand is situated within the Eurasian plate which is surrounded by the convergent margins, namely the Andaman subduction zone in the west, Sunda and Java trenches in the south and Philippine trench in the east. Within the Eurasian plate, there are few smaller combined crustal plates and of which the related movement is low compared with the larger plates (Metcalf, 1996, Charusiri et al., 1997, 2002). In the end of Mesozoic (Bunopas and Vella, 1992, Charusiri et al., 2002, Morley, 2004), the major tectonic evolution of Thailand formed coincidentally with the collision between Indian and Eurasian plates (Rhodes et al., 2004). The Indian-Eurasian collision began about 40-50 Ma (Searle et al., 1987, Peltzer and Tapponnier, 1988) and

then shortening across the Himalayan orogen occurred as well as the Indochina extruded to the southeast along the Red River strike-slip fault (Peltzer and Tapponnier, 1988, Lee & Lawver, 1994, Golonka, 2002) and

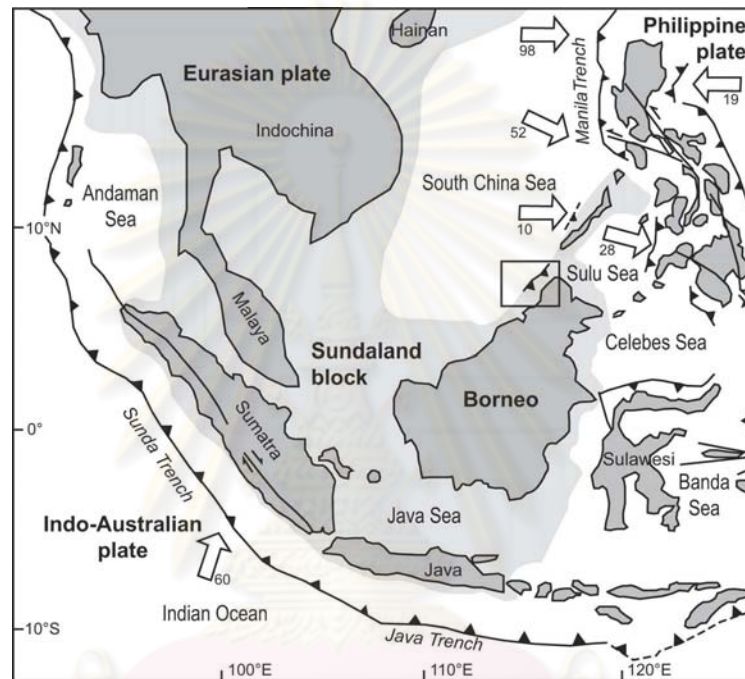


Figure 2.3 Tectonic map of Southeast Asia (www.gsabulletin.gsapubs.org).

rotated clockwise during Oligocene-Miocene (20-30 Ma). This event produced the sinistral displacement along the main strike-slip faults in Southeast Asia. Because of differential slip between those strike-slip faults, transtensional situation happened resulting the opening of many fault-controlled Tertiary basins in Southeast Asia (Ducrocq et al., 1992). Many basins that are bounded by linear escarpments are believed still active (Siribhakdi, 1986, Charusiri, 2007). The climax of extensional tectonic is the eruption of alkaline basalts during late Tertiary and early to middle Quaternary (Hoke and Campbell, 1995). Because of the Indo-Australian plate subducting beneath the Eurasian plate in the Andaman Sea, Mergui basin developed rapidly as a series of north trending half-

garbens with north trending normal faults during Late Oligocene (25 Ma). Similarly, this situation can be observed in Thailand's Tertiary basins of which the trend is in N-direction and the structures are pull-apart garben and half-graben developed since Late Oligocene (20-25 Ma) (Braun et al., 1976). The total amount of Cenozoic extension at the northern part of the Gulf of Thailand is about 50 km (Olinstad et al., 1989). A lot of basins with linear escarpment on their boundaries are interpreted that they are still active structures (Siribhakdi, 1986).

The seismotectonic provinces for Thailand were firstly classified and mapped by Santoso (1982) as shown in Figure 2.4. Based on the data on structural geology,

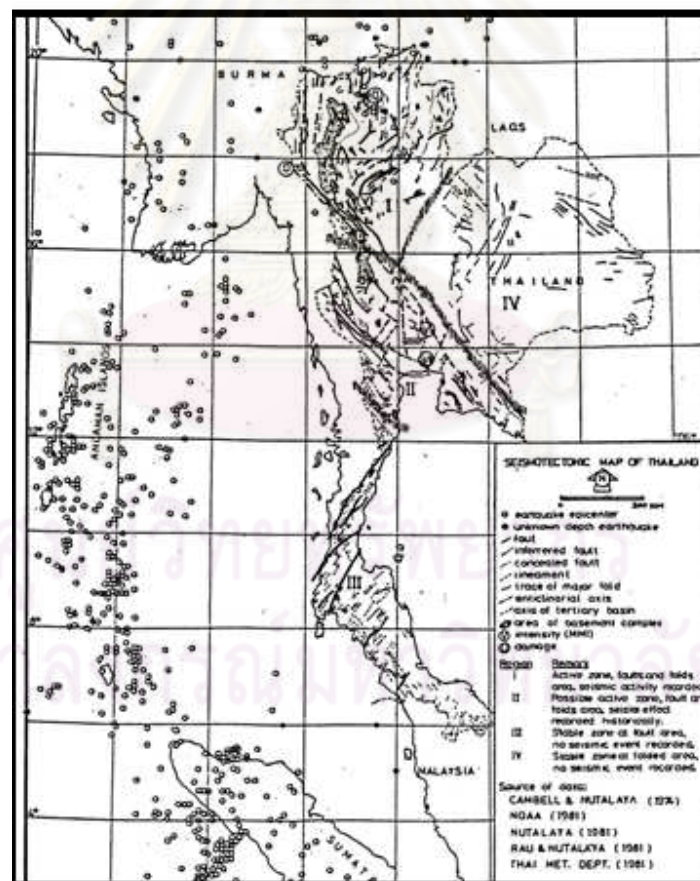


Figure 2.4 Seismotectonic map of Thailand (Santoso, 1982).

earthquake epicenters and earthquake intensity of Thailand, this seismotectonic zone map is composed of 4 zones: (1) Zone I, active province at the northern Thailand, (2) Zone II, possible active zone covering the central, the east and the upper part of the south of Thailand, (3) Zone III, stable area with faulted structures including the southern Thailand and (4) Zone IV, stable area with folded structures at the northeastern Thailand.

Nutalaya et al. (1985) produced the seismotectonic map of Thailand and adjacent areas as shown in Figure 2.5. This map is depicted based on the distribution of historical earthquakes from 1910-1979. The seismotectonic setting of Thailand and nearby region is divided into 12 zones. The southern Thailand is not defined into any seismotectonic zone due to no earthquake events.

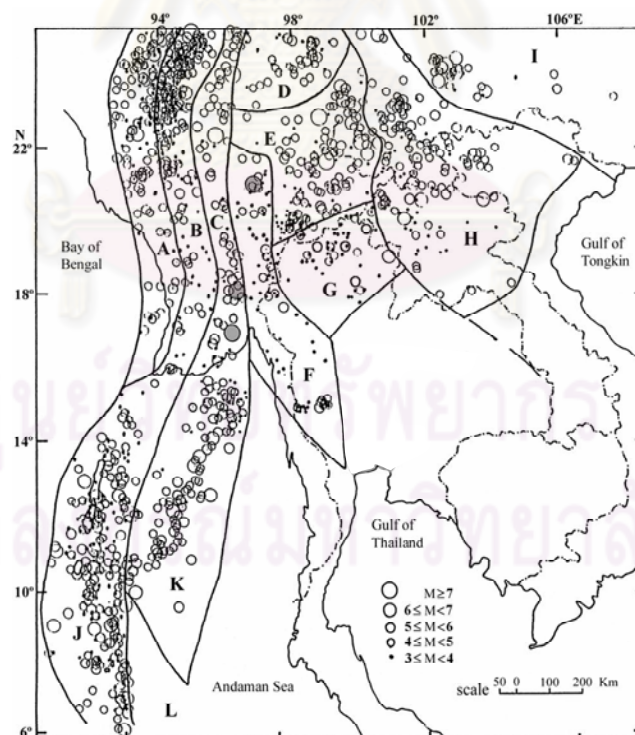


Figure 2.5 Regional seismic source zones of Thailand and nearby region, and earthquake epicenters recorded during 1910-1979 (Nutalaya et al., 1985).

With additional geologic, heat flow and fault activity data, Woodward–Clyde Federal Service (WCFS, 1996) modified the seismotectonic zones for Thailand as shown in Figure 2.6. The seismotectonic zones are divided into 6 zones-- northern basin and range, eastern fold belt, Khorat plateau, central plain, western highlands, and Malay peninsula zones. The southern part of Thailand is located in the Malay peninsula zone.

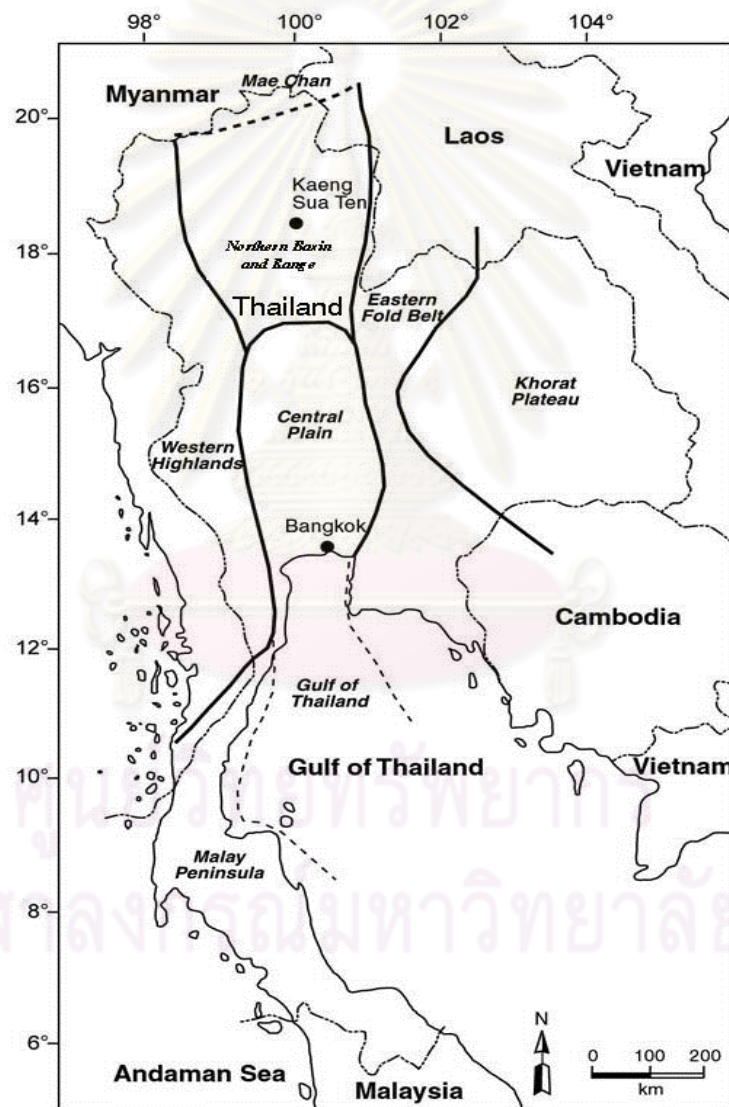


Figure 2.6 Seismotectonic zone map of Thailand (WCFS, 1996).

In 2000, applying data from remote sensing interpretation, field geologic investigation, geo-chemistry of igneous rocks and fossils, Charusiri et al. (2000) established the seismotectonic zoned map for Thailand as shown in Figure 2.7. It consists of 4 lithospheric plates, i.e. (1) Shan-Thai plate in the western and southern Thailand, (2) Lampang-Chiang Rai plate in the middle of northern Thailand, (3) Nakhon Thai plate in the east of Northern Thailand, and (4) Indochina plate in the eastern Thailand.

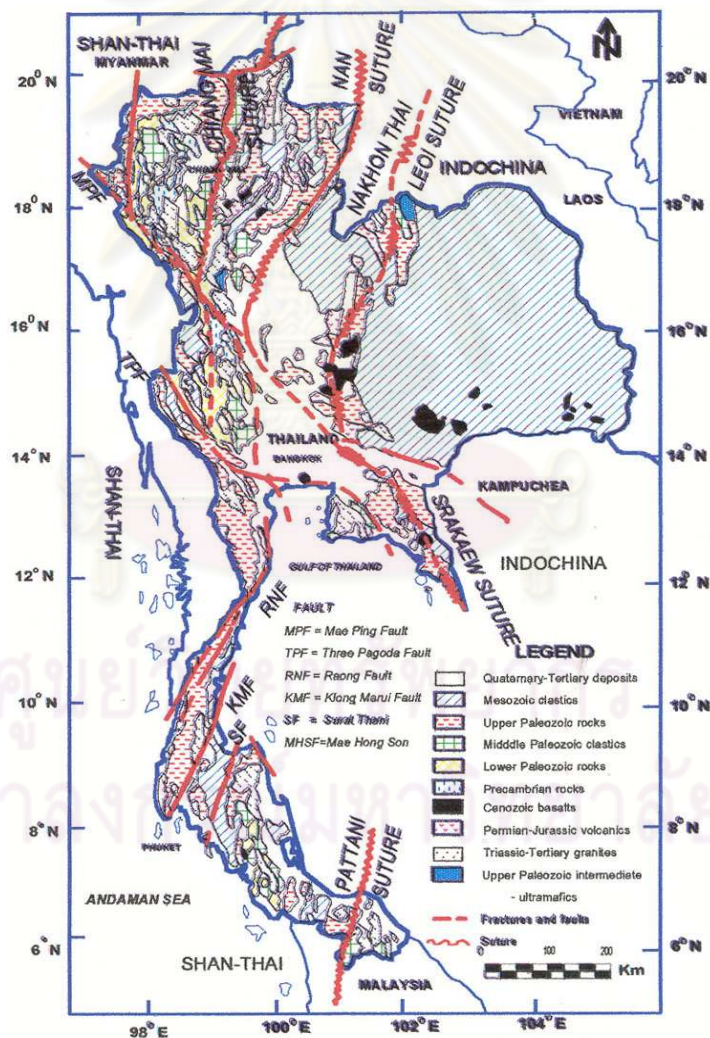


Figure 2.7 Seismotectonic province in Thailand (Charusiri et al., 2000).

The Nutalaya et al.(1985)'s seismotectonic zone map was modified with integrating the geological setting, geological structure, tectonic setting and seismological information by Charusiri et al. (2005). As a result, 21 seismotectonic provinces were classified as shown in Figure 2.8.

2.3 Earthquake Data

The historical earthquake records can be divided into pre-instrumental and instrumental data. Uniform earthquake detection and orientation of earthquake data in Thailand has probably only been possible in the last 20-25 years.

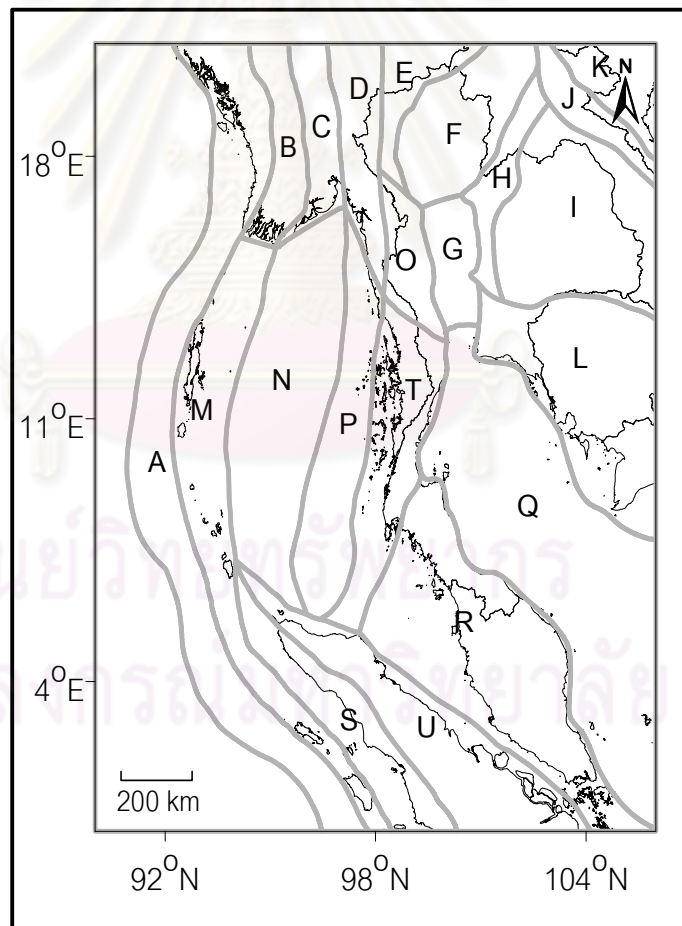


Figure 2.8 Seismotectonic zones in Southeast Asia (Charusiri et al., 2005).

2.3.1 Pre-instrumental Seismicity

Reports of earthquakes in Thailand during the period of unavailable earthquake-detecting equipment reveal where the earthquakes are felt and do not inform where they are located (Nutalaya et al., 1985). They are mainly based on direct observation and felt reports. No earthquakes are felt in the south of Thailand in the pre-instrumental period as well.

2.3.2 Instrumental Seismicity

The first earthquake-monitoring station established in Thailand in 1963 is the Worldwide Seismographic Stations Network at Doi Suthep, Chiang Mai province (CHTO). The second station was constructed at Songkla province (SNG) in 1965. These stations were not used to record smaller local earthquakes in Thailand and could not be used to locate earthquake epicenters in the site region. Until 1970, several stations were installed by the Thai Meteorological Department (TMD) to record the local earthquakes. In the south of Thailand, the first two stations were installed at Nnong Plab (NNT) in 1982 and at Phuket (PKT) in 1994.

After the completion of construction of the Ratchaprapha dam at Surat Thani province, the Electricity Generating Authority of Thailand (EGAT) installed three mobile earthquake stations around the reservoir of the Ratchaprapha dam. They could detect the reservoir-triggered seismicity events (RTS) with magnitudes of M_L 0.3-3.4 located in the reservoir area. At present only one station has been left at the Ratchaprapha dam. It could record the M_L 1.4 earthquake on 27 October 2006. Its epicenter could be calculated with a distance away from the Ratchaprapha dam about 16 km. It is believed to be the RTS.

After the large earthquake with a magnitude of M 9.3 occurred at the northwest of the Sumatra Island on 26 December 2004, the Department of Physics, Prince of Songkla University placed four temporary earthquake-recording instruments at Phuket, Phang Nga

and Krabi province during 14 January-30 June 2005. The instruments could detect a lot of small aftershock earthquakes that are located along the southern RNF and KMF (Duerrast, 2007) as shown in Figure 2.9.

At the present, there are several earthquake stations that were built in the south of Thailand as follows:

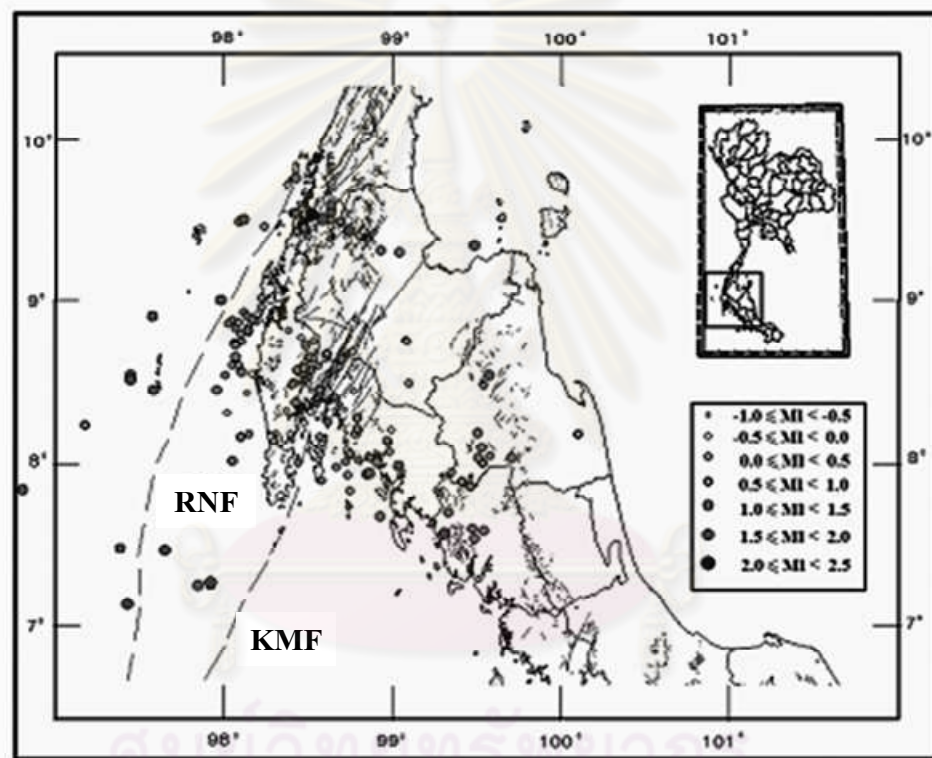


Figure 2.9 A map of southern Thailand showing epicenters recorded between 14 January 2005 and 30 June 2005 (Duerrast, 2007).

1. Four stations of Tha Sae Dam Project of the Royal Irrigation Department (RID) consist of:

- TSKT station at Khuring sub-district office, Khuring sub-district, Tha Sae district, Chumporn province,
 - TSJK station at Khlong Kracha dam, Thapsakae district, Prachuab Khirikhun province,
 - TSLC station at Lamchoo weir, Bang Saphan Noi district, Prachuab Khirikhun province, and
 - TSPJ station at Nikhom Sang Ton Eng Ban Pak Chun, Kra Buri district, Ranong province
2. A station owned by the EGAT was installed at the Ratchaprapha dam, Ban Ta Khun district, Surat Thani province.
3. Eight stations established by the Thai Meteorological Department (TMD) are:
- RNTT station at Ratchaprapha dam, Ban Ta Khun district, Surat Thani province,
 - PKDT station at Bang Wad dam, Katoo district, Phuket province,
 - TRTT station at Khlong Tha Ngiew dam, Tha Ngiew district, Trang province,
 - SKLT station at Rupchang hill, Muang district, Songkla province,
 - SURA station at Thathong weir, Donsak district, Surat Thani province,
 - SRIT station at Khlong Din Daeng dam, Phipun district, Nakhon Srithamarach province,
 - KRAB station at Bang Kumprat dam, Khao Phanom district, Krabi province.

From 1912 to 2008, besides the small aftershock earthquakes that were recorded by the mobile recorders (Duerrast, 2007), eight earthquake events were recorded in the southern Thailand during the years 2006-2008 (Figure 2.10) as below.

1. There are earthquakes with a magnitude of M_b 4.5 (USGS) occurring on 28 September 2006 and with a magnitude of M_b 4.9 (USGS) on October 8, 2006. The USGS

reported that they happened in the Gulf of Thailand but the TMD and the Department of Mineral Resources (DMR) reported that they occurred in Myanmar along Tenessarim fault.

2. On 19 November 2007, the earthquake with a magnitude of M_L 2.76 was detected by the TSPJ station. Its epicenter could not be computed.

3. There are earthquakes with a magnitude of M_b 4.5 (USGS) occurring on 28 September 2006 and with a magnitude of M_b 4.9 (USGS) on October 8, 2006. The USGS reported that they happened in the Gulf of Thailand but the TMD and the Department of Mineral Resources (DMR) reported that they occurred in Myanmar along Tenessarim fault.

4. On 19 November 2007, the earthquake with a magnitude of M_L 2.76 was detected by the TSPJ station. Its epicenter could not be computed.

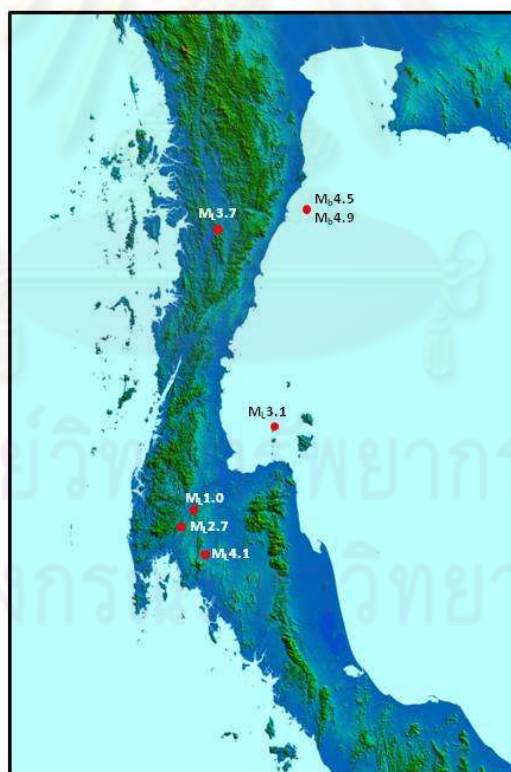


Figure 2.10 Earthquakes were detected in the southern Thailand and Myanma during the years 2006-2008.

5. There are earthquakes with a magnitude of M_b 4.5 (USGS) occurring on 28 September 2006 and with a magnitude of M_b 4.9 (USGS) on October 8, 2006. The USGS reported that they happened in the Gulf of Thailand but the TMD and the Department of Mineral Resources (DMR) reported that they occurred in Myanmar along Tenessarim fault.

6. On 19 November 2007, the earthquake with a magnitude of M_L 2.76 was detected by the TSPJ station. Its epicenter could not be computed.

7. On 4 May 2008, the earthquake occurred at Khao To sub-district, Plai Phraya district, Krabi province. The TMD reported that the earthquake produced the magnitude of M_L 2.7 at latitude of 8.6389°N and longitude of 98.7361°E but the RID revealed that the magnitude is M_L 3.88. The people widely perceived the earthquake ground shaking.

8. On 24 May 2008, the TMD reported that there is an M_L 1.0 earthquake at Phanom district, Surat Thani province (8.8273°N 98.8942°E).

9. On 24 July 2008, the earthquake happened with a magnitude of M_L 3.70 that was computed by the RID's TSTK station. Its epicenter at 11.70°N / 98.90°E in southern Myanma.

10. On 4 September 2008, the occurrence of an M_L 3.1 earthquake at Surat Thani province. The TMD reported that its epicenter is located at 9.256°N / 98.619°E (in the mountainous area at the boundary between Ranong and Surat Thani provinces) but the EGAT stated that it is situated at 9.66°N / 99.65°E (in Ang Thong Island belt).

11. On 23 December 2008, an M_L 4.1 earthquake was detected. Its epicenter was reported at Phra Saeng district, Surat Thani province ($8^\circ37'\text{N}$ / $99^\circ0'0''\text{E}$). The people in various areas could feel the ground shaking.

2.4 Earthquake Sources

Two types of earthquake sources influencing the southern part of Thailand to which many previous studies have mentioned are active faults and area source zones. The

followings are summary of earthquake sources in the south of Thailand and adjacent areas identified by many researchers.

2.4.1 Fault Sources

Based on satellite image interpretation and field investigation, Chuaviroch (1991) classified active faults in Thailand into 13 fault zones as shown in Figure 2.11. These fault Zones

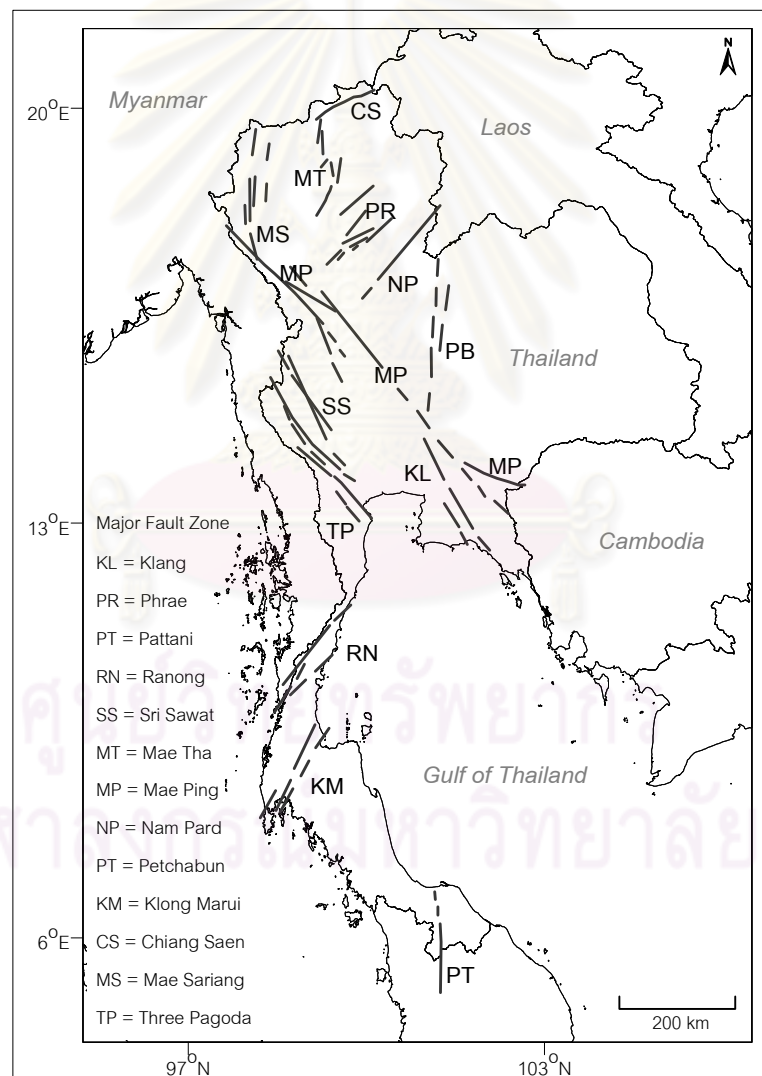


Figure 2.11 Fault Map of Thailand showing 13 fault zones (Chuaviroch, 1991).

consist of Pattani (PT), Klang (KL), Klong Marui (KM), Chiang Saen (CS) or Mae Chan, Mae Ping (MP), Mae Sariang (MS), Mae Tha (MT), Nam Pard (NP) or Uttaradit, Petchabun (PT), Phrae (PR), Ranong (RN), Sri Sawat (SS), and Three Pagoda (TP) fault zones. For the south of Thailand, he reported that there are 3 fault zones, namely RNF, KMF and PT fault zones, of which orientations are approximately NE to NNE trending. It can be believable that they are left-lateral strike-slip faults.

In 1997, applying results of historical seismicity compilation, satellite image interpretation, field investigation and Thermoluminescence (TL) age dating, Hinthong categorized 22 fault zones into four classification of active faults in Thailand —(1) potentially active fault zones (2) historically and seismologically active fault zones (3) neotectonically active faults and (4) tentatively active faults and fault zones (Figure 2.12). In the south of Thailand, active faults are identified into two classes, i.e. the neotectonically active faults consisting of following minor faults: Khok Pho, Saba Yoi, Yala and Betong fault zones, and the tentatively active faults composed of the RNF, KMF, Ao Luk, Khlong Thom and Kantang fault zones.

Charusiri et al. (2002) produced the seismically active belts (SAB) map. The map shows 17 fault zones in Thailand. These fault zones are divided into 3 groups based on TL age dating data, i.e. active, potentially active and tentatively active fault zones as shown in Figure 2.13. For the southern part of Thailand, there are two group of fault activity consisting of four fault zones. The first group is the tentatively active fault zones: RNF, Khlong Thom and Pattani fault (PTF) zones. The second group is the potentially active fault zone: KMF zone.

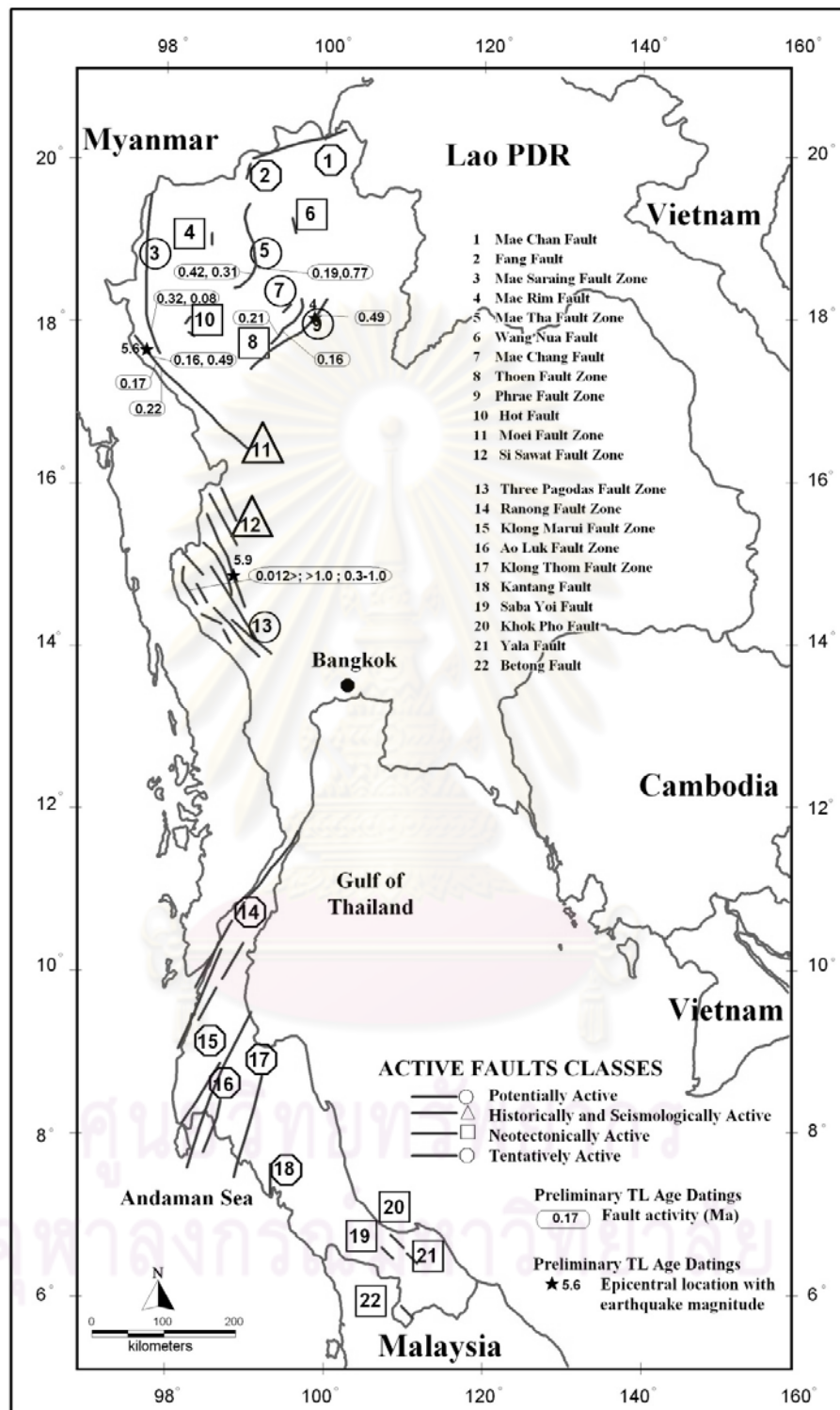


Figure 2.12 A map showing 22 active faults in Thailand (Hinthong, 1997).

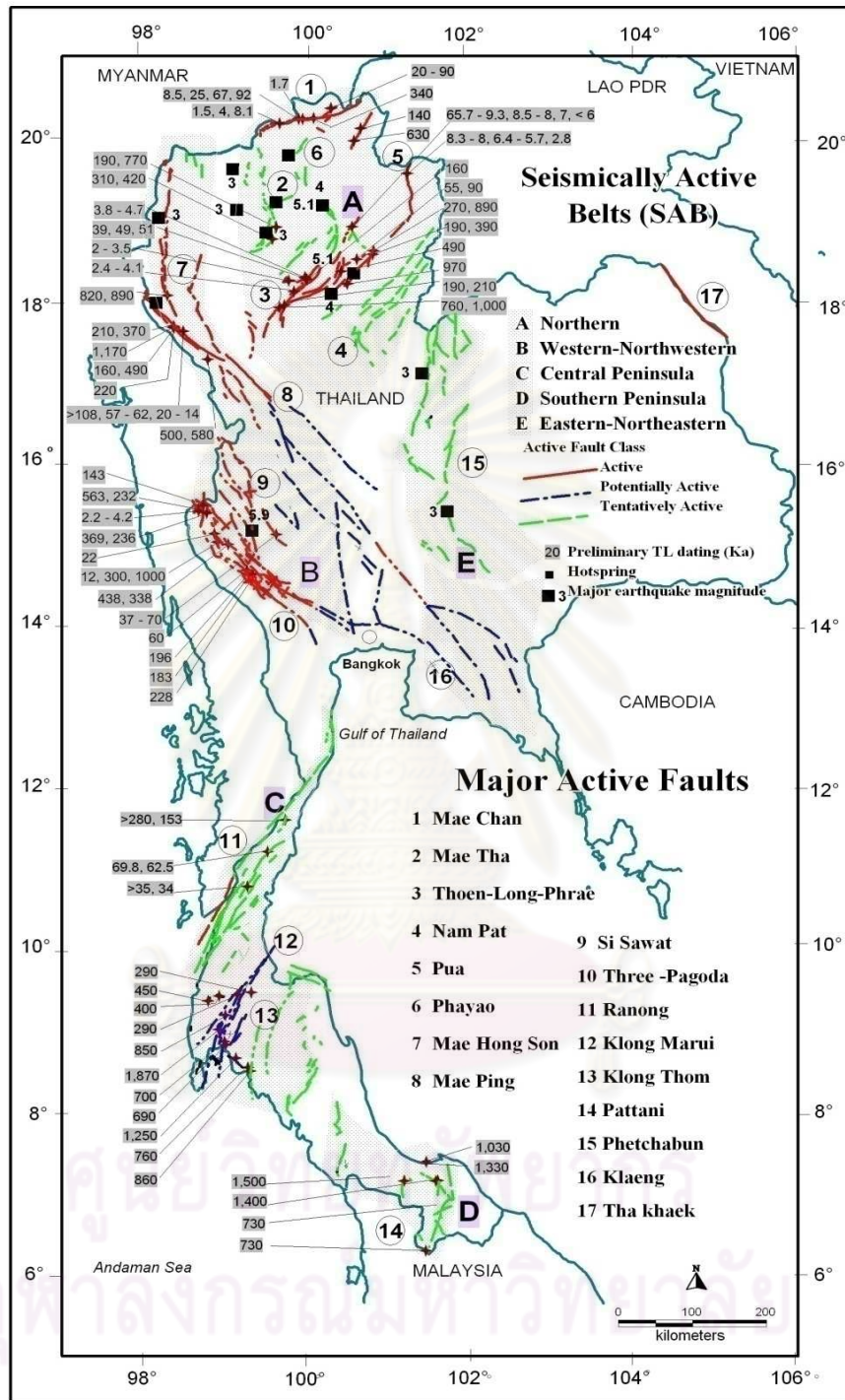


Figure 2.13 Seismically active belt map showing three groups of 17 faults as active, potentially active and tentatively active faults (Charusiri et al., 2002).

The last official version of the active fault map is illustrated in the Department of Mineral Resources' website as shown in Figure 2.14 (DMR, 2006). Thirteen active fault zones were mapped. They are named as Mae Hong Son, Mae Tha fault, Phrayao fault, Mae Chan fault, Mae Ing fault, Mae Yom fault, Pua fault, Thoen fault, Uttaradi faultt, Tha Khaek fault, Si Sawat fault, TPF, RNF and KMF zones. Only two active fault zones—RNF and KMF zones—exist in southern Thailand

Besides the seismic sources located in Thailand, the sources in Myanma and Andaman Sea affecting the ground shaking in the south of Thailand where some researchers mentioned can be summarized as follows:

Wong et al.(2005) concluded that the RNF and KMF are inactive but there are three active faults in Myanma—TNF, KYF and TVF-- on the northwest of Prachuap Khiri Khan and Kanchanaburi provinces as shown in Figure 2.15. Based on the geomorphic expression, the TNF is divided into three segments, namely northern, central and south segments with a length of approximately 80 km, 80 km and 40 km, respectively, and the KYF has the length about 55 km. Results of remote sensing imagery analysis indicate that both faults are active. Moreover, at the west of Kanchanaburi province in Myanma, the TVF is interpreted from remote sensing data as the active fault. It is a north-northwest-striking right-lateral strike-slip fault.

There are two types of earthquake sources occurring in the Sumatra-Andaman subduction zone: (1) interplate earthquakes that occur along the megathrust separating the subducting plate and the overlying plate, and (2) intraplate or intraslab earthquakes that occur within the subducting plate. The slip rate of the megathrust is 53 mm/year. The largest earthquake of the megathrust that occurred in December 2004 was firstly reported with a magnitude



Figure 2.14 Active fault map in Thailand (www.dmr.go.th).

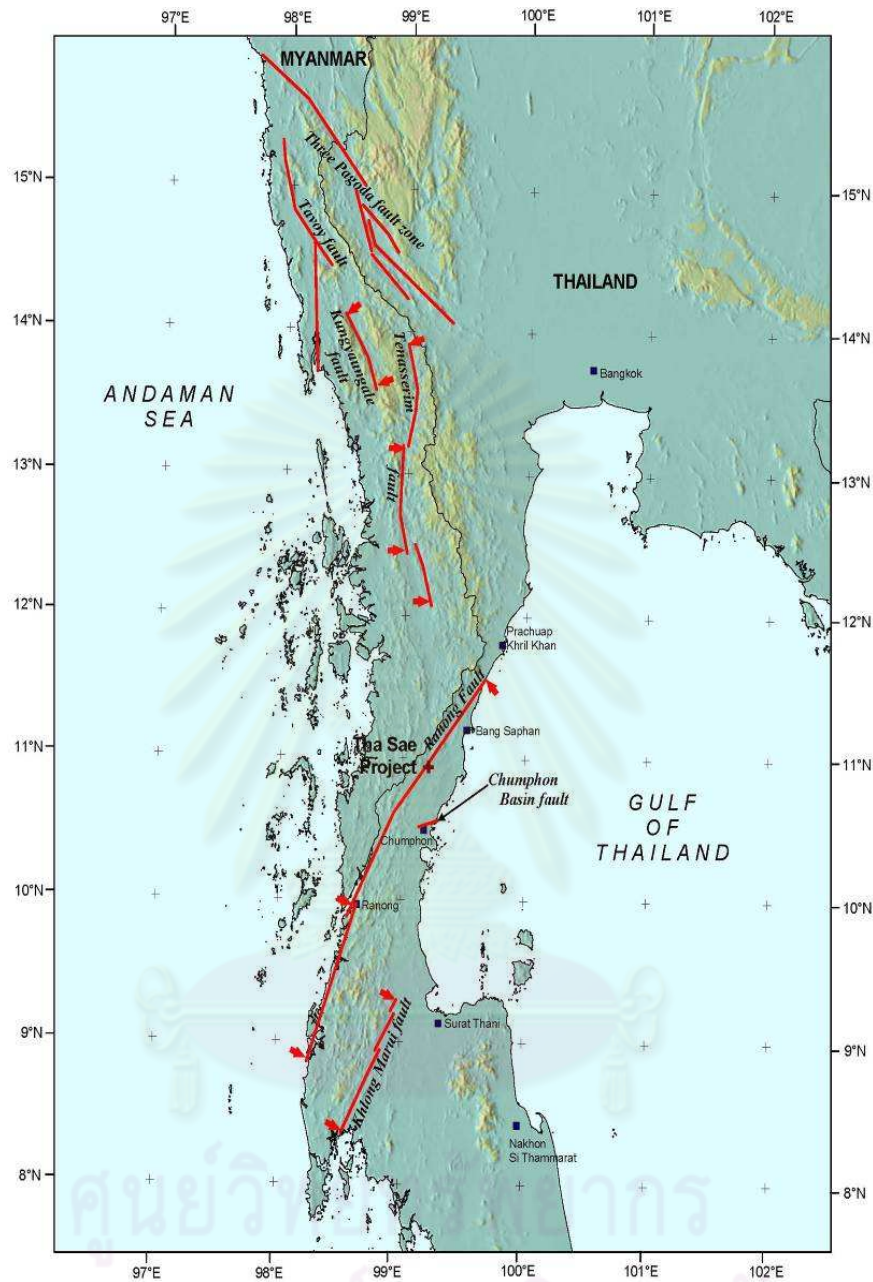


Figure 2.15 Active faults in the southern Thailand and Myanma (Wong, 2005).

of M_w 9.0 to 9.3 (USGS, 2005a, Bilham, 2005, Stein and Okal, 2005) but at present is given in the USGS's website with the magnitude of M_w 9.1 (based on Park, 2005). The magnitude

of the intraslab had a magnitude of M 7.3 (Wong, 2005) adopted from aftershock of the 2004 Andaman-Sumatra mainshock.

2.4.2 Area Sources

The twelve seismotectonic zones of Thailand and nearby countries (Figure 2.5) depicted by Nutalaya et al. (1985) were applied by many researchers (Shrestha, 1986, Lisantono, 1994, Warnitchai and Lisantono, 1997, Warnitchai, 1998) to be the seismic area sources.

For USGS's Southeast Asia seismic hazard map preparation, 11 seismic source zones are identified as shown in Figure 2.16. The south of Thailand is situated in an inactive Sunda plate that is considered to be a background seismic source zone. This zone not only includes southern Thailand but also Malaysian peninsula, western Borneo, and portions of eastern Thailand.

Pailoplee (2009) and Palasri and Ruangrassamee (2010) applied the seismic source zones as the seismic area sources that were proposed by Charusiri (2005) as illustrated in Figure 2.8 to establish the seismic hazard map of Thailand and adjacent areas.

2.5 Attenuation Relationships

Many strong ground motion attenuation relationships that describe the general decay of peak acceleration and response spectral amplitudes with magnitude and distance were developed from recorded earthquake ground motions for both crustal and subduction zone earthquakes (Douglas, 2001).

Hattori (1980) used an attenuation model that was developed Oliveira (1975) and McGuire (1974) to construct the seismic risk maps in the Asian countries including Thailand.

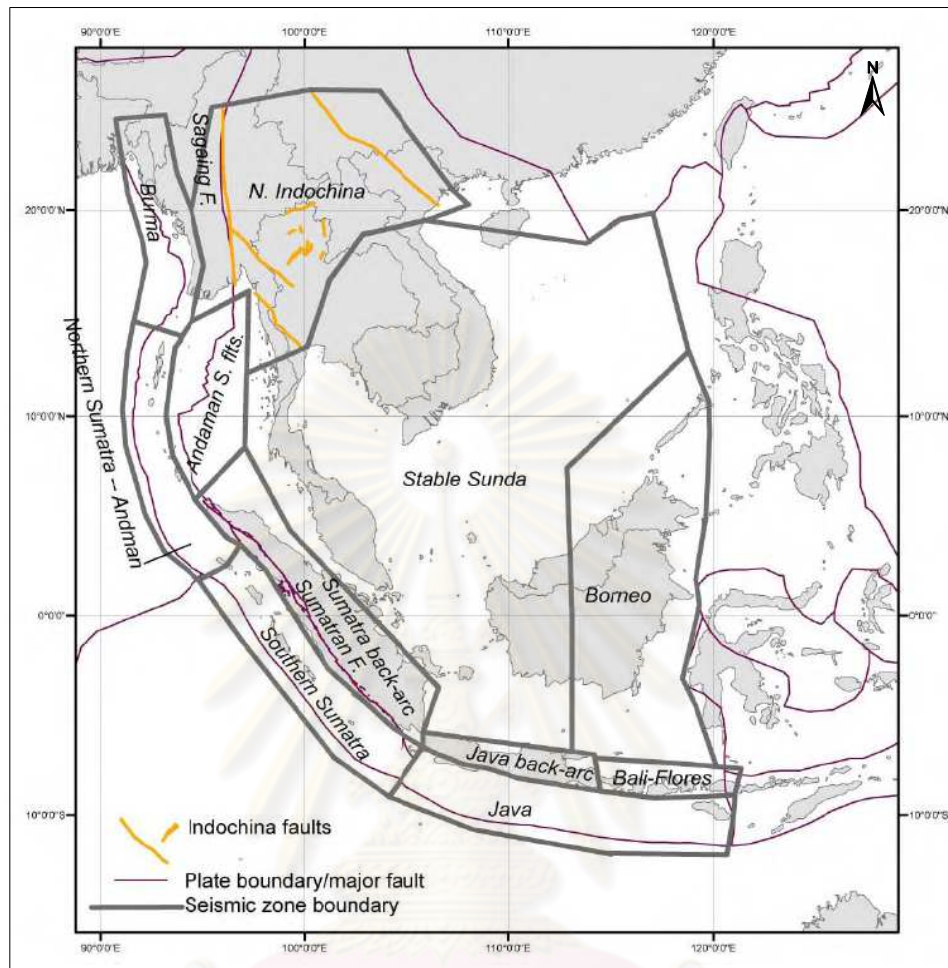


Figure 2.16 Map of shallow-depth earthquake source zones for southeast Asia
(Petersen et al., 2007).

Santoso (1982) adopted Katayama's and Kanai's attenuation models (Hattori, 1980) to establish the seismic zoning map of Thailand in terms of acceleration and velocity, respectively.

Shrestha (1986) compared computed peak ground acceleration using different models with the actual measured acceleration at Srinagarind and Khao Laem dams. He

concluded that the Esteva's model (Esteva and Villavarde, 1973) was reliable for this region. He applied the Esteva's model to construct iso-acceleration and iso-particle velocity maps of Thailand.

Lukkunaprasit and Kuhatasanadeekul (1993) and Lisantono (1994) also used the Esteva's model to depict the peak ground acceleration and velocity maps of Thailand.

WCFS (1996, 1998) and Wong (2005) applied the attenuation models used in the western part of USA. The selected relationships are Abrahamson and Silva (1997), Campbell and Bozorgnia (2003), Sadigh *et al.* (1997), Boore *et al.* (1997), and Pankow and Pechmann (2004) for crustal earthquakes, Youngs *et al.* (1997), Atkinson and Boore (2003), and Gregor *et al.* (2002) for subduction zone megathrust earthquakes, and Youngs *et al.* (1997) and Atkinson and Boore (2003) for subduction zone intraslab earthquakes.

Petersen *et al.* (2007) applied the attenuation models from Western United States to calculate ground motion for all crustal faults in Thailand. These models were developed by Boore and Atkinson (2007), Campbell and Bozorgnia (2007), and Chiou and Youngs (2007). For calculation of ground motions caused by the subduction zone, attenuation relations proposed by Youngs *et al.* (1997), Atkinson and Boore (2003), and Zhao *et al.* (1997) were chosen.

Chintanapakdee *et al.* (2008) evaluated twenty attenuation equations that were developed for shallow crustal earthquakes and subduction zones by comparing with forty five existing earthquakes recorded during 2006-2007 by the TMD. They summarized that the attenuation relationships established by Idriss (1993), Sadigh *et al.* (1997) and Toro (2002) are suitable for shallow crustal earthquake analysis while Crouse (1991) is appropriate for subduction zone earthquake calculation.

Pailoplee (2009) compared the strong ground motion that were recorded in Thailand with Estava and Villaverdi (1973)'s, Idriss (1993)'s and Sadigh et al. (1997)'s attenuation models. He concluded that the Idriss's attenuation relationship is most suitable to apply for the seismic hazard analysis.

Palasri and Ruangrassamee (2010) selected the Idriss (1993)'s and Sadigh et al (1997)'s attenuation equations for analyzing shallow crustal earthquakes and Petesen et al.'s attenuation model (2004) was chosen for computing Sumatra-Andaman subduction zone earthquakes.

2.6 Previous Paleoseismic Investigation

Paleoseismic investigation in southern Thailand was started by the Royal Irrigation Department (RID) for Tha Sae dam project, Chumporn province in 2006. The paleoseismic investigation concentrated along the RNF. The investigation included data collection, satellite and aerial photograph images interpretation, field reconnaissance, trenching and fault age dating. A total of 12 trenches and exposures were logged in details to determine the relations between faults and recent geological deposits. 25 soil samples were collected for thermoluminescence (TL) age dating. Results of the study concluded that the RNF has not moved in the latter part of Quaternary and is not considered an active fault.

In 2007, the Department of Mineral Resources (DMR) engaged the Department of Geology, Faculty of Science, Chulalongkorn University to determine the recurrence intervals of RNF and KMF in Prachuabkhirikhun, Chumporn, Ranong, Surat Thani, Krabi, Phang Nga and Phuket provinces. This performance comprises data collection and compilation, remote sensing and aerial photograph interpretation, field reconnaissance, detailed topographic survey, geological mapping, radon detection, trenching, and ^{14}C -, TL- and electron spin

resonance (ESR) age dating. Ten trenches were excavated along the KMF while seven trenches along the RNF. Eighty seven soil samples were collected for TL age-dating and eight soil samples were kept for electron spin resonance (ESR) age-dating. Fifteen charcoal were sampled for ^{14}C AMS age-dating. As a result, it can be stated that at least 5 time of movement of RNF and KMF. Firstly, the RNF fault moved 40,000 years ago with a slip rate of 0.7 mm/yr. Secondly, the movement of both RNF and KMF occurred about 9,000 years ago with the slip rate of 0.18 mm/yr and 9,400 years ago with the slip rate of 0.08-0.11 mm/yr, respectively. Thirdly, the KMF displaced approximately 4,700 years ago and its slip rate is 0.17 mm/yr. Fourthly, the displacement of KMF happened in the range of 2,700-3,000 years ago and the slip rate is 0.43-0.5 mm/yr. Finally, the occurrence of both RNF's and KMF's movements at the age about 2,000 years ago with a slip rate of 0.27 mm/yr and 0.5 mm/yr, respectively.

In 2008, Sutiwanich et al. presented that the paleoseismic investigation along the KMF was carried out for the RID's Khlong Tham dam project in Phang Nga province. Steps of investigation follow general methods--data collection, satellite and aerial photograph images interpretation, field reconnaissance, trenching and fault age dating. A total of 13 trenches and exposures, i.e. 4 trenches along the RNF and 10 trenches/exposures along the KMF, were done. 54 soils were sampled for TL-age dating. As a result, there is an evidence indicating that the KMF was displaced before 3,000 years ago. The study concluded that the KMF is active.

Pananont et al. (2009) performed the paleoseismic investigation along the northern part of the RNF for the earthquake hazard risk study in Prachuabkhirikhan province and adjacent areas. The methodology used in the study consists of satellite and aerial photograph interpretation, field reconnaissance, ground penetration radar survey, trenching

and logging, and TL-age dating of soil sample. 2 trenches were excavated and 16 soil samples were collected. The study summarized that the RNF is an active fault.

2.7 Previous Seismic Hazard Maps of Thailand

The first seismic hazard map of Thailand was established by Hattori (1980). The main purpose of his study is to produce the seismic hazard map (he called seismic risk map) with the return period of 100 years for Southeast Asia. Oliveira's and McGuire's models were used to analyze the earthquake ground motion. As a result, seismic hazard maps consisting of two types: (1) the maximum particle velocity (kine) on the base rock (2) the maximum acceleration (gal) on the ground were prepared. The maximum ground acceleration in southern Thailand for the return period of 100 years is less than 20 gal or 0.02g as shown in Figure 2.17.

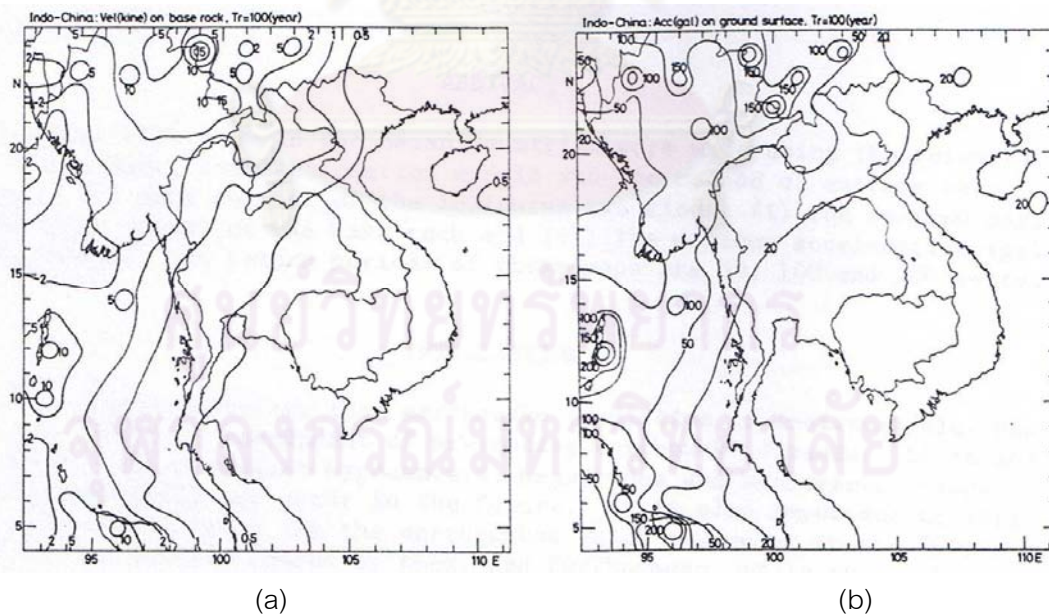
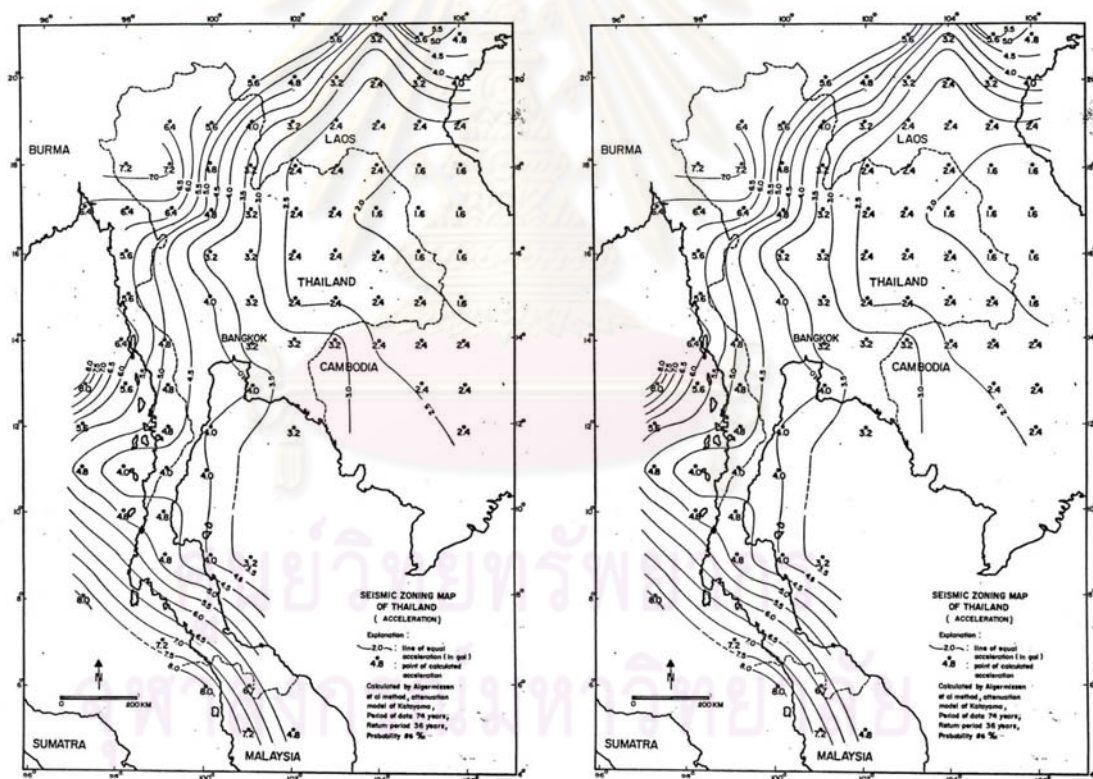


Figure 2.17 Seismic risk maps for the return period of 100 years of Southeast Asia (a) maximum acceleration map in gal (b) maximum velocity map in kine (Hattori, 1980).

Santoso (1981) constructed the ground motion map based on 74-year earthquake data. He adopted the method of seismic hazard analysis proposed by Karnik and Algermissen (1978) and applied the attenuation model suggested by Katayama and Kanai mentioned in Hattori (1980)'s paper. His evaluation excluded consideration of seismic sources and frequency of earthquake occurrence. The ground acceleration maps for 36 and 74 years corresponding to 86% and 63% probabilities, respectively, are shown in Figure 2.18. The ground acceleration of the southern Thailand for 36 years (86% probability) is 4.0-7.0 gal or 0.004–0.007 g while for 74 years (63% probability) is 4.5-8.0 gal or 0.0045-0.008 g.



(a)

(b)

Figure 2.18 Ground acceleration map for (a) 36 years corresponding to 86% and (b) 74 years corresponding to 63% probabilities (Santoso, 1981).

In 1985, Nutalaya et al. depicted the maximum earthquake intensity map for Thailand and adjacent areas as shown in Figure 2.19. The map shows that Thailand is located in the earthquake intensity zone III in the east up to the zone VII in the west. The southern Thailand has the maximum earthquake intensity level VI.

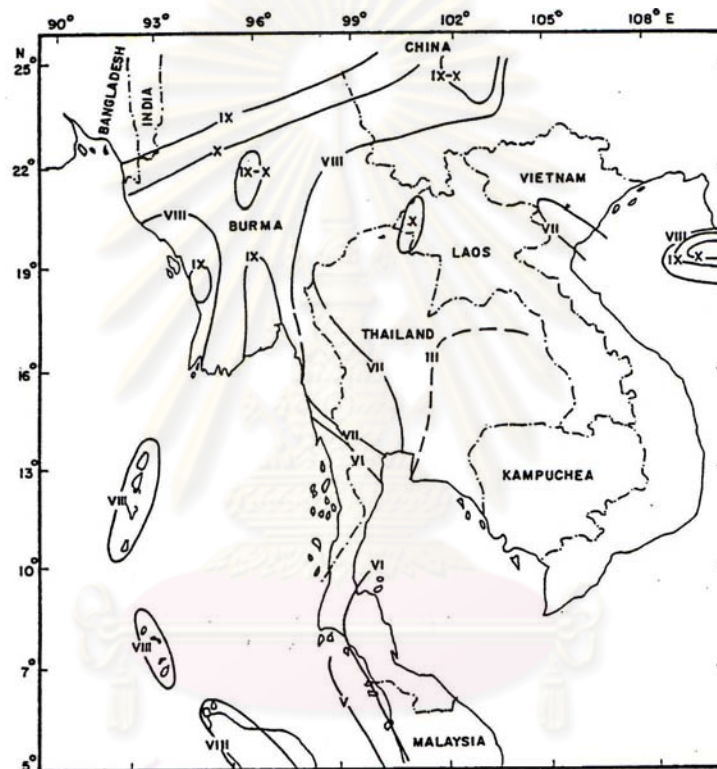


Figure 2.19 Maximum earthquake intensity map for Thailand and adjacent areas

(Nutalaya et al., 1985).

Shrestha (1986) revised Santoso's seismic hazard maps using the Esteva's model (Esteva & Villaverde, 1973) that is the different from Santoso-adopted attenuation model. He applied the seismic source zones that were identified by Nutalaya (1985). The peak

ground acceleration and peak particle velocity maps for the return period of 90 and 13 years corresponding to the 20% and 80% probabilities of exceedance were developed as shown in Figure 2.20. For the southern part of Thailand, the peak ground acceleration with the return period of 90 years (20% probability of exceedance) is mostly less than 10 gal or 0.01 g, except the northern part at Prachuab Khirikhun province about 10-20 gal or 0.01-0.02 g while that with the return period of 13 years (80% probabilities of exceedance) is less than 5 gal or 0.005 g. He also concluded that the southern part of Thailand is seismic hazard free area.

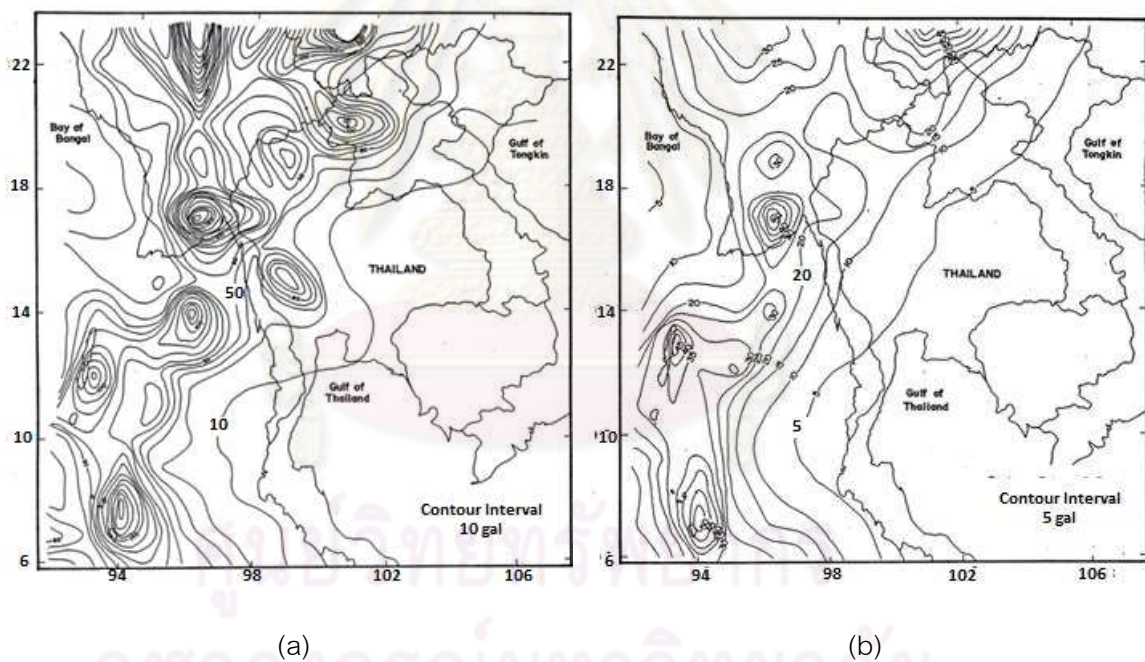


Figure 2.20 Peak ground acceleration map with the return period of (a) 90 years or 20% probability of exceedance and (b) 13 years or 80% probability of exceedance of Thailand and nearby region (Shrestha, 1986).

Lukkunaprasit and Kuhatasanadeekul (1993) also employed the Esteva's attenuation model to estimate the peak ground acceleration using 1,000 earthquake events. His peak ground acceleration map is shown in Figure 2.21. He found that seismic zoning for Thailand by

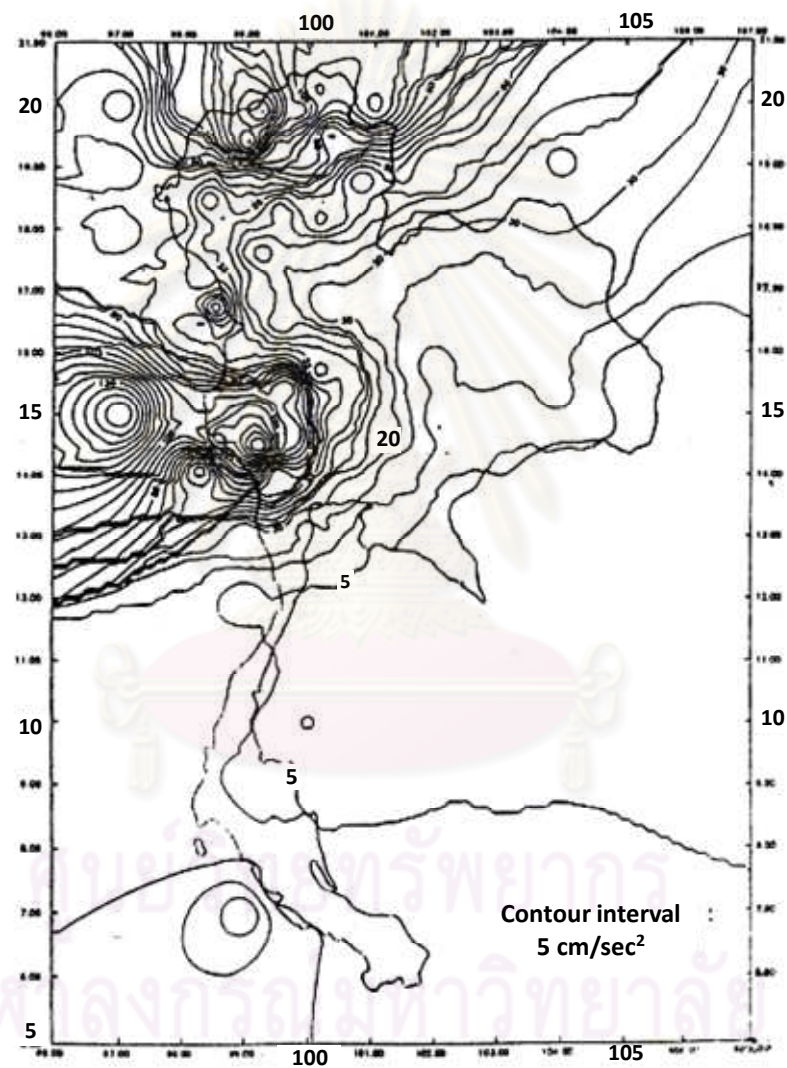


Figure 2.21 Peak ground acceleration map of Thailand (Lukkunaprasit and Kuhatasanadeekul (1993).

directly following UBC is not appropriate and then he developed the seismic zone map with slightly smaller seismic coefficient in each zone than the UBC values. The map consists of three zones: (1) zone 1, the peak ground acceleration is not greater than 6%g (2) zone 2, the peak ground acceleration is 6-10%g and (3) zone 3, the peak ground acceleration is 10-14%g. The southern Thailand is located in the zone with the peak ground acceleration less than 5 gal or 0.005 g.

Lisantono (1994) compiled the earthquake data during 1910-1989 from SEASEE Book Volume II (Nutalaya, 1985) and 1984-1989 from the TMD, and applied the Nutalaya's twelve seismotectonic provinces (1985) to be seismic source zones, excluding the zone L. All earthquake data in each seismic source zone was used to find relations between the earthquake magnitude and recurrence (Gutenberg and Richter, 1954). Moreover, each seismic source zone was sub-divided into various small seismic source blocks of which the center was assumed as the seismic point source as shown in Figure 2.22(a). The possible ground shaking analysis was based on the Cornell's method (1968) and analyzed by using Esteva's attenuation model (Esteva & Villaverde, 1973). As a result, the peak ground acceleration and seismic zoning map of Thailand with 10% probability of exceedance in 50 years based on Uniform Building Code 1991 was developed as shown in Figure 2.22 (b). The seismic zone of Thailand can be divided into five zones—(1) zone 0: the peak ground acceleration is less than 0.05g, (2) zone 1: the peak ground acceleration is 0.050g-0.075g, (3) zone 2A: the peak ground acceleration is 0.075g-0.15g, (4) zone 2B: the peak ground acceleration is 0.15g-0.20g, and (5) zone 3: the peak ground acceleration is 0.20g-0.30g. Results of this study were re-printed a few times in public conferences in Thailand (Warnitchai and Lisantono, 1997, Warnitchai, 1998).

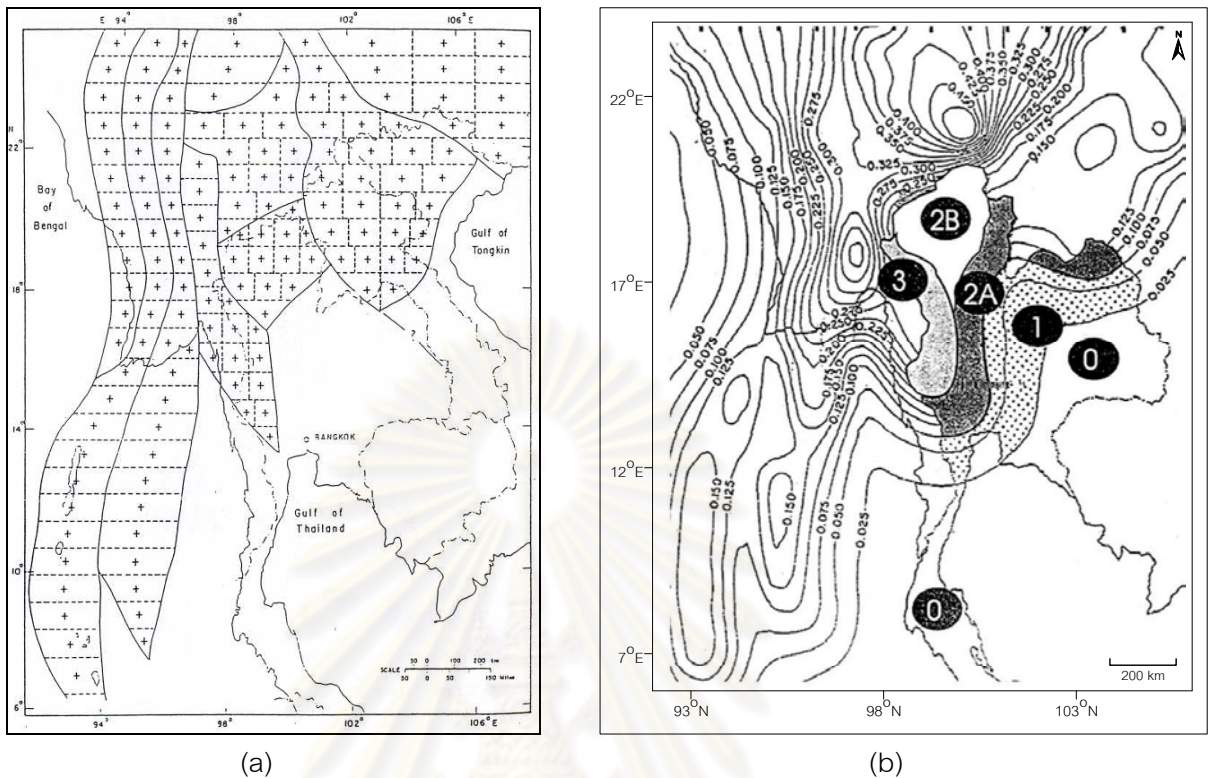


Figure 2.22 (a) Small seismic source blocks and their centers assumed to be seismic source points (b) Peak ground acceleration and seismic zoning map of Thailand with 10% probability of exceedance in 50 years based on Uniform Building Code 1991 Map (Lisantono, 1994, Warnitchai and Lisantono, 1997, Warnitchai, 1998).

Chrusiri et al. (1997) classified the seismic hazard areas in Thailand into 4 zones (Figure 2.23) as follows: (1) Zone 0, no seismic hazard in the lower half of northeastern and southern Thailand, (2) Zone 1, low seismic hazard in the upper part of northeastern and the east of central Thailand, (3) Zone 2, low to moderate seismic hazard in the east of northern and the west of central Thailand, and (4) Zone 3, moderate to high seismic hazard in the remaining northern Thailand.

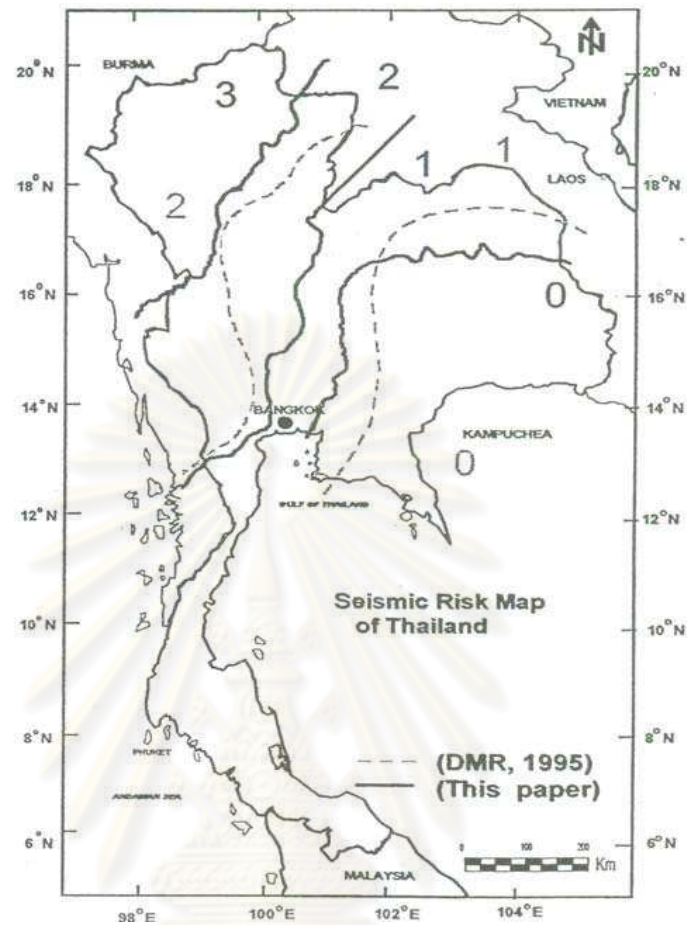


Figure 2.23 Seismic hazard zoned map of Thailand (Charusiri et al., 1997).

After M_w 9.1 Sumatra-Andaman earthquake of 26 December 2004 and following devastating tsunami, the Department of Mineral Resources (DMR, 2005) revised and improved their old seismic hazard map. The new seismic hazard map can be divided into 4 zones (Figure 2.24), namely (1) Zone 0, intensity less than III Mercalli scale, no seismic hazard, no need for building design resisting earthquake ground shaking, in the east of eastern and northeastern Thailand, (2) Zone 1, intensity III-IV Mercalli scale, slight damage, in the central, the north of northeastern, the west of eastern, and the east of the lower part of southern Thailand, (3) Zone 2A, intensity V-VII Mercalli scale, slight to moderate damages,

in the north, the central, the west and the upper part of the southern Thailand, and (4) Zone 2B, intensity VII-VIII, moderate damage, in the west of northern and central Thailand.

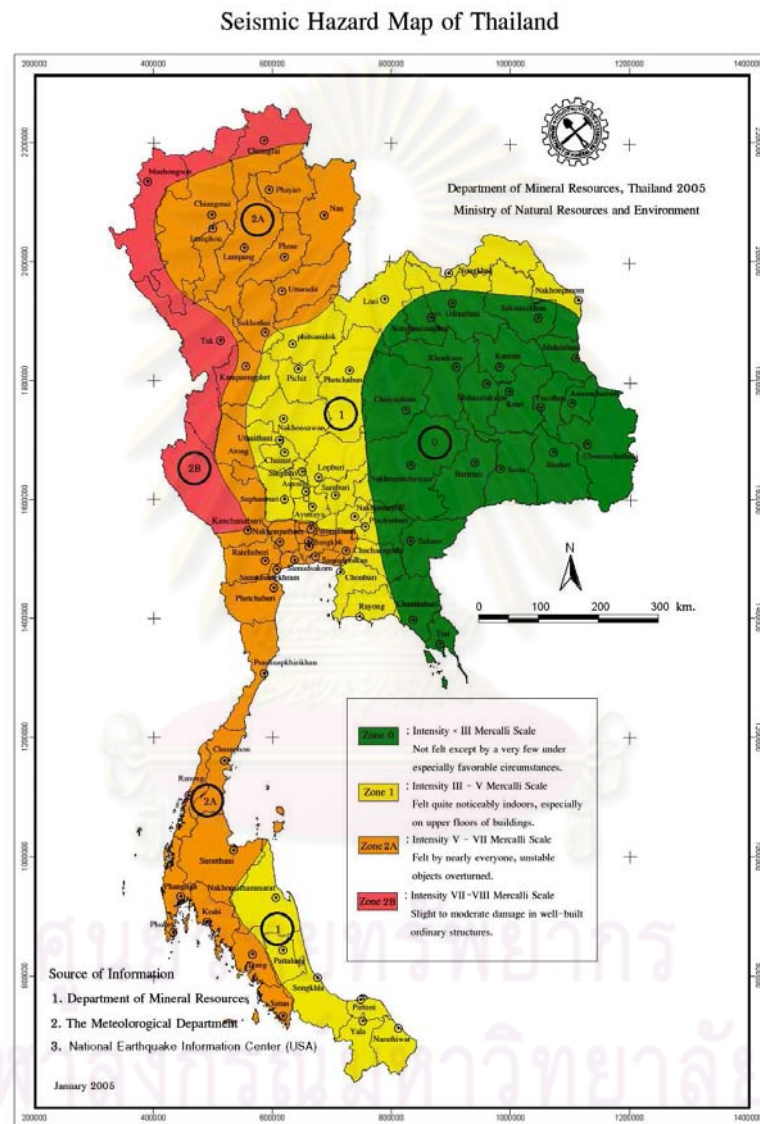


Figure 2.24 Seismic intensity map of Thailand (DMR, 2005).

Under the Southeast Asia Seismic Hazard Project funded through a United States Agency for International Development (USAID), Petersen et al. (2007) produced the seismic

hazard map of Southeast Asia. Various revisions on basic data for probability seismic hazard analysis was performed. Firstly, up-to-date earthquake data were compiled and evaluated. Secondly, seismic source zones were re-classified as shown in Figure 2.16. Finally, present fault data collected from countries in Southeast Asia were summarized and selected for seismic hazard analysis. For the southern part of Thailand, the RNF and KMF as well as the stable Sunda were included as seismic sources. However, the KMF was still considered as inactive fault with the recurrence interval of 127,398 years, slip rate of 0.01 mm/yr and a maximum magnitude of $M_w 7.5$. The RNF was specified that its recurrence interval, slip rate and a maximum earthquake magnitude are 8,473 years, 0.1 mm/yr and $M_w 7.5$, respectively. The stable Sunda was identified that it will produce background earthquakes with a maximum magnitude of $M_w 7$. The established hazard maps are composed of (1) the peak ground acceleration map with 2- and 10-percent probabilities of exceedance in 50-yr hazard level for firm rock site condition (Figure 2.25), (2) the 1-Hz spectral acceleration map with 2- and 10-percent probabilities of exceedance in 50-yr hazard level for firm rock site condition (Figure 2.26), and (3) the 5-Hz spectral acceleration map with 2- and 10-percent probabilities of exceedance in 50-yr hazard level for firm rock site condition (Figure 2.27). It can be seen that the southern Thailand will be faced with the peak ground acceleration of 2-5% g and 10-15% g for 10% and 2% probability of exceedance in 50-year, respectively.

Pailoplee (2009) established the ground acceleration maps of Thailand based on the deterministic and probabilistic methods. He applied the seismic areal source zones that were proposed by Charusiri et al. (2005) and fault sources in the analysis. He compiled the earthquake data from 1963 to 2007. The b-values of areal source zones and fault sources were

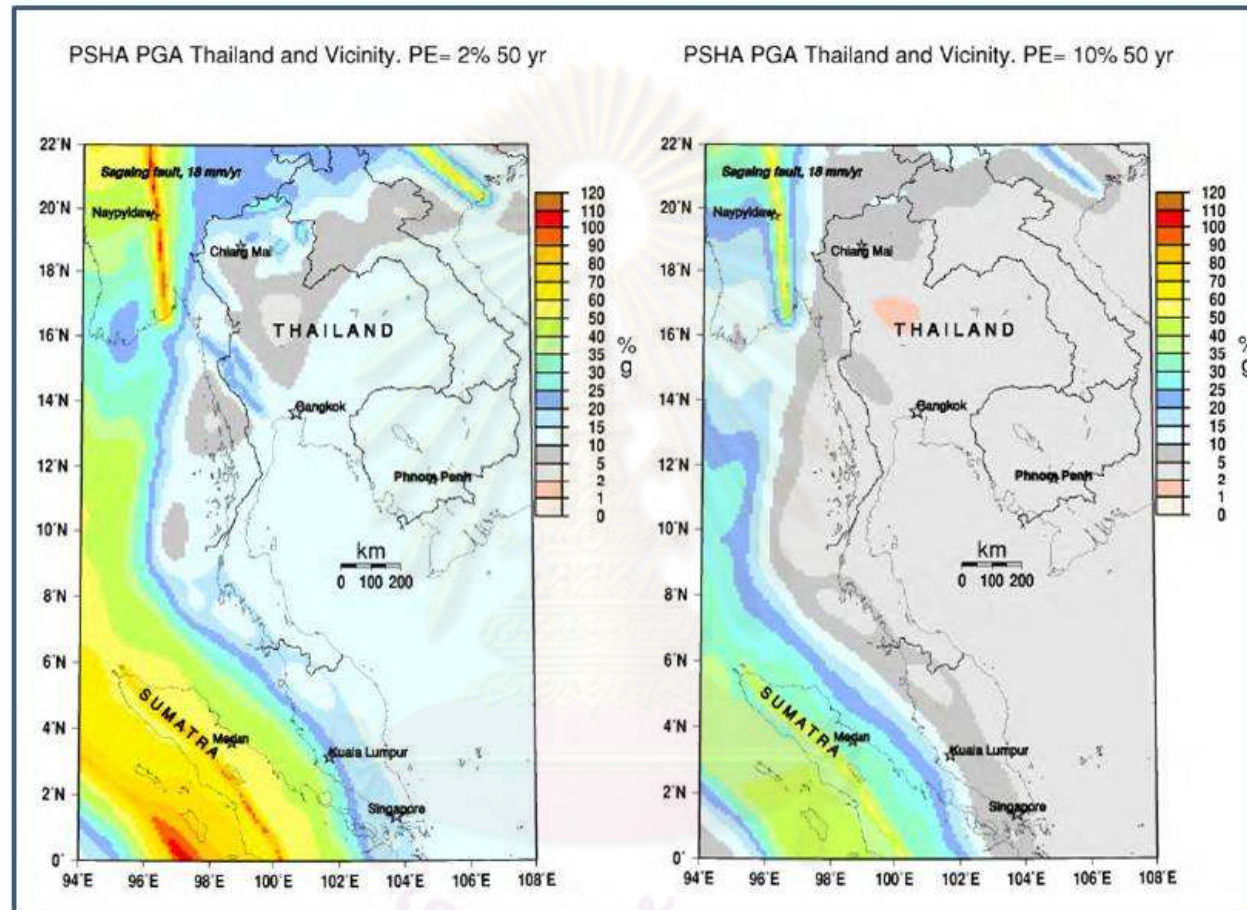


Figure 2.25 Probabilistic seismic hazard maps for Southeast Asia showing the PGA with (a) 10% and (b) 2% probability of exceedance in 50-year return period for the rock site condition (Petersen et al., 2007).

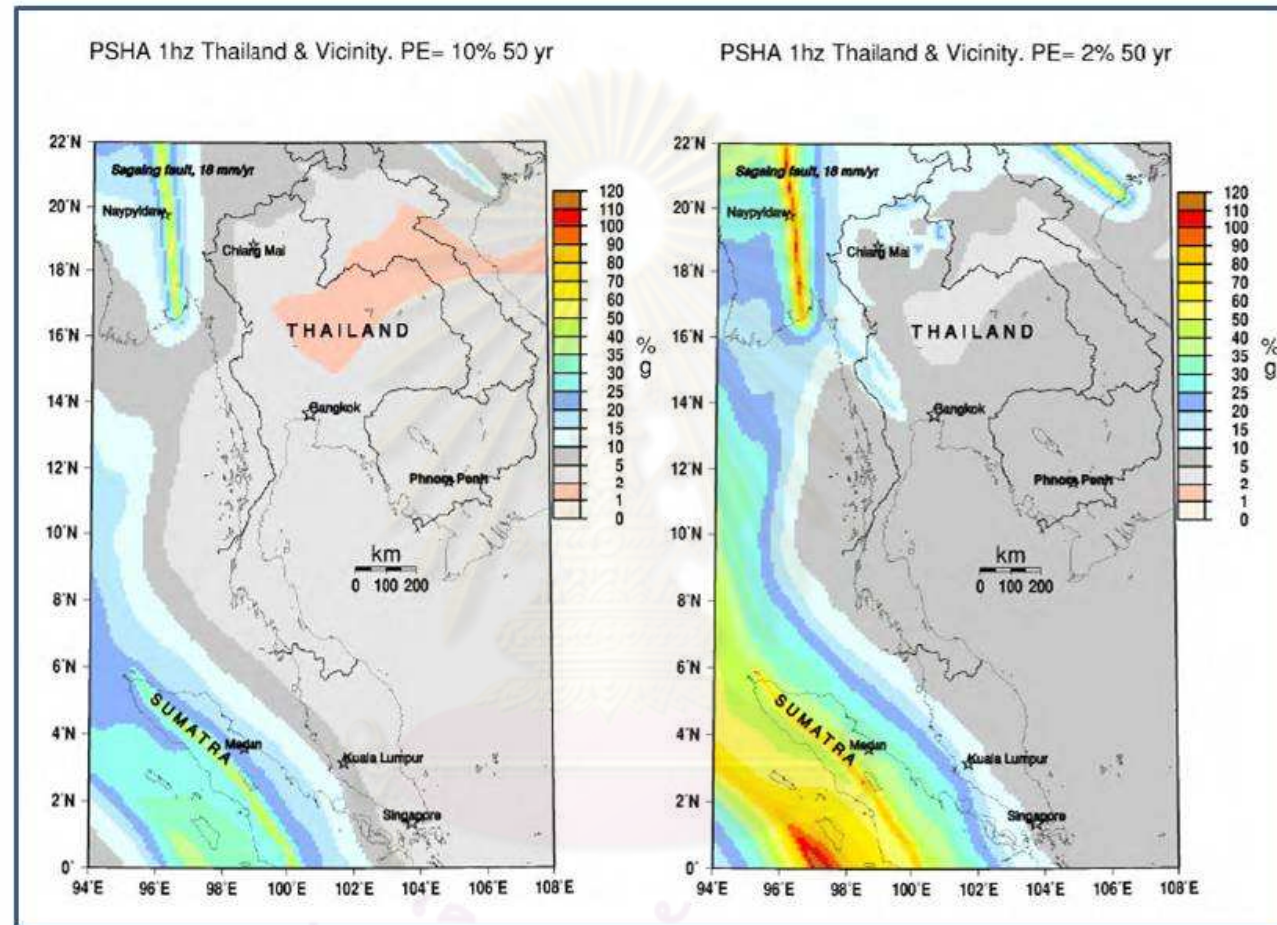


Figure 2.26 Probabilistic seismic hazard maps for Southeast Asia showing 1-Hz spectral acceleration with (a) 10% and (b) 2% probability of exceedance in 50-year return period for the rock site condition (Petersen et al., 2007).

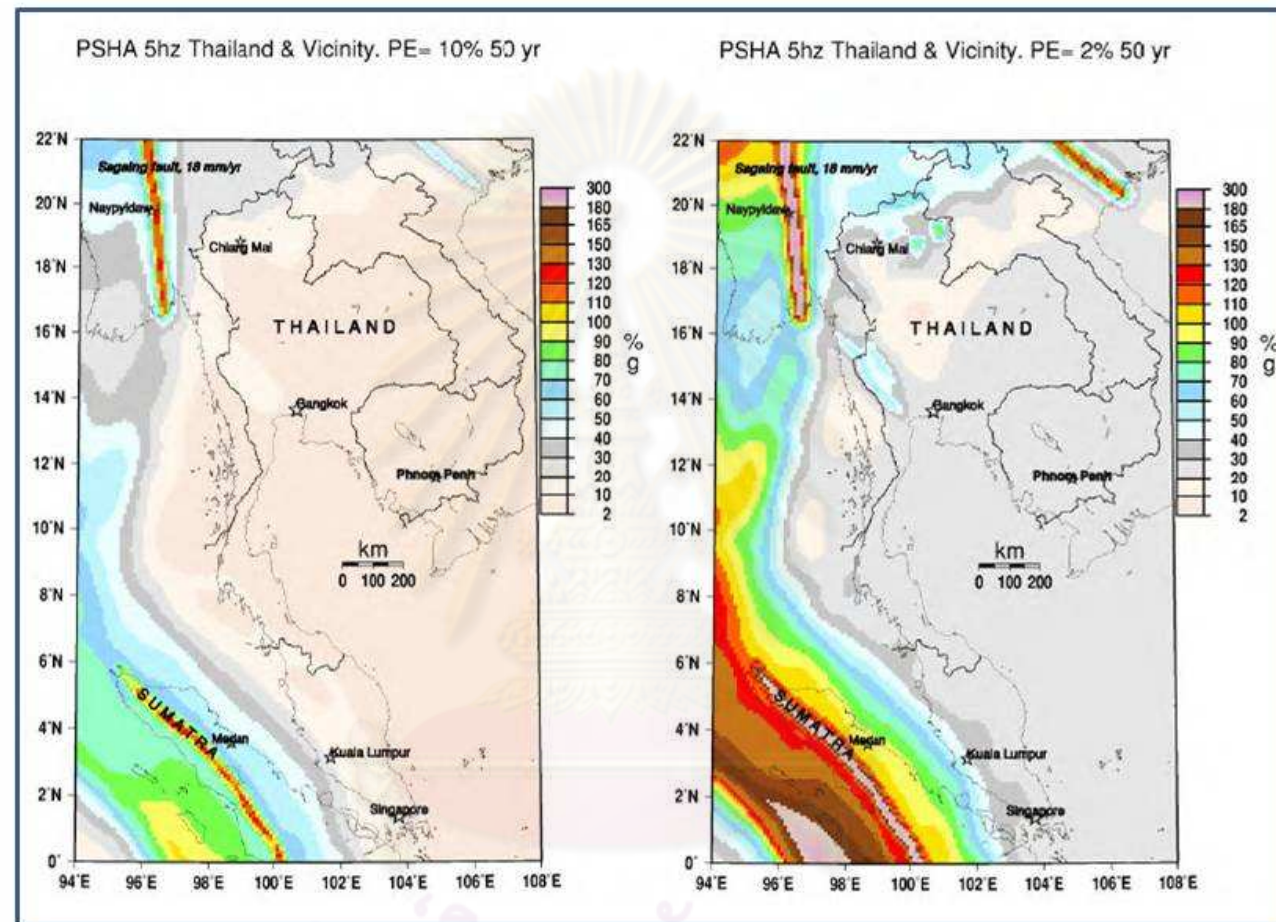


Figure 2.27 Probabilistic seismic hazard maps for Southeast Asia showing 5-Hz spectral acceleration with (a) 10% and (b) 2% probability of exceedance in 50-year return period for the rock site condition (Petersen et al., 2007).

computed and referred from other studies. Compared with moderate and strong ground motions detected by the instruments in Thailand, the Idriss (1993)'s attenuation relationship was selected for the hazard analysis. On the basis of the deterministic approach, the acceleration of the southern Thailand is in the range of 0.1g-0.3g as shown in Figure 2.28. The maximum acceleration appears along the RNF

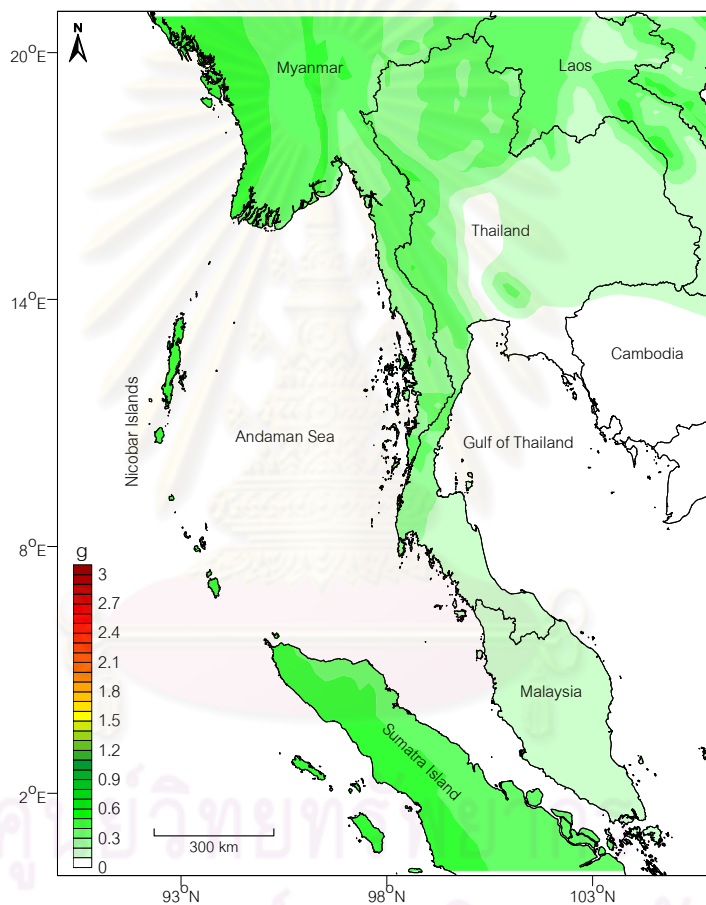


Figure 2.28 Possible maximum acceleration map of Thailand and adjacent areas computed by the deterministic method (Pailoplee, 2009)

For the probabilistic analysis, the seismic hazard maps consisting of the peak ground acceleration maps with 2% and 10% probability of exceedance in 50 years and 100 years

are shown in Figure 2.29. As a result, it can be seen that the maximum peak ground acceleration in southern Thailand varies from 0.6g for the 10% probability of exceedance in 50 years to 1.1g for 2% probability of exceedance in 100 years.

The latest seismic hazard map of Thailand was presented by Palasri and Ruangrassamee (2010). They used up-to date earthquake data (1912 to 2006) from the TMD and U.S. Geological Survey (USGS) and adopted Charusiri et al.'s seismotectonic provinces (2005) to be the areal seismic sources (Figure 2.8). Petersen et al. (2004)'s attenuation relationship was applied for the Sumatra-Andaman subduction zone while Sadigh et al. (1997)'s and Idriss (1993)'s attenuation models were weighted equally for the zones outside the subduction zone. Consequently, the seismic hazard maps with 2% and 10% probability of exceedance in 50 years were prepared as shown in Figure 2.30. This seismic hazard map shows that the southern Thailand is in the zone of low seismic hazard. The maximum accelerations for 10% probability of exceedance in 50 years is 0.08g and for 2% probability of exceedance in 50 years is 0.1g, respectively, along the Andaman coast. The minimum accelerations for 10% probability of exceedance in 50 years is less than 0.01g and for 2% probability of exceedance in 50 years is 0.01g, respectively, along the coast of the Gulf of Thailand.

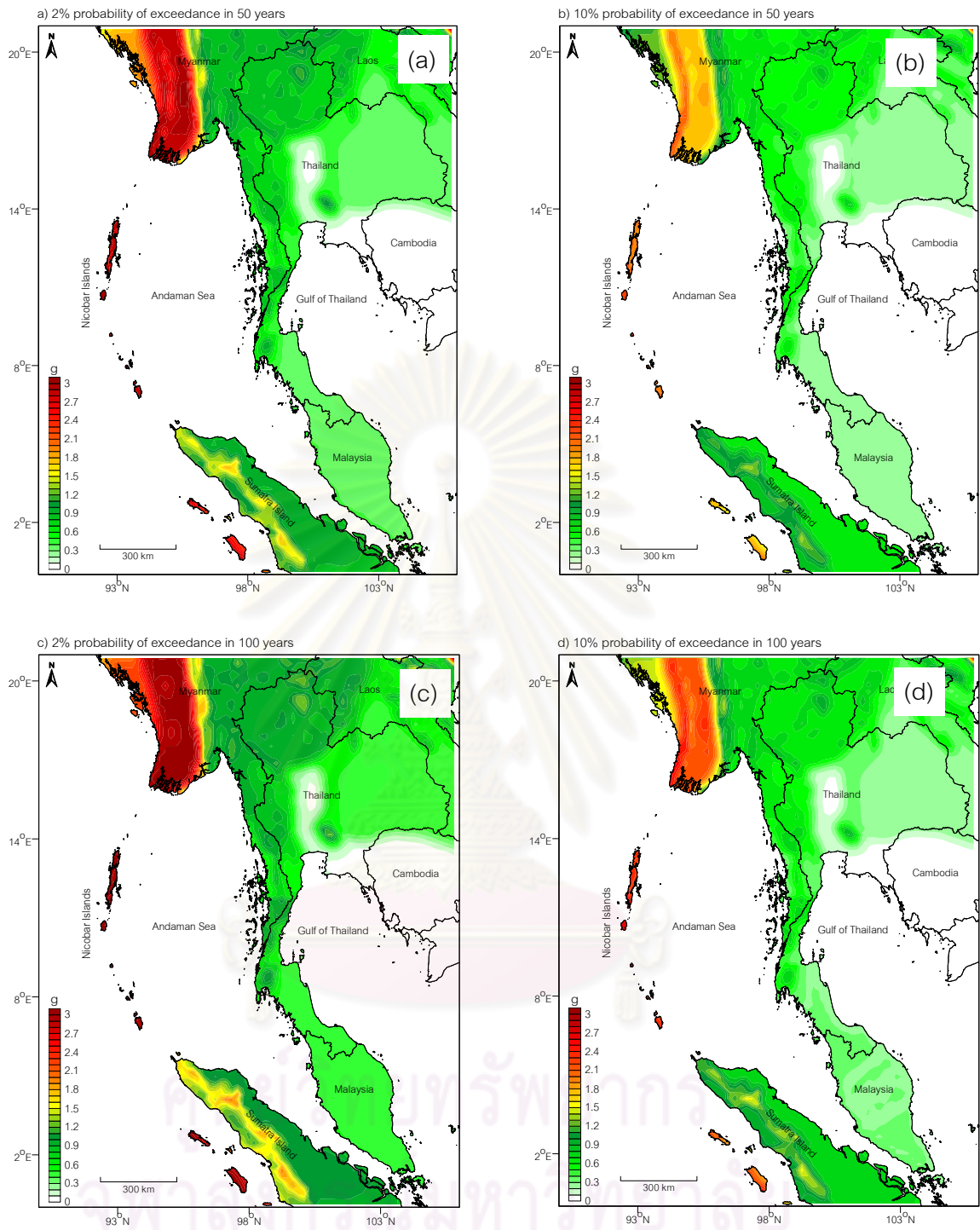


Figure 2.29 The peak ground acceleration maps with (a) 2% and (b) 10% probability of exceedance in 50 years as well as (c) 2% and (d) 10% probability of exceedance in 100 years (Pailoplee, 2009).

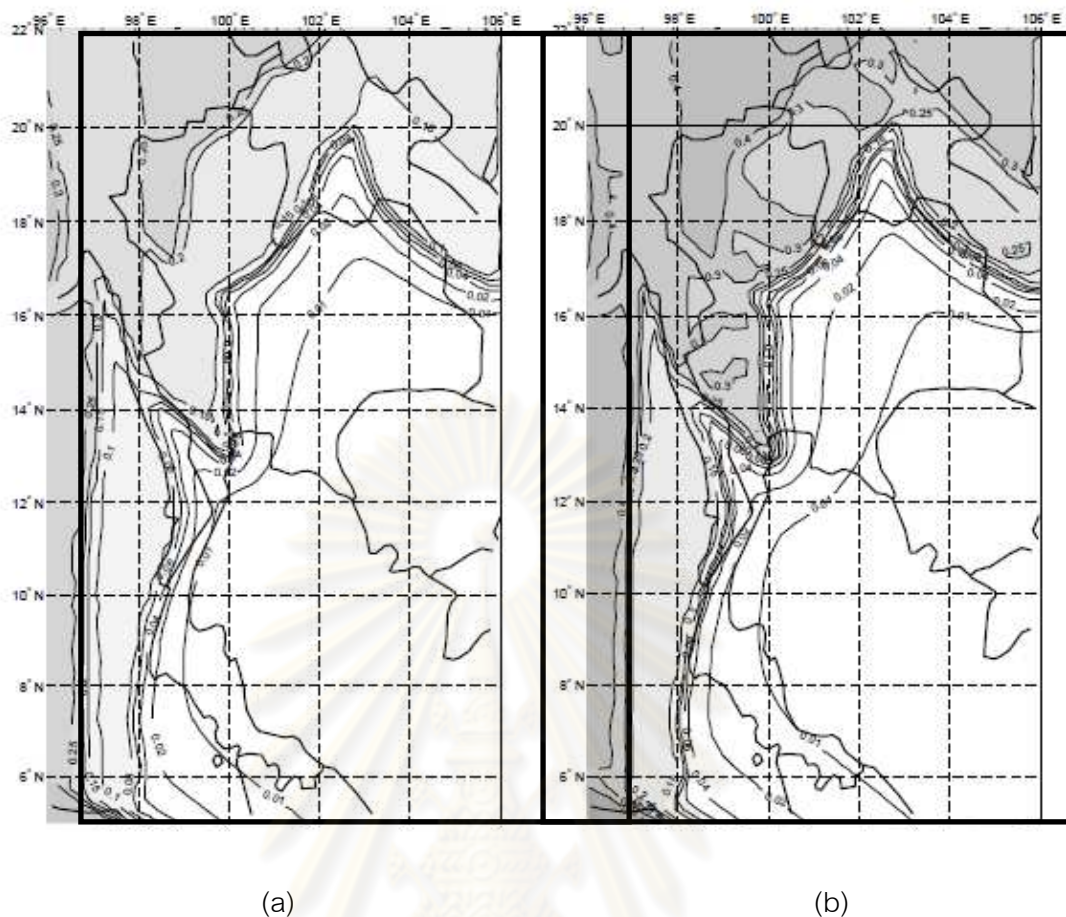


Figure 2.30 Probability seismic hazard map of Thailand and nearby region (a) 10% probability of exceedance in 50 years (b) 2% probability of exceedance in 50 years (Palasri and Ruangrassamee, 2010).

ศูนย์วิทยทรัพยากร
จุฬาลงกรณ์มหาวิทยาลัย

CHAPTER III

APPROACH AND METHODOLOGY

3.1 Approach

Seismic hazard is a term used to identify the potential damage phenomena that are associated with earthquakes such as ground shaking, landslides, liquefaction and tsunami. In this study seismic hazard analysis concerns the quantitative estimation of the ground motion hazard at the specified site in the period of interest. The methodology for assessing the seismic hazard can be carried out as the deterministic and probabilistic analyses (Kramer, 1996). The deterministic seismic hazard analysis (DSHA) involve the calculation of the ground shaking resulted from a particular earthquake at the specified site while the probabilistic seismic hazard analysis (PSHA) concerns the evaluation of the ground motion caused by earthquakes with uncertainties in the size, location and recurrence rate. Because the PSHA includes uncertainties in the size and location of the earthquake sources, produced magnitudes and ground motion characteristics that can give more complete picture of the seismic hazard (Kramer, 1996), the probabilistic approach is selected and applied in this study to establish the seismic hazard map of southern Thailand. The process of the construction of the probabilistic seismic hazard maps can be illustrated as a flow chart in Figure 3.1 and can be explained as below:

1. The first step of the process is to identify and characterize all earthquake sources that can affect the ground shaking at the site. In general practice, the earthquake occurrence is always specified to distribute uniformly within the sources. Combined with the source geometry, the earthquake distribution will provide probability

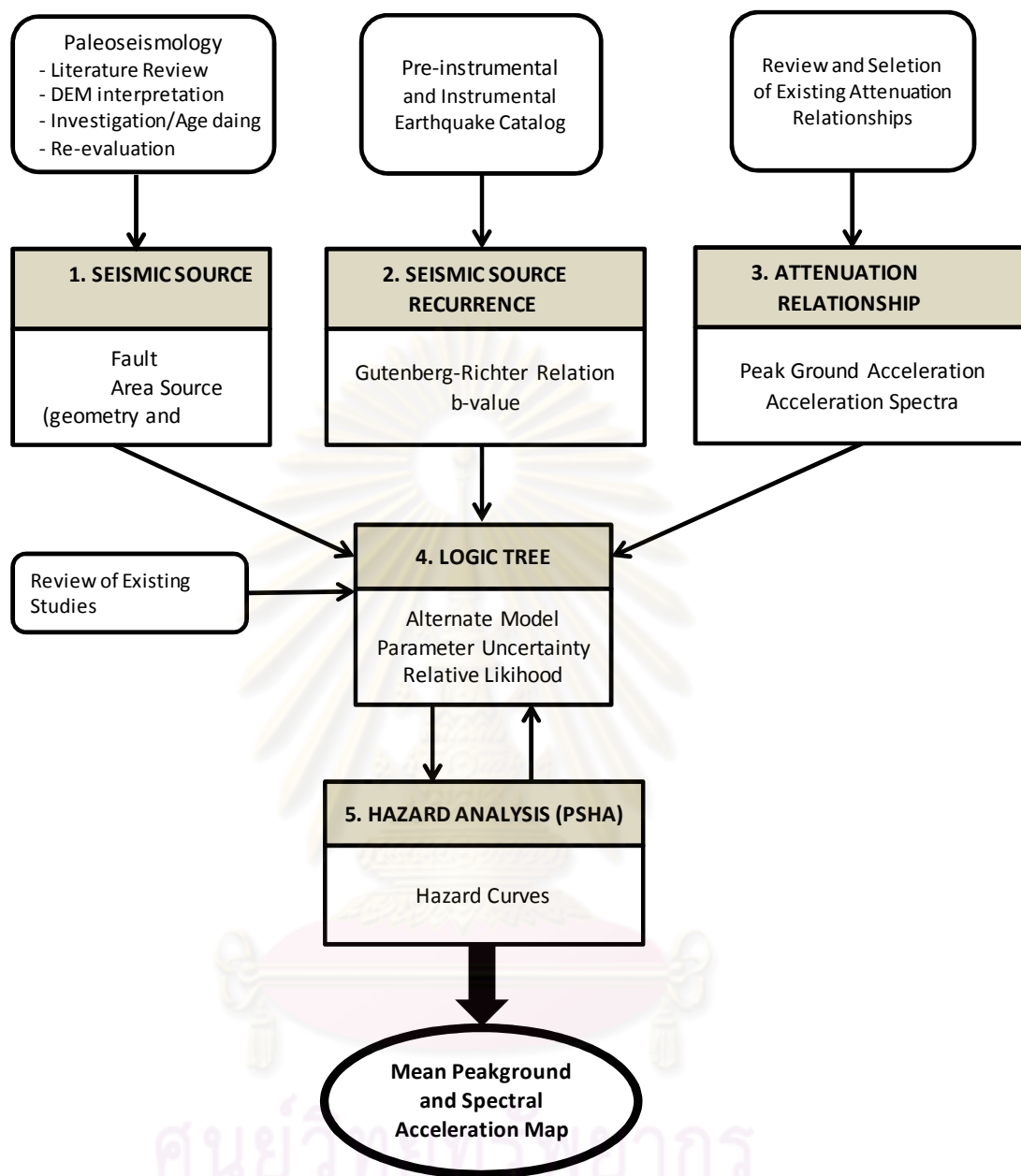


Figure 3.1 Flow chart showing steps of work in this study.

distribution of the source-to-site distance. The source characteristics can be identified by interpretation of Digital Elevation Model (DEM), field check, sample collection and age dating, and re-evaluation of the results of previous paleoseismic investigations of the KMF and RMF, and re-view of the previous works of other faults.

2. The second step is to establish the recurrence rate which is an average rate of some earthquake magnitude for each source by using the Gutenberg-Richter model, based on pre-instrumental and instrumental earthquake data catalogs,

3. The third step is to review and select existing attenuation models for the analysis of the ground motion at the site produced from any earthquake magnitude at any point within each source.

4. The fourth step is to identify the possible earthquake process, parameters of seismic source characteristics and attenuation models, and then prescribe the weight of each possibility by applying the logic tree methodology.

5. The final step is to compute ground acceleration with probability of exceedance for the specified year from uncertainties of earthquake sources and attenuation models for each source. The exceedance rate for each ground acceleration is multiplied with the weight given in the logic tree. After that the hazard curves for each source and integrated hazard curve at any site are depicted and then peak ground acceleration and spectral acceleration maps are prepared.

3.2 Methodology

3.2.1 Seismic Sources Characterization

Seismic source characterization is related to (1) the identification of prominent earthquake sources affecting the mapped area. (2) the maximum magnitudes produced from these sources. All earthquake sources with demonstrated and trusted Holocene movement that could produce the ground motion hazard in the southern Thailand due to their activities, length, or distance to the southern Thailand (approximately within 200 km based on ICOLD, 1989) are included in the analysis.

1. Source Type Identification

In general, there are three types of the seismic sources—fault, areal and point sources. Based on the active fault map of Thailand (DMR, 2006) and previous study as well as unavailable point source such as volcanoes, southern Thailand and nearby area (200 km away from the southern Thailand) have possible two source types, namely fault and areal sources. The active fault sources included in this study comprise the KMF, RNF, TNF, KYF, TVF, TPF and Sumatra-Andaman subduction zone.

In this study, the Digital Elevation Model (DEM) downloaded from the shuttle radar topography mission website is used to interpret the faults and lineaments in the KMF and RNF zones in order to check their orientations and lengths. Other fault sources data are obtained from the previous studies. For the areal sources, based on the occurrence of the earthquakes, there are two types to be classified, i.e. (1) reservoir-triggered seismicity and (2) background earthquakes of which the epicenters are not related to identified surface faults.

2. Source Geometry Determination

All faults in the analysis are modeled as independent planar sources. Variations of the geologic structures of the faults that are potentially significant parameters in the hazard analysis are considered by including a variety of models of fault rupture and fault geometries. The geometric of fault sources consists of fault location, segmentation, dip and thickness of seismogenic zone. The dip angle for all fault sources in this study is assumed to be 90 degrees similar to Petersen et al. (2007)'s application. Based on the estimated seismogenic depth of faults in the northern Thailand that is 15 km (Bott et al., 1997) and the seismogenic thickness of various continental areas that is equal to 15 ± 5 km. (Chen and Molnar, 1983), in this study the seismogenic thickness of the faults is assumed to be 10, 15, and 20 km. and the seismogenic depth of the background

earthquakes in any areal sources is specified as 15 km. For the reservoir triggered seismicity (RTS), the seismogenic depth is identified as 8, 10, and 15 km based on studies on the RTS recorded at the reservoirs of Srinagarind and Wachiralongkorn dams (WCFS, 1996, 1998, Wong et al., 2005).

3. Magnitude Computation

The most common practice to estimate the maximum magnitude applies the empirical relationships between fault rupture length or fault rupture area and magnitude. In this study, application of fault rupture length is the parameter to calculate the maximum magnitude. The author conservatively assume that the maximum fault rupture length is equal to the maximum length of the fault identified on the DEM images. The author do not adopt the fault rupture area for calculating the maximum magnitude because the dip angle and seismogenic depth of the faults that are used to estimate the down dip width of the fault rupture plains are not exactly known. Furthermore, all fault sources are the strike-slip faults. So, maximum magnitudes of the faults or fault segments can be calculated from the fault rupture length by applying Well and Coppersmith's empirical relationships (1994) for strike slip fault as given in equation (3.1).

$$M_w = 1.12 \cdot \log(\text{SRL}) + 5.16 \quad (3.1)$$

where M_w is the maximum magnitude and SRL is the surface rupture length.

The standard deviation of the above regression relationship is 0.28 or approximately 0.3. The maximum magnitudes of each fault derived from above equation are therefore added a ± 0.3 magnitude unit in this study.

For areal source zones, the earthquakes are assumed to occur randomly and modeled as point sources uniformly distributing in their volumes. The parameters that are used in the hazard analysis include the areas, seismogenic depth, maximum magnitude and recurrence parameters. The areal sources are applied to the areas where the occurrence of earthquakes are randomly distributed. The author adopt the maximum magnitude of $M_w 6.5 \pm 0.3$ similar the maximum magnitudes for the background earthquakes in northern Thailand estimated by WCFS (1996). In case of the reservoir triggered seismicity, the maximum magnitudes are assigned to be $M_w 5$ and $M_w 5.5$ based on the RTS recorded at the reservoirs of Srinagarind and Wachiralongkorn dams (WCFS, 1996, 1998, Wong et al., 2005).

4. Field Investigation and Fault Age Determination

Outcrops and RID's trenches located along the KMF and RNF zones are investigated. Additional soil samples are collected from some exposure and trench walls carried out by the Royal Irrigation Department (RID) and tested on the Thermoluminescence (TL) age dating. The detailed technique of TL-age dating is based on the methodology performed by Pailoplee (2009). Also, previous age dating results that were carried out by the RID (2006, 2009) and the DMR (2007) are re-evaluated to finalize the age of the faults found in each site.

5. Calculation of Recurrence Interval and Slip Rate

The methodology to identify and clarify the recurrence interval and slip rate includes review of previous studies (Pananon, 2009, Pailoplee, 2009, Sutiwanich et al., 2008, DMR, 2007, Petersen et al., 2007, 2006, Wong et al., 2005, Charusiri et al., 2000, Fenton et al., 1997 and 2003, WCFS, 1996 and 1998), and re-evaluation of the results of the paleoseismic investigations for the KMF and RNF carried out by the RID and the DMR, additional data from field checking and TL-age dating in this study.

All fault events are grouped by depicting a space-time diagram. Different time between a pair of consecutive fault events is the recurrence interval. The mean recurrence interval can be calculated from the average of all recurrence intervals (Martel, 2002).

According to Reid's elastic rebound concept (1910), a fault slip rate is the average slip rate of the fault for the whole time of fault movement. The slip rate of the fault can be determined by applying the assumption that the slip of the fault is constant rate without creep. The slip rate is calculated from the cumulative displacement of dated landforms or deposits (McCalpin, 1996). The total displacement of the fault in the exploratory trenches is measured from the offset of sediment layers or shortening of folded layers based on the assumption that the observed offset is true slip or the exposure and trench walls are parallel to the principle stress. So, the slip rate can be computed by the equation (3.2).

$$S = D/T \quad (3.2)$$

Where S is the fault slip rate (mm/yr), D is the total fault displacement (mm) or shortening distance (mm), and T is the total time of fault slip or shortening (yr).

3.2.2 Seismic Source Recurrence Establishment

The seismic source recurrence can be determined from the historical earthquakes and geologic evidences. The steps of works to construct the recurrence relationships from the historical earthquake data are as follows:

1. **Compilation of Historical Seismicity Catalogue** All seismicity catalogues are compiled for the study area and nearby regions. Primary data sources of the catalogue include:

- 1) a historical earthquake catalogue for Thailand and adjacent areas compiled by Nutalaya et al. (1985) for the period 624 B.C. to 1984,
- 2) the TMD seismicity catalogue,
- 3) the U.S. Geological Survey (USGS)
- 4) the International Seismological Center (ISC) catalogue and the International Seismological Summaries (ISS),
- 5) the National Earthquake Information Service (NEIC) Preliminary Determination of Epicenter (PDE)
- 6) seismicity located by the EGAT's earthquake stations at Ratchaphapha dam, and
- 7) seismicity measured by the Department of Geophysics, Prince of Songkhla University.

2. Manipulation of Historical Earthquake Data

1) Usually, most of earthquake events in the catalog for which the magnitudes are recorded as the body wave magnitude (m_b), the surface wave magnitude (M_s) or the local magnitude (M_L) and many events are listed without the magnitudes. The m_b , M_s and M_L are converted to be M_w by using the relationship between m_b , M_s , M_L and M_w established by Idriss (1985).

2) Due to the main shock representing the exact seismic stress released from the tectonic activities (Cornell, 1968), dependent events, i.e. induced seismicity, foreshocks, aftershocks and smaller earthquakes within an earthquake swarm, are

identified and cleaned out from the catalogue using the technique developed by Gardner and Knopoff (1974)

3) From completely filtered catalogue the set of earthquakes of which the magnitude is more than the chosen threshold magnitude or so-called lower bound magnitude (equal or more than $M_w 4$) are selected for further analyses.

3. Establishment of Recurrence Relationships

The derived historical seismicity data is used to construct a magnitude-recurrence relationships for each seismic source according to Gutenberg-Richter Recurrence Law. This relationship specifies the average rate at which an earthquake of some size will be exceeded. Due to limitation of earthquake data for the fault sources in the south and the west of Thailand and adjacent areas, the background earthquakes are collected to estimate the historical recurrence rate (b-value) based on the maximum likelihood procedure developed by Weichert (1980) similar to the estimation performed by WCFS (1998), Wong et al. (2005) and RID (2006). We assume that the background recurrence rate corresponds to the fault recurrence.

The calculation of the background earthquake recurrence for the south of Thailand by using the earthquake data (from the past to 2005) of the region located within 500 km surrounding the Tha Sae dam site in Chumporn province that was adopted by Wong et al. (2005) and RID (2006) is applied in this study. The independent earthquake events from 2005 to 2008 are compiled and classified in this study. Re-analysis of the recurrence is then performed. A similar method is undertaken for the computation of the recurrence of the background earthquake for the Three Pagoda fault in the western Thailand and for the Sumatra-Andaman subduction zone,

The recurrence relationships for the fault sources used in this study are the exponentially truncated Gutenberg-Richter and the characteristic models. Only the

truncated exponential recurrence model is assumed to be suitable for the areal sources. Concepts of these two models can be summarized as follows:

1. Truncated Exponential Model

Based on the standard Gutenberg-Richter recurrence law, it suggests that the earthquake is exponential distribution and covers an infinite range of magnitudes as shown in the equation (3.2).

$$\begin{aligned} \text{Log } \lambda_m &= a - bm \\ \text{or } \lambda_m &= 10^{a - bm} = \exp(\alpha - \beta m) \end{aligned} \quad (3.2)$$

where λ_m = annual rate of recurrence, $\alpha = 2.303a$ and $\beta = 2.303b$. Because in engineering view the lower earthquake magnitudes, usually less than M_w 4, cause insignificant damages and the larger earthquake magnitudes do not have exponentially lower mean rate of exceedance, the truncated exponential or bounded Gutenberg-Richter model was proposed (Cornell and Vanmarcke, 1969, McGuir and Arabasz, 1990). This recurrence model has the finite upper and lower bound magnitudes of m_{max} and m_0 as shown in Figure 3.2 The mean annual rate of exceedance can be estimated from the following equation (3.3).

$$\lambda_m = \frac{v \exp[-\beta(m - m_0)] - \exp[-\beta(m_{max} - m_0)]}{1 - \exp[-\beta(m_{max} - m_0)]} \quad (3.3)$$

Where λ_m is the annual frequency of occurrence of earthquakes greater than the minimum magnitude (m_0),

β is equal to $b \ln(10)$,

b is the Gutenberg-Richter parameter obtained from a slope of the

recurrence curve,

m_{max} is a maximum magnitude being able to occur on the source,

m_0 is a lower threshold magnitude.

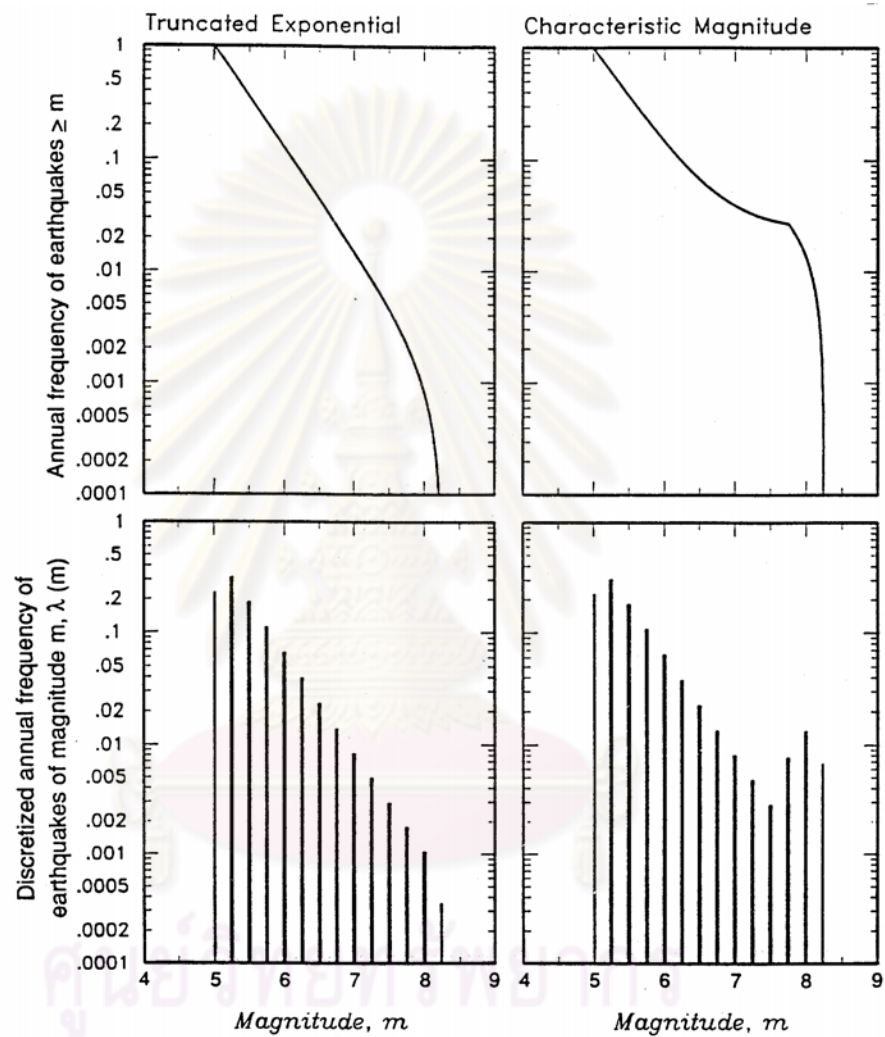


Figure 3.2 Typical earthquake recurrence curves and discretized occurrence rates (US Army Corps of Engineers, 1999).

The bounded Gutenberg-Richter recurrence model can be expressed as a probability density function $[f_M(m)]$ as given in the equation (3.4).

$$f_M(m) = \frac{\beta \exp[-\beta(m - m_0)]}{1 - \exp[-\beta(m_{max} - m_0)]} \quad (4 \quad (3.4))$$

2. Characteristic Model

The characteristic model means that the fault reproduces the earthquake of similar size at or near the maximum magnitude (Schwartz and Coppersmith, 1984, Youngs and Coppersmith, 1985). Resulting from geologic evidences, it shows that the characteristic earthquakes occur more often than the frequent rate obtained from the extrapolation of the Gutenberg-Richter model (Figure 3.2). Based on the same values of the maximum magnitude, b-value and slip rate, comparison between the characteristic model (Youngs and Coppersmith, 1985) and the bounded Gutenberg-Richter model (Figure 3.3) illustrates that the characteristic model gives the higher exceedance rates at the magnitude near the characteristic magnitude and lower rates at lower magnitude.

The characteristic model can be demonstrated by probability density function, $f_M(m)$, as given in the equation (3.5).

$$f_M(m) = \begin{cases} 0 & \text{for } m < m_0 \\ \frac{\beta \exp[-\beta(m - m_0)]}{1 - \exp[-\beta(m_{max} - m_0 - \Delta m_2)]} \frac{1}{1 + C} & \text{for } m_0 \leq m \leq m_c = m_{max} - \Delta m_2 \\ \frac{\beta \exp[-\beta(m_{max} - m_0 - m_1 - \Delta m_2)]}{1 - \exp[-\beta(m_{max} - m_0 - \Delta m_2)]} \frac{1}{1 + C} & \text{for } m_c = m_{max} - \Delta m_2 \leq m \leq m_{max} \\ 0 & \text{for } m > m_{max} \end{cases} \quad (3.5)$$

Where

$$c = \frac{\beta - \exp[-\beta(m_{\max} - m_0 - m_1 - \Delta m_2)]}{1 - \exp[-\beta(m_{\max} - m_0 - \Delta m_2)]} \Delta m_2$$

$\beta = b \ln 10$ (b is the b -value of the Gutenberg-Richter relationship),

m_{\max} and m_0 are the maximum and minimum magnitudes of interest,

m_c is the characteristic magnitude,

Δm_1 and Δm_2 are the magnitude intervals below and above the m_c , respectively

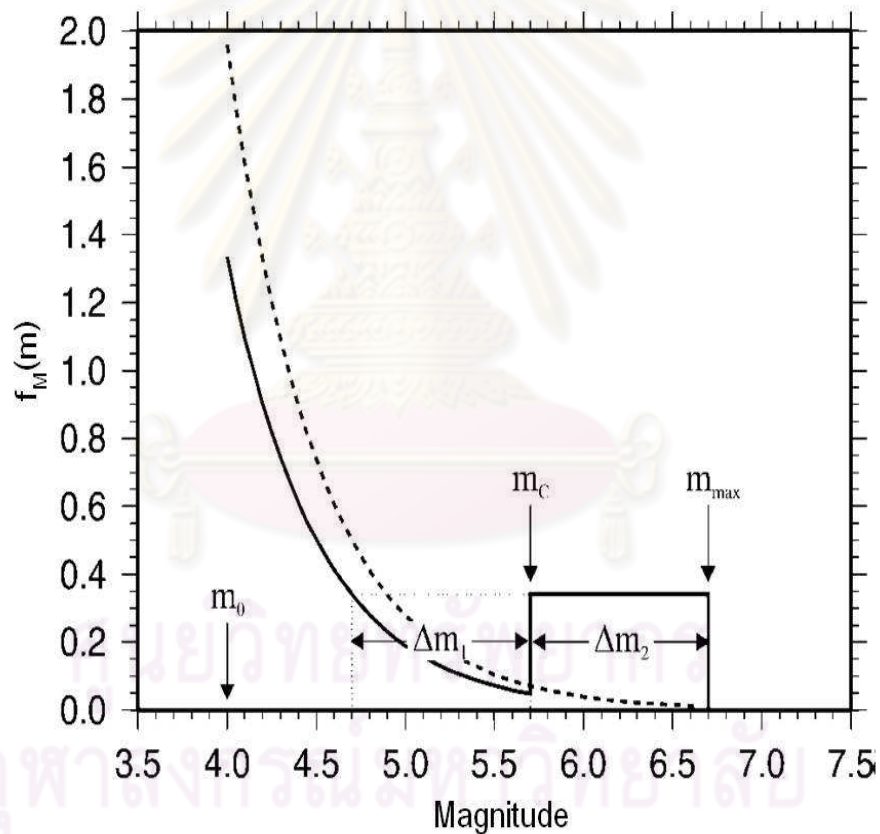


Figure 3.3 Graphs plotted between the annual rate of exceedance and magnitude for the characteristic earthquake-recurrence model (black line) and for the truncated exponential earthquake-recurrence model (dashed line) (Convertito et al., 2006)

The values of Δm_1 and Δm_2 are defined as 1.0 and 0.5, respectively, by Youngs and Coppersmith (1985) but in this study they are applied as both values of 1.0 (Convertito et al., 2006).

In general, the magnitudes of the characteristic earthquakes are in the range of m_{max} and m_c as a horizontal part of the solid line in Figure 3.3. The activity rate (λ_m) between m_c and m_{max} can be given in the equation (3.6).

$$\lambda_m = \lambda_{NC} \frac{\beta \Delta m_2 - \exp[-\beta(m_{max} - m_0 - m_1 - \Delta m_2)]}{1 - \exp[-\beta(m_{max} - m_0 - \Delta m_2)]} \quad (3.6)$$

The activity rate for the non-characteristic part (λ_{NC}) is $m_0 \leq m \leq m_c$ and can be illustrated as the following equation (3.7) and (3.8).

$$\lambda_{NC} = \frac{\mu A S [1 - \exp[-\beta(m_{max} - m_0 - \Delta m_2)]]}{K M_0^{max} - \exp[-\beta(m_{max} - m_0 - \Delta m_2)]} \quad (3.7)$$

and

$$K = \frac{b 10^{-c \Delta m_2}}{c - b} + \frac{b \exp(\beta \Delta m_1) (1 - 10^{-c \Delta m_2})}{c} \quad (3.8)$$

where

μ = the shear modulus

A = the total area of the fault plane

S = the average slip rate along the fault

M_0^{max} = the seismic moment related to the moment magnitude M_w by

the Hanks and Kanamori's relationship (1979) as given in the equation (3.9).

$$M_w = 2/3 \text{Log} M_0 - 10.7 \quad (3.9)$$

3.2.3 Attenuation Relationship Application

The most important factor concerning the calculation of the ground motion at the site is how the seismic wave attenuates with distance from the source. The decrease of the ground motion with the distance from the earthquake sources is dependent upon many factors, namely geometrical spreading, damping or absorption by the earth, scattering, reflection, refraction, diffraction and wave convection. This phenomenon can be predicted by using empirical attenuation models that were developed from numerous strong ground motion records by applying the statistical regression method. Usually, the attenuation relationships can be used only in the region where they were developed. However, they may be adopted in the other regions where the seismotectonic settings are similar. In Thailand, there are a few strong ground motion records that are not enough for developing the attenuation models. The applied attenuation models have to be selected from other places. However, all over the world there are so many attenuation models developed as summarized by Douglas (2001). These models were empirically established from the strong ground motion triggered by many crustal faults and subduction zones. In this study, both crustal earthquake and subduction zone sources are included. Therefore, the most suitable attenuation models developed from the crustal earthquake and subduction zone have to be chosen for the hazard analysis.

1. Crustal Fault Attenuation Models

In the southern Thailand, the RID (2006, 2008, 2009) proved and reported that four strong ground motion models developed in the western North America for crustal earthquakes, i.e. Boore et al.(1997), Abrahamson and Silva (1997), Campbell and Bozorgnia(2003), and Sadigh et al. (1997), are suitable for seismic hazard application in the southern part of Thailand. Moreover, Pailoplee (2009) correlated Sadigh et al (1997)'s model with the available strong ground motion recorded in Thailand and then

he concluded that it is proper application for Thailand's hazard analysis. Based on similar geology between Thailand and the western North America (Harnpattanapanich, 2010) and above reasons, these four attenuation relationships are selected for the seismic hazard analysis in this study.

The followings are details of each relationship showing the attenuation of the acceleration depending on the source-to-site distance for the rock condition with a damping value of 5%.

(1) **Boore et al. (1997)** The attenuation relationship for a strike-slip fault is given in the equation (3.10)

$$\ln(PGA) = b_1 + b_2 (M_W - 6) + b_3 (M_W - 6)^2 + b_5 \ln(r) + b_V \ln(V_S/V_A) \quad (3.10)$$

$$r = (r_{jb}^2 + h^2)^{1/2}$$

where PGA is a peak ground acceleration, g , r_{jb} is shortest horizontal distance between the epicenter and the site, V_S is average shear wave velocity of soils and rocks with a thickness of 30 m, m/sec^2 , V_A is reference shear wave velocity, m/sec^2 , b_1 , b_2 , b_3 , b_5 , b_V , and V_A are the constants that are given in Appendix A.

(2) **Abrahamson and Silva (1997)** For the strike-slip fault, the attenuation relationship can be given in the equations (3.11) and (3.12).

- If M_W less than or equal to C_1 :

$$\ln(PGA) = a_1 + a_2 (M_W - c_1) + a_{12} (8.5 - M_W)^n + (a_3 + a_{13} (M_W - c_1)) \ln(R) \quad (3.11)$$

- If M_w more than C_1 :

$$\ln(PGA) = a_1 + a_4(M_w - c_1) + a_{12}(8.5 - M_w)^n + (a_3 + a_{13}(M_w - c_1)) \ln(R) \quad (3.12)$$

where R is equal to $(r_{rup}^2 + c_4^2)^{1/2}$, PGA is a peak ground acceleration, g , r_{rup} is the shortest distance from a site to the fault plane, km, a_1 , a_2 , a_3 , a_4 , a_{12} , a_{13} , c_1 , c_4 , and n are the constants that are summarized in Appendix A.

(3) Campbell and Bozorgnia (2003) The attenuation relationship can be written as in the equation (3.13).

$$\begin{aligned} \ln(PGA) = & c_1 + c_2 M_w + c_3(8.5 - M_w)^2 + c_4 \ln(r_{seis}^2 + (c_5 + 0.5c_6 + 0.5c_7)^2 (\exp(c_8 M_w \\ & + c_9(8.5 - M_w)^2))^{1/2} + 0.5c_{13} + 0.5c_{14} \end{aligned} \quad (3.13)$$

where PGA is the peak ground acceleration, g , r_{seis} is the shortest distance from a site to the seismogenic rupture, km, c_1 , c_2 , c_3 , c_4 , c_5 , c_6 , c_7 , c_8 , c_9 , c_{13} , and c_{14} are the constants that are given in Appendix A.

(4) Sadigh et al. (1997) The proposed attenuation relationship is shown in the following equation (3.14):

$$\begin{aligned} \log(PGA) = & b_1 + b_2(M_w - 6) + b_3(M_w - 6)^2 + b_5 \log(r_{jb}^2 + h^2)^{1/2} \\ & + B_V (\log 310 - \log 910) \end{aligned} \quad (3.14)$$

where PGA is the peak ground acceleration, g , r_{jb} is the shortest horizontal distance from the site to the epicenter, km, b_1 , b_2 , b_3 , b_5 , h , B_W and the standard deviation are stated in Appendix A.

2. Subduction Zone Attenuation Models

The calculation of the ground motion in southern Thailand generated by the Sumatra-Andaman subduction zone is applied by using the attenuation relationships developed by Youngs et al. (1997) and Atkinson and Boore (2003). These two relationships were established from the strong motion data from Japan, Mexico, Chile, and the 2001 Nisqually earthquake in the Puget Sound of Washington (U.S.). They were developed for the distance less than 500 km so the relation extrapolation is applied in the study. Both relationships can be given as below.

(1) Youngs et al. (1997)

The attenuation relationship was developed from 171 earthquake events with the magnitudes of larger than 5 and the distances to the source of 10-500 km. The attenuation equation is given in the equation (3.15).

$$\begin{aligned} \ln(PGA) = & 0.2418 + 1.414M_W + c_1 + c_2(10 - M_W)^3 \\ & + c_3 \ln(r_{rup} + 1.7818 e^{0.554M_W}) + 0.00607H + 0.3846Z_T \end{aligned} \quad (3.15)$$

$$\sigma = c_4 - c_5 M_W$$

where σ is the standard deviation (if the magnitude is larger than M_W 8, it is equal to σ of M_W 8), PGA is the peak ground acceleration, g , r_{rup} is the shortest distance from the site to

the fault plane, km, c_1 , c_2 , c_3 , c_4 , and c_5 are given in Appendix A, H is the depth, km, Z_T is 0 for the earthquakes occurring along the interplate or 1 for the earthquakes occurring in the intra-slab.

(2) Atkinson and Boore (2003)

The attenuation relationship was developed from worldwide earthquakes with the magnitude of M_W 5 to M_W 8.3 occurring along the interplate and in the intra-slab. The relationship can be written as the equation (3.16).

$$\text{Log} (PGA) = c_1 + c_2 M_W + c_3 h + c_4 R - g \text{Log} R \quad (3.16)$$

where PGA is the peak ground acceleration, g , R is $(D_{fault}^2 + (0.00724 \times 10^{0.507M})^{1/2})$, D_{fault} is the shortest distance from the site to the fault plane, km, c_1 , c_2 , c_3 , and c_4 are given in Appendix A.

3.2.4 Logic Tree Approach

The logic tree approach was first introduced into the probabilistic seismic hazard analysis by Power et al. (1981) and then become a standard method used in the analysis (Coppersmith and Youngs, 1986; Reiter, 1990). The seismic hazard analysis has various uncertainties due to not completely understanding of the earthquake phenomena. Assumptions on the constrained parameters for the seismic hazard analysis are composed of earthquake locations and sizes, potential occurrence of future earthquakes, and what earthquake affects. A best approach to deal with these uncertainties for the probabilistic seismic hazard analysis is a logic tree concept. The logic trees can be applied and implemented easily with a common form. The methods of the logic tree analysis comprise

two steps: (1) to specify the sequence of the hazard analyses, and (2) to define the uncertainties in each of these analyses in a sequence manner.

The logic tree is a decision flow path consisting of nodes and branches as shown in Figure 3.4. Each branch represents a discrete choice of a parameter and is assigned a likelihood of being correct. The nodes are connecting points between input elements. Practically, various branches are specified in a given node to sufficiently represent the uncertainties in the estimated parameters. Probabilities or weights are assigned in each parameter usually based on the subjective judgments. The summation of the probability at each node is unity.

In this study, discrete values representing the likelihood of actual one of the earthquake source parameters have been included in the logic tree approach. These

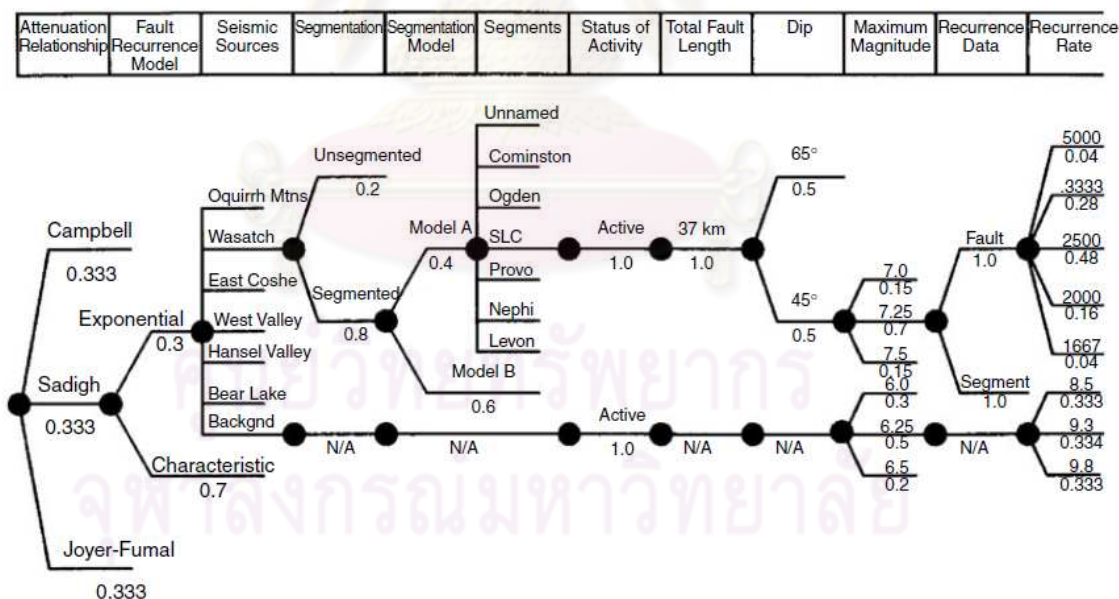


Figure 3.4 Example of the logic tree applied for the probabilistic analysis of earthquake ground shaking along the Wasatch Front, Utah (Youngs et al., 1987).

input parameters consist of seismogenic crustal thickness, fault segmentation, maximum magnitude, probability of activity, and slip rate. Other than the source characteristic, the

attenuation relationships and recurrence model are also considered in the logic tree approach. The input parameters such as seismogenic crustal earthquake, maximum magnitude and slip rate are normally defined by three values consisting of a preferred value and a range of higher and lower values that is similar to the normal or lognormal statistical distribution (US Army Corp of Engineer, 1999). Weights are assigned to each parameter in order to specify the distribution based on the results of statistical analyses studied by Keefer and Bodily (1983) and subjective judgments. The results of Keefer and Bodily's study (1983) show that the best discrete approximation of the continuous distribution is the three point distribution with 5th, 50th and 95th percentiles weighted about 0.2, 0.6 and 0.2, respectively. These weighted values are applied to the weight of the seismogenic depth and magnitude in this study. Furthermore, Keefer and Bodily (1983) found that if the data is limited to determine the 5th and 95th percentiles of the distribution, the 10th, 50th and 90th percentiles weighted about 0.3, 0.4 and 0.3, respectively, can be applied. So, these weights were adopted for the weight of the slip rate in this study. In case of two branches, the strongly preferred branch is weighted as 0.9 and the remained branch as 0.1 (US Army Corp of Engineer, 1999). These weights were applied to the earthquake source types of the KMF. The weights of the KMF's line and areal sources are 0.1 and 0.9, respectively.

In case of earthquake source activity, the probability of activity and slip rate are characterized. The weights assigned to the activity of the sources are derived from the ability of the sources to produce independently the earthquake and the possibility that it is still active within the present stress field. Any fault that has evidences of active fault (Based on USGS's definition, active faults means the fault has moved one or more times in the last 10,000 years) is defined as the weight of activity of 1.0.

The attenuation models used for the crustal seismic sources and the Sumatra-Andaman subduction zone are not developed in Thailand. Furthermore, strong ground motion data in Thailand is insufficient to prove which model is most suitable application. So, the four attenuation relationships for the crustal earthquakes were equally weighted and two attenuation relationships for Sumatra-Andaman subduction zone earthquakes were also weighted even.

3.2.5 Probabilistic Seismic Hazard Analysis (PSHA)

The outputs of the seismic hazard analysis are the hazard curve of the specified site and then the acceleration maps are finally prepared.

The PSHA approach applied in this study is based on the methodology initially developed by Cornell (1968). The occurrence of earthquakes generated by fault movements is usually assumed to be a Poisson probability process. It can be stated that the Poisson model is widely accepted and used. The ground motion exceeding a specific level at the site will be accounted to be in the Poisson process if there are:

1. the earthquake occurrence is a Poisson process and
2. the probability of the earthquake event that produces the ground motion at the site exceeding the specific level is not dependent upon the other earthquake events.

From above properties, the earthquake events of Poisson process occur randomly without memory of the time, size or location of any preceding earthquake events (Kramer, 1996, 2009). The probability of exceedance, $p_z (Z>z)$, of a ground motion level "Z" exceeding a specific level "z", in an exposure time or design time period, t , at a site is related to the annual frequency (or rate) of ground motion exceedance at the site, $v(z)$, is given in the equation (3.17).

$$P(Z>z) = 1 - \exp[-(v(z) t)] \quad (3.17)$$

The return period for the ground motion exceedance can be calculated from the reciprocal of $v(z)$. The annual mean number of events can be computed by summing the contribution from all seismic sources as given in the equation (3.18).

$$v(z) = \sum_n v_n(z) \quad (3.18)$$

where $v_n(z)$ is the annual mean number (or rate) of events on source n for which Z exceeds z at the site. This annual frequency of ground motion exceedance can be determined from the below equation (3.19).

$$v(z) = \sum_{n=1}^N \sum_{m_i=m_{min}}^{m_i=m_{max}} \lambda_n(m_i) \sum_{r_j=0}^{r_j=r_{max}} P_n(R=r_j/m_i) * P(Z>z/m_i, r_j) \quad (3.19)$$

where $\lambda_n(m_i)$ is the annual mean rate of recurrence of earthquakes with the magnitude increment m_i on the source n ,

$P(R = r_j / m_i)$ is the probability of an earthquake of magnitude m_i on source n occurring at a certain distance r_j from the site, r_j is the closet distance increment from the rupture surface to the site,

$P(Z > z / m_i, r_j)$ is the probability that ground motion level z will be exceeded, given an earthquake of magnitude m_i at distance r_j from the site.

The recurrence function ($\lambda_n(m_i)$) is the average number of the earthquake of each magnitude that is expected to happen on the seismic source. This incremental recurrence rate ($\lambda_n(m_i)$) is derived from the recurrence relationships. Two recurrence models are usually applied in the probabilistic seismic hazard analysis (PSHA). They are the exponential truncated (modified Gutenberg-Richter) and characteristic recurrence models. In this study, both the truncated exponential and characteristic

recurrence models are adopted for the fault sources whereas only the truncated (exponential recurrence model is applied for the background earthquakes or the areal sources.

The distance function ($P(R = r_j / m_i)$) is the probability of site-to-source distances for which the earthquakes will occur at the source in the future. It can be estimated from the geometry of the seismic source—distance, dip, length, depth and fault segmentation—and from the earthquake rupture—rupture length, rupture width, and depth of rupture.

The attenuation function ($P(Z > z / m_i, r_j)$) is the probability of exceedance of the ground motion to the specified value with the given magnitude and distance. It can be computed by using the attenuation relationships.

Steps of development of the probabilistic seismic hazard maps for southern Thailand can be described as the following

1. Computation of Annual Rate of Exceedance

The annual rates of exceedance of the assigned sites were calculated with the relationships 3.19 by using the CRISIS 2007 computer program developed by Ordaz, Aquila and Arboleda (2007). The inputs and outputs of the program can be given in Appendix B. The analyses are performed at two hundred twenty four sites, in southern Thailand covering the southernmost Yala province northward to Phetchaburi province. The sites are determined by a grid system basis starting from latitude of 5.58°N to 13.5°N , and longitude of 97.5°E to 102.12°E as shown in Figure 3.5. Each point of grid crossing has a spacing about 0.33° or approximately 36 km.

The computation of the mean annual rate of exceedance of the site with specified rock ground motions (acceleration) and time periods is carried out for all branches of the proposed logic trees. After that in each branch of the logic tree, the derived annual rates of exceedance are multiplied by the total weight of the branch with using the Microsoft Excel program. Then, summation of annual rates of exceedance for each assigned time period and rock ground acceleration from all logic tree branches of each earthquake source is undertaken.

2. Establishment of Hazard Curves

As above-mentioned, for each earthquake source, the received values of mean annual rate of exceedance for each ground acceleration were taken to plot mean hazard

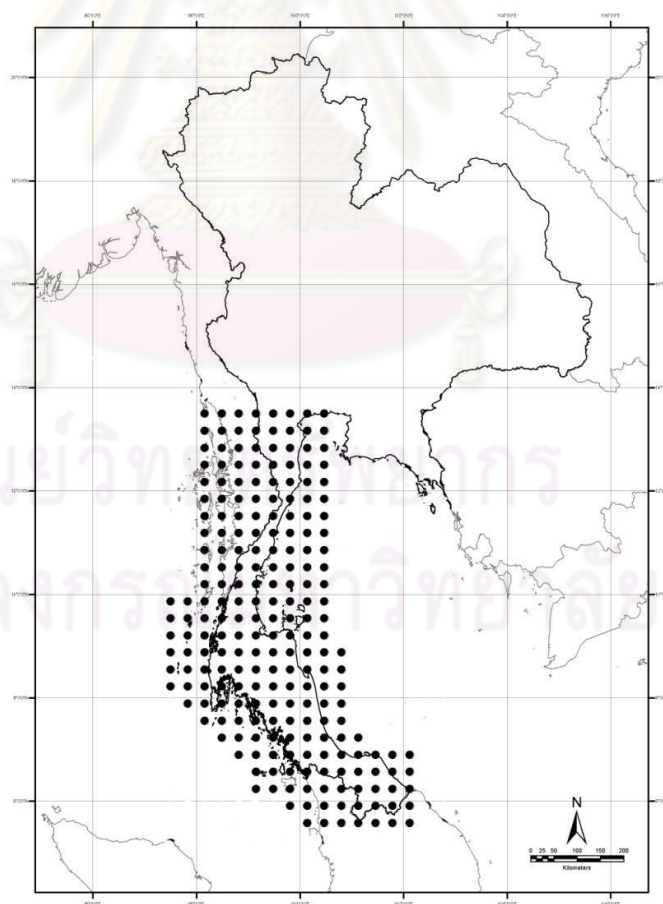


Figure 3.5 Location map showing calculated 224 sites (black circles) for PSHA in this study.

curves at the selected site. The mean hazard curve of the site is the combination of all sources-produced hazard curves. As a result, there are four mean hazard curves for each site. They are composed of a mean peak horizontal acceleration and mean 0.2-, 0.3-, and 1.0-second horizontal spectral acceleration hazard curves.

3.2.6 Development of Hazard Maps

From the hazard curves, the peak ground and spectral accelerations for given time period can be read from the curve when the annual rate of exceedance is known. Based on the equation 3.17, the annual rate of exceedance can be calculated from the probability of exceedance in specified time period. So, 10%, 5%, 2% and 0.5% probabilities of exceedance in 50 years equal to the annual rate of exceedances of approximately 0.002, 0.001, 0.0004, and 0.0001, respectively. An example of determination of mean peak ground acceleration for 500, 1,000, 2,500 and 10,000 years or 10%, 5%, 2% and 0.5% probabilities of exceedance in 50 years can be shown in Figure 3.6. It can be seen that the mean peak ground accelerations for 10%, 5%, 2% and 0.5% probabilities of exceedance in 50 years are equivalent to 0.158g, 0.192g, 0.255g, and 0.346g, respectively. Similarly, these peak ground computations have to be carried out for all another 223 sites. Then hazard maps are prepared by drawing the contour lines of equal acceleration. Finally, 16 hazard maps are prepared.

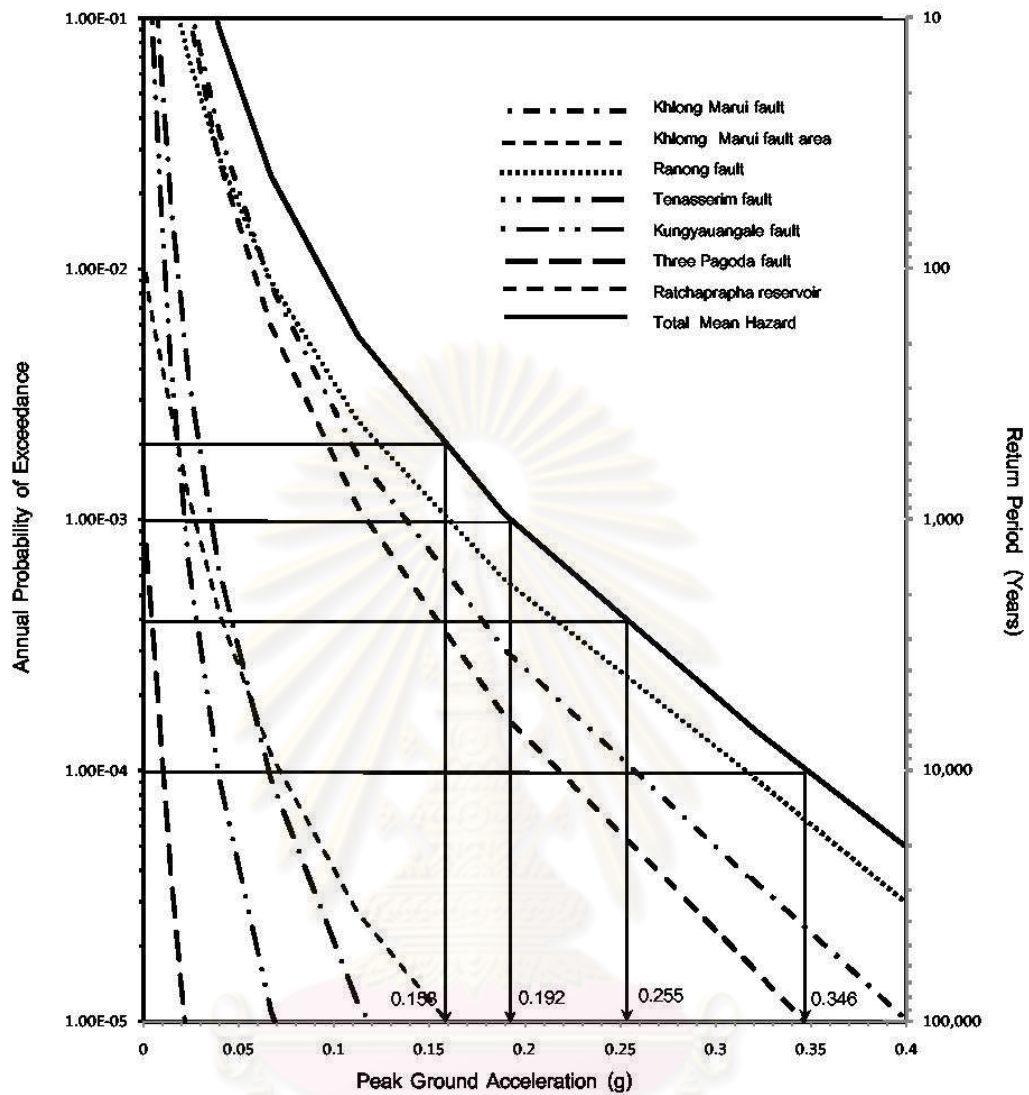


Figure 3.6 An example hazard curve showing the mean peak ground accelerations for 10%, 5%, 2% and 0.5% probabilities of exceedance in 50 years at the specified site.

CHAPTER IV

RE-EVALUATION OF ACTIVE FAULTS IN SOUTHERN THAILAND

The objective of this chapter will present the results of re-evaluation of the paleoseismic investigation data of the KMF and RNF carried out by the RID (2006, 2008, 2009), the DMR (2007), and Pananont (2009) as well as additional data obtained from this study. The followings describe how to re-evaluate and what values of derived characteristics of the KMF and RNF that will be included in the seismic hazard analysis in Chapter V.

4.1 Fault Orientation and Length

The satellite image interpretation was re-interpreted to confirm the orientation and the length of both the KMF and RNF as well as the geomorphologic features representing the active fault on the earth surface, for example lineaments, triangular facets, scarps etc. The Shuttle Radar Topography Mission (STRM)'s Digital Elevation Model (DEM) images with the resolution of 90 m x 90 m were applied. The alignment and length of the KMF and RNF can be shown in Figure 4.1, and Figures 4.2 and 4.3, respectively.

Analysis of DEM images show that the Khlong Marui fault zone extends from Muang and Thap Put districts of Phang Nga province, and Ao Luk and Khao Phanom districts of Krabi province on the Andaman coast to Viphavadi and Muang districts of Surat Thani province on the Gulf of Thailand. The major faults in the Khlong Marui fault zone orientate in the direction of $N30^{\circ}E$ while the minor faults or conjugate faults lie in the direction of $N5^{\circ}W$ to $N5^{\circ}E$ and $N60^{\circ}E$ to $N80^{\circ}E$.

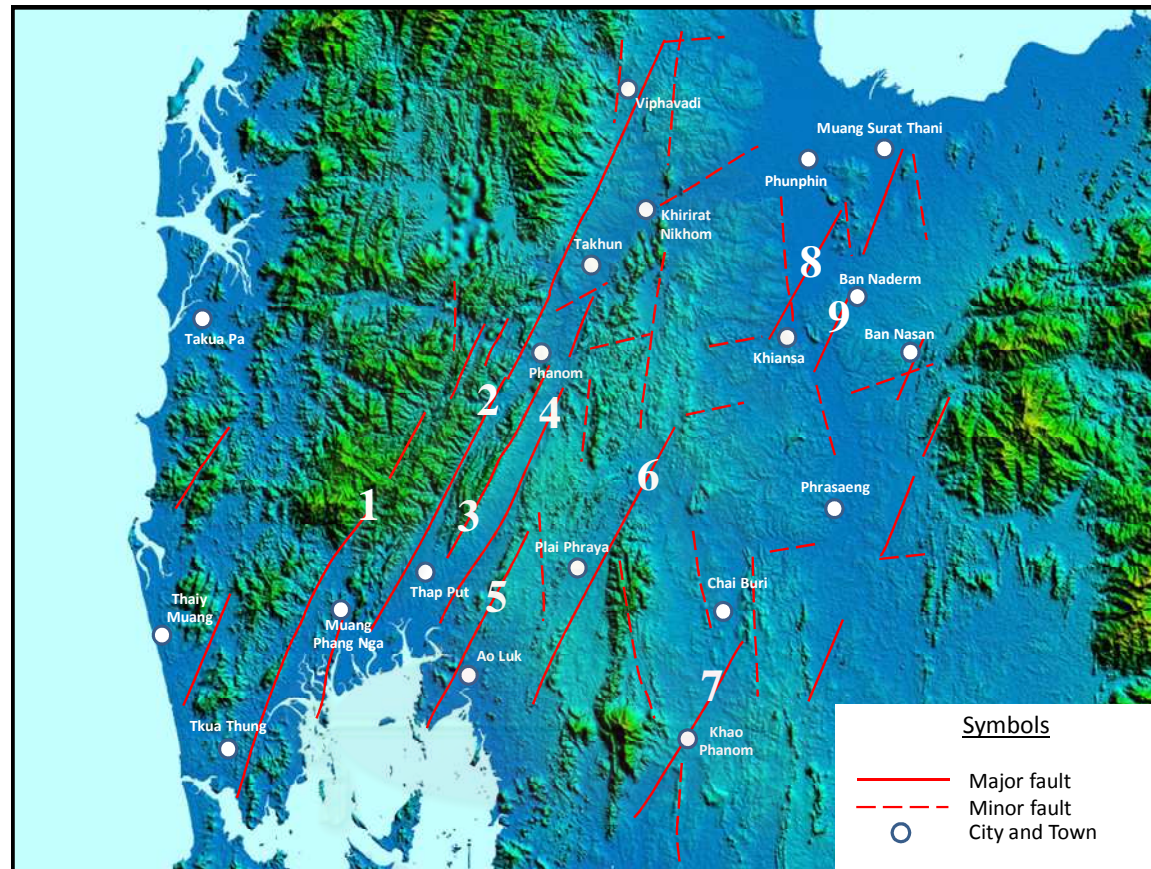


Figure 4.1 Major and minor faults in the KMF zone newly interpreted from the DEM image in this study. Major fault segments are :
 1 = Takua Thung fault, 2 = Khlong Marui fault, 3 = Thap Put fault, 4 = Phanom fault, 5 = Ao Luk fault, 6 = Plai Phraya
 fault, 7 = Khao Phanom fault, 8 = Khian Sa fault, 9 = Ban Naderm fault

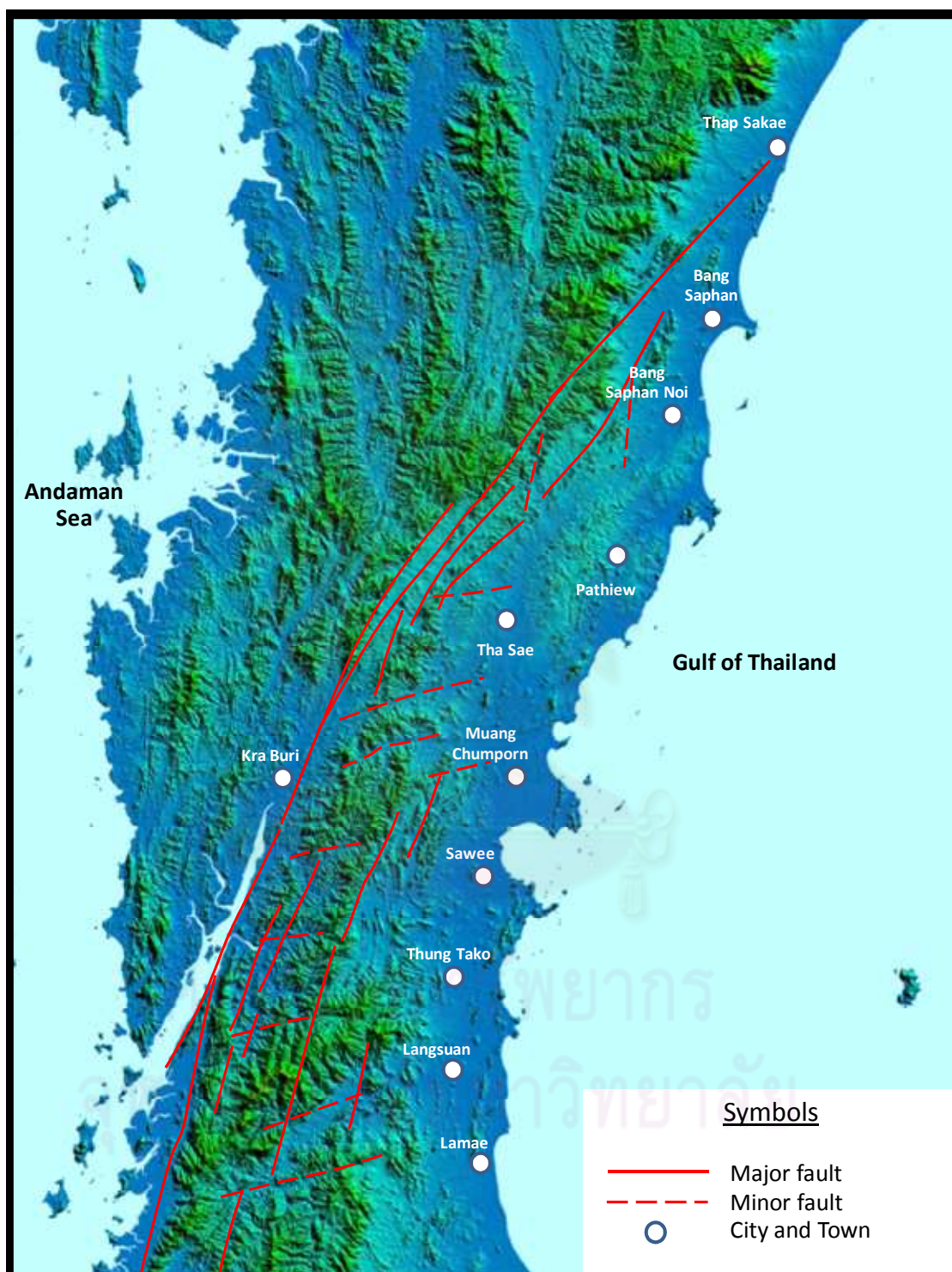


Figure 4.2 Major and minor faults in the northern RNF zone newly interpreted from the DEM image in this study.

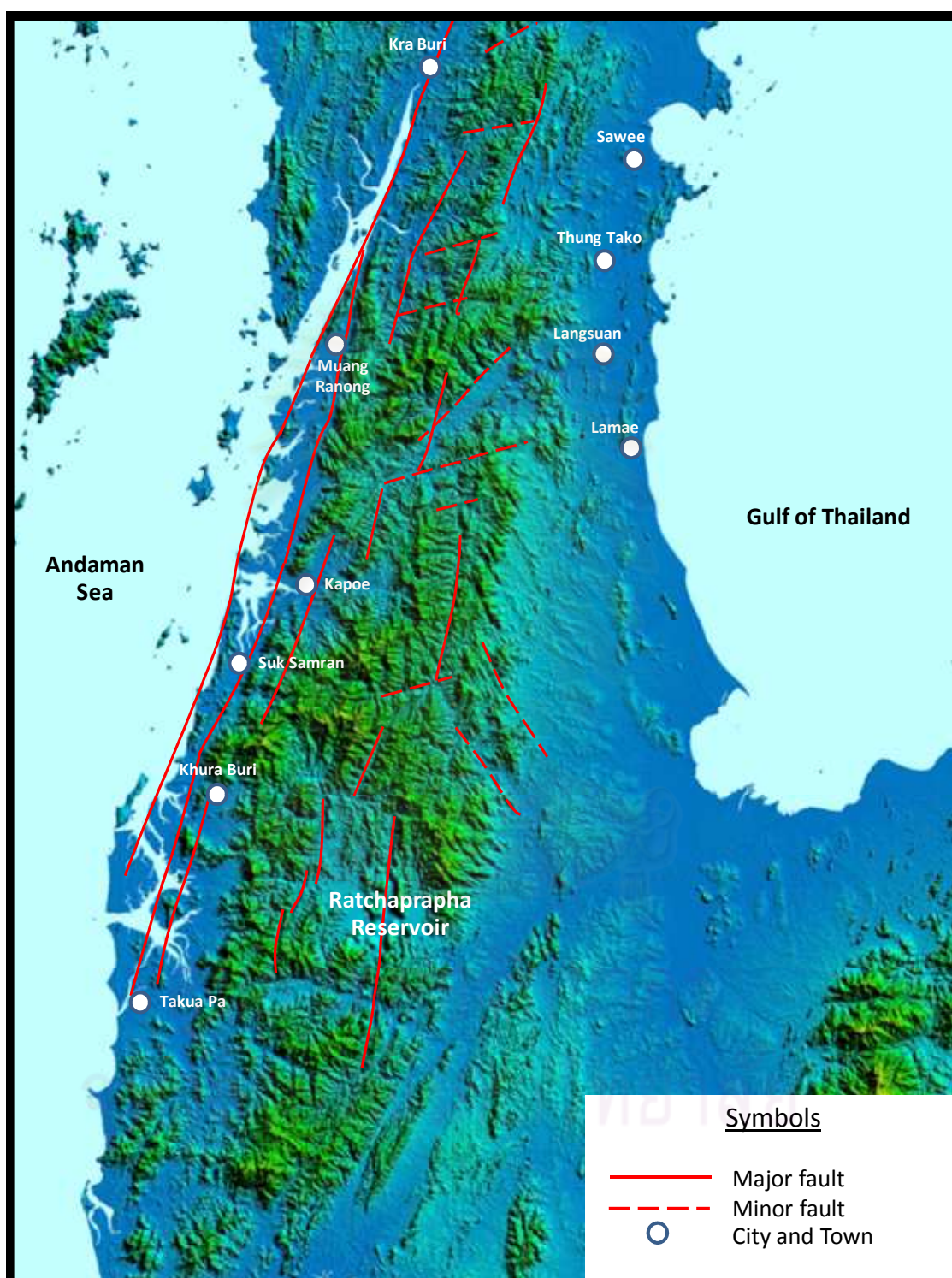


Figure 4.3 Major and minor faults in the southern RNF zone newly interpreted from the DEM image in this study.

The longest fault is located along the toe of the mountain on the west extending from Thap Put district of Phang Nga province northeast toward Viphavadi district of Surat Thani province. Its total length is approximately 115 kilometer. It was specified as the active fault in the active fault map of Thailand (DMR, 2008).

The RNF zone lies from Thap Sakae district of Prachuab Khirikun at the Gulf of Thailand passing to Chumporn province and ends at Takua Pa district of Phang Nga province. Based on the fault orientation, the RNF zone can be divided into two parts, namely the northern and southern parts. The trend of the major fault varies from $N20^{\circ}E$ in the northern part to $N40^{\circ}E$ in the southern part. The conjugate faults express the strike of approximately $N75^{\circ}-85^{\circ}E$. The longest fault that was mapped as the active fault in Thailand by DMR (2008) can be divided into two segments. The first segment starts from Thap Sakae district of Prachuab Khirikun province at the coast of the Gulf of Thailand to Kra Buri district of Ranong province. Its escarpment is low angle and dips to the east. The second segment extends from the first segment at Kra Buri district, then goes along the Andaman coast, and ends at Takua Pa district of Phang Nga province. It express as west-facing scarps. The northern segment is 180 km long whereas the southern segment is 160 km long.

4.2 Recurrence Intervals and Slip Rates

1. KMF Zone

The data on fault trenching and dating from the Lam Rooyai dam project owned by the RID, and additional data on the field investigation and sediment age dating from this study were used to re-estimate the recurrence interval and slip rate of the KMF. Twelve trenches, forty nine soil samples and one charcoal sample were carried out in the project.

Additionally, ten soil samples were collected from five exposure and trench walls to carry out the TL-age dating in this study. Results of additional TL-age dating done in this study are summarized in Table 4.1 and Appendix C. The ages of soils derived from this study are in the same range of values that obtained from the RID's study in case of similar soil layers. So, the data from eleven trenches, one trench excavated at Ban Don Chan, Thaiy Muang district, Phang Nga province expressing no traced fault was omitted, and newly dated data in this study were inspected and re-analyzed. Re-interpretation of fault events, re-estimation of fault time, and re-calculation of recurrence interval and slip rate were performed in this study. Locations of the trenches, and logs and photos of the trench walls are attached in the Appendix C

Table 4.1 Results of TL-age dating in this study

Site No.	Location			Fault Segment	Sample No.	Soil Unit	Age (year)
	Village	District	Province				
3	Chong Maliew	Phanom	Surat Thani	Khlung Marui	CML1	D	5,500±600
					CML2	B	54,600±7,100
					CML3	B	30,200±4,500
6	Khao To	Plai Phraya	Krabi	Ao Luk	BKT2	D	12,000±1,100
7	Naiprab	Khian Sa	Surat Thani	Plai Phraya	WNP-4	M	13,100±1,000
8	Palm field	Muang	Krabi	Khao Phanom	SHP5	C	5,700±400
					SHP6	C	5,800±300
					SHP8	C	5,600±400
9	Thung Saingam school	Thap Put	Phang Nga	Thap Put	TSG3	H	5,200±800
					TSG6	D	19,700±3,100

It is believed that the upper constrain of the faulting time (younger side) is more representative of the faulting age than the lower constrain (older side). Reasons are the age of the lower constrain mainly receives from the layer underlying the laterite that is mostly weathered bed rocks (difficult to collect samples) and the long-period formation of laterite. Furthermore, the main purpose of the paleoseismic investigation is to find out the recurrence interval and slip rate of the KMF zone. Therefore, the assumption that depositional age of sediments overlying the layer with the end of the tectonic event is approximate age of the event was applied in this study.

Fault events derived from each trench were re-evaluated and can be summarized as follows:

(1) Site No.1: Ban Phophana, Takuktai sub-district, Viphavadi district, Surat Thani province

Exposures in the borrow pit located at the northern part of the KMF segment were investigated. The basal bedrock unit is intercalation of sandstone, conglomerate and mudstone (Unit A). Unit B is highly to completely weathered rocks. A sequence of gravels (Unit C, D) overlies the bedrock. A brown lateritic layer (Unit E) overlying the Unit D was found. The topmost layer is silty sand (Unit F). It can be divided into two formations—Unit F1 is an original deposit and Unit F2 is a reworked F1 after the tectonic movement. The bedrock was cut by a series of faults and fractures. Fractures cut into the overlying lateritic gravels (Unit E). 3 soil samples from Unit F1 and F2 were collected for TL age dating. The depositional age of the Unit F1 is 6,240-7,440 cal yr B.P. while that of the Unit F2 is 1,930-2,340 cal yr B.P. It can be stated that at least three tectonic movements were observed. The first uplift event happened after the deposition of the white-colored gravel (Unit C) causing the Unit C disappears at the exposure no.1. After the formation of laterite

(Unit E), the second terrain uplift occurred and then absence of laterite was found at the exposure no.1. Representing both mentioned events, a photograph as shown in Figure 4.4(a) expresses the sequence of deposits without the Unit C and the laterite Unit E, and the faults cutting from the bed rock Unit A to the Unit D. The third movement event appeared after the deposition of the reworked yellowish brown silty sand (Unit F2) as encountered in the exposure no.2. Various faults and fractures can be observed in the Unit F2 and some laterite (Unit E) was moved upward as shown in Figure 4.4(b). Based on the deposition age

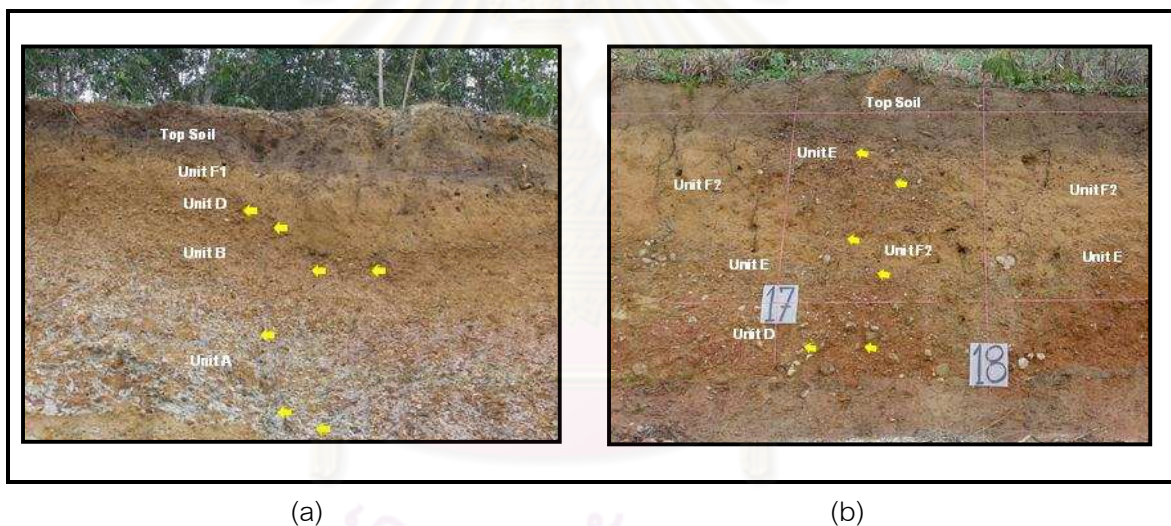


Figure 4.4 Photographs show (a) faults (pointed by yellow arrows) cutting through Units A, B and D and absence of Unit C (b) faults (pointed by yellow arrows) cutting through Units D, E and F2 and a block of Unit E embedded in Unit F2

of sediments overlying the layer with the end of the tectonic event, only the age of second and third of the tectonic movement can be determined. The age of second movement based on the age of the Unit F1 is approximately 6,240-7,440 cal yr B.P. The third faulting

event occurred after the deposition of the reworked F1 (Unit F2). It was assumed that the faulting appeared as soon as the Unit F2 deposited completely. So, the age of the third faulting event is approximately 1,930-2,340 cal yr B.P.

(2) Site No.2: Ban Song Phinong, Phanom sub-district, Phanom district, Surat Thani province.

It is situated at the northern part of the Takua Thung fault segment. The basement rock (Unit A) is sandstone that is covered by colluviums (Unit B and C). The topmost layer overlying the Unit B and C is yellow silt (Unit D). Folded and faulted structures could be observed in the colluviums Unit B and C as shown in Figure 4.5. Results of the dating show

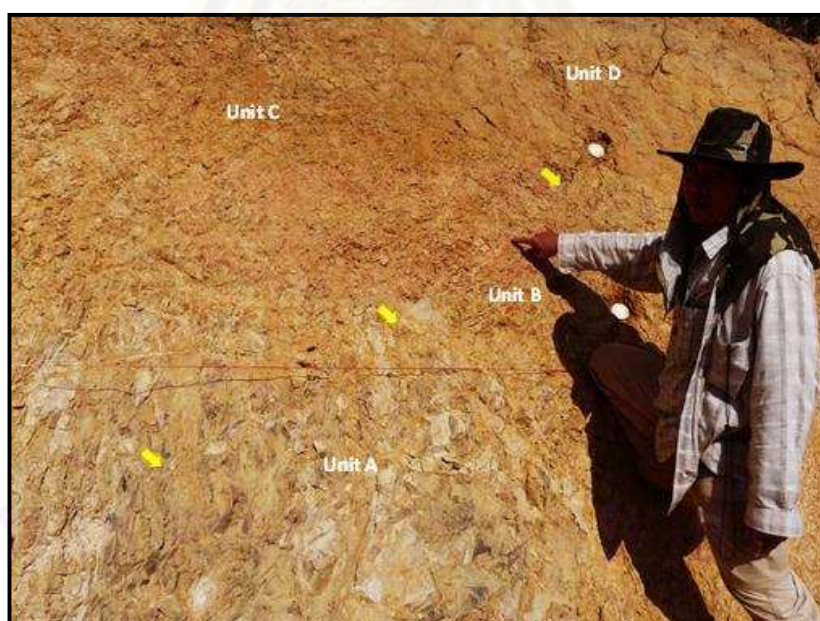


Figure 4.5 Fault (pointed by yellow arrows) cutting through Unit A, and Unit B.

that the age of soils in the sandstone fissure that are expected to re-deposit during the fault movement is 11,940-14,140 cal yr B.P. and that of the Unit D is 2,640-2,840 cal yr B.P. and 3,240-4,040 cal yr B.P. It can be concluded that at least two faulting time can be determined in this area i.e. the first occurred after the deposition of the Unit B with the age of activity about 11,940-14,140 cal yr B.P. and the second moved after the deposition of the Unit C during the period of 2,640-4,040 cal yr B.P.

(3) Site No.3 : Ban Chong Maliew, Phanom sub-district, Phanom district, Surat Thani province

Two exposures in a borrow pit located on the Phanom fault segment were investigated. The bed rock is sandstone and conglomerate that are highly to completely weathered with relics of original structures (Unit A). The top part of Unit A is white- and brown-colored clay (Unit B) derived from completely weathered sandstone and conglomerate. Folded and faulted laterite (Unit C) was found overlying the Unit B and underlying yellow- to orange-colored silty sand layer (Unit D). Two samples from the Unit B yielded ages of 13,540-15,940 cal yr B.P. (CML-5) and 11,640-13,440 cal yr B.P. (CML-7). Another two samples from the Unit B (CML2 and CML3) were tested in this study. They give the age of 25,580-61,640 cal yr B.P. These results indicate that the formation age of the Unit B is between 11,640 cal yr B.P. and 61,640 cal yr B.P. The TL ages that were determined from the Unit D are 5,540-6,140 cal yr B.P. (CML-4), 2,950-3,350 Cal yr B.P. (CML-6), and 4,840-6,040 cal yr B.P. (CML1 performed in this study). At this site only one faulting activity could be observed after the formation of the laterite. For example, the tectonic features representing this event are the faults and fractures propagating from the bed rock Unit A until the lateritic layer Unit C as illustrated in Figure 4.6 to 4.8. Its movement period is 4,840-6,140 cal yr B.P.



Figure 4.6 Fault (pointed by yellow arrows) with the orientation of $N12^{\circ}W72^{\circ}E$ extending from the bed rock Unit A and ending at the laterite Unit C at the station 54-57 m of the exposure no.1.

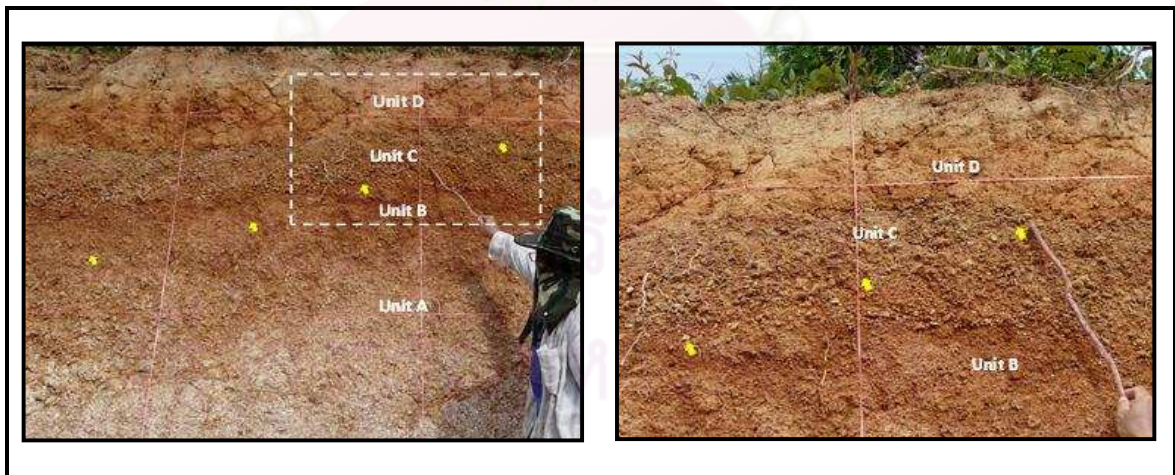


Figure 4.7 The fracture (pointed by yellow arrows) appears in the bed rock Unit A and continues up to the laterite Unit C. Its orientation is $N45^{\circ}E34^{\circ}NW$. Close up photograph in a white rectangle (left figure) is illustrated in the right figure.

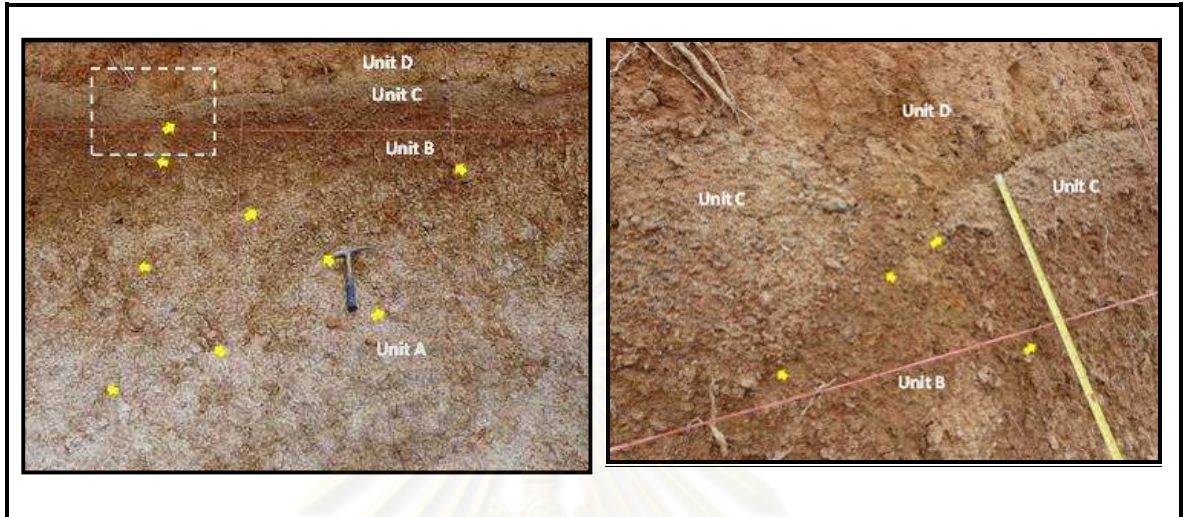


Figure 4.8 Faults (pointed by yellow arrows) were observed. They cut the bed rock Unit A, weathered bed rock Unit B and the laterite Unit C. Close up photograph in the white rectangle (left figure) is shown in the right figure

(4) Site No.4 : Ban Nongtao, Ao Luek Tai sub-district, Ao Luek district, Krabi province.

A road cut exposure situated on Ao Luk fault segment was studied. Mainly the exposure is rocks (Unit A) consisting of sandstone, siltstone and conglomerate. Covering some part of the Unit A, thin laterite (Unit B) is folded and faulted. The topmost layer overlying the laterite and the rocks is clayey sand (Unit C). Various faults and fractures were observed continuously from the Unit A to the Unit B. Bedding of the Unit A orientates mainly in the trend of NE-SW and the dip of NW. Results of TL-age dating show that the age of the Unit C is in the range of 3,640-13,440 cal yr B.P. Based on our interpretation, two fault movements were activated. The first movement occurred as evidenced by folded and

faulted laterite under compression force situation. This event represents the depositional age of the Unit C overlying the laterite (Unit B) which is about 11,840-13,440 cal yr B.P. The second movement is regarded to be a strike-slip faulting as shown by a prominent fissure (McCalpin, 1996) in the Unit A. The date of the reworked Unit C in the fissure is interpreted as the age of fault movement of approximately 4,140-4,940 cal yr B.P.

(5) Site No.5 : Ban Bangsai, Thap Put sub-district, Thap Put district, Phang Nga province.

A road cut exposure that is located on the Thap Put fault segment was investigated. A bottommost layer is sandstone interbedded with siltstone (Unit A) of which the upper part is weathered completely. Laterite (Unit B) lies over the rocks (Unit A) and underlies gray clay (Unit C) and yellowish brown sandy clay (Unit D). Many faults and fractures cut through the rocks (Unit A) into the laterite (Unit B) as shown in Figure 4.9. Two samples

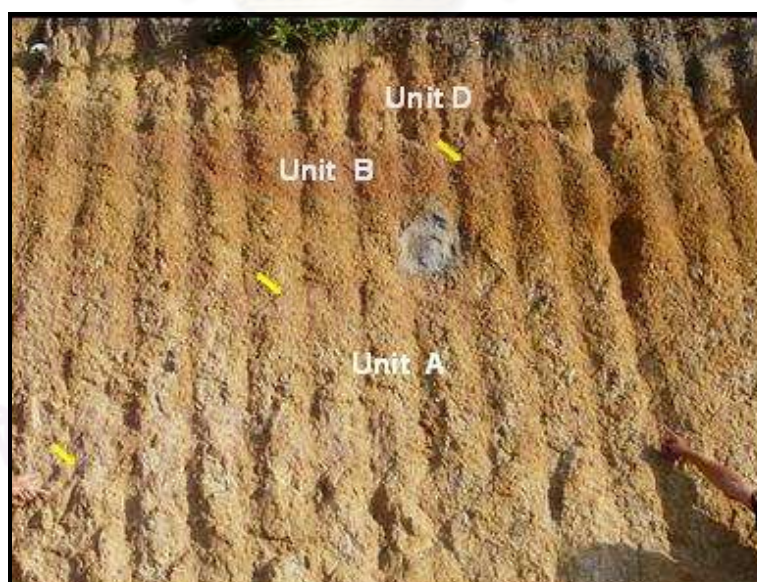


Figure 4.9 Excavation wall at site no.5 at Ban Bangs, Phang Nga province showing faults, pointed by yellow arrows, cutting from the bed rock Unit A to the laterite Unit B.

were collected from the completely weathered rocks yielded TL date of 7,340-12,440 cal yr B.P. Two samples from layers overlying the laterite (Unit C and D) show TL ages of 4,640-5,840 cal yr B.P. Only one tectonic fault movement event can be interpreted, occurring after the formation of the laterite Unit B. This faulting event time is in the range of approximately 4,640-5,840 cal yr B.P. in accordance with the depositional age of Units C and D.

(6) Site No.6 : Ban Khao To, Khao Khane sub-district, Plai Phraya district, Krabi province.

An exposure in a borrow pit lying on the Phanom fault segment was studied. A bottom part of the exposure is inclined semi-consolidated sand and gravel beds (Unit A) overlain by Unit B comprising gravels of mainly quartz and sandstone. Laterite (Unit C) lies on the Unit B. The uppermost layer is pale brown clayey sand (Unit D). Faults and fractures were found cutting from the Unit A to the Unit C (Figure 4.10). Two samples from the Unit A reveal the TL ages of 17,240-24,040 cal yr B.P. and 8,750-10,530 cal yr B.P. (another sample with the age of 11,940-14,460 cal yr B.P. from this study) while two samples from the Unit D give ages of 2,230-2,250 cal yr B.P. and 5,240-6,040 cal yr B.P. Therefore, the depositional age of the Unit D is between 2,230 cal yr B.P. and 6,040 cal yr B.P. In this section, one faulting event can be interpreted. The event occurred postdating the laterite formation. The age of the fault movement is approximately 5,240-6,040 cal yr B.P.

(7) Site No.7 : Naiprab temple, Tha Sadej sub-district, Khian Sa district, Surat Thani province.

A slope cut and a trench located on the Khian Sa fault segment were studied. From the bottom to the top of the trench and exposure, faulted sequence of sand

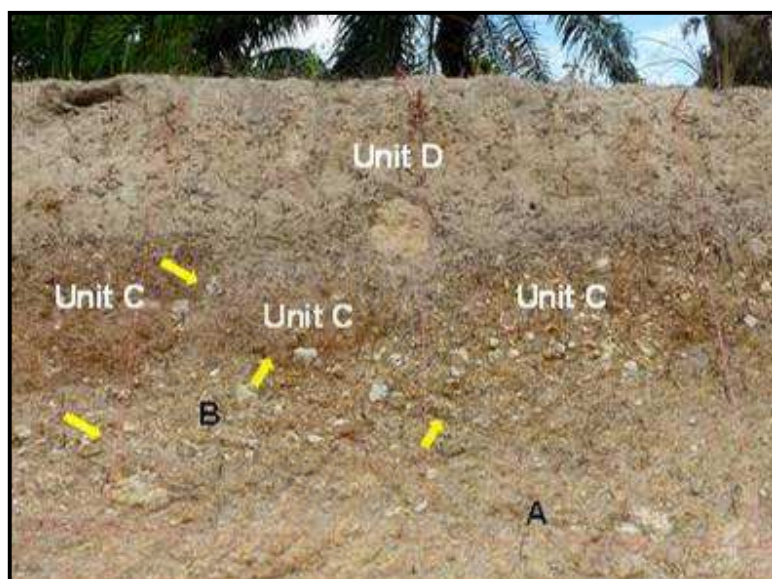


Figure 4.10 Trench wall of site no. 6 showing faults (pointed by yellow arrows) passing from the bed rock Unit A up to the laterite Unit C

and silt (Units A, B, C, D, E) is overlain by brown-colored laterite (Unit F). Overlying the Unit F, there is a white-gray sequence of calcrete nodules and manganese layers (Units G, H, I and J). The topmost two layers are yellow brown-colored sands (Unit K) and orange brown-colored sand (Unit L). Numerous faults and fractures cut through Unit A, B, C, D, E, F, and K but not into Unit L. No faults and fractures can be observed in the Units G, H, I and J because they are loose materials and eroded. However, it is believed that faulting activities happened after these units occurred because faults and fractures were found in the younger Unit K. Based on TL-age dating of Unit K and L, it can be concluded that at least two tectonic activities occurred. The first event occurrence is evidenced by folded and faulted of laterite Unit F during 11,640-12,440 cal yr B.P. (in accordance with the depositional age of Unit K). The second event is shown by faults in the Unit K of which the

time of occurrence is about 8,640-14,040 cal yr B.P. based on the depositional age of unfaulted Unit L.

(8) Site No.8 : a palm field, Krabi Noi sub-district, Muang district, Krabi province

An L-shaped trench is situated on the Khao Phanom fault segment was excavated. The sequences of sediment layers consisting, from the bottom to the top, of pale yellow silty sand (E), yellowish brown silty sand (D), orange silty sand (C), laterite (B) and white sandy clay with brown and yellow mottles (A) units. Many faults and fractures cut from the bottom Unit A to Unit D. For example, fractures appear in the laterite Unit B as shown in Figure 4.11. The Unit C overlaying faulted and folded laterite yielded calibrated dates of 5,240-

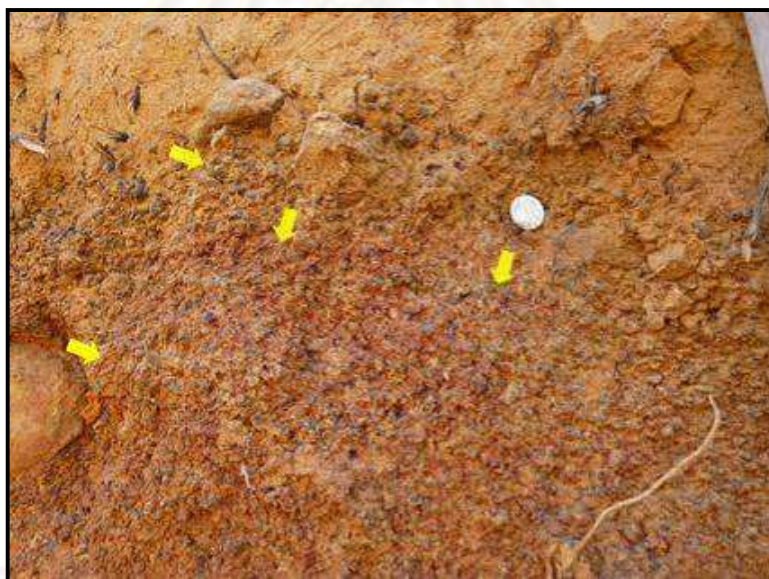


Figure 4.11 Trench wall of site no.8 showing fractures (pointed by yellow arrows) cutting through the laterite Unit B observed

6,040 cal yr B.P. Unit D, faulted and embedded with laterite blocks, obtained calibrated date of 2,580-2,900 cal yr B.P. (SHP-1), 3,340-3,540 cal yr B.P., and 3,640-3,840 cal yr B.P.,

thus indicating a depositional age of 2,580-3,840 cal yr B.P. The nearest faulting time for the first movement is the depositional age of the Unit C about 5,240-6,040 cal yr B.P. and for the second movement is the depositional age of the Unit D approximately 2,580-3,840 cal yr B.P.

(9) Site No.9 : Thung Saingam school, Thap Put district, Phang Nga province.

A trench and an exposure are located on the Thap Put fault segment were excavated and cleaned. Bedrocks consisting of sandstone (Unit A), siltstone and mudstone (Unit B) are exposed in the trench striking NW–SE and dipping to NE. Tectonic activity was found in the exposure. Overlying completely weathered bedrocks (Unit C and D) and inclined gravel beds (Unit E and F), folded and faulted laterite (Unit G) underlies the topmost layer of faulted and fractured yellowish brown to orange brown silt (Unit H) and whitish gray silt (Unit I). The Unit D yielded TL dates of 13,040-14,040 cal yr B.P. while the Unit F dated at 10,240-13,240 cal yr B.P. Soil sample derived from the Unit H was deposited in a fissure of the laterite (Unit G) as illustrated in Figure 4.12 during the faulting time. It obtained TL dates of 5,340-5,940 cal yr B.P. Folded and faulted detrital charcoal as shown in Figure 4.13 that were collected from the Unit I shows that the age is in the range of 3,980-4,060 cal yr B.P. while a soil sample obtained from the Unit I yielded TL-dating age of 2,940-3,140 cal yr B.P. This indicates that depositional age of the Unit I between 2,940 and 4,060 cal yr B.P. It can be stated that at least three faulting events can be observed in this area. The first movement is the uplift of the bed rocks. The author apply the age of paleosol (Unit D) to be approximate age of the faulting time. The second movement is the formation of the fissure of laterite after the deposition of laterite. The age of soil in the fissure that deposited during the movement represents the faulting age of 5,340-5,940 cal yr B.P. The third movement occurred after the deposition of the Unit I with the movement time of 4,060

to 2,940 cal yr B.P. This latest event can be confirmed from evidences observed in the Unit I-- folded and faulted charcoal, fractures as shown in Figure 4.14 (a)-- and silt lumps of Unit H embedded in laterite Unit G as shown in Figure 4.14(b).

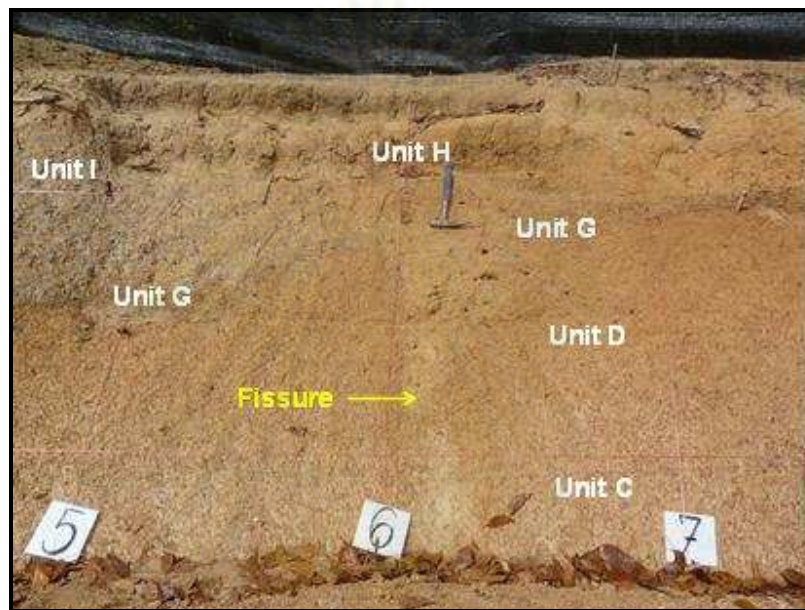


Figure 4.12 Fissure occurs in Units C, D and G.

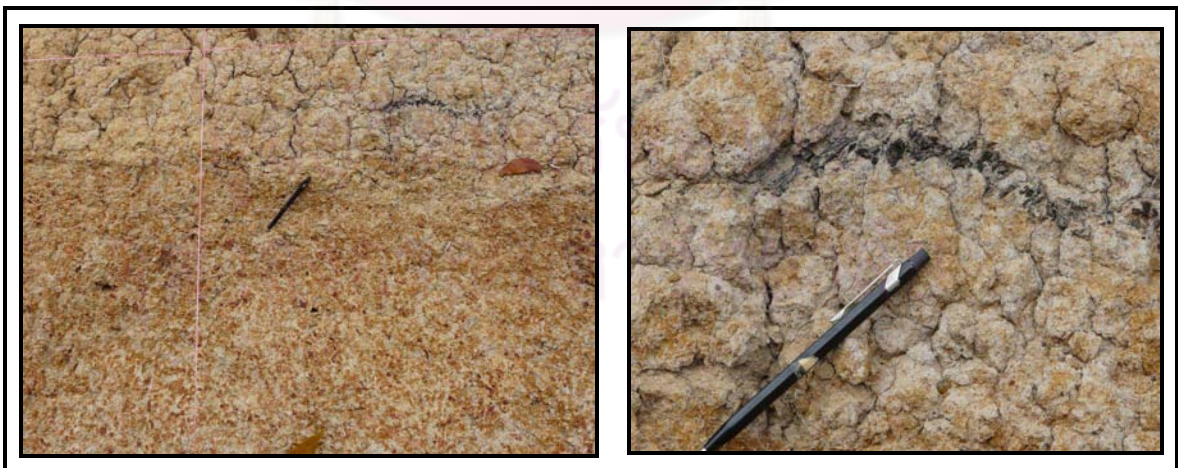
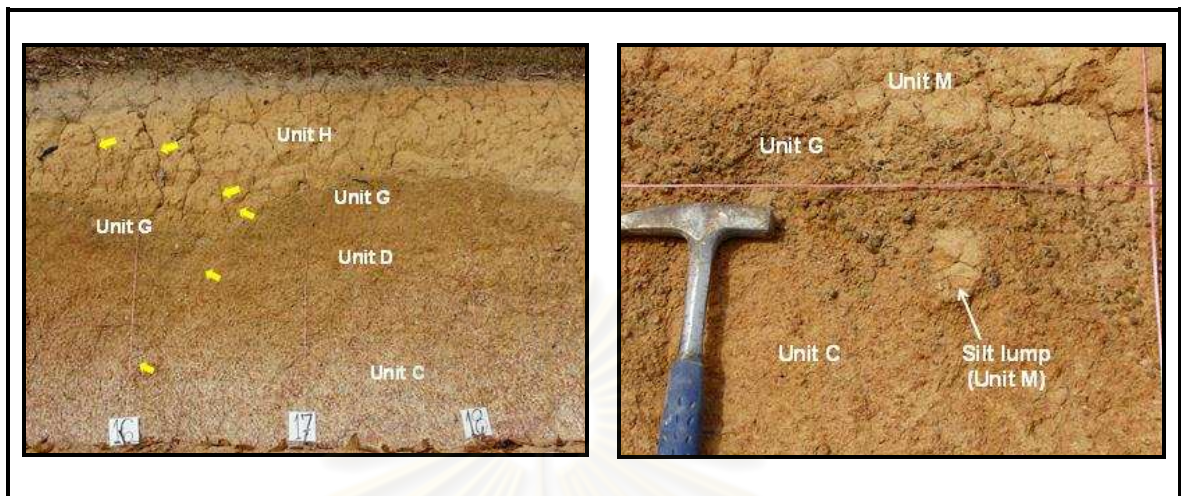


Figure 4.13 Folded and faulted charcoal layer, orientation of a black pencil indicating fault direction, the right photograph is a close-up charcoal picture.



(a)

(b)

Figure 4.14 (a) Faults and fractures (pointed by yellow arrows) in Unit C, D, G and H, (b) Silt lump of the Unit M embedded in laterite Unit G

(10) Site No.10 : Ban Lum Kriab, Thap Put sub-district, Thap Put district, Phang Nga province

A T-shaped trench excavation lying on the Thap Put fault segment was carried out. Six sediment layers consisting of gray silt (Unit A), sandy gravel (Unit B), white and red brown sand (Unit C), brown silty gravel (Unit D), yellow brown silty gravel (Unit E), laterite (Unit F) and pale brown fine sand (Unit G) were observed. The trench did not reach the basement rocks. Faults cut from the layers at the bottom of the trench (Unit A) up to the Unit F. Soil samples of the Unit G were collected for the TL age dating. Results of the age dating show that the sediment samples have the age of 1,130-2,840 cal yr B.P. Many faults were observed in the trench walls. Only one faulting activity was able to be dated. This

faulting time based on the age of soil filled in the fissure of laterite is about 1,640-1,840 cal yr B.P.

(11) Site No.11 : Ban Torua, Thap Put sub-district, Thap Put district, Phang Nga province.

A road cut exposure is situated on the Thap Put fault segment was investigated; Two sediment layers were observed overlying completely-weathered sandstone (Unit A). The lower sediment layer is folded and faulted laterite (Unit B) and the upper sediment layer is yellowish brown silt (Unit C) as shown in Figure 4.15. Moreover, silty lumps (expected to be reworked Unit C due to tectonic activity) are impregnated in the Unit A and B (Figure 4.16). Two samples were collected from the lower part of Unit C that were disturbed and filled up in a open fissure of the laterite. TL-age dating results reveal that the age is 1,640-1,840 cal yr B.P. and 2,140-2,340 cal yr B.P. The other two samples were collected from the undeformed upper part of the Unit C of which TL dates give ages of 890-1,040 cal yr B.P. and 830-950 cal yr B.P. (BTR-4). It can be stated that the undeformed upper part of the

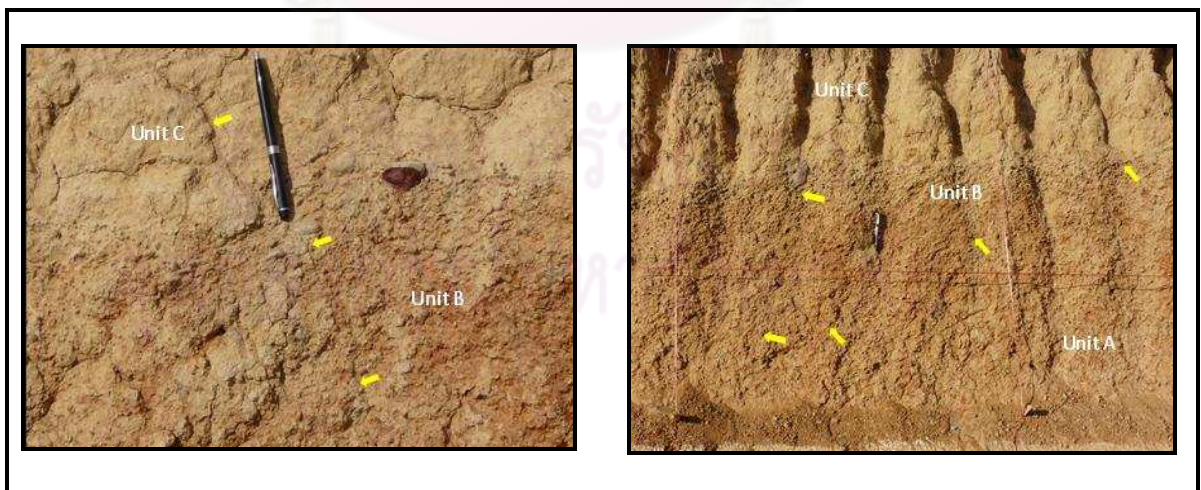


Figure 4.15 Fault (pointed by yellow arrows) passing through laterite Unit B.



Figure 4.16 Slit lump impregnated in the lateritic layer and the completely weathered rock, the right photograph is a close up silt lump picture at stations 36-37 m.

Unit C deposited about 830-1,040 cal yr B.P. The faulting time is the depositional age of silt in the fissure of laterite. It is approximately 1,640-2,340 cal yr B.P.

Moreover, based on the evaluation of the results of trenching along the KMF that were carried out by the DMR (2007), the fault events can be re-established as follows:

(1) Site No.1 : Ban Bang Wo, Phluthoen sub-district, Phanom district of Surat Thani province

The trench was excavated on the KMF segment. Four soil layers were found in the trench. From the upper to the lower layers, brown clayey sand (Unit D), brown gravels (Unit C), yellowish brown gravels (Unit B) and reddish brown clay (Unit A). Fault was traced in the Unit A, B, and C. Due to the TL age was not consistent, ^{14}C -age was selected to specify the age of faulting. The deposition age of the Unit D was estimated to be the fault time. It is approximately 10,120-10,440 years ago (or 10,073-10,393 cal yr B.P.).

(2) Site No.2 : Ban Phet Kled, Viphavadi district, Surat Thani provin

The exposure lying on the KMF segment was investigated. Soil and rock layers found on the trench wall consist of sandstone (Unit A), dark brown sandy gravels (Unit B) and pale brown sand (Unit C). Faults occurred in these units. Both TL- and ^{14}C -age dating techniques were performed. Results of TL date show very high ages. The ^{14}C age seems to be reasonable, so it was selected to determine the age of the fault. The faulting event was estimated to be 5,530-6,110 years ago (or 5,483-6,063 cal yr B.P.).

(3) Site No.3 : Ban Bang Luk, Thap Put district, Phang Nga province

Two trenches were excavated along the KMF segment. The first trench, called Bang Luk trench, expresses the intercalation of clay, sand and gravel layers (Unit A, B., C, D, E, F, H, I and J. The uppermost layer (Unit J) was not faulted. So, the oldest depositional age of the Unit J was applied to be the fault age. TL- and ESR-age dating methods were carried out. However, the TL dates is very high and not reasonable to be used. The ESR-ages, therefore, was adopted. The fault age is 1,690-2,310 years ago or 1,643-2,263 cal yr B.P. The second trench, named Bang Luk 2 trench, shows three soil layers, namely Unit A: weathered sandstone, conglomerate and mudstone, Unit B: dark brown colluvial gravels, and Unit C: brown silty sand. The fault was observed in the Unit A and B. The depositional age of the Unit C was applied to be the fault age. Both TL- and ^{14}C -age dating method were tested. But TL ages are very high and unreasonable to be used. The ^{14}C dates were applied. The fault age is 6,060-6,140 years ago or 6,013-6,093 cal yr B.P.

(4) Site No.4 : Ban Khuan Sabai, Ao Luk district, Krabi province

The trench was excavated on the northern part of the Thap Put fault segment. Three soil and rock layers were encountered in the trench. They are weathered sandstone and shale (Unit A), brown colluvial gravels (Unit B) and brown silty sand (Unit C). The fault occurred in the Unit A and B. The depositional age of the Unit C was used to be the fault age. Based on ^{14}C age, the movement period is between 2,260 and 2,340 years ago or 2,213-2,293 cal yr B.P.

The ages of each fault event derived from this study were grouped to establish a space-time diagram as shown in Figure 4.17. From the diagram, it can be concluded that at least six possible large earthquake events of the KMF zone occurred in the past. Discussion on the sedimentary evidence for each of six events is given as follows:

The latest event (E1) is about 1,640 to 2340 cal yr B.P. The chronological limit is the age of silt of the lower part of Unit C that deposited in the opened fissure of folded and faulted laterite (Unit B) in the trench at the Ao Luek fault, Ban Torua, Thap Put district, Phang Nga province. Due to appearance of silt lumps of Unit C embedded in laterite (Unit B), it can be believed that the event E1 occurred after deposition of the lower part of Unit C and the event may have occurred near 1,640-2,340 cal yr B.P. The event E1 occurred from the movement of the KMF and Thap Put fault segments.

The penultimate event (E2) occurred approximately during 2,580 – 4,040 cal yr B.P. The upper chronological limit is defined by the ages of silt (Unit D) that deposited over folded and faulted colluvium (Unit B) of the trench excavated at Ban Song Phinong, Phanom district, Surat Thani province. The ages are between 2,640 and 4,040 cal yr B.P. The lower

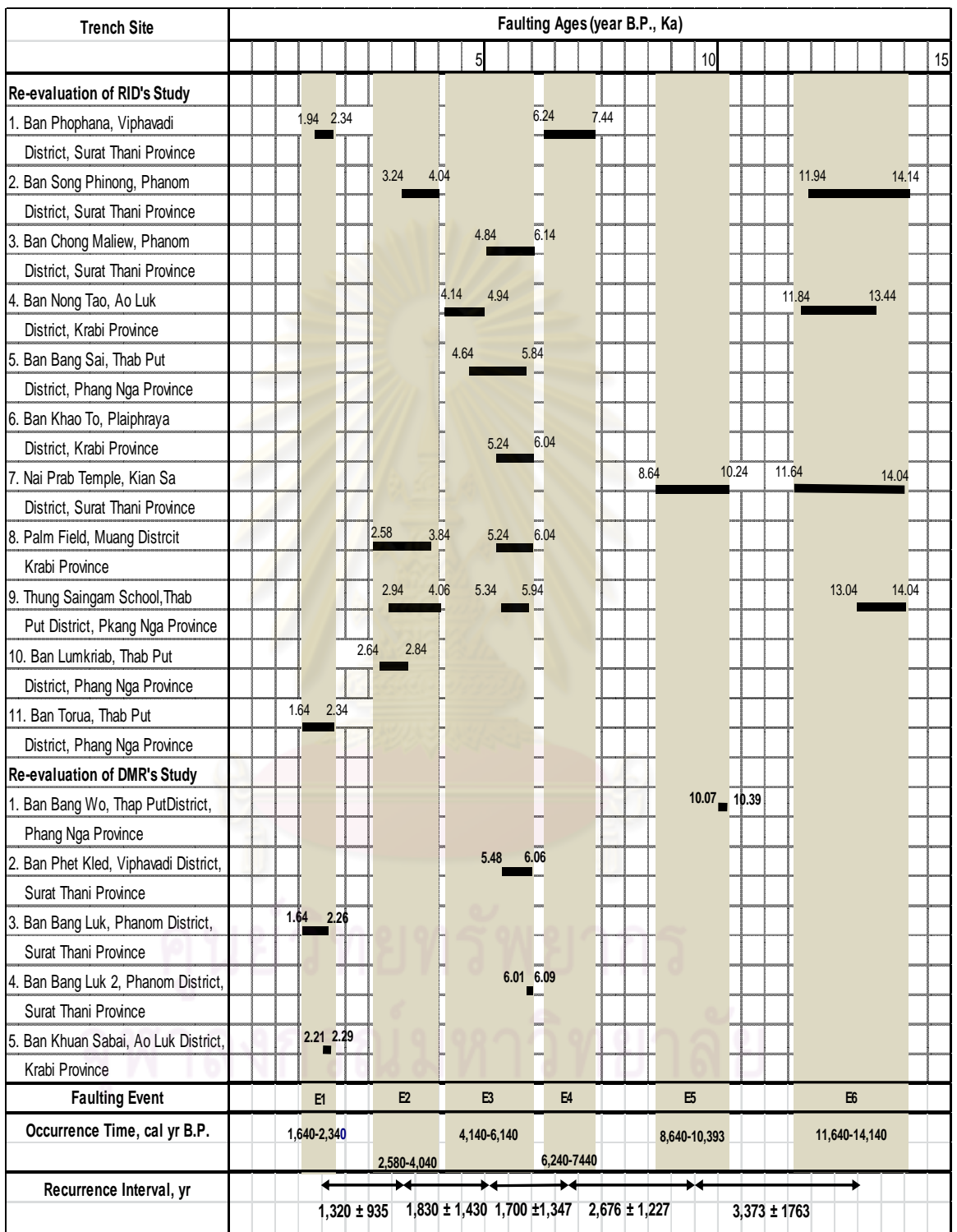


Figure 4.17 Space-time diagram of the KMF zone, southern Thailand.

chronological limit is derived from the ages of unfaulted silty sand (Unit D) encountered at the NE wall of the trench at the palm field, Muang district, Krabi province. Its ages are between 2,580 and 2,900 cal yr B.P. The occurrence of the event E2 was also observed in the trenches excavated Ban Lum Kriab and Thung Saingam school, Thap Put district, Phang Nga province as well as at Ban Bang Luk, Phanom district, Surat Thani province (DMR, 2007). It means that the movement occurred along the Thap Put and Khao Phanom fault segments.

The third event (E3) is recognized by the depositional ages of sediments overlying folded and faulted laterite that is expected to be the ages near to the faulting time. This event can be observed on the walls of exploratory trenches and exposures investigated at the palm field of Muang district, and Ban Nong Tao of Ao Luek district and Ban Khao To of Plai Phraya district, Krabi province, Thung Saingam school and Ban Bang Sai, Thap Put district, Phang Nga province, Ban Chong Maliew, Phanom district and Ban Phet Kled, Viphavadi district, Surat Thani province. It can be summarized that the event E3 occurred during 4,140-6,140 cal yr B.P. The KMF, Thap Put, Khao Phanom, Phanom and Ao Luk fault segments moved during this period.

The fourth event (E4) is defined from the depositional ages of the lower part of the Unit E lying over folded and faulted gravel layer found at the exploratory exposure at Ban Phonphana, Viphavadi district, Surat Thani province. The event is likely to occur between 6,240 and 7,440 cal yr B.P. along the KMF segment.

The fifth event (E5) is obtained only from the depositional age of yellowish brown sand (Unit M) overlying faulted and fractured range-brown sand (Unit L). This event was found on the exposure at Naiprab temple, Khian Sa district, Surat Thani province and at Ban

Bang Wo, Phanom district, Surat Thani province. The ages of the event are approximately 8,640-10,393 cal yr B.P. The movement occurred along the KMF and Khian Sa fault segments.

The sixth event (E6) is identified from the trenches and exposures at Ban Nong Tao, Ao Luek district, Krabi province, Naiprab temple, Khian Sa district, Surat Thani province, Thung Saingam school, Thap Put district, Phang Nga province, and Ban Song Pinong, Phanom district, Surat Thani province. The upper chronological limit of the event is defined by the sediment was deposited in the open fissure of the bed rock of the exposure at Ban Song Phinong with the ages of about 11,940-14,140 cal yr B.P., and by the deposition before tectonic movement at Thung Saingam school with the age of approximately 13,040-14,040 cal yr B.P. The lower chronological limit of the event is derived from the ages of sediments covering activated laterites observed at Ban Nong Tao, Ao Luek district, Krabi province (11,840-13,440 cal yr B.P) and Naiprab temple, Khian Sa district, Surat Thani province (11,640-12,440 cal yr B.P.). So, the event E6 occurred along the Thap Put, Khian Sa, Ao Luk, and Takua Thung fault segments in the period of 11,640-14,140 cal yr B.P.

Based on the time between the oldest event (E6) and the last faulting event (E1), the mean recurrence interval of the large earthquake of the KMF zone is approximately 2,200 years. The recurrence times calculated between each successive pair of earthquake events are approximately 1,300, 1,800, 1,700, 2,700 and 33,700. The standard deviation of 5 recurrence intervals associated with 6 earthquake events is about 830 years.

Six out of eleven RID's exploratory trenches and exposures, and four DMR's trenches show evidences for determining the fault slip rate. Results of estimated slip rate

can be summarized in Table 4.2. It can be concluded that the slip rate of the Khlong Marui fault zone is in the range of 0.08-0.5 mm/yr.

Table 4.2 Summary of the slip rates of the KMF zone.

Site No.	Location	Displacement		Approximate Faulting Time (yr)	Slip Rate (mm/yr)
		Type	Distance (m)		
RID (2009)					
1	Ban Phonphana, Viphavadi district, Surat Thani province	Folding	0.55	6,900	0.08
3	Ban Chong Malew, Phanom district, Surat Thani province	Fault Offset	0.6	5,900	0.10
5	Ban Bang Sai, Thap Put district, Phang Nga province	Fault Offset	0.4	5,300	0.08
8	Palm field, Muang district, Krabi province	Fault Offset	0.65	5,700	0.11
9	Thung Saingam School, Thap Put district, Phang Nga province	Folding	0.45	5,700	0.08
10	Ban Lum Kriab, Thap Put district, Phang Nga province	Folding	0.15	1,800	0.08
DMR (2007)					
1	Ban Bang Wo, Phanom district, Surat Thani province	Fault Offset	1.2	10,390	0.12
2	Ban Phet Kred, Viphavadi district, Surat Thani province	Fault Offset	0.8	6,070	0.13
3	Ban Bang Luk, Thap Put district, Phang Nga province	Fault Offset	1	2,000	0.50
4	Ban Khuan Sabaj, Ao Luk district, Krabi province	Fault Offset	1	5,200	0.19

2. RNF Zone

Based on results of paleoseismic investigation of the Tha Sae dam project in Chumporn province carried out by the RID in 2006 and the study on recurrence interval of faults in Prachub Khirikhun, Chumporn, Ranong, Surat Thani, Krabi, Phangnga and Phuket provinces (RNF and KMF) performed by the DMR in 2007, the recurrence intervals and the slip rates of the RNF were re-checked and re-estimated.

Four trenches were excavated along the RNF zone by the RID. Data from two trenches, namely Ban Sai Khao trench at Tha Sae district of Chumporn province and Ban Hin Yai trench at Kra Buri district of Ranong province, can be used to estimate the fault age. Fault events derived from each trench were re-evaluated and can be summarized as follows:

(1) Site No.1 : Ban Sai Khao, Tha Sae district, Chumporn province

The exposure was studied and logged. The bed rock is faulted and weathered fine grained diorite (Unit A) that is overlain by completely weathered or oxidized zone of the bed rock (Unit B). Overlying the Unit B, the colluvium, the red-brown silt and clay with sub-angular quartz clasts (Unit C) underlies the Unit D that can be divided into the lower unit (Unit D1) and the upper unit (Unit D2). The Unit D1 comprises red-brown silt and clay while the Unit D2 consists of yellow gray sand and silt. Fault was observed cutting in the Unit A and B. The disappearance of the Unit B and Unit C were found at some part of the exposure. This characteristic means that after the deposition of the Unit B and C, the terrain was uplifted. So, the deposition age of the Unit D1 that overlies the Unit A can be applied as

the approximate age of the fault activity. This age is in the range of 26,600-41,600 years ago or 26,540-41,540 cal yr B.P.

(2) Site No.2 : Ban Hin Yai, Kra Buri district, Ranong province

A trench was excavated and logged. The bed rock is phyllite of which the upper part becomes brown clay (completely weathered phyllite) with rock fragments. It is overlain by the colluvium that is brown clay with sub-angular to sub-round quartz clasts. The top most layer is yellow-brown colluvial sand and clay. Faults can be observed in the bed rock. The fault age can be determined by the age of the completely weathered phyllite that is 20,900-21,100 years ago or 20,840-21,040 cal yr B.P.

Two trenches performed by the DMR including the age dating results were re-evaluated to identify the Ranong fault activities as below.

(1) Site No.1 : Ban Bang Nonnai, Muang district, Ranong province.

Faults were observed to cut from the lower to the upper layers—Unit A:siltstone and mudstone, Unit B:clayey gravel with iron-oxide nodules, Unit C:clay with sandstone fragments, and Unit D:sandy gravels. Unfaulted Unit E that is sandy clay lies on the Unit D. TL- and ^{14}C -age dating was carried out. Results of TL-age dating give very high ages and is not consistent. So, in this study the author apply the age derived from ^{14}C -age dating. The fault activity occurred after the deposition of the Unit D. So, the depositional age of the Unit D represent the faulting time of 9,280-9,400 years ago or 9,220-9,340 cal yr B.P.

The latest event (E1) occurred during 8,240-8,330 cal yr B.P. The event was encountered at Ban Noen Kruat, Bang Saphan district, Prachuab Khirikhun province. The penultimate event (E2) with the age of 9,220-9,340 cal yr B.P. is derived from the trench excavated at Ban Non Nai, Bang Non sub-district, Muang district, Ranong province. The third event (E3) was found at Ban Hin Yai, Chor Por Ror sub-district, Kra Buri district, Ranong province. The fault age is 20,840-21,040 cal yr B.P. The fourth event (E4) was interpreted from the trench located at Ban Sai Khao, Song Phinong sub-district, Tha Sae district, Chumphon province. The older and younger chronological limits are 41,540 and 26,540 cal yr B.P., respectively.

Based on the time between the oldest event (E4) and the latest faulting event (E1), the mean recurrence interval of the large earthquake of the Ranong fault zone is approximately 8,300 years. The recurrence times calculated between each successive pair of earthquake events (E1, E2 and E3) are approximately 1,000, 11,700 and 13,100 years. The standard deviation of two recurrence intervals associated with three earthquake events is about 6,600 years. Re-estimated slip rate can be computed from the observed fault offset and the faulting time as summarized in Table 4.3. It can be concluded that the slip rate of the RNF zone is in the range of 0.04-0.17 mm/yr.

4.3 Probability of Large Earthquake Occurrence of KMF

Based on the displacement of the fault segments found in the KMF zone as given in Table 4.2, the potential large earthquake can be computed from the equation (4.1) (Wells and Coppersmith, 1994) as below.

Table 4.3 Summary the slip rate of the RNF zone.

Site No.	Location	Displacement		Approximate Faulting Time (yr)	Slip Rate (mm/yr)
		Type	Distance (m)		
1	Ban Bang Nonnai, Muang district, Ranong province	Fault Offset	1.60	9,340	0.17
2	Ban Pracha Seri, Sawee district, Chumporn province	Fault Offset	2.8	64,500	0.04
3	Ban Noen Kruat, Bang Saphan district, Prachuab Khirkhun province	Fault Offset	0.6	8,340	0.07

$$M_w = 6.81 + 0.78 \log D \quad (4.1)$$

where M_w is the moment magnitude and D is displacement in meter.

It was found that the great earthquake is in the range of M_w 6.1- M_w 7.1. The probability of the large earthquake event of the KMF can be estimated by normally-distributed recurrence approach or randomly-distributed approach (Poisson distribution). Examples for calculation of these two methods are attached in Appendix D. If it is supposed that the distribution of recurrence intervals is normally distributed about the mean recurrence interval, the probability density curve from the mean recurrence intervals can be plotted as shown in Figure 4.19. So, the probability of large earthquake occurrence on the KMF in any years from the year 2009 can be computed by applying the area under the curve from 2009 to considered year divided by the area from 2009 to infinity. Figure 4.20 shows the probability of the large earthquakes expected to be occurred from 2009 up to

4000. For example, the probability of a large earthquake on the KMF in the year 2005 from the year 2009 is about 40.4%. Based on the assumption that the earthquakes are distributed randomly (Poisson distribution), the probability of occurrence of the earthquake in a given interval of time can be shown in Figure 4.21. It can be concluded that the maximum probability of getting one earthquake event in 2,180 years is approximately 37%.

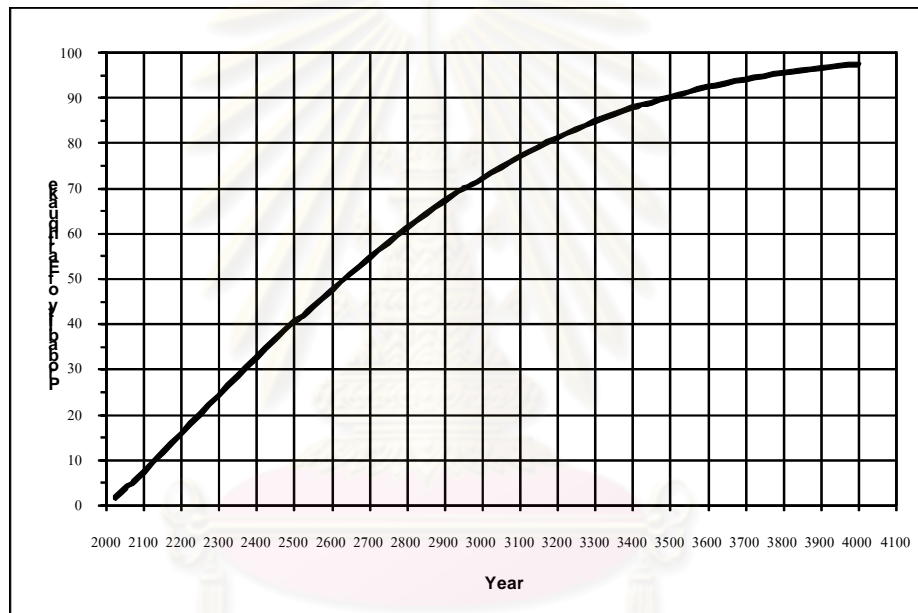


Figure 4.19 Probability of large earthquakes produced by the KMF.

ศูนย์วิทยบริการ
จุฬาลงกรณ์มหาวิทยาลัย

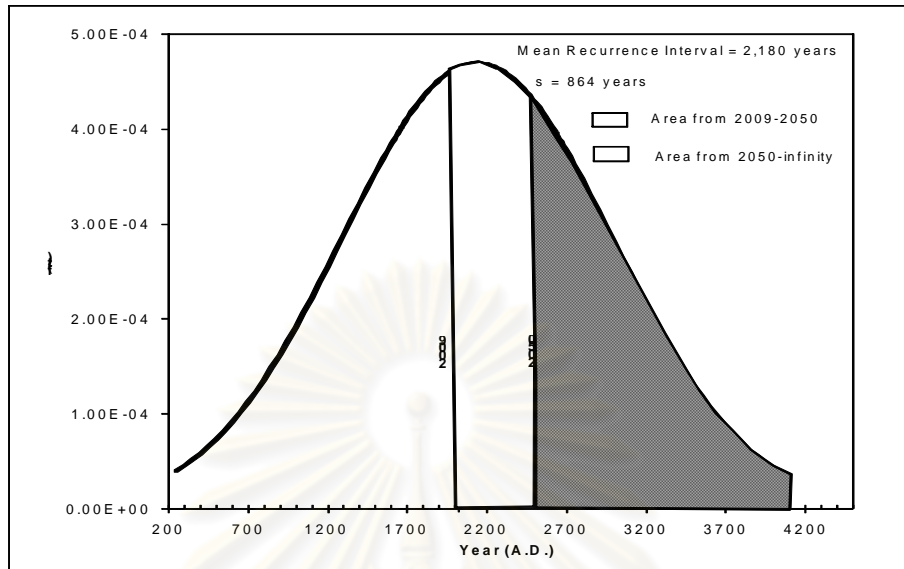


Figure 4.20 Probability of the KMF's large earthquake occurrence in any year from the year 2009 based on the normally-distributed recurrence approach.

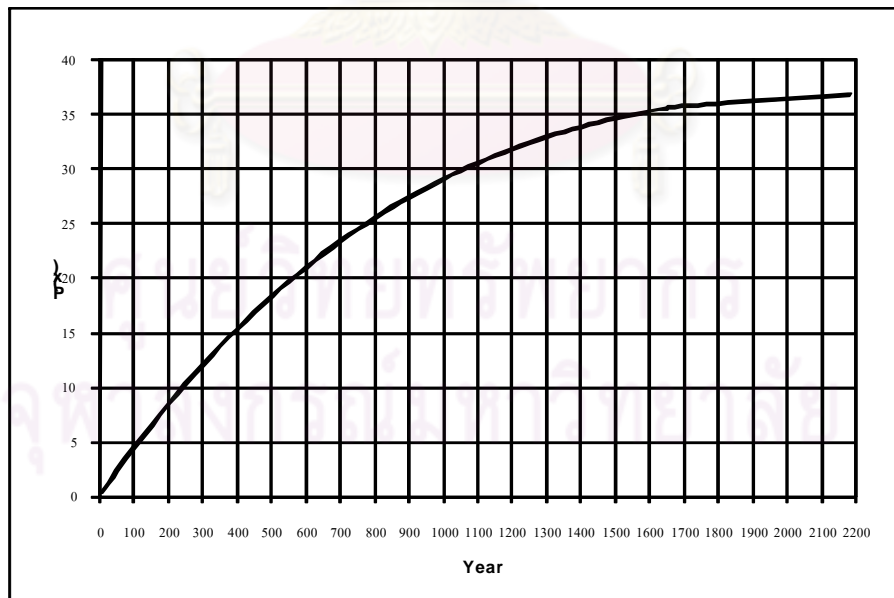


Figure 4.21 Probability of the KMF's large earthquake occurrence in any year from the year 2009 based on the randomly-distributed approach.

CHAPTER V

RESULTS OF PROBABILISTIC SEISMIC HAZARD ANALYSIS

5.1 Seismic Sources Characterization

Seismic source characterization is related to (1) the identification of prominent earthquake sources affecting the mapped area. (2) the maximum magnitudes produced from these sources, and (3) the recurrence rates of their occurrences. All earthquake sources with demonstrated and trusted Holocene movement that could produce the ground motion hazard in the southern Thailand due to their activities, length, or distance to southern Thailand (approximately within 300 km) were included in the analysis. These sources can be divided into two types as below.

1. **Fault Sources** They consist of the RNF, KMF, KYF, TNF, TVF and TPF, and the Sumatra-Andaman subduction zone,
2. **Areal Sources** These sources is named as the KMF areal source located in the east of the main KMF covering Krabi, Phang Nga and Surat Thani provinces, and the reservoir area of the Ratchaphapha dam in Surat Thani province that has produced the reservoir-triggered seismicity (RTS).

Locations of these sources are shown in Figure 5.1. The characteristics of each source obtained from this study and compiled from other studied can be summarized as follows:

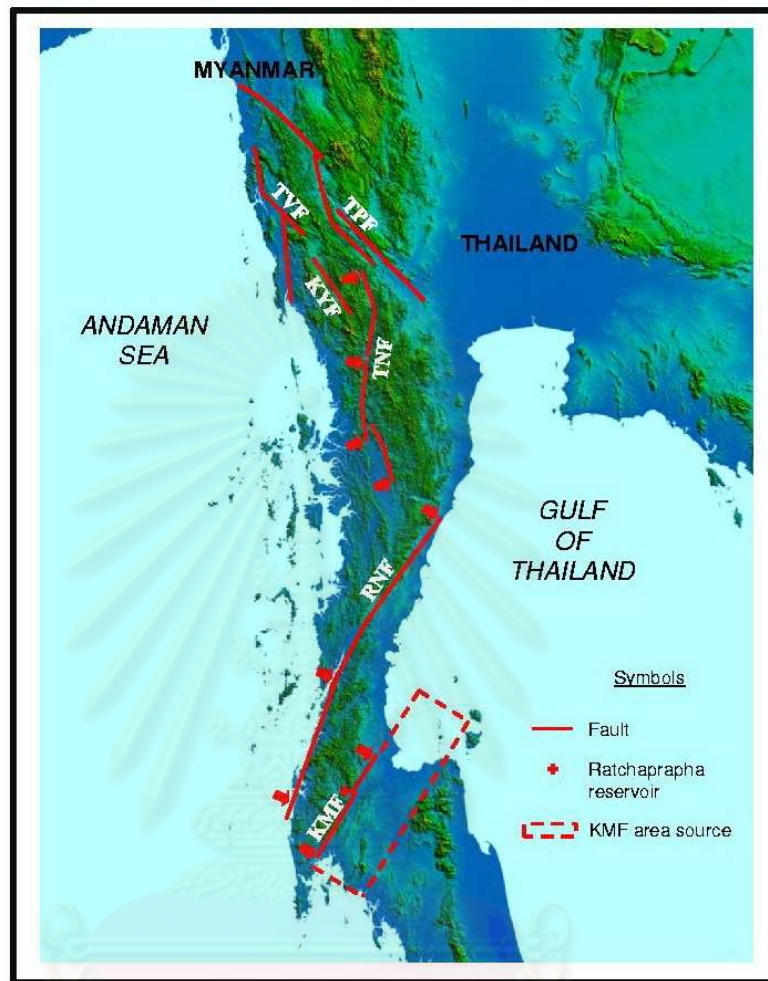


Figure 5.1 Seismicity sources in southern Thailand and adjacent areas, KMF = Khlung Marui fault, RNF = Ranong fault, TNF = Tenasserim fault, KYF = Kungyauangale fault, TVF = Tavoy fault, and TPF = Three Pagoda fault.

5.1.1 KMF

The longest segment of the KMF zone extends from the southwestern Thap Put district, Phang Nga province northeastward passing through Phanom district, Surat Thani province up to Viphavadi district, Surat Thani province. Its total length is about 115 km. Based on the re-evaluated movement of the KMF zone, it can be said that the KMF zone is

the active fault zone that the latest movement happened about 1,700-2400 years ago with the slip rate of 0.08-0.5 mm/yr.

Based on four earthquake events occurred at Krabi and Surat Thani provinces in 2008 (Figure 2.10 in Chapter II), it can be accounted that the KMF zone as an active aerial source zone. In this study, the author specified it as the KMF aerial source zone for the seismic hazard analysis. The parameters of the characteristics and activities of the KMF zone including their weights for the probabilistic seismic hazard analysis are illustrated as the logic tree in Figure 5.2 and summarized in Table 5.1.

Three possible two seismic source scenarios are incorporated in the analysis. They are:

1. **Scenario I: Line Source** This source was identified as the longest segment of the KMF zone in the west. It can be divided into two scenarios of earthquake occurrences as below.

- **Unsegmentation** The longest KMF segment was presumed to rupture simultaneously the entire length of 115 km from Thap Put district, Phang Nga province to Viphavadi district, Surat Than province. It can generate the maximum earthquake of $M_w 7.4 \pm 0.3$,
- **Floating Earthquake** It is assumed that the earthquake can occur freely along the fault with the maximum magnitude of $M_w 6.5 \pm 0.3$.

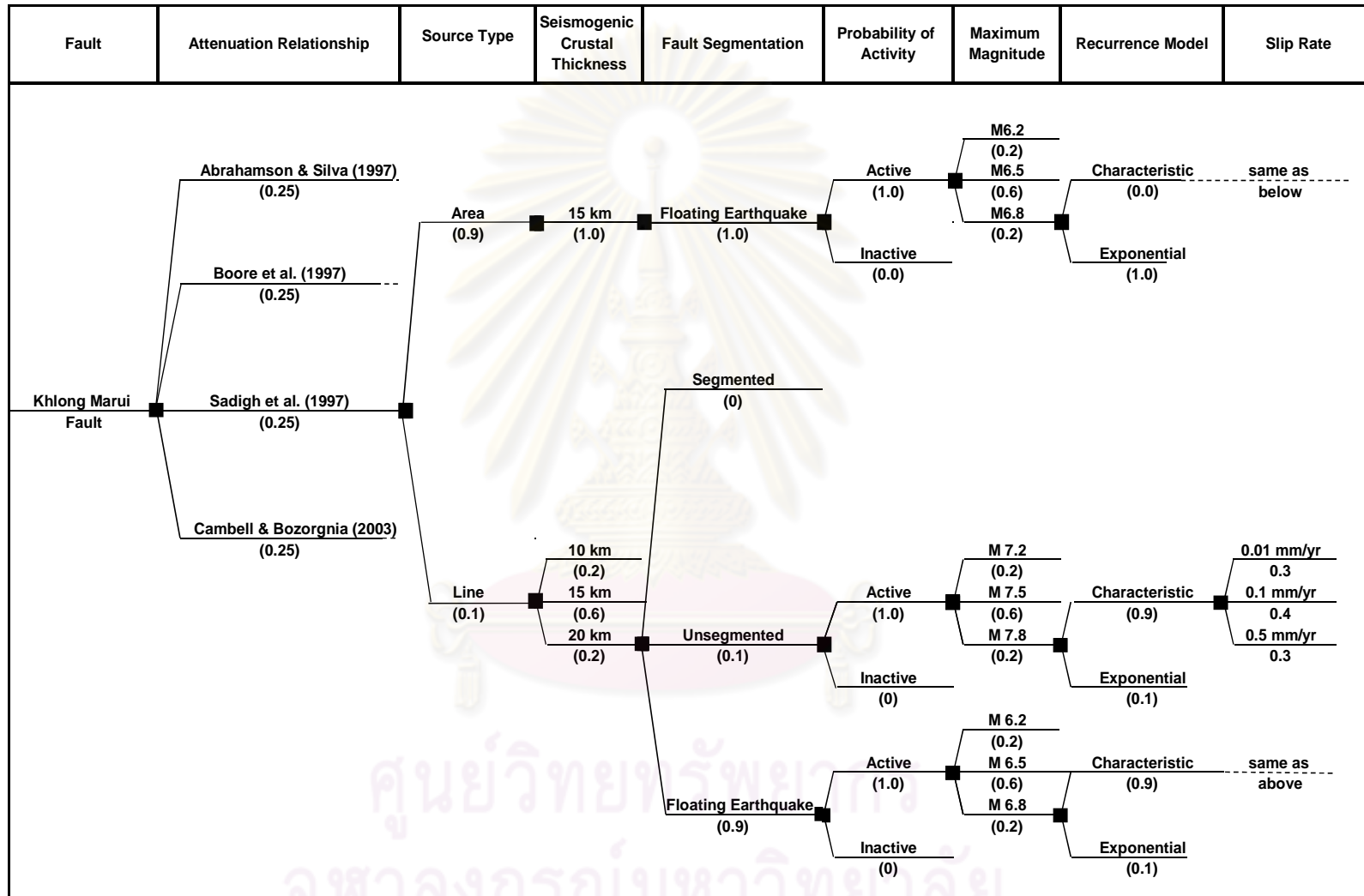


Figure 5.2 Logic tree for the KMF.

Table 5.1 KMF zone model.

Fault	Total Fault Length (km)	Fault Width		Earthquake Source		Rupture Scenario				Magnitude		Slip Rate			
		(km)	Weight	Type	Weight	Rupture Type	Weight	Rupture Length (km)	Prbability of Activity	(M)	Weight	(mm/yr)	Weight		
Khlung Marui	115	15	1.0	Aera	0.9	Floating earthquake	1.0		1.0	6.2	0.2	0.01 ^{1,2}	0.3		
										6.5	0.6			0.1 ^{1,3}	0.4
										6.8	0.2			0.5 ¹	0.3
			10	0.3	Line	0.1	Unsegmented	0.1	115	1.0	7.2	0.2			
			15	0.4							7.5	0.6			
			20	0.3							7.8	0.2			
							Floating earthquake	0.9		1.0	6.2	0.2			
											6.5	0.6			
											6.80	0.2			

Note : data from ¹ this study ² Petersen et al. (2007) ³ Pailoplee (2009)

1. **Scenario II: Aerial Source** It is believed that background earthquakes with a maximum magnitude of $M 6.5 \pm 0.3$ can be generated in the KMF zone covering the areas of Thap Put district of Phang Nga province, Plai Phraya and Ao Luk districts of Krabi province, and Viphavadi districts of Surat Thai province on the northwest to Phanom district of Krabi province, and Phrasaeng and Nasan districts of Surat Thani province in the southeast as well as northeast toward to Group of Ang Thong Islands.

The scenario I and II are given weights of 0.1 and 0.9, respectively. Moreover, the weights of rupture scenarios for the KMF line source are equal to 0.1 for the complete rupture and 0.9 for the floating earthquakes.

Based on the re-estimated slip rate, the maximum, preferred, and minimum slip rate of the KMF is approximately 0.5, 0.1, and 0.01 mm/yr. The weights of their slip rates are assigned to be 0.3, 0.4, and 0.3, respectively.

5.1.2 RNF

Based on the DEM interpretation and re-evaluation of the RNF zone activity, the RNF zone is located from Thap Sakae district of Prachuab Khirikun at the Gulf of Thailand passing Chumporn province and ends at Takua Pa district of Phang Nga province, and Ban Ta Khun district of Surat Thani province. The prominent and longest segment is situated on the west boundary of the zone. It can be divided into two segments.

The first segment starts from Thap Sakae district of Prachuab Khirikun province at the coast of the Gulf of Thailand to Kra Buri district of Ranong province with the length of

180 km. The second segment extends from the first segment at Kra Buri district, then goes along the Andaman coast, and ends at Takua Pa district of Phang Nga province with the length of 160 km. In accordance with re-evaluated RNF activity, it can be stated that the RNF is active with the latest movement occurred about 8,300 years ago, the mean recurrence interval of approximately $8,300 \pm 6,400$ years, and slip rate of 0.04-0.17 mm/yr.

The parameters of the characteristics and activities of the RNF including their weights for the probabilistic seismic hazard analysis are illustrated as the logic tree in Figure 5.3 and summarized in Table 5.2.

In this study, the longest segment is included in the seismic hazard analysis. Three rupture scenarios are assumed as below.

1. **Scenario I: Unsegmentation** The RNF ruptured completely its whole length of 340 km from Prachuab Khirikhun to Ranng provinces. It could produce the maximum earthquake of $M_w 7.9 \pm 0.3$
2. **Scenario II: Segmentation** The RNF ruptured independently as the north and south sections. The north and south sections can generate the maximum earthquake magnitude of $M_w 7.7 \pm 0.3$ and $M_w 7.5 \pm 0.3$, respectively.
3. **Scenario III: Floating Earthquake** The earthquake is presumed to occur anywhere along the entire RNF. The maximum size of the earthquake is estimated as $M_w 6.75 \pm 0.25$.

The scenarios I, II and III are given weights of 0.05, 0.05 and 0.9, respectively.

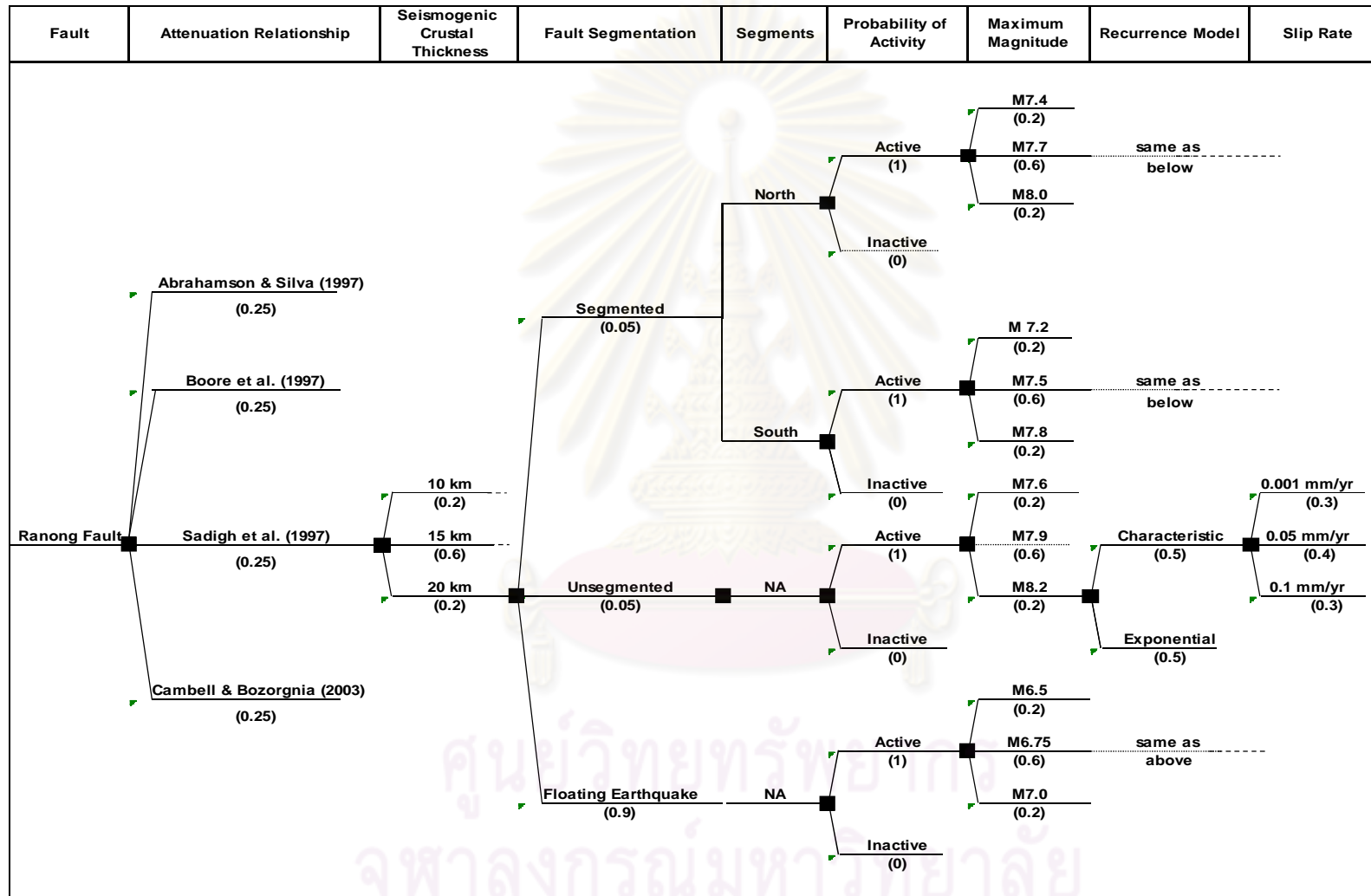


Figure 5.3 Logic tree for the RNF.

Table 5.2 RNF zone model

Fault	Total Fault Length (km)	Fault Width		Rupture Scenario				Magnitude		Slip Rate				
		(km)	Weight	Rupture Type	Weight	Rupture Length (km)	Prbability of Activity	(M)	Weight	(mm/yr)	Weight			
Ranong	340	10	0.2	Unsegmented	0.05	340	1.0	7.6	0.2	0.001 ^{1,2}	0.3			
			15					0.6	7.9			0.6	0.05 ¹	0.4
			20					0.2	8.2			0.2	0.1 ^{1,3}	0.3
		North segment	0.05	180	1.0	7.4	0.2	0.05 ¹	0.4					
						7.7	0.6							
						8	0.2							
		South segment	0.05	160	1.0	7.2	0.2	0.1 ^{1,3}	0.3					
						7.5	0.6							
						7.8	0.2							
		Floating earthquake	0.9		1.0	6.5	0.2	0.001 ^{1,2}	0.3					
						6.75	0.6							
						7.00	0.2							

Note : data from ¹this study ²Wong et al. (2005) ³Petersen et al. (2007)

According to the re-estimated slip rate in this study and Fenton et al.(2003), the preferred slip rate is 0.05 mm/yr, the minimum slip rate is 0.001 mm/yr (this study, Wong et al., 2005) and the maximum slip rate is 0.1 mm/yr (this study, Petersen et al., 2007). The weights of the minimum, preferred and maximum slip rates are equal to 0.3, 0.4 and 0.3, respectively.

5.1.3 TNF

According to Wong et al. (2005) and RID (2006, 2008, 2009), results of the satellite image study show that the TNF located in Myanmar west of Prachuab Khirikhun province is a 200-long northwest- to north-northwest-striking, right-lateral strike-slip fault. Based on

geomorphic expression, the fault can be classified into three sections. The first one called north section with the length of 80 km tranverses an upland area to the north of the valley of the Tenasserim river. The second one called central section with the length of 100 km is the upper reach of the Tenasserim river valley. The third one called south section with the length of 55 km is along the Tenasserim river valley. Its characteristics with the weights are tabulated in Table 5.3. The logic tree adopted for the TNF is shown in Figure 5.4.

The rupture scenarios of the TNF are specified as below.

1. **Scenario I: Unsegmentation** The rupture of the entire fault is an unlikely event because there are the width of the step-over zone about 5 km or larger between these three sections to act as barriers to rupture propagation. However, the rupture of the whole length of the fault appearing to produce the maximum earthquake of $M_w 7.6 \pm 0.3$ is still included in the hazard analysis,
2. **Scenario II: Segmentation** Due to extremely geomorphic difference between these three sections, it is believed that each fault segment ruptured in different time. According to Well and Coppersmith (1994), the length of the north, central and south sections can generate the maximum size of the earthquakes of $M_w 7.2$, 7.3 , and 7.0 , respectively. In the hazard analysis, these maximum magnitudes are also added plus and minus $M_w 0.3$.

Table 5.3 TNF model.

Fault	Total Fault Length (km)	Fault Width		Rupture Scenario				Magnitude		Slip Rate						
		(km)	Weight	Rupture Type	Weight	Rupture Length (km)	Prbability of Activity	(M)	Weight	(mm/yr)	Weight					
Tenasserim	235	10	0.2	Unsegmented	0.1	235	1.0	7.3	0.2	0.1 ¹	0.3					
		15	0.6					7.6	0.6	2 ¹						
		20	0.2					7.9	0.2	4 ^{1,2}						
				North segment	0.9	80	1.0	6.9	0.2	7.2	0.6	7.5	0.2			
								Central segment	100					1.0	7.0	0.2
															7.3	0.6
				South segment	0.9	55	1.0	6.7	0.2	7.0	0.6	7.30	0.2			
								7.0	0.6							
								7.30	0.2							

Note: data from ¹ Wong et al. (2005) ² Pailoplee (2009)

The weight of entire rupture of 0.1 is given and that of the independent rupture of 0.9 is specified. The slip rate of the TNF is assumed to be 2 mm/yr. The upper and lower bounds are prescribed to be 4 and 0.1 mm/yr, respectively.

5.1.4 KYF

The orientation, characteristic and other parameters of the KYF for the hazard analysis are derived from the reports studied by Wong et al. (2005) and RID (2006, 2008, 2009) and given in Table 5.4.

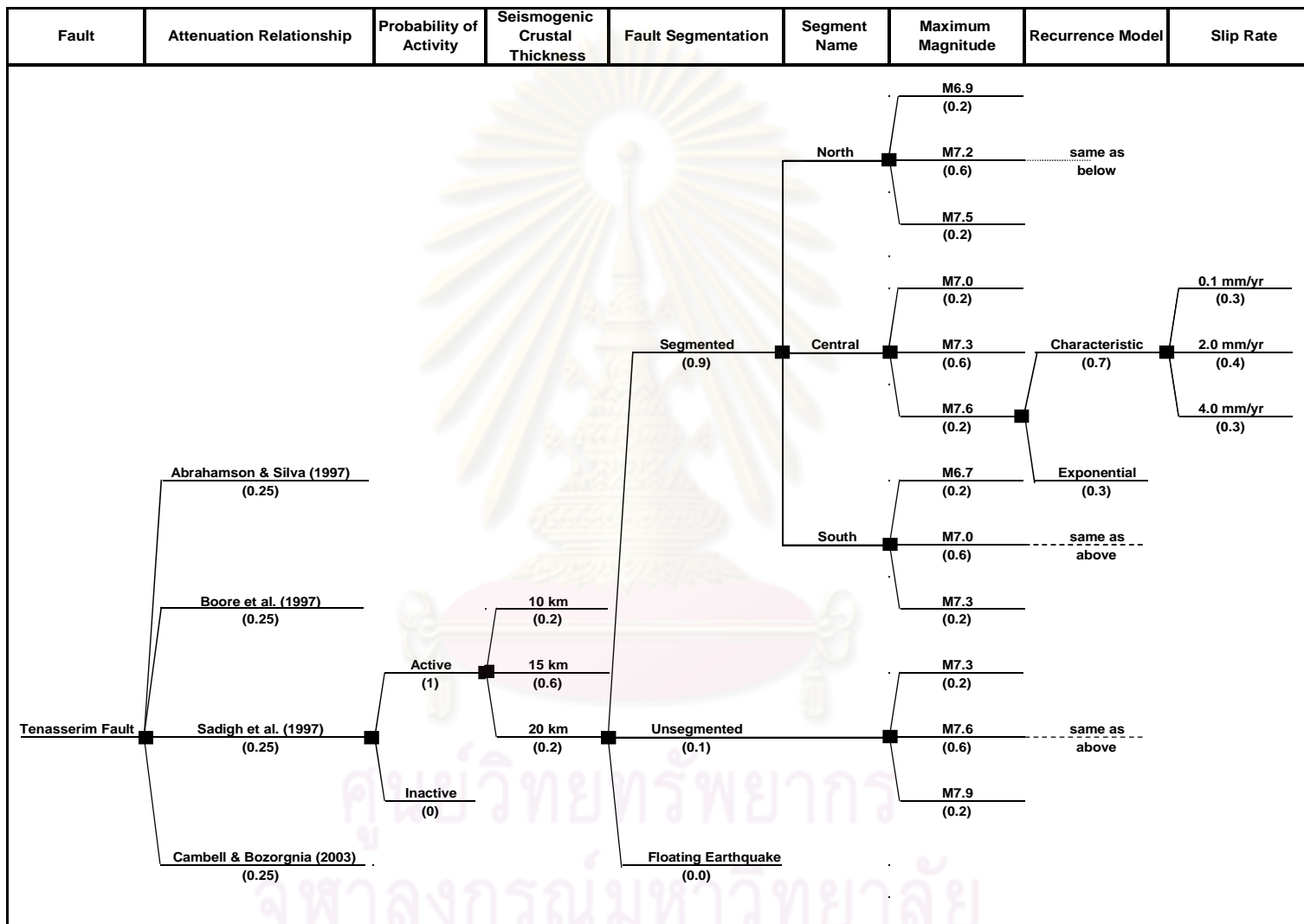


Figure 5.4 Logic tree of the TNF.

Table 5.4 KYF and TVF models.

Fault	Total Fault Length (km)	Fault Width		Rupture Scenario				Magnitude		Slip Rate			
		(km)	Weight	Rupture Type	Weight	Rupture Length (km)	Prbability of Activity	(M)	Weight	(mm/yr)	Weight		
Kungyauangale	235	10	0.2	Unsegmented	0.9	235	1.0	6.7	0.2	0.1	0.3		
		15	0.6					7.0	0.6			2.0	0.4
		20	0.2					7.3	0.2				
				Floating earthquake	0.1		1.0	6.2	0.2				
								6.5	0.6				
								6.8	0.2				
Tavoy	300	10	0.2	Unsegmented	1.0	300	1.0	7.2	0.2	1.0	0.3		
		15	0.6					7.5	0.6			4.0	0.6
		20	0.2					7.8	0.2				

It can be summarized that the KYF is 55-km long, northwest striking fault located in Tenasserim province of Myanmar. On the satellite images, the geomorphologic features of the fault indicate that it is an active right lateral strike-slip fault. The applied logic tree of the KYF is shown in Figure 5.5.

The rupture scenarios of the fault can be given as follows:

1. **Scenario I: Unsegmentation** Without the data on fault segmentation, it is assumed that the fault ruptures entirely and generates the maximum magnitude of $M_w 7 \pm 0.3$,
2. **Scenario II: Floating Earthquake** The floating earthquake of $M_w 6.5 \pm 0.3$ is also presumed to occur anywhere along the fault line.

The given occurrence weight of the entire rupture scenario is 0.9 while the floating earthquake is 0.1. Because the geomorphic expression of the KYF is similar to that of the TNF, the slip rate is supposed to be similar distribution.

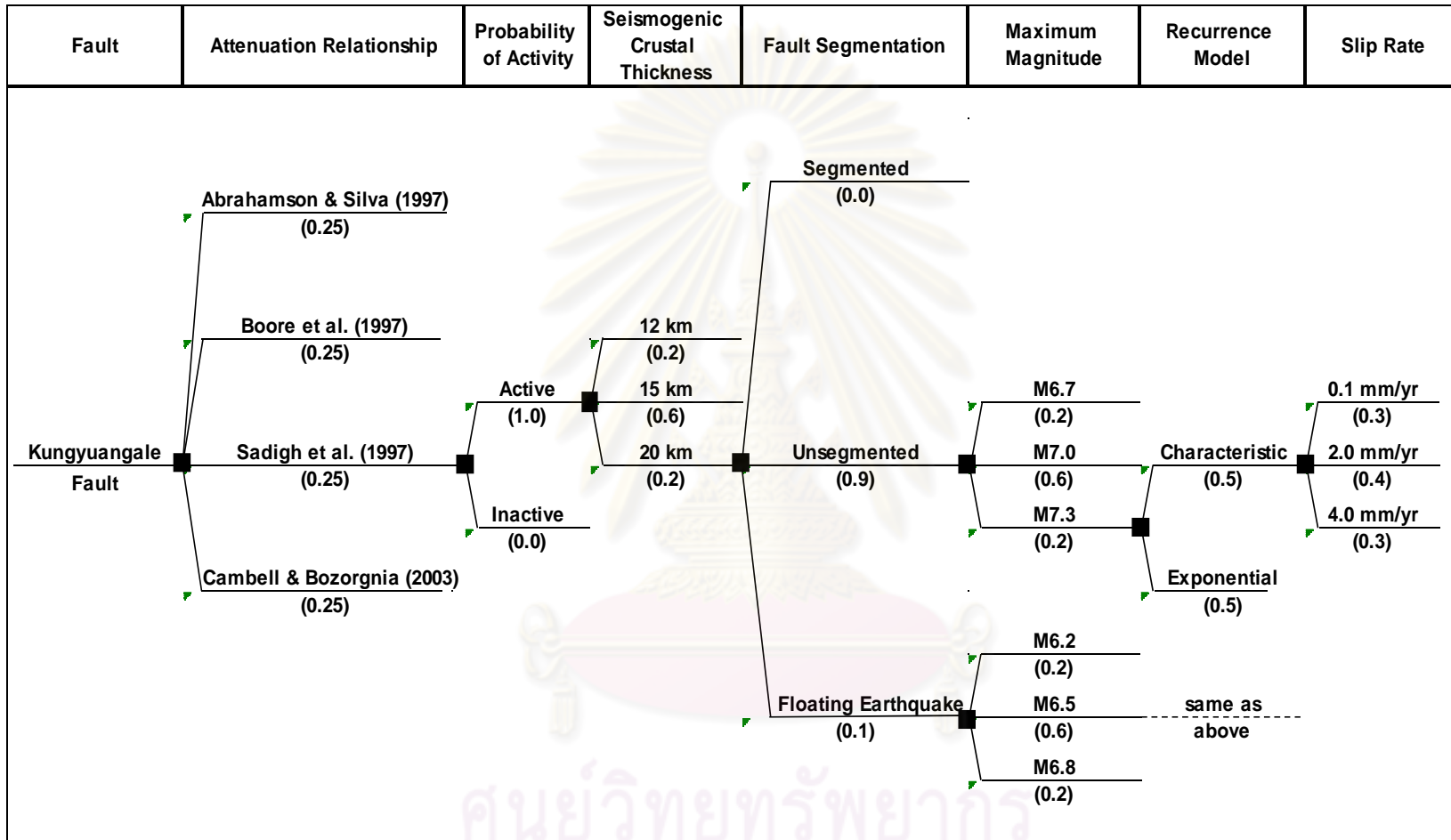


Figure 5.5 Logic tree of the KYF.

5.1.5 TVF

The characteristics of the TVF are derived from the report on the seismic hazard evaluation of Khao Laem and Srinagarind dams written by WCFS (1998) as stated in Table 5.4. The TVF is a north-northwest-striking right-lateral strike-slip fault. Results of the remote sensing analysis show that the TVF is 300 km long. The rupture behavior of the TVF is assumed to be unsegmentation in a more limited manner that generates the maximum earthquake of $M_w 7.5 \pm 0.3$. This earthquake event is believed to occur anywhere along the whole length of the fault. The slip rates of the fault are defined as 1, 4, and 10 mm/yr. The depicted logic tree of the TVF is shown in Figure 5.6.

5.1.6 TPF

The TPF is extended from Myanmar southeastward to the northwest of Kanchanaburi province, passing through the Khao Laem and Srinagarin dams. The fault orientates in the northwest-southeast direction and has right-lateral movement. In terms of geomorphology, the fault is an active structure and can be divided into four segments, namely a 165-km-long north segment (in Myanmar), a 90- to 100-km-long central segment, a 70-km-long southwest segment, and a 80-km-long southeast segment (WCFS, 1998). The characteristics can be given in Table 4.7. The logic tree for the TPF is shown in Figure 5.7.

Only the scenario of individually segmented rupture of the fault is applied as given below.

1. **North Segment** It can generate the earthquake with the maximum magnitude of $M_w 7.5 \pm 0.3$. It is more active than the other segments.

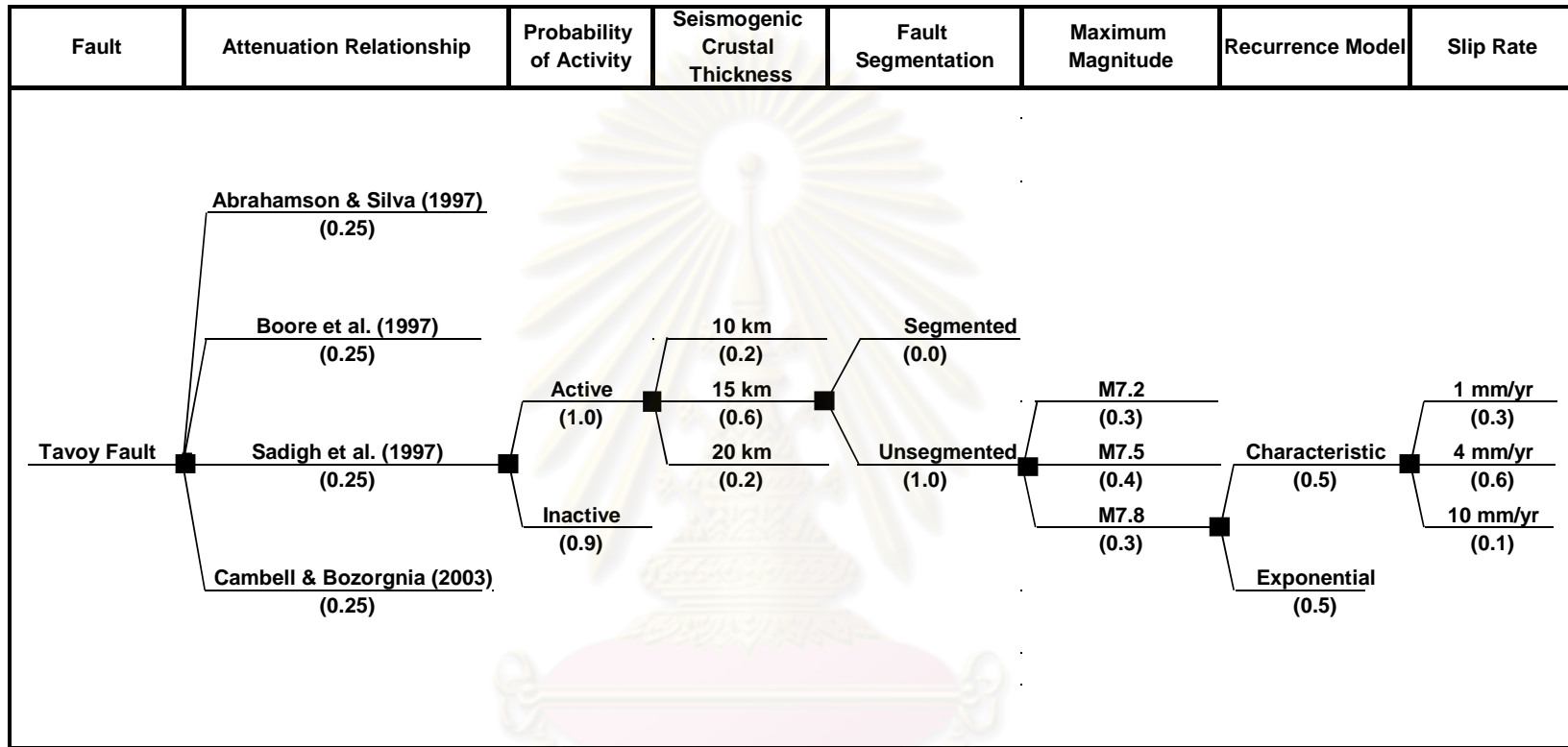


Figure 5.6 Logic tree for the TVF.

ศูนย์วิทยบริการ
จุฬาลงกรณ์มหาวิทยาลัย

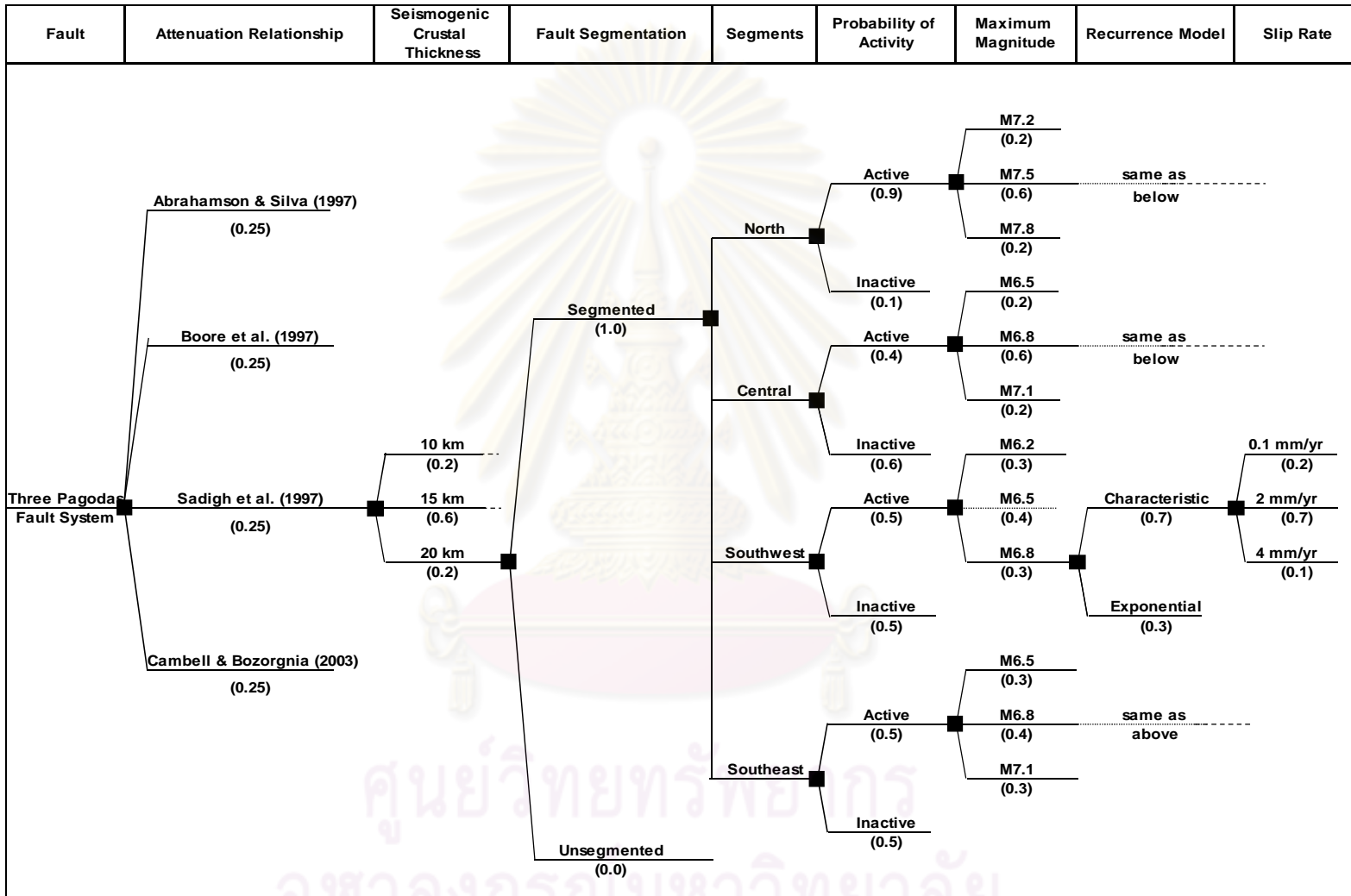


Figure 5.7 Logic tree for the TPF.

Table 5.5 TPF model.

Fault	Total Fault Length (km)	Fault Width		Rupture Scenario				Magnitude		Slip Rate			
		(km)	Weight	Rupture Type	Weight	Rupture Length (km)	Prbability of Activity	(M)	Weight	(mm/yr)	Weight		
Three Pagoda	415	10	0.2	North segment	1	165	0.9	7.2	0.2	0.1	0.2		
								7.5	0.6			2.0	0.7
								7.8	0.2				
		15	0.6	Central segment		100	0.4	6.5	0.2	6.5	0.2		
								6.8	0.6				
								7.1	0.2				
		20	0.2	Southwest		70	0.5	6.2	0.3	6.5	0.4		
								6.5	0.4				
								6.8	0.3				
		Southeast	80	0.5		80	0.5	6.5	0.3	6.5	0.3		
								6.8	0.4				
								7.1	0.3				

Based on the prominently geomorphologic evidence, it is assigned the weight of activity of 0.9

2. **Central Segment** The central segment can produce the maximum size of the earthquake of M_w 6.8 ± 0.3 . Due to less evidence of activity than other segments, the weight of activity is assumed to be 0.4.
3. **Southwest Segment** The maximum magnitude is calculated to be M_w 6.5 ± 0.3 . The fault segment is given the weight of activity equal to 0.5 because uncertainty of activity appears for this segment.
4. **Sotheast Segment** The maximum magnitude of M_w 6.8 ± 0.3 can be generated from this fault segment. As similar reasons to the southwest segment, the weight of activity is specified as 0.5.

The maximum slip rate for all segments is based on the slip rate of 4 mm for the Red River fault in Vietnam (Allen et al., 1984) while the minimum slip rate is in accordance to the slip rate of 0.1 for the active fault with recognizable tectonic geomorphology in Thailand (Fenton et al., 2003). The preferred slip rate for the north segment where is located nearby the more active Sagiang fault is assigned as 2 mm/yr while that for the remaining segments is applied as 4 mm/yr (WCFS, 1998).

5.1.7 Sumatra-Andaman Subduction Zone

The Sumatra-Andaman subduction zone or Sunda subduction zone can be divided into four major sections: the Burma, Northern Sumatra-Andaman, Southern Sumatra, and Java zones (Petersen et al., 2007). The Northern Sumatra-Andaman section appears to be the most significant zone affecting the ground shaking in the southern Thailand. This section is included in the hazard analysis. The earthquakes occurring in the section can be divided into two types as follows:

1. **Megathrust** The megathrust earthquake happens along an interplate boundary separating a subducting plate and an overlying plate. The maximum magnitude of M_w 9.1 (Park, 2005) detected on 26 December 2004 is adopted in the hazard analysis. The subduction rate is in the range of 20 mm/yr to 40 mm/yr with the higher rate to the south (Rajendran et al., 2007; Socquet et al. (2006); and Chlieh et al., 2006).
2. **Intraslab Zone** The earthquake occurs within the subducting plate. The largest historical earthquake was recorded as M_w 7.3 aftershock of the great 2004 Sumatra-Andaman mainshock.

The earthquake produced from the megathrust with the magnitude of $M_w 9.1 \pm 0.3$ is considered in the hazard analysis. On the contrary, the earthquake generated from the intraslab is excluded in the analysis because the intensity of earthquakes originated from the intraslab rapidly decrease with the distance (Atkinson & Boore, 2003).

The characteristics of the megathrust applied in the hazard analysis are summarized in Table 5.6. The logic tree for the Sumatra-Andaman megathrust earthquake is illustrated in Figure 5.8.

Table 5.6 Megathrust of Sumatra-Andaman subduction zone and Ratchaphra reservoir.

Fault	Fault Width		Rupture Scenario			Magnitude		Slip Rate	
	(km)	Weight	Rupture Type	Weight	Prbability of Activity	(M)	Weight	(mm/yr)	Weight
Megathrust	40	1.0	Unsegmented	1.0	1.0	8.9	0.2	20	0.5
Sumatra-Andaman						9.1	0.6	40.0	0.5
subduction zone						9.3	0.2		
Ratchaphra	8	0.2	Floating earthquake	1.0	1.0	5.0	0.2		
reservoir area	10	0.6				5.5	0.6		
	15	0.2							

5.1.8 Ratchaphra Reservoir Area

The construction of the Ratchaphra dam was completed on June 1988. Twenty four reservoir-triggered seismicities (RTS) with the magnitudes of $M_L 0.4-3.4$ occurred from June 1988 to December 1993 due to impoundment of the Ratchaphra reservoir (TEAM, 1995). The latest RTS event of $M_L 1.4$ was recorded by the EGAT on 27 October 2006.

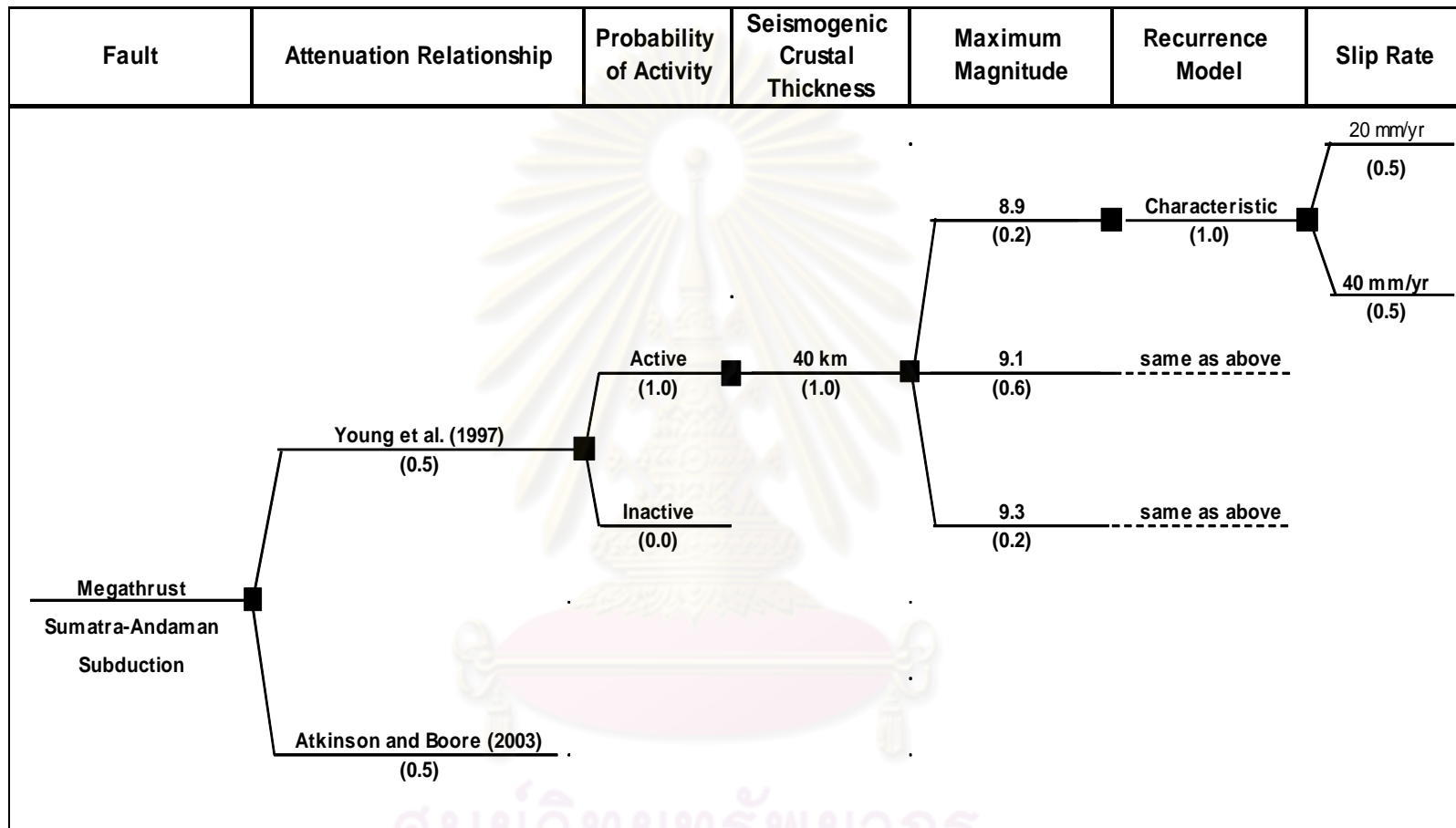


Figure 5.8 Logic tree for the Sumatra-Andaman megathrust earthquake.

In the hazard analysis, the preferred seismogenic depth of the RTS is 10 km based on the RTS recorded at the reservoirs of Srinagarind and Wachiralongkorn dams (Wong, 2005) and the maximum magnitude is M 5.5 (WCFS, 1998). The application of the logic tree can be written as in Figure 5.9 and characteristics are given in Table 5.6.

5.2 Earthquake Recurrence

There are a few earthquakes associated with all fault sources in southern Thailand and adjacent areas as shown in Figure 5.10, except the Sumatra-Andaman subduction zone.

It is not possible to develop the recurrence relationships of each fault source. So, the application of all available background (floating or random) earthquakes (all fault-associated earthquakes to be removed) to estimate the earthquake recurrence in the region are required

5.2.1. Southern Thailand and Adjacent Areas

The recurrence relationships of the background earthquakes in the southern Thailand and adjacent areas was developed by Wong (2005) using the earthquake events collected from the past to 2005. Those earthquakes are located within 500 km distance around the Tha Sae dam site, Tha Sae district, Chumporn province covering the southern, eastern, western and central Thailand, and the Andaman Sea. Additionally, this study compiled and classified independent earthquake events from 2005 to 2008. Totally, 47 earthquake events were obtained for evaluation. Their epicenters are shown in Figure 5.11. These events are classified as quantity of earthquakes in 0.5 M_w magnitude interval as given in Table 5.7. The study area is approximately 800,500 km². Then, the recurrence

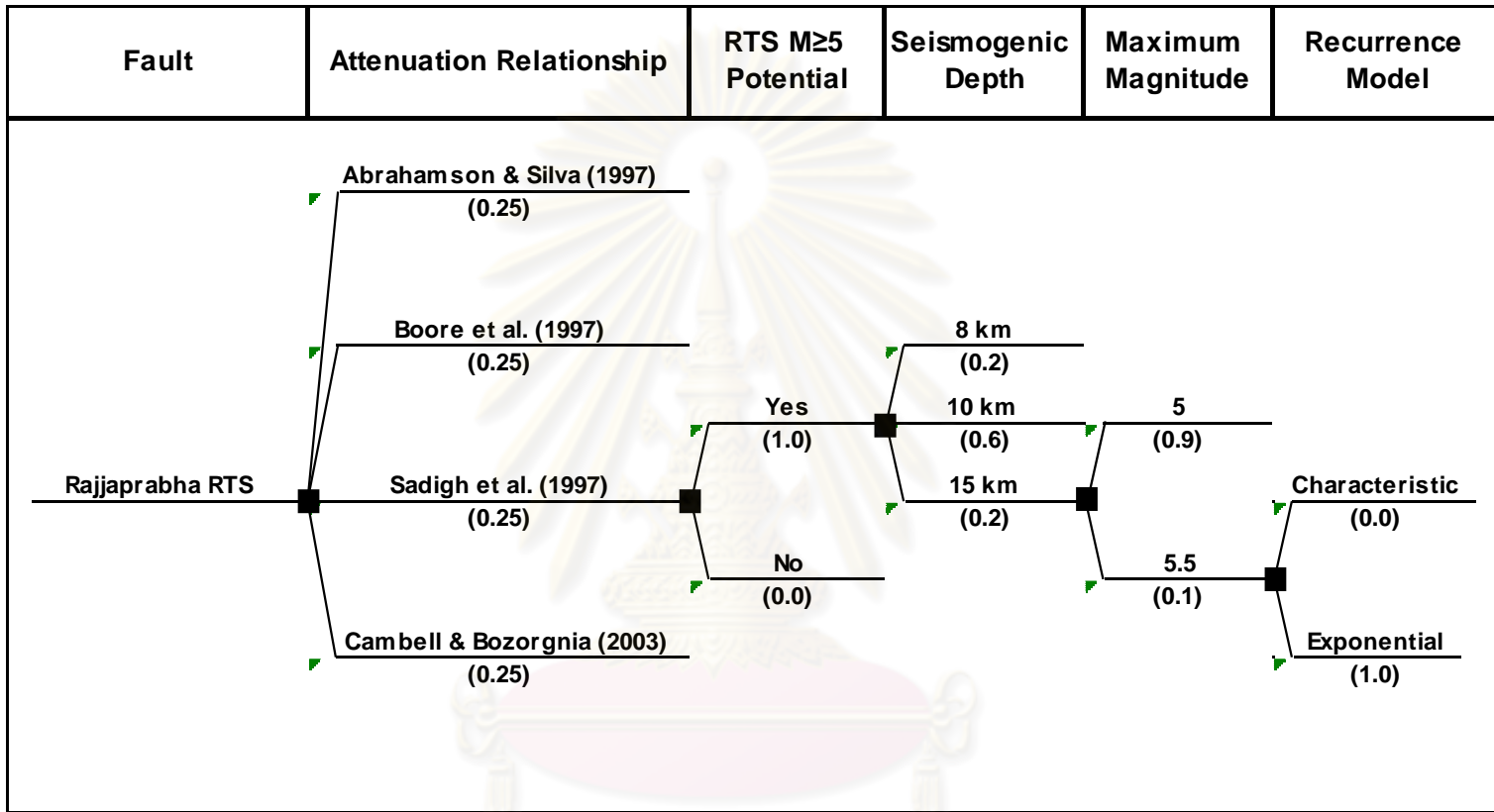


Figure 5.9 Logic tree for the Ratchaprabha RTS.

ศูนย์วิทยทรัพยากร
จุฬาลงกรณ์มหาวิทยาลัย

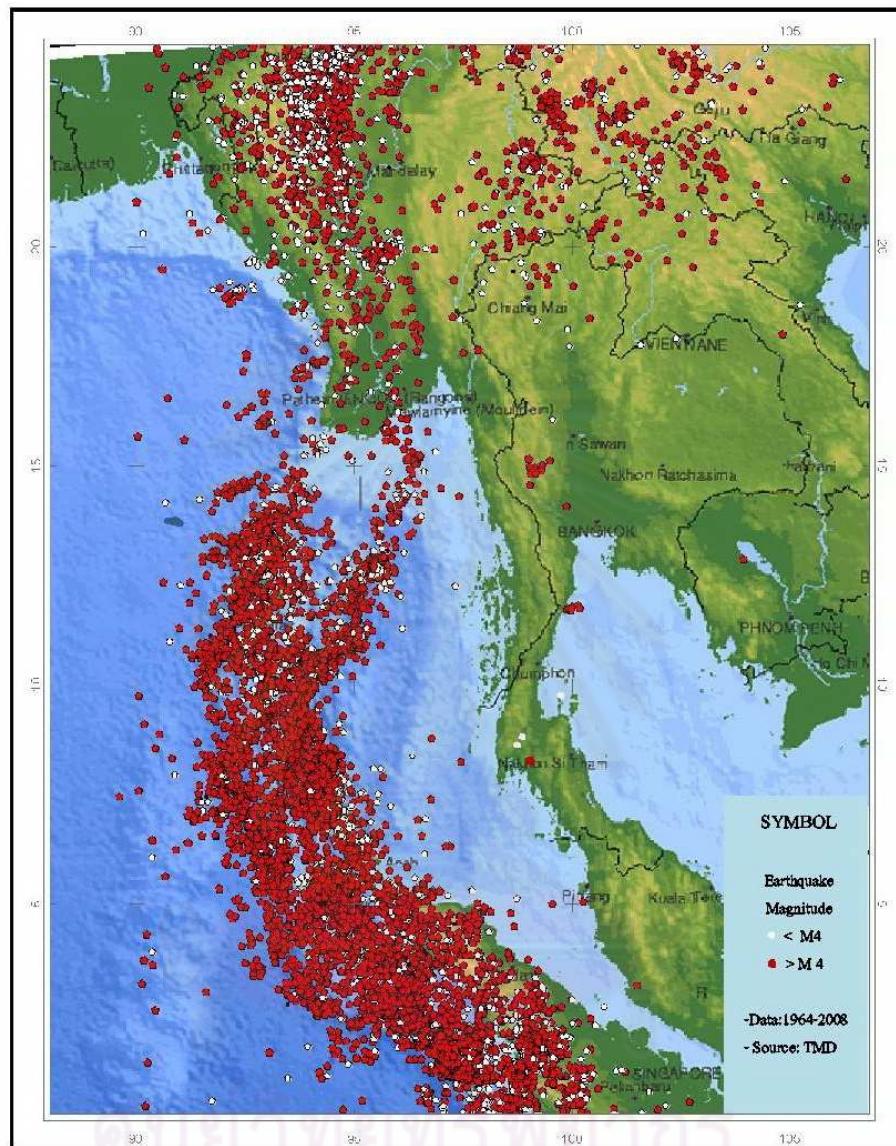


Figure 5.10 Map of epicenters for the period of 1964-2008, data obtained from the TMD.

curve is plotted as shown in Figure 5.12. The computed recurrence curve fits the data quite well. The b-value is 1.03 (almost equal to the global average of 1.00) with the standard deviation (σ) of 0.04.

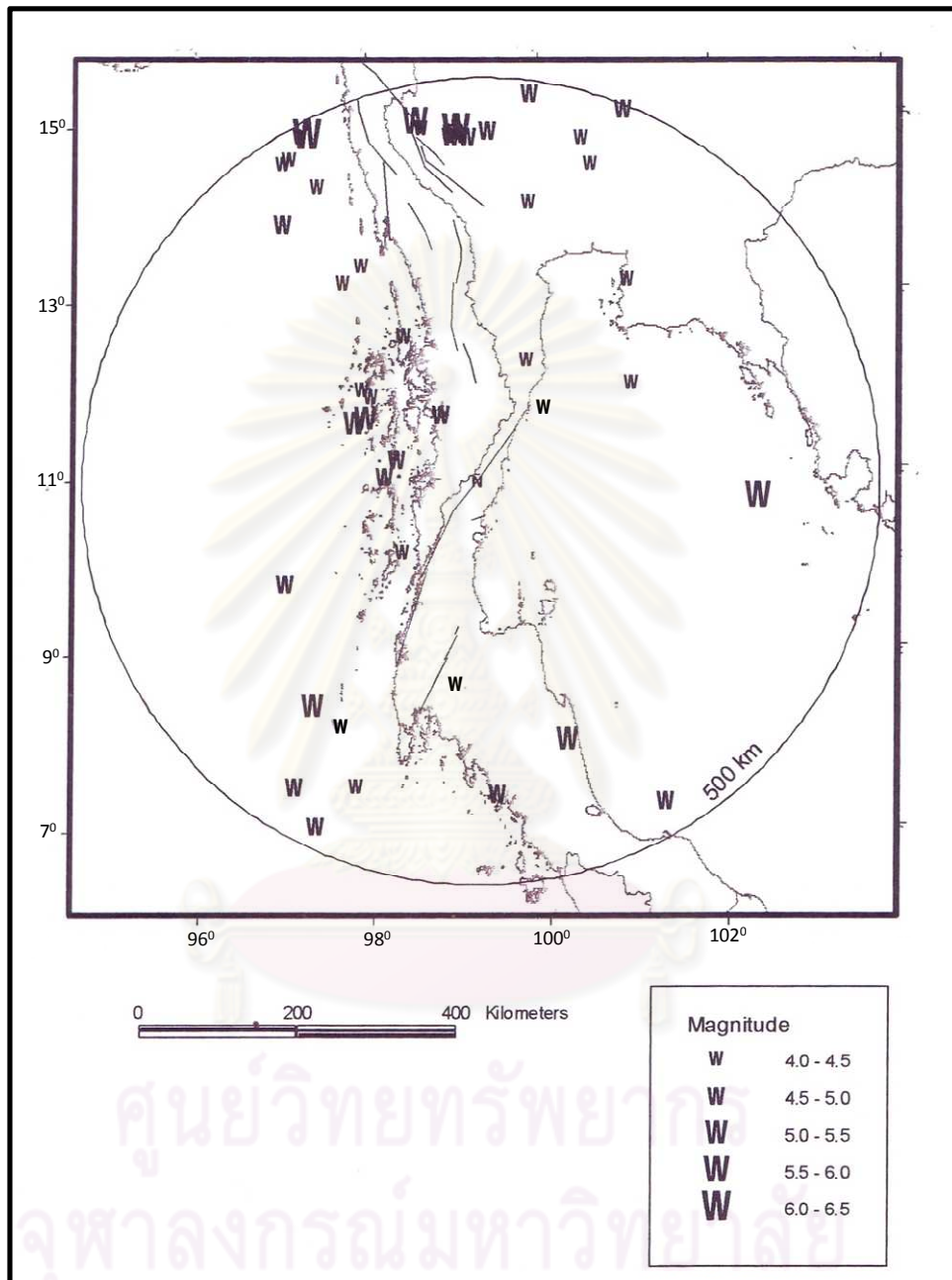


Figure 5.11 Map showing epicenters used in the calculation of crustal earthquake recurrence (modified from Wong, 2005).

Table 5.7 Earthquake catalog completeness and number of events used in recurrence for southern Thailand and adjacent areas.

Magnitude Range (M)	Time Period	Number of Events
4.0 - 4.5	1982 - 2008	20
4.5 - 5.0	1965 -2008	18
5.0 - 5.5	1965 -2008	4
5.5 - 6.0	1900 - 2008	2
6.0 - 6.5	1768 - 2008	2
6.5 -7.0	1968 - 2008	1

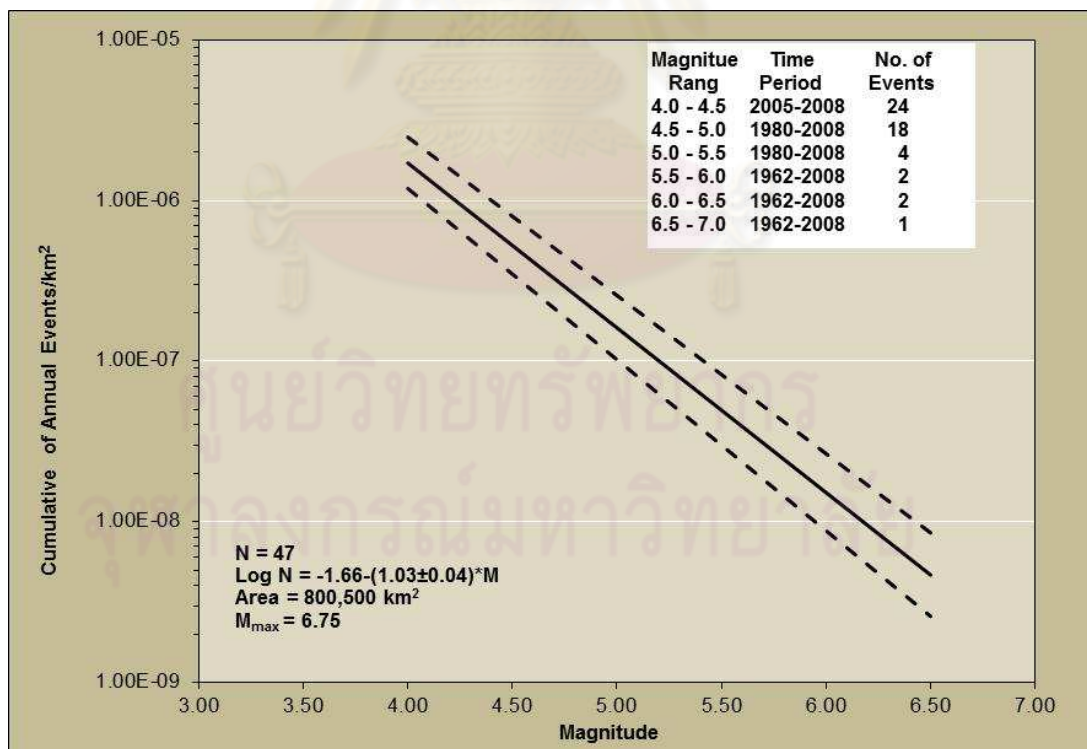


Figure 5.12 Earthquake recurrence for southern Thailand and adjacent areas.

5.2.2 Sumatra-Andaman Subduction Zone

In similar to the recurrence calculation of the southern Thailand and adjacent areas, the recurrence of the Sumatra-Andaman subduction zone can be analyzed. The earthquake data with the magnitude of M_w 4.0-7.5 were compiled from the past to 2008. The total 522 independent were defined and then were classified as the number of earthquakes in each 0.5 M_w magnitude range as given in Table 5.8. After that the recurrence curves including the mean and plus and minus one standard deviation were depicted as shown in Figure 5.13. The b-value is 0.91 (almost equal to the global average of 1.00) with the standard deviation (σ) of 0.05.

Table 5.8 Earthquake catalog completeness and number of events used in recurrence for the Sumatra-Andaman subduction zone.

Magnitude Range (M)	Time Period	Number of Events
4.0 - 4.5	2005 - 2008	24
4.5 - 5.0	1980 -2008	299
5.0 - 5.5	1980 -2008	122
5.5 - 6.0	1962 - 2008	57
6.0 - 6.5	1962 - 2008	11
6.5 -7.0	1962 - 2008	6
7.0-7.5	1962 - 2008	3

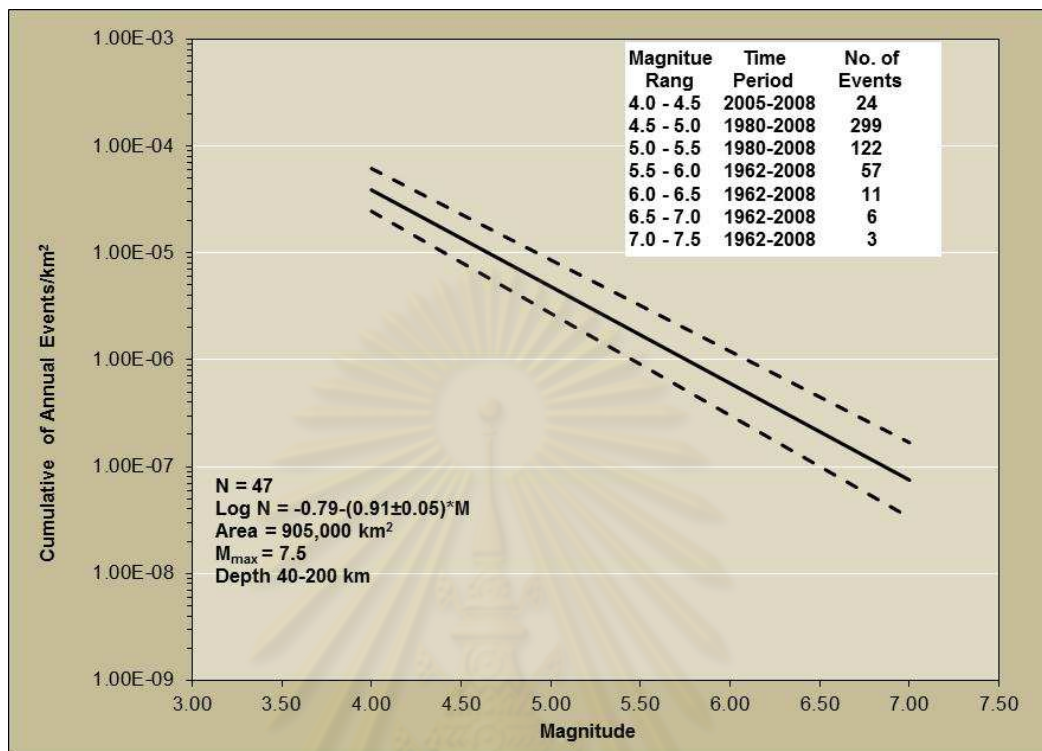


Figure 5.13 Earthquake recurrence for the Sumatra-Andaman subduction zone.

5.2.3 Western Thailand

The background earthquakes in the western part of Thailand at which the TPF is located covering the area of 86,540 km² are compiled. The earthquake data from the past to 1997 were collected by WCFC (1998) and that from 1998 to 2009 were gathered by this study. A number of independent earthquakes in the study area is totally 44 events. These events are classified into each magnitude interval of 0.5 M_w as given in Table 5.9. The recurrence relationship is received as shown in Figure 5.14. The b-value is equal to 0.94 ± 0.16.

Table 5.9 Earthquake catalog completeness and number of events used in recurrence for western Thailand.

Magnitude Range (M)	Time Period	Number of Events
3.0 - 3.5	1982 - 2010	12
3.5 - 4.0	1976 - 2010	12
4.0 - 4.5	1963 - 2010	14
4.5 - 5.0	1768 - 2010	0
5.0 - 5.5	1768 - 2010	6

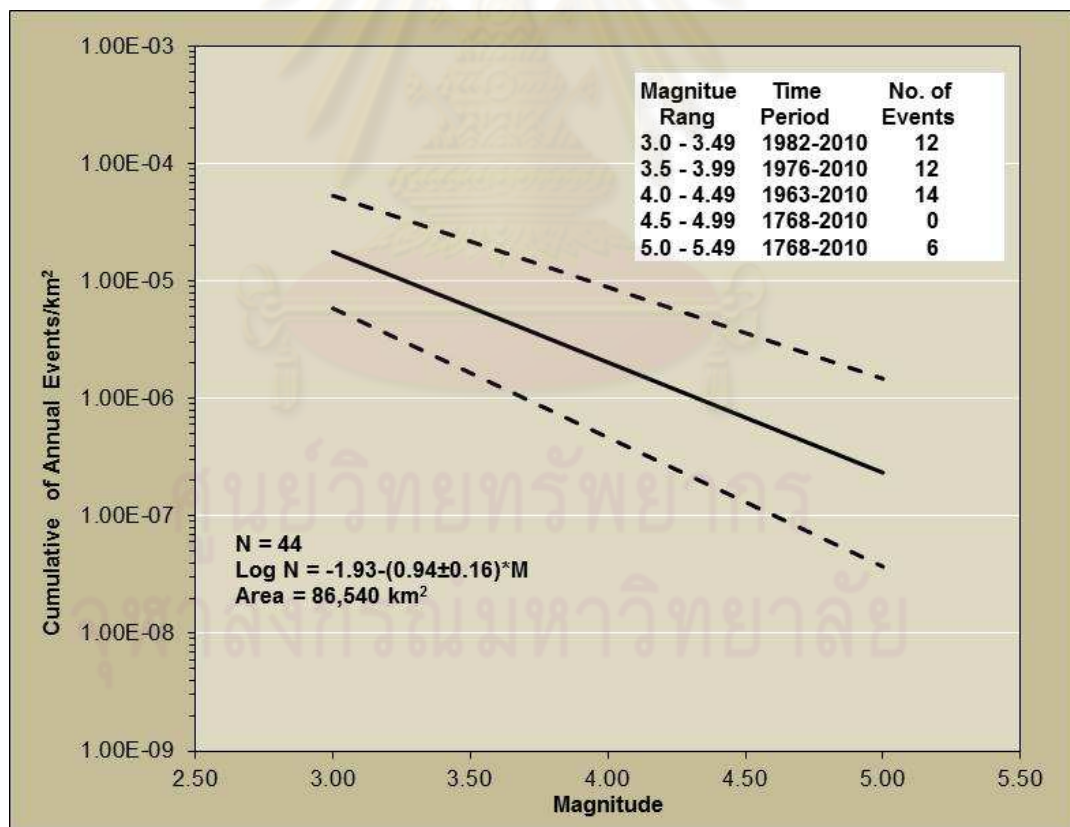


Figure 5.14 Earthquake recurrence for western Thailand.

5.3 Probabilistic Seismic Hazard Map Development

Steps of development of the probabilistic seismic hazard maps for the southern Thailand can be described as the following:

5.3.1 Computation of Annual Rate of Exceedance

The annual rate of exceedance values of the assigned sites are calculated with the relationships 4.3 to 4.10 by using the CRISIS 2007 computer program developed by Ordaz et al. (2007) (input data for this program is summarized in Appendix C). The analyses were performed at two hundred twenty four sites in southern Thailand covering the southernmost Yala province northward to Phetchaburi province. The sites are determined by a grid system basis starting from latitude of 5.58°N northward to 13.5°N , and longitude of 97.5°E eastward to 102.12°E as shown in Figure 5.15.

The computation of the mean annual rate of exceedance of the site with specified acceleration and time periods was carried out for all branches of the proposed logic trees. After that in each branch of the logic tree, the derived annual rate of exceedances were multiplied by the total weight of the branch with using the Microsoft Excel program. Then, summation of annual rate of exceedance for each assigned time period and rock ground acceleration from all logic tree branches of each earthquake source was undertaken.

5.3.2 Establishment of Hazard Curves

As above-mentioned, for each earthquake source the received values of mean the annual rate of exceedances were taken to plot the mean hazard curves at the selected site. The mean hazard curve of the site is the combination of all sources-produced hazard

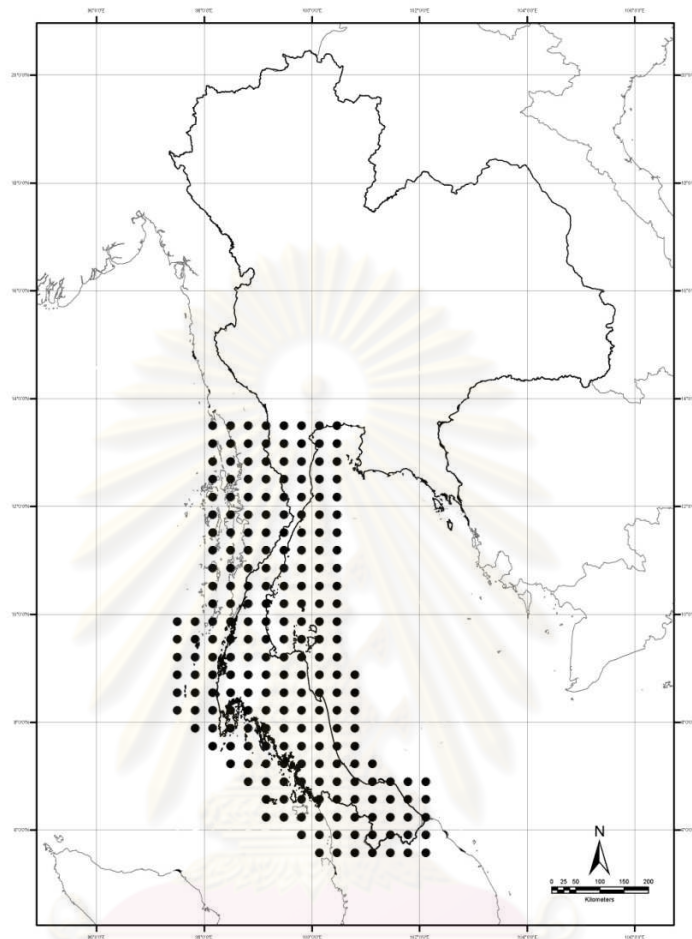


Figure 5.15 Location map showing 224 sites (black circles) performed the PSHA.

curves. As a result, there are four mean hazard curves for each site. They are composed of a mean peak horizontal acceleration and mean 0.2-, 0.3-, and 1.0-second horizontal spectral acceleration hazard curves (Appendix F). For example, the mean peak horizontal acceleration hazard curve of the site at longitude of 98.82°E and latitude of 9.59°N can be depicted as shown in Figure 5.16. The different seismic sources contribute the different values of the ground motion (acceleration) at the site. It can be seen that the contribution of

the various seismic sources to the mean peak horizontal hazard at this site. The KMF controls the peak horizontal acceleration hazard up to the return period of 100 years and then the RNF controls at the longer return periods. The least contribution is derived from the TPF

5.3.3 Development of Hazard Maps

The probabilistic seismic hazard maps generated in this study are derived from seismic hazard curves calculated on a grid of sites across southern Thailand and express the peak ground acceleration and spectral acceleration at 0.2, 0.3, and 1.0 seconds for 500, 1,000, 2,500 and 10,000 years corresponding to 10%, 5%, 2% and 0.5% probabilities of exceedance in 50 years. From the hazard curves, the peak ground and spectral accelerations for given time period can be read from the curve when the annual rate of exceedance is known. Based on the equation 3.19, the annual rate of exceedance can be calculated from the probability of exceedance in specified time period. So, 10%, 5%, 2% and 0.5% probabilities of exceedance in 50 years equal to the annual rate of exceedances of approximately 0.002, 0.001, 0.0004, and 0.0001, respectively. An example of determination of mean peak ground acceleration for 500, 1,000, 2,500 and 10,000 years or 10%, 5%, 2% and 0.5% probabilities of exceedance in 50 years at the site with longitude of 98.82°E and latitude of 9.59°N can be shown in Figure 5.17. It can be seen that the mean peak ground accelerations for 10%, 5%, 2% and 0.5% probabilities of exceedance in 50 years are equivalent to 0.158g, 0.192g, 0.255g, and 0.346g, respectively. Similarly, these peak ground computations have to be carried out for all another 223 sites. Then hazard maps are prepared by drawing the contour lines of equal acceleration. Finally, 16 hazard maps are prepared.

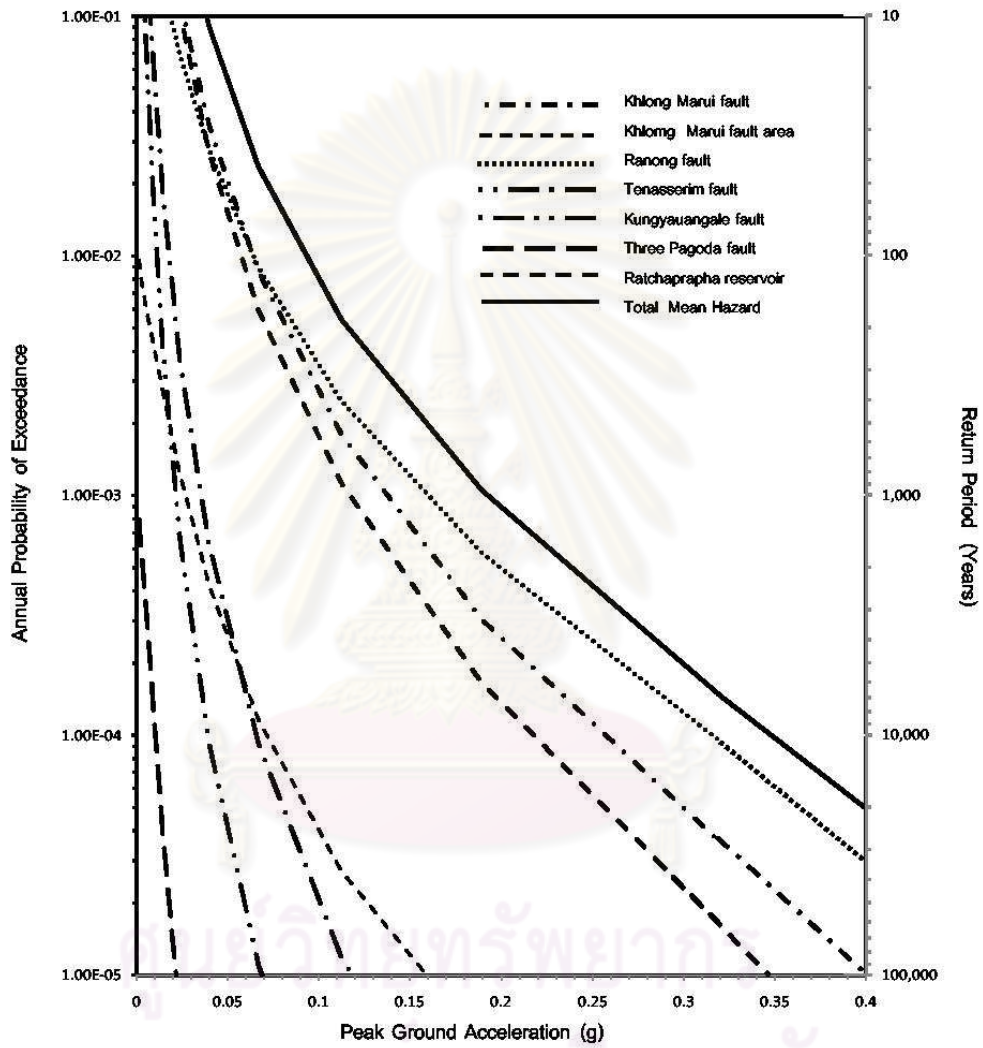


Figure 5.16 Mean peak horizontal acceleration hazard curve contributed from various seismic sources at the site with longitude of $98.82^{\circ}E$ and latitude of $9.59^{\circ}N$.

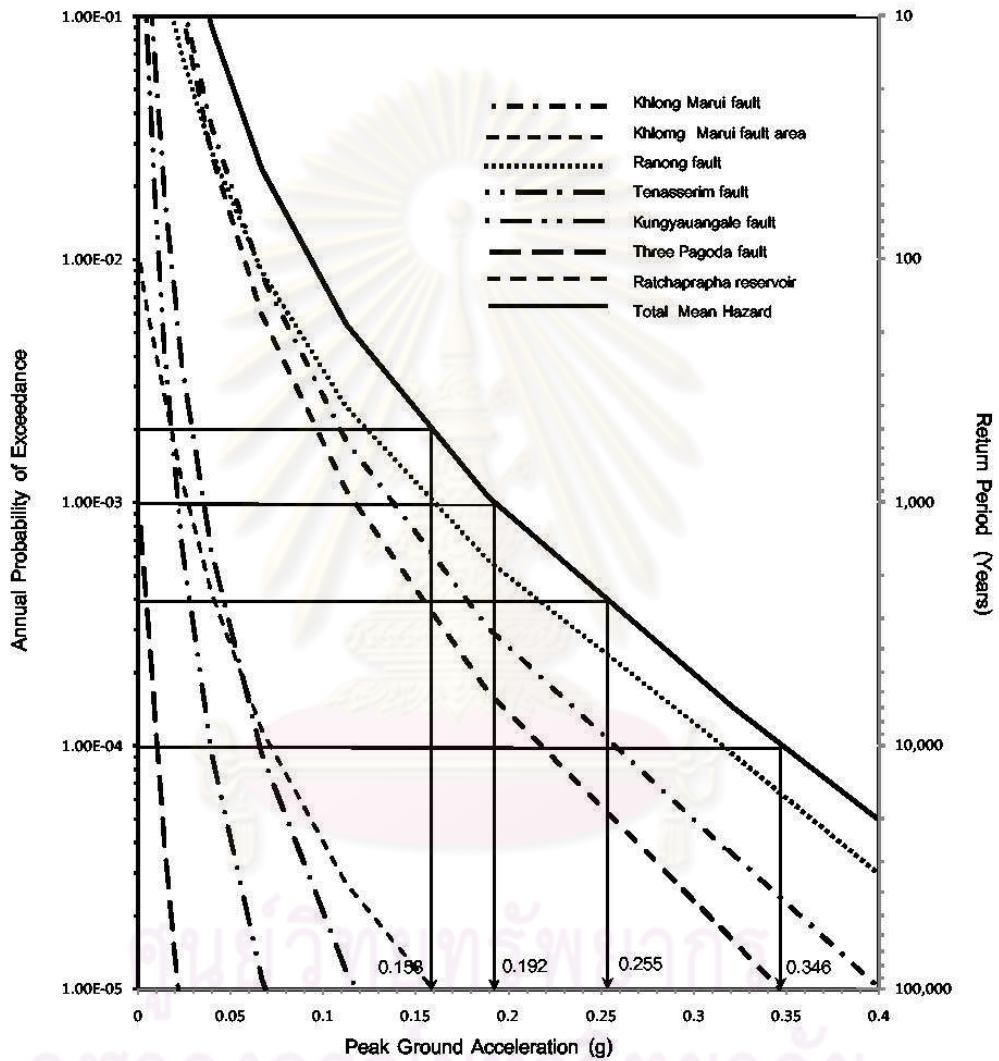


Figure 5.17 Mean peak ground accelerations for 10%, 5%, 2% and 0.5% probabilities of exceedance in 50 years at the site with longitude of $98.82^{\circ}E$ and latitude of $9.59^{\circ}N$.

The hazard maps of southern Thailand showing mean peak ground accelerations and the spectral acceleration at 0.2, 0.3, and 1.0 seconds with a 10%, 5%, 2% and 0.5% probability of exceedance in 50-year hazard levels for rock site condition are shown in Figure 5.18 to 5.33. It can be concluded that the highest hazard areas are mainly Surat Thani province, and some parts of northern Krabi, eastern Phang Nga and northern Nakhon Sri Thammarat provinces while the lowest hazard areas are deepest southern part of Thailand consisting of Yala, Pattani and Narathiwat provinces. The ranges of accelerations at specified time period with defined return periods for each province in southern Thailand can be summarized as given in Table 5.10..



ศูนย์วิทยทรัพยากร
จุฬาลงกรณ์มหาวิทยาลัย

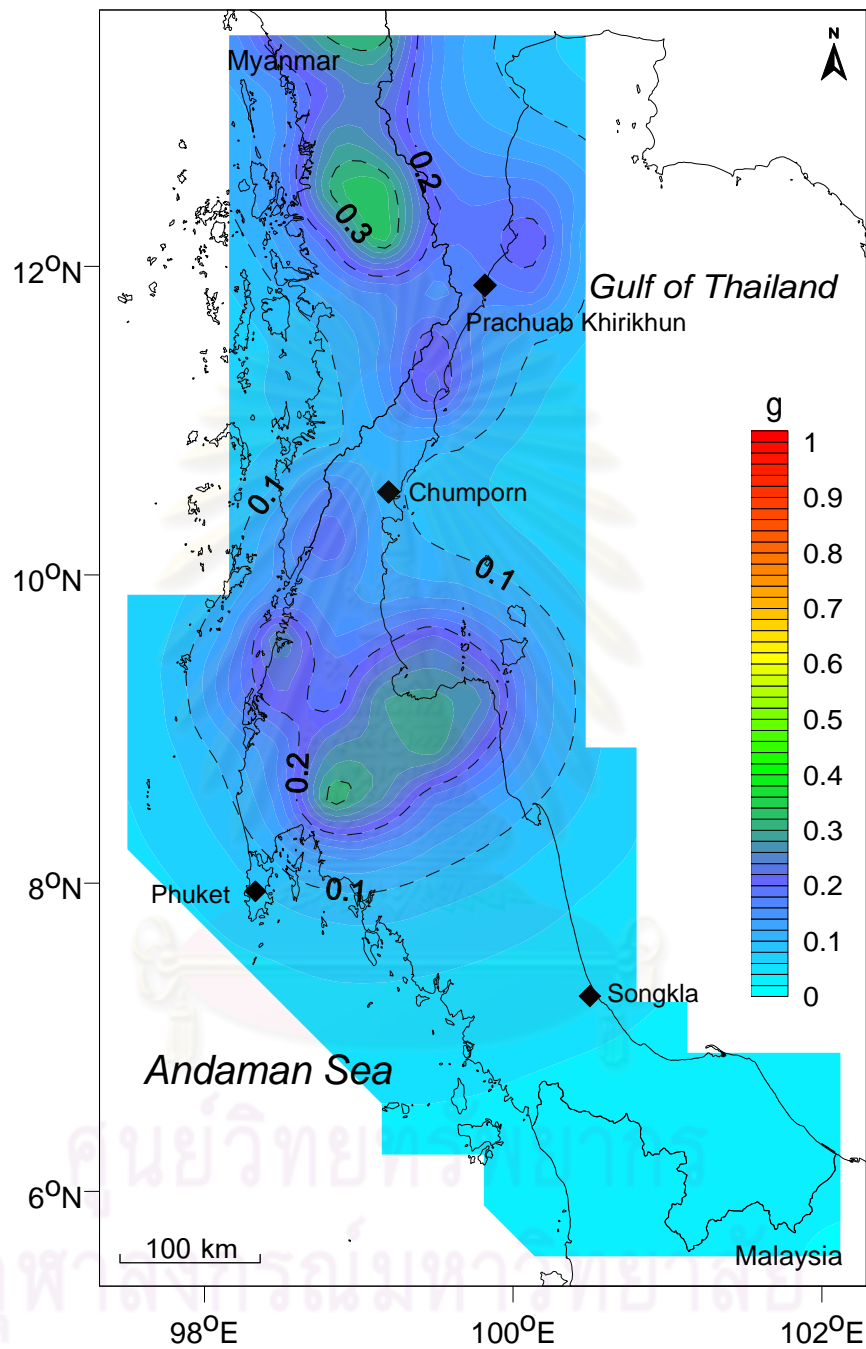


Figure 5.18 Seismic hazard map showing mean peak horizontal acceleration with 10% probability of exceedance in 50 years or for 500 years for the rock site condition in southern Thailand.

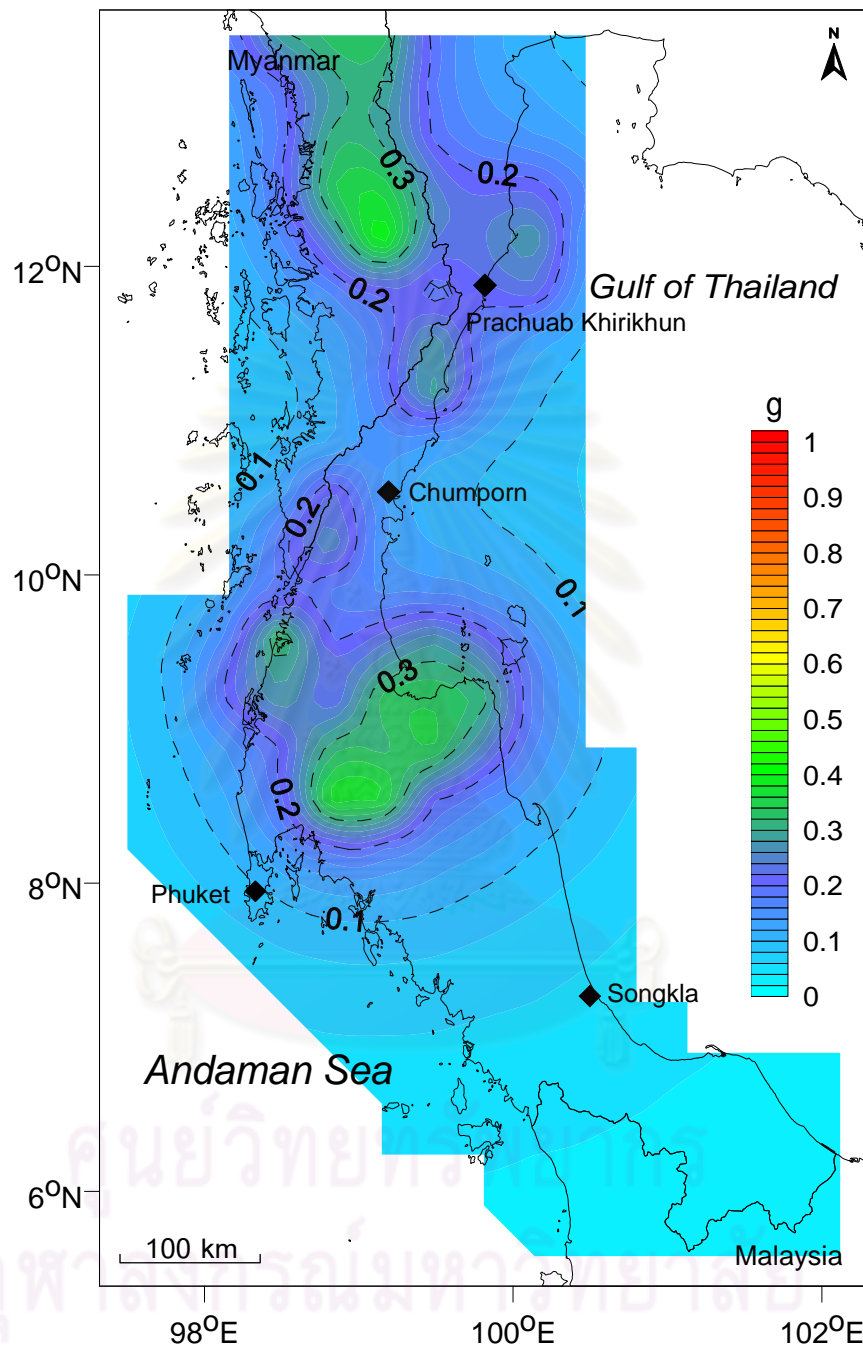


Figure 5.19 Seismic hazard map showing mean peak horizontal acceleration with 5% probability of exceedance in 50 years or for 1,000 years for the rock site condition in southern Thailand.

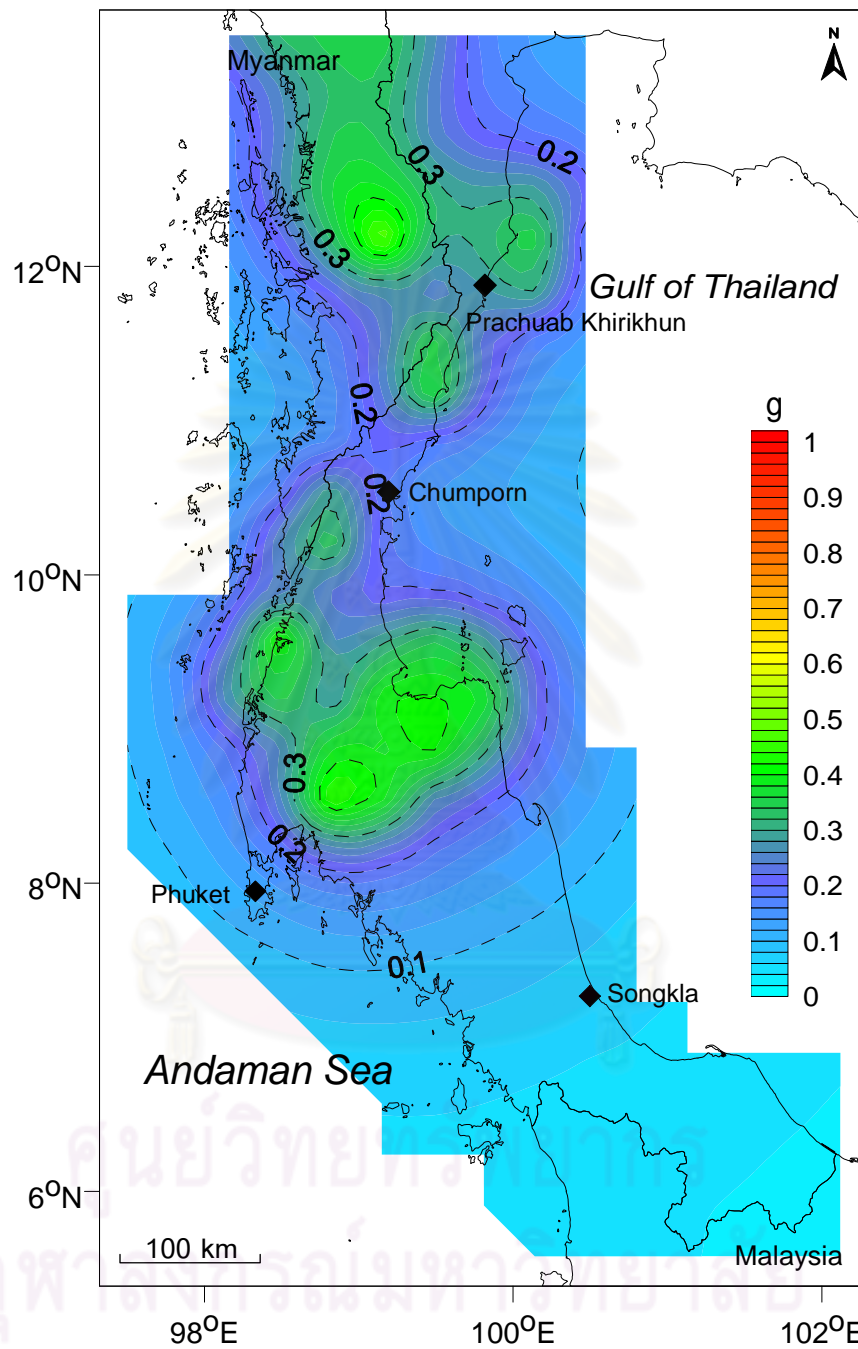


Figure 5.20 Seismic hazard map showing mean peak horizontal acceleration with 2% probability of exceedance in 50 years or for 2,500 years for the rock site condition in southern Thailand.

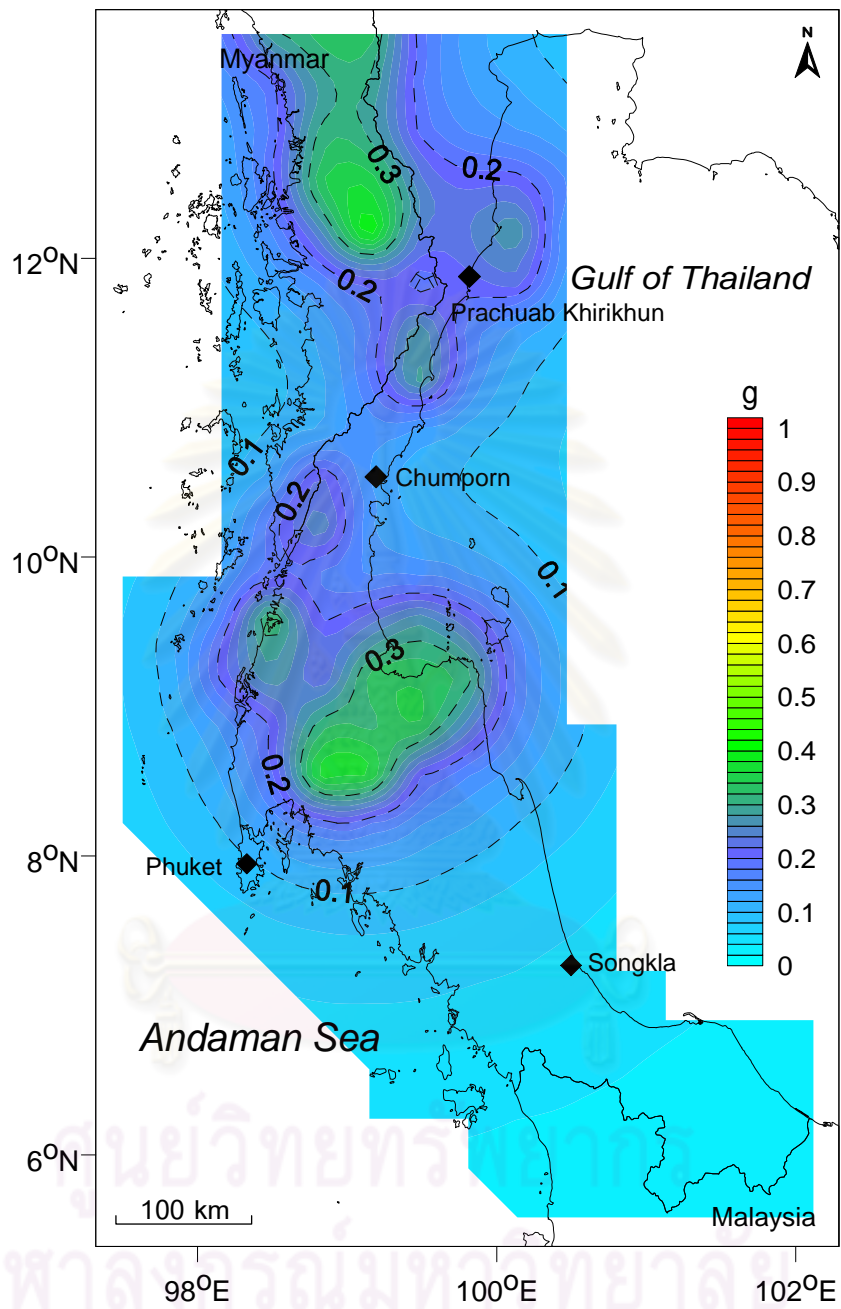


Figure 5.21 Seismic hazard map showing mean peak horizontal acceleration with 0.5% probability of exceedance in 50 years or for 10,000 years for the rock site condition in southern Thailand.

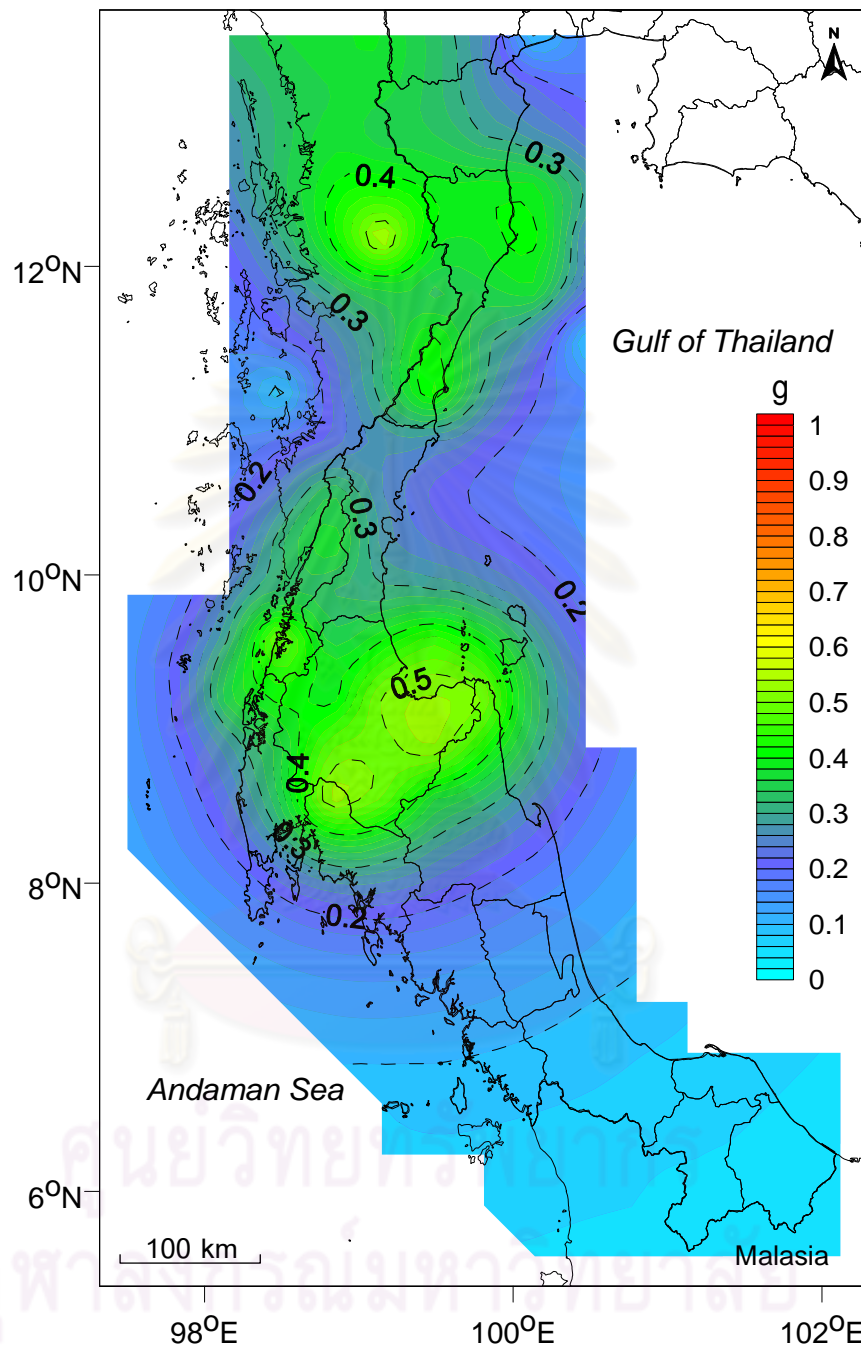


Figure 5.22 Seismic hazard map showing mean 0.2 sec horizontal spectral acceleration with 10% probability of exceedance in 50 years or for 500 years for the rock site condition in southern Thailand.

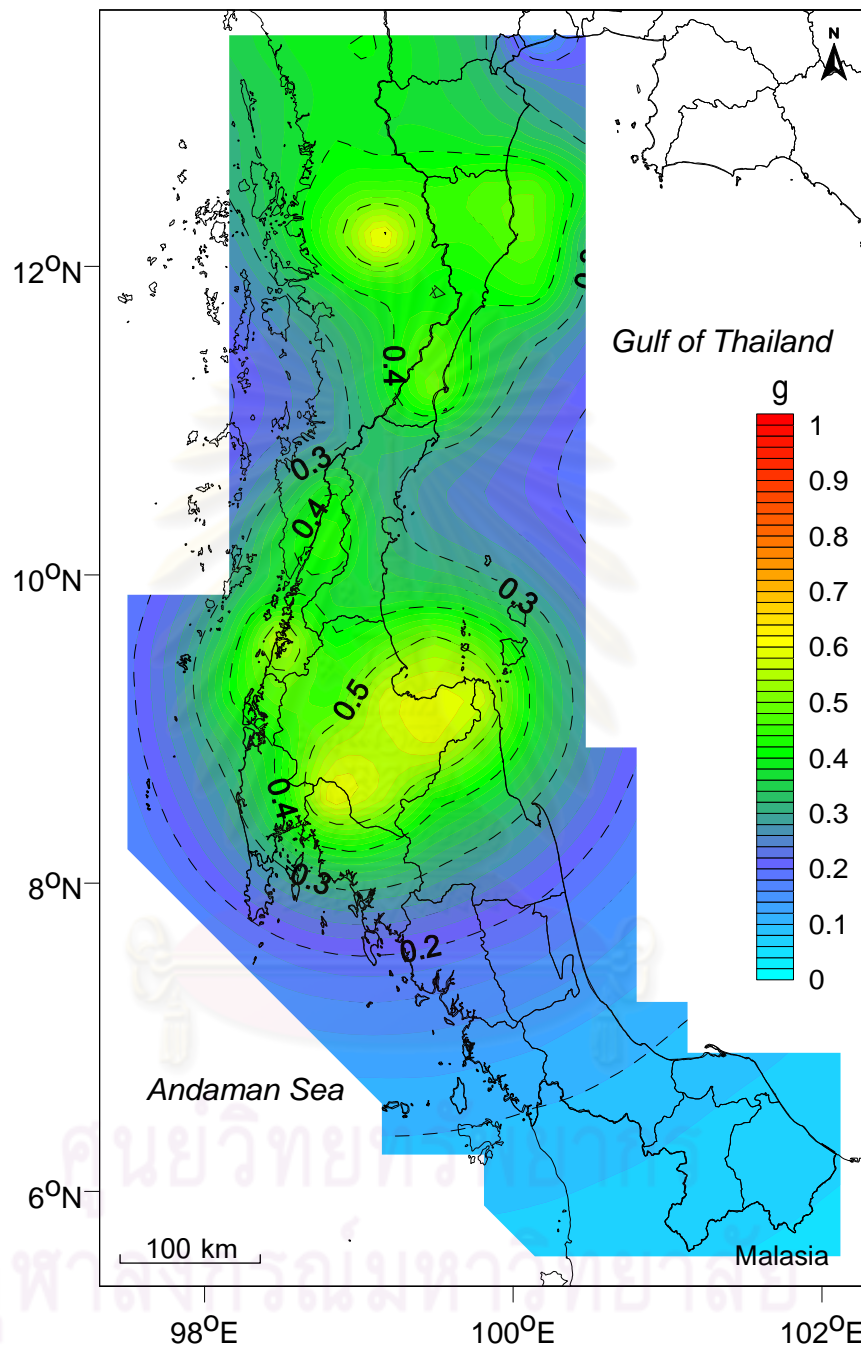


Figure 5.23 Seismic hazard map showing mean 0.2 sec horizontal spectral acceleration with 5% probability of exceedance in 50 years or for 1,000 years for the rock site condition in southern Thailand.

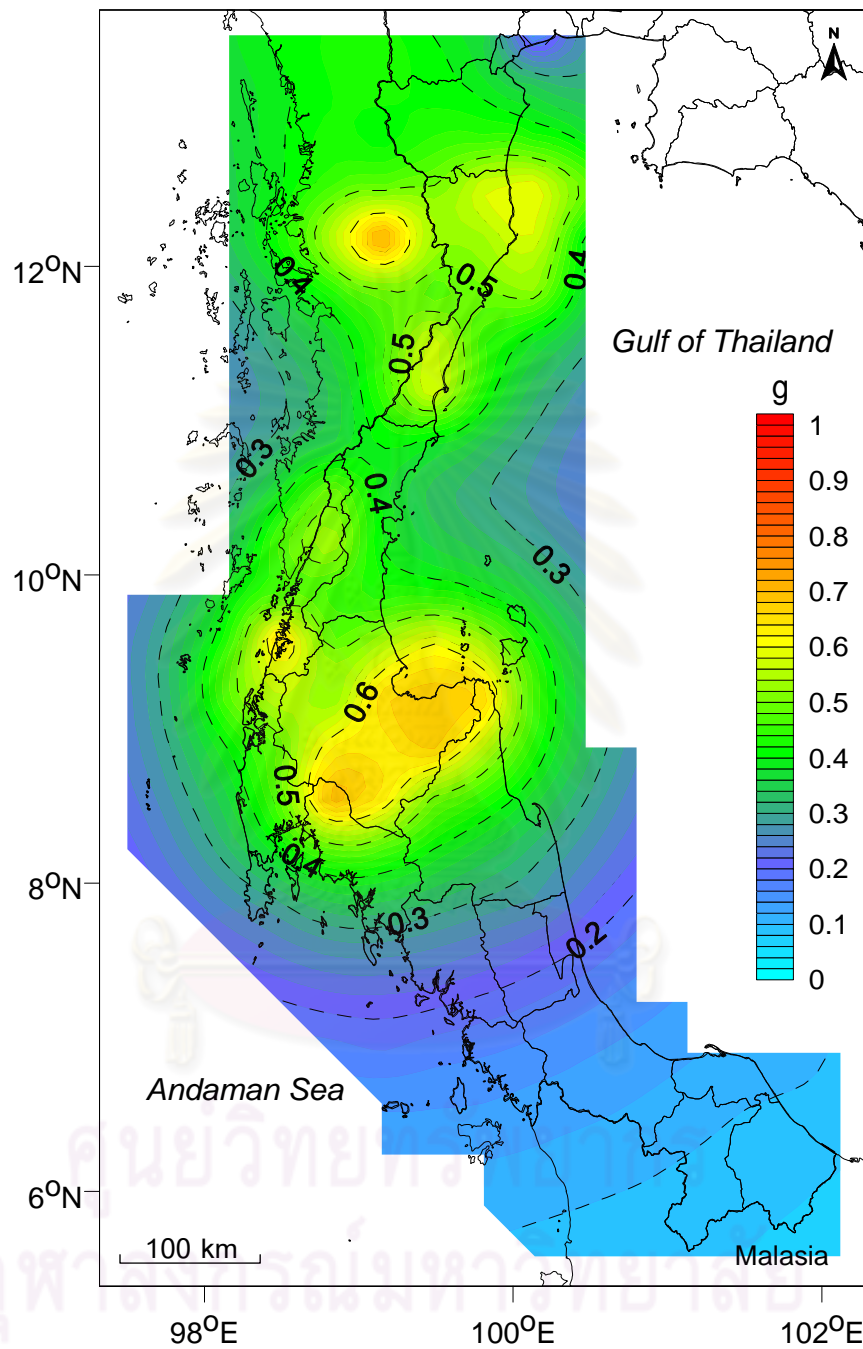


Figure 5.24 Seismic hazard map showing mean 0.2 sec horizontal spectral acceleration with 2% probability of exceedance in 50 years or for 2,500 years for the rock site condition in southern Thailand.

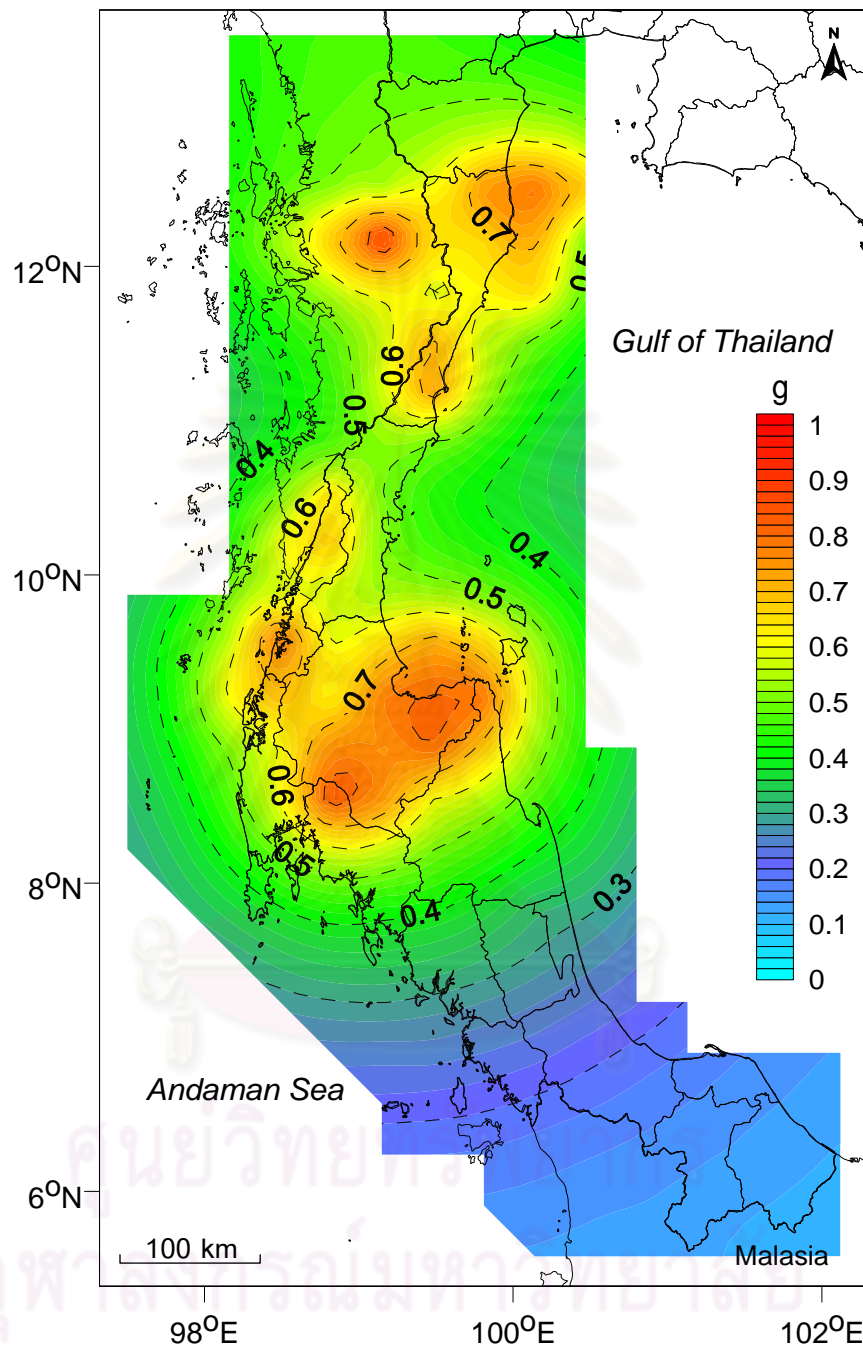


Figure 5.25 Seismic hazard map showing mean 0.2 sec horizontal spectral acceleration with 0.5% probability of exceedance in 50 years or for 10,000 years for the rock site condition in southern Thailand.

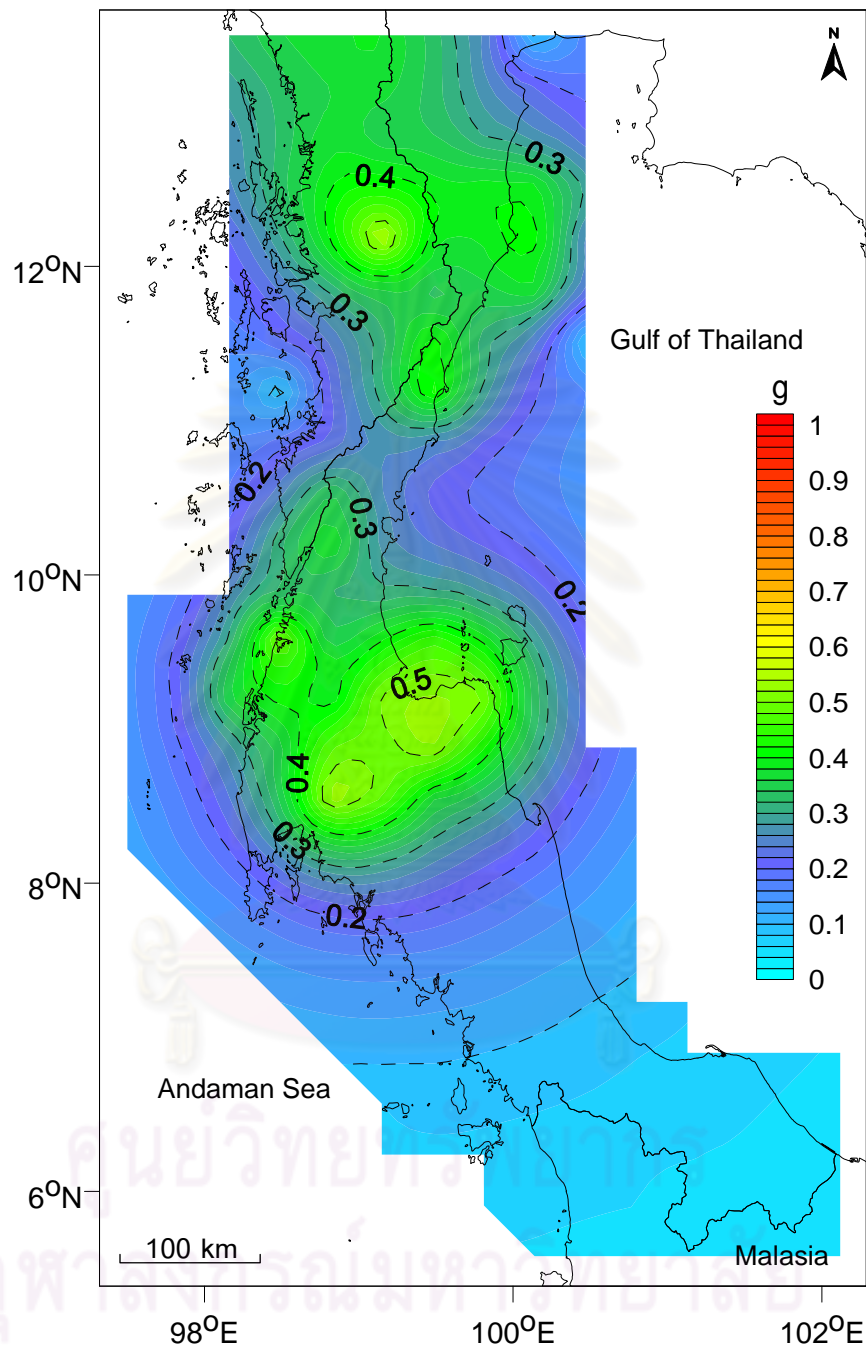


Figure 5.26 Seismic hazard map showing mean 0.3 sec horizontal spectral acceleration with 10% probability of exceedance in 50 years or for 500 years for the rock site condition in southern Thailand.

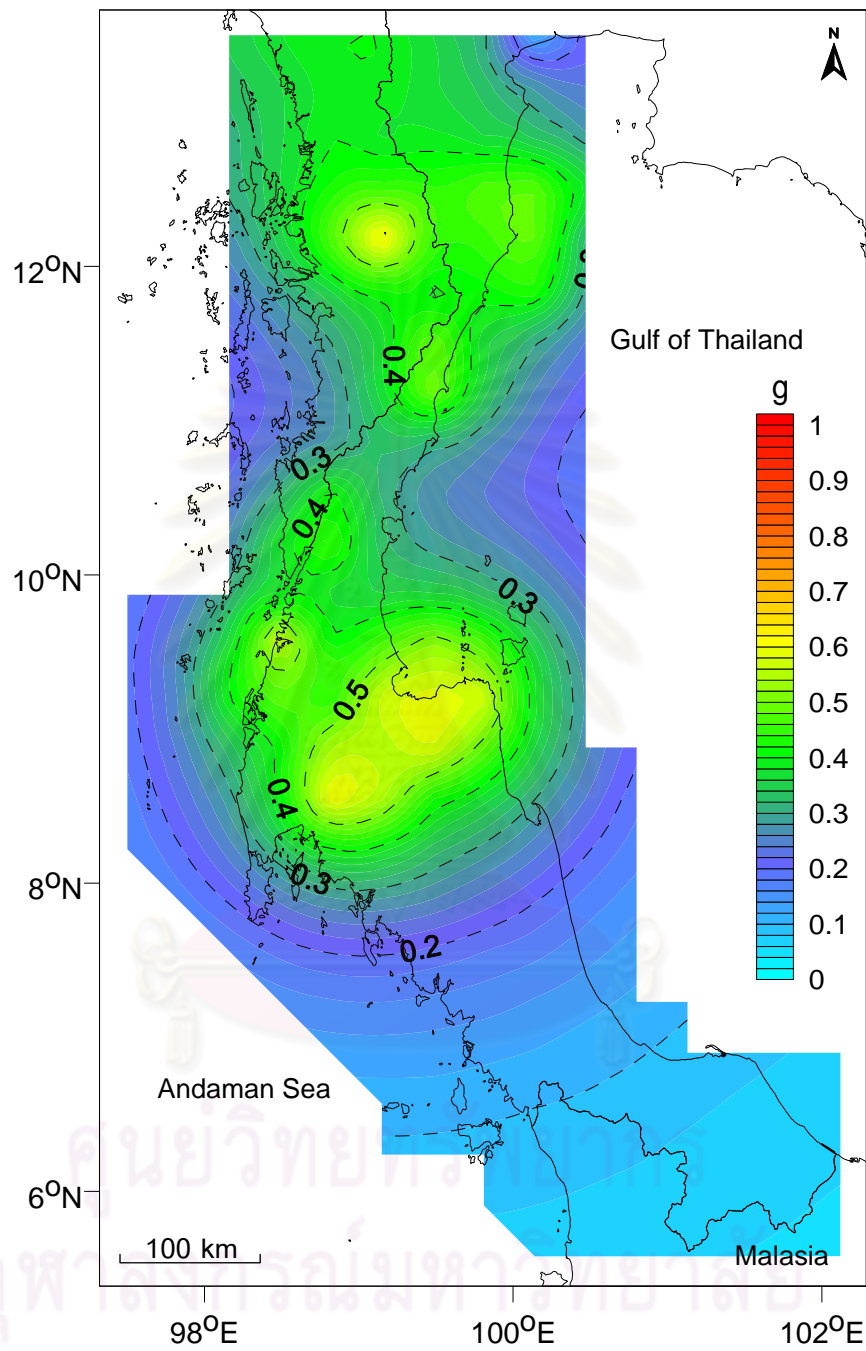


Figure 5.27 Seismic hazard map showing mean 0.3 sec horizontal spectral acceleration with 5% probability of exceedance in 50 years or for 1,000 years for the rock site condition in southern Thailand.

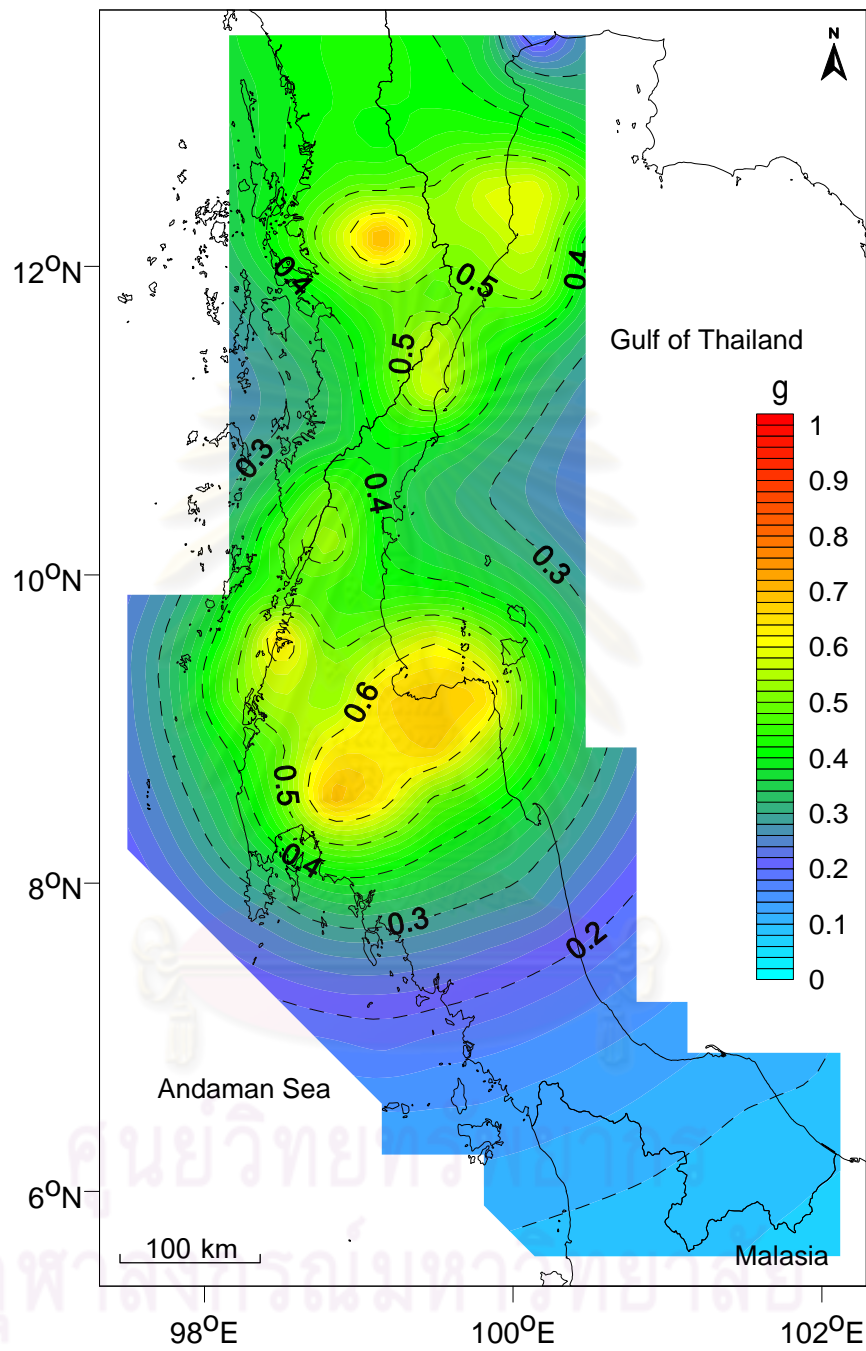


Figure 5.28 Seismic hazard map showing mean 0.3 sec horizontal spectral acceleration with 2% probability of exceedance in 50 years or for 2,500 years for the rock site condition in southern Thailand.

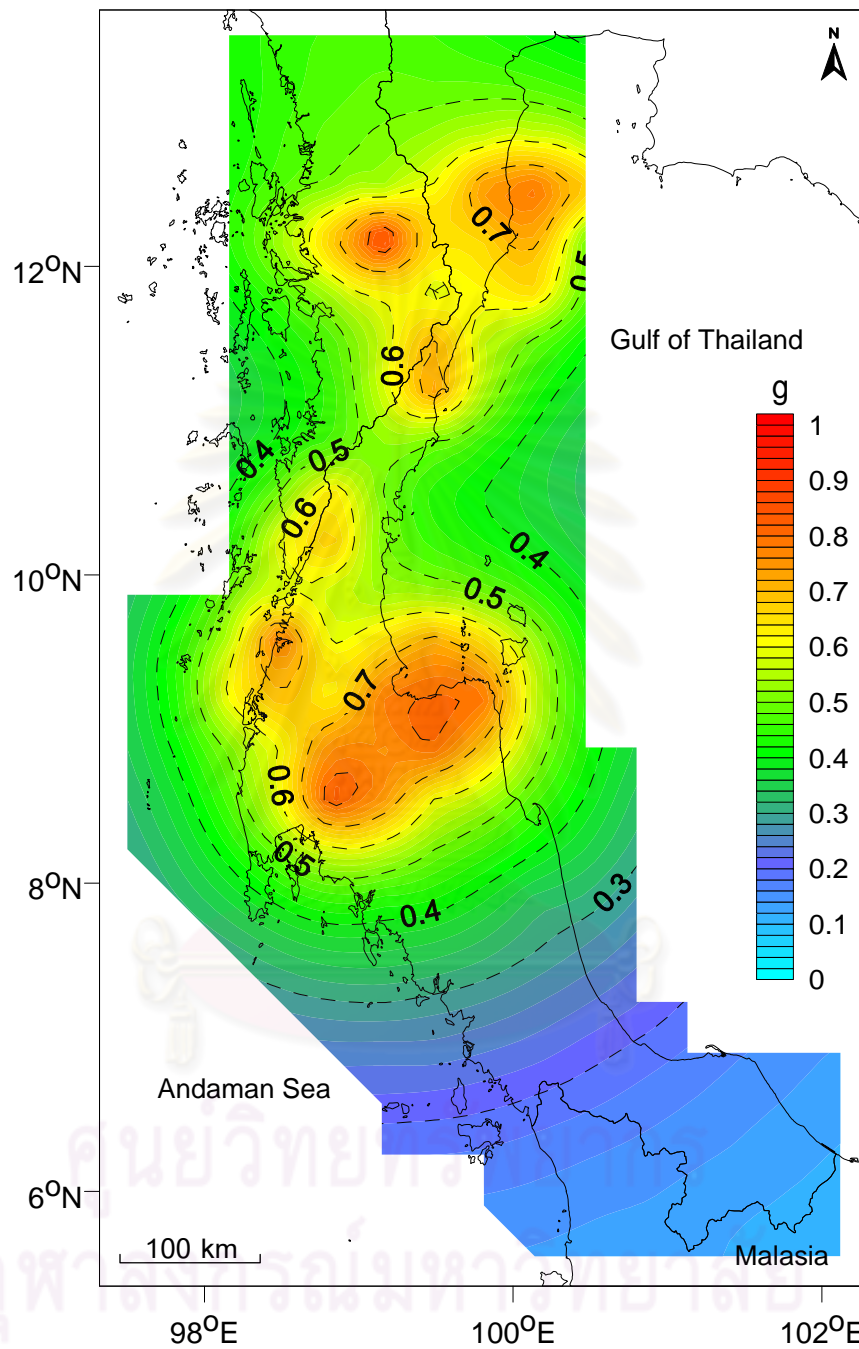


Figure 5.29 Seismic hazard map showing mean 0.3 sec horizontal spectral acceleration with 0.5% probability of exceedance in 50 years or for 10,000 years for the rock site condition in southern Thailand.

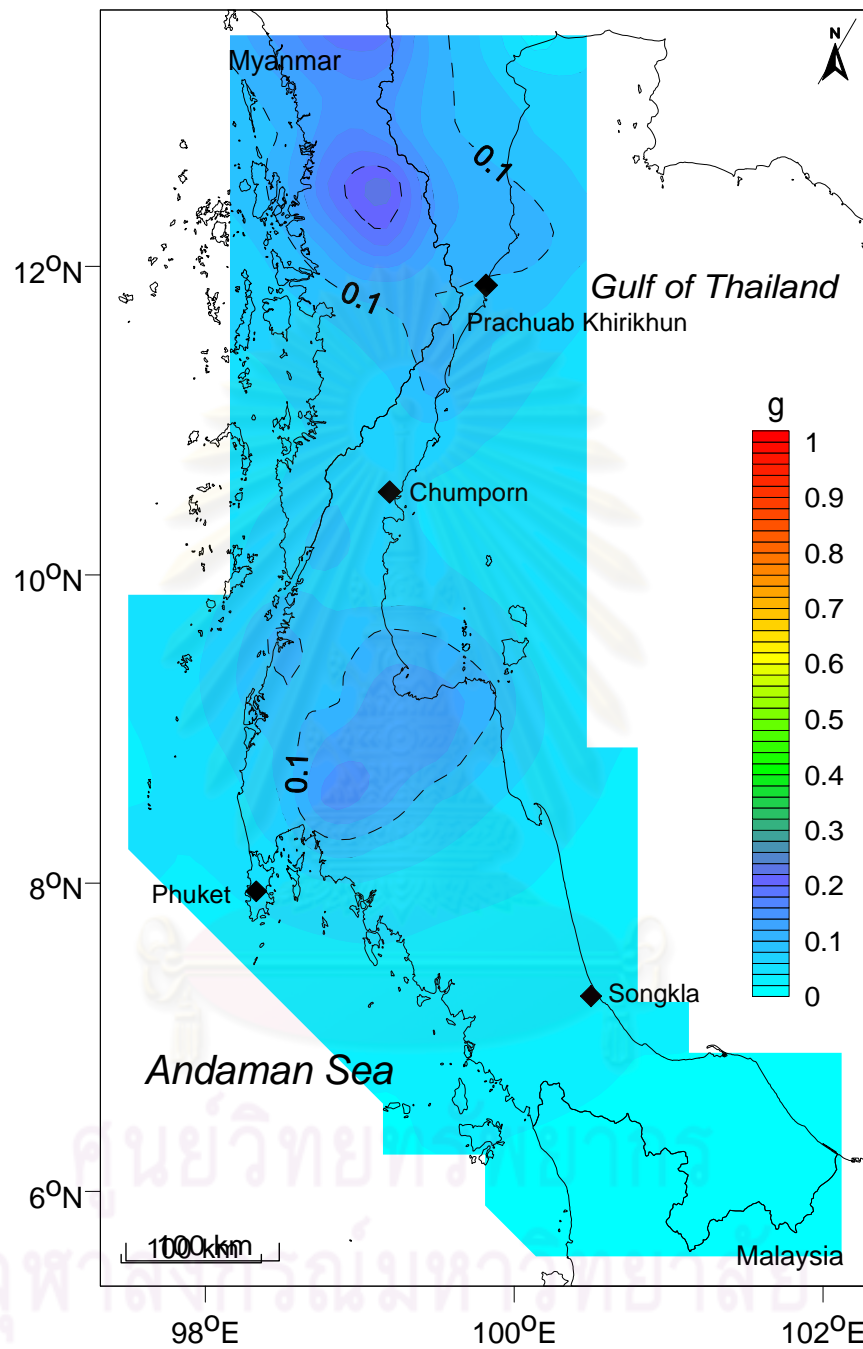


Figure 5.30 Seismic hazard map showing mean 1.0 sec horizontal spectral acceleration with 10% probability of exceedance in 50 years or for 500 years for the rock site condition in southern Thailand.

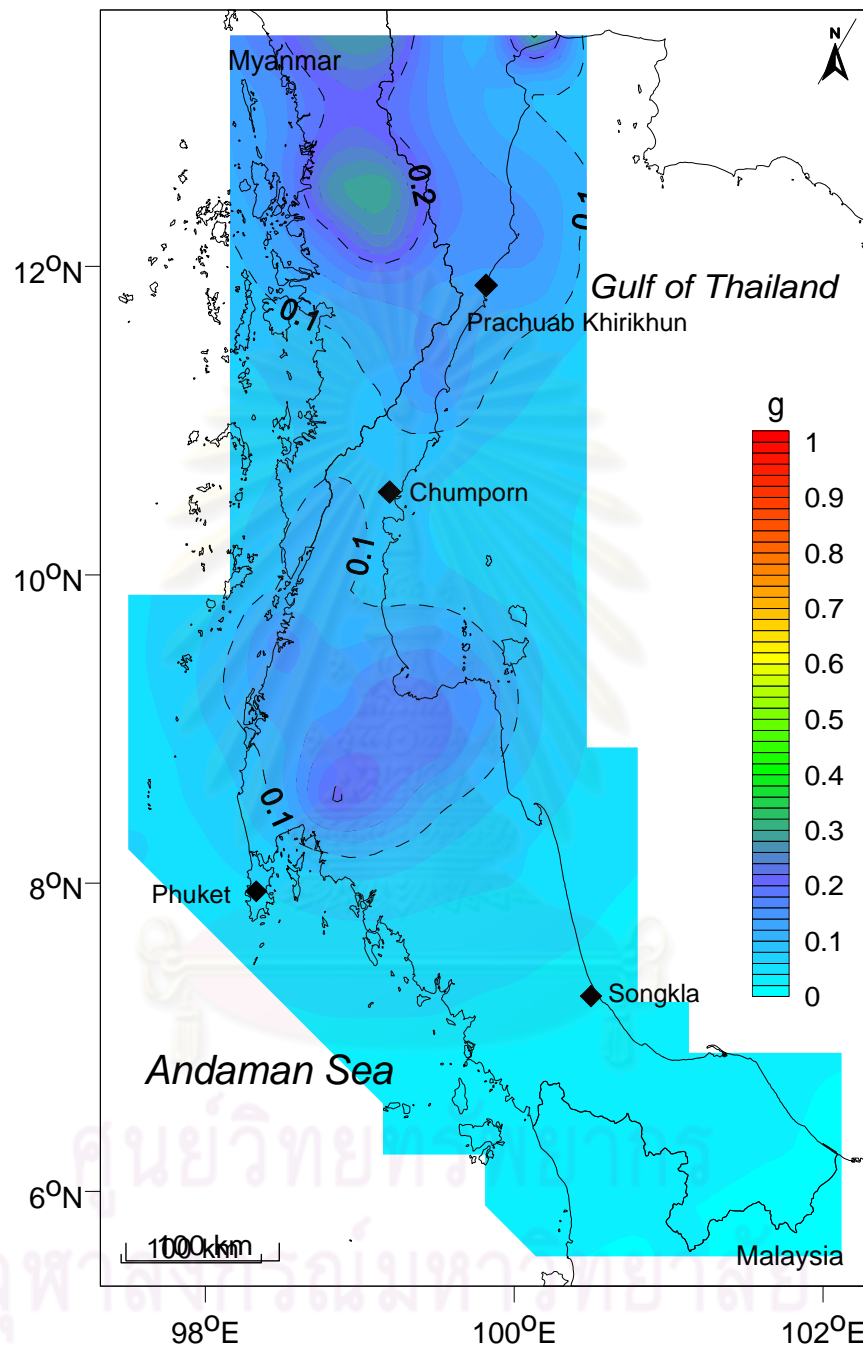


Figure 5.31 Hazard map showing mean 1.0 sec horizontal spectral acceleration with 5% probability of exceedance in 50 years or for 1,000 years for the rock site condition in southern Thailand.

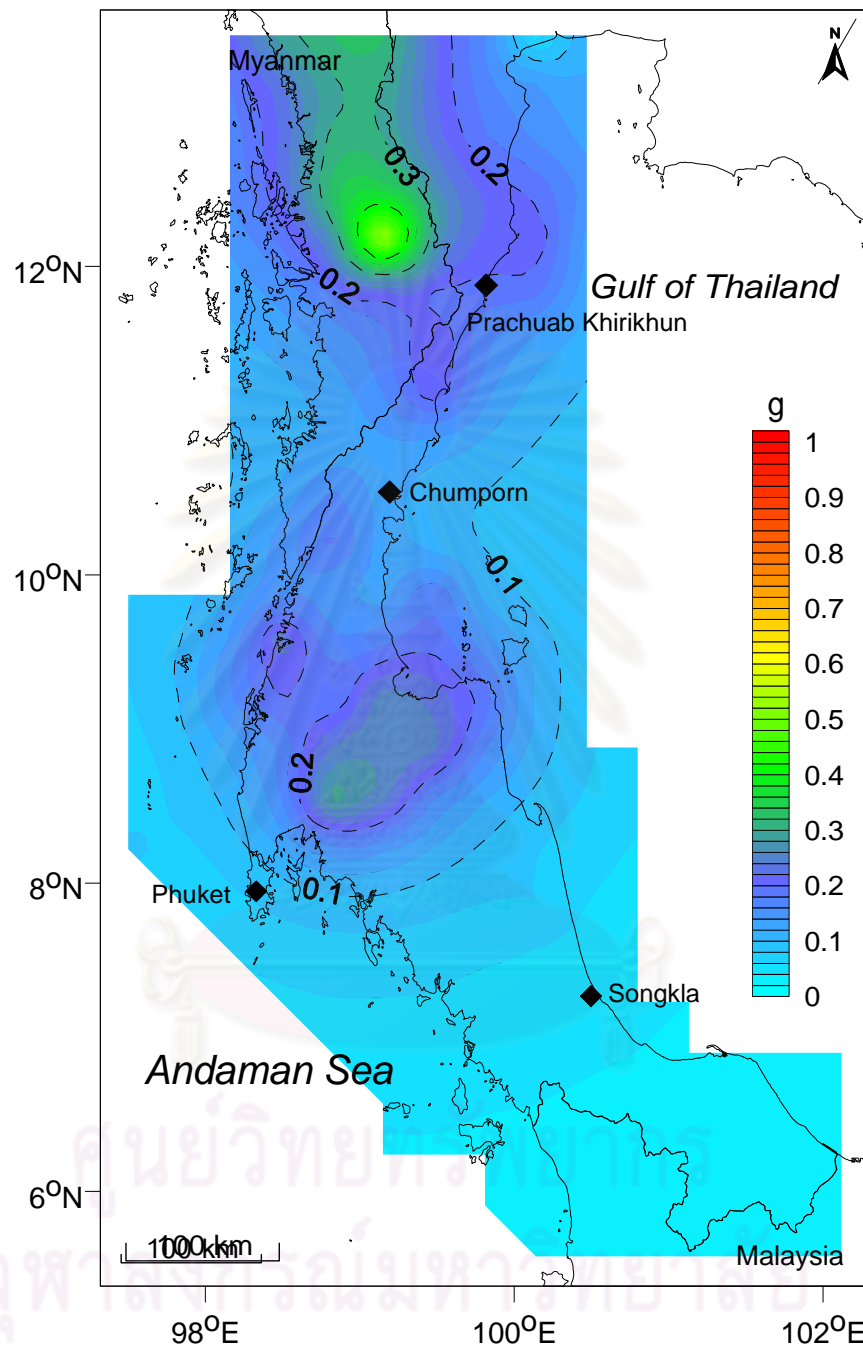


Figure 5.32 Hazard map showing mean 1.0 sec horizontal spectral acceleration with 2% probability of exceedance in 50 years or for 2,500 years for the rock site condition in southern Thailand.

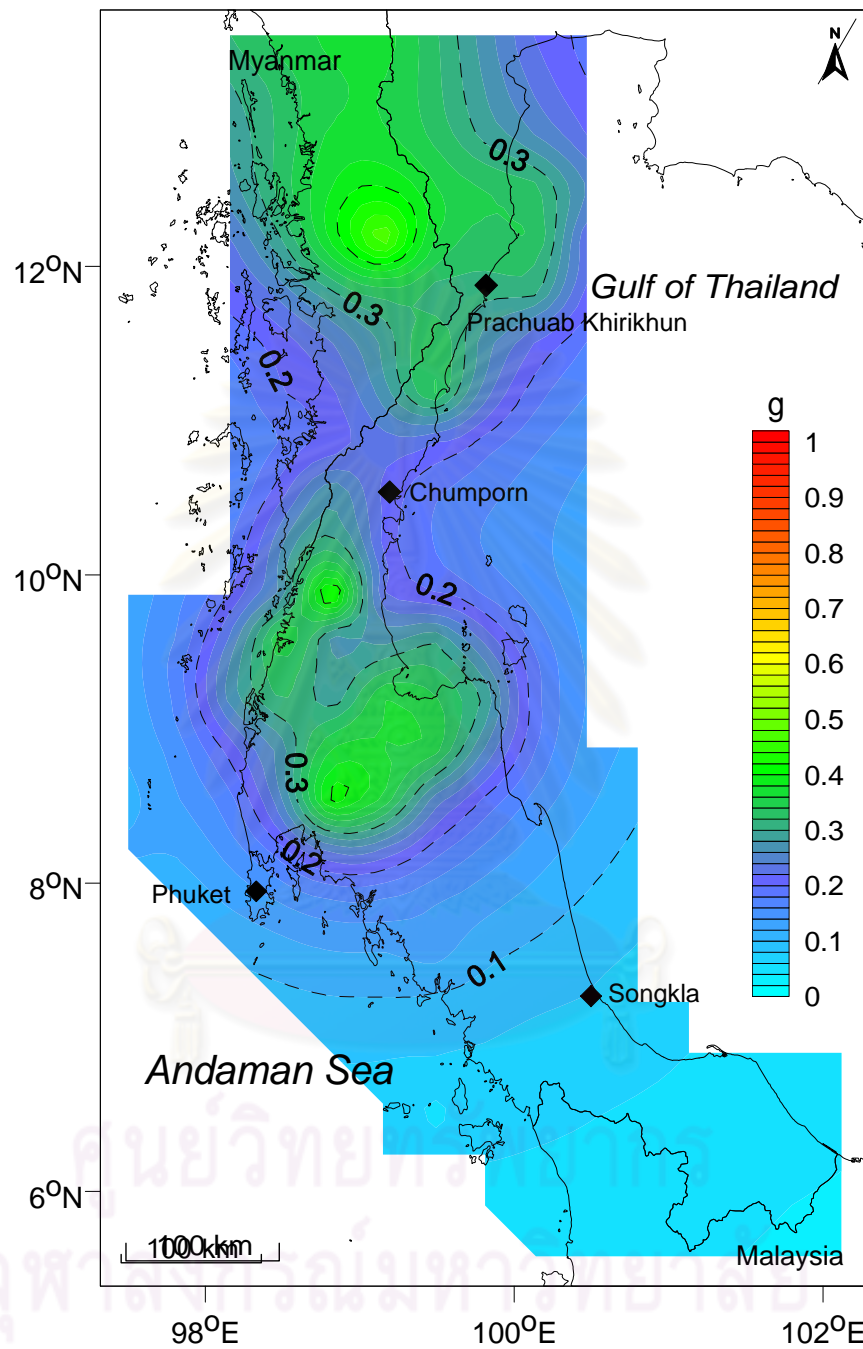


Figure 5.33 Hazard map showing mean 1.0 sec horizontal spectral acceleration with 0.5% probability of exceedance in 50 years or for 10,000 years for the rock site condition in southern Thailand.

Table 5.10 Mean peak ground accelerations and the spectral acceleration at 0.2, 0.3, and 1.0 seconds with a 10%, 5%, 2% and 0.5% probability of exceedance in 50-year hazard levels (500, 1,000, 2,500, and 10,000 years) for rock site condition at each province in southern Thailand.

Province	Minimum-Maximum Acceleration (g)															
	500 return years				1,000 return years				2,500 return years				10,000 return years			
	PGA (g)	Spectral Acceleration (g)			PGA (g)	Spectral Acceleration (g)			PGA (g)	Spectral Acceleration (g)			PGA (g)	Spectral Acceleration (g)		
		0.2 sec	0.3 sec	1.0 sec		0.2 sec	0.3 sec	1.0 sec		0.2 sec	0.3 sec	1.0 sec		0.2 sec	0.3 sec	1.0 sec
Phetchaburi	0.1-0.22	0.24 - 0.38	0.20 - 0.35	0.07 - 0.16	0.13 - 0.28	0.30 - 0.42	0.26 - 0.39	0.1 - 0.22	0.16 - 0.32	0.34 - 0.52	0.32 - 0.48	0.14 - 0.30	0.24 - 0.38	0.44 - 0.70	0.44 - 0.64	0.25 - 0.37
Prachuab Khirilhun	0.14-0.22	0.22 - 0.40	0.18 - 0.35	0.06 - 0.10	0.18 - 0.28	0.28 - 0.48	0.22 - 0.42	0.08 - 0.20	0.26 - 0.34	0.32 - 0.58	0.26 - 0.52	0.15 - 0.30	0.34 - 0.46	0.56 - 0.76	0.55 - 0.68	0.25 - 0.32
Chumphon	0.12-0.16	0.28 - 0.38	0.20 - 0.30	0.08 - 0.09	0.16 - 0.22	0.30 - 0.42	0.26 - 0.38	0.09 - 0.12	0.18 - 0.30	0.36 - 0.48	0.33 - 0.45	0.12 - 0.18	0.26 - 0.40	0.48 - 0.64	0.47 - 0.58	0.20 - 0.40
Ranong	0.12 - 0.24	0.26 - 0.44	0.22 - 0.34	0.07 - 1.00	0.16 - 3.0	0.32 - 0.52	0.28 - 0.42	0.1 - 0.14	0.20 - 0.38	0.40 - 0.60	0.34 - 0.50	0.14 - 0.20	0.30 - 0.50	0.52 - 0.74	0.44 - 0.64	0.23 - 0.38
Surat Thani	0.16 - 0.28	0.34 - 0.52	0.30 - 0.44	0.08 - 0.14	0.20 - 0.34	0.40 - 0.58	0.34 - 0.50	0.15 - 0.18	0.26 - 0.42	0.48 - 0.66	0.42 - 0.58	0.16 - 0.26	0.34 - 0.52	0.58 - 0.80	0.52 - 0.72	0.26 0.38
Phangnga	0.10 - 0.26	0.24 - 0.46	0.19 - 0.42	0.05 - 0.09	0.12 - 0.30	0.28 - 0.52	0.24 - 0.48	0.07 - 0.18	0.16 - 0.38	0.34 - 0.62	0.30 - 0.56	0.10 - 0.24	0.22 - 0.48	0.44 - 0.68	0.40 - 0.68	0.16 - 0.36
Krabi	0.08 - 0.3	0.18 - 0.52	0.14 - 0.44	0.04 - 0.14	0.10 - 0.34	0.22 - 0.58	0.18 - 0.52	0.05 - 0.18	0.12 - 0.42	0.28 - 0.68	0.24 - 0.60	0.08 - 0.26	0.16 - 0.54	0.38 - 0.80	0.34 - 0.73	0.13 - 0.40
Phuket	0.07 - 0.09	0.14 - 0.20	0.14 - 0.19	0.04 - 0.05	0.08 - 0.10	0.20 - 0.28	0.18 - 0.24	0.05 - 0.07	0.11 - 0.15	0.24 - 0.32	0.23 - 0.31	0.07 - 0.10	0.16 - 0.22	0.36 - 0.46	0.32 - 0.40	0.12 - 0.16
Nakho Sri Thammarat	0.07 - 0.26	0.14 - 0.48	0.13 - 0.42	0.03 - 0.12	0.08 - 0.30	0.20 - 0.56	0.16 - 0.47	0.05 - 0.16	0.10 - 0.36	0.26 - 0.65	0.22 - 0.55	0.07 - 0.22	0.14 - 0.46	0.32 - 0.78	0.30 - 0.67	0.11 - 0.32
Trang	0.05 - 0.09	0.11 - 0.22	0.10 - 0.19	0.03 - 0.07	0.06 - 0.12	0.14 - 0.26	0.12 - 0.24	0.04 - 0.06	0.08 - 0.14	0.18 - 0.34	0.16 - 0.30	0.05 - 0.09	0.11 - 0.18	0.27 - 0.44	0.24 - 0.40	0.06 - 0.18
Phatthalung	0.05 - 0.07	0.11 - 0.18	0.09 - 0.15	0.03 - 0.04	0.06 - 0.10	0.13 - 0.22	0.11 - 0.19	0.03 - 0.06	0.07 - 0.12	0.17 - 0.29	0.15 - 0.26	0.05 - 0.08	0.10 - 0.17	0.24 - 0.38	0.23 - 0.33	0.08 - 0.13
Songkhla	0.02 - 0.06	0.07 - 0.16	0.06 - 0.13	0.01 - 0.05	0.04 - 0.06	0.08 - 0.21	0.07 - 0.16	0.02 - 0.05	0.05 - 0.07	0.11 - 0.26	0.10 - 0.22	0.04 - 0.09	0.07 - 0.14	0.16 - 0.32	0.14 - 0.31	0.05 - 0.11
Satun	0.03 - 0.05	0.08 - 0.11	0.07 - 1.00	0.02 - 0.03	0.04 - 0.06	0.10 - 0.14	0.09 - 0.12	0.03 - 0.04	0.06 - 0.08	0.13 - 0.18	0.11 - 0.16	0.04 - 0.05	0.08 - 0.11	0.18 - 0.27	0.17 - 0.24	0.06 - 0.09
Yala	0.02	0.05 - 0.07	0.05 - 0.06	< 0.02	0.02 - 0.04	0.07 - 0.09	0.06 - 0.08	0.02 - 0.03	0.04 - 0.05	0.09 - 0.11	0.08 - 0.11	0.02 - 0.04	0.05 - 0.07	0.12 - 0.16	0.11 - 0.15	0.04 - 0.06
Narathiwat	0.02	0.05 - 0.06	0.04 - 0.05	< 0.02	0.02 - 0.04	0.06 - 0.07	0.05 - 0.07	0.02 - 0.03	0.04 - 0.05	0.08 - 0.10	0.07 - 0.09	0.02 - 0.04	0.05 - 0.06	0.11 - 0.14	0.11 - 0.16	0.04 - 0.05
Pattani	0.02	0.06 - 0.07	0.05 - 0.07	< 0.02	0.02 - 0.04	0.07 - 0.09	0.07 - 0.08	0.02 - 0.03	0.03 - 0.04	0.10 - 0.12	0.09 - 0.11	0.02 - 0.04	0.06 - 0.07	0.14 - 0.18	0.14 - 0.16	0.05 - 0.06

CHAPTER VI

DISCUSSION

The peak ground and spectral acceleration maps produced from this study are derived from the effect of all active faults and known area sources in the southern Thailand and adjacent areas. The characteristics of the KMF and RNF were re-studied and re-evaluated. Moreover, the logic tree approach and western America's attenuation relationships were applied in the hazard analysis. Compared with previous studies, different earthquake sources and their characteristic, different assumptions and models as well as dissimilar seismic hazard maps are discussed as follows.

6.1 Length, Recurrence Interval and Slip Rate

6.1.1 KMF

Based on the DEM interpretation, the area with lineaments lying in the NE-SW direction and paralleling the KMF, that is illustrated in the active fault map of Thailand (DMR, 2006), is defined as the KMF zone. This zone covers the large area from Thap Put district of Phang Nga province southeast toward Khao Phanom district of Krabi province, and northeast toward Viphavadi, Muang and Ban Nasan districts of Surat Thani province. Geomorphologic features indicate that the northern part of the KMF ends at Viphavadi district, not extends to the Gulf of Thailand as mentioned by Wong et al. (2005), DMR (2007) and RID (2006, 2008, 2009). The total length of the KMF is about 115 km compared with 140 km reported by Wong et al. (2005) and RID (2006, 2008 2009).

According to the re-evaluation of the data from the paleoseismic investigation of the KMF done by DMR (2007) and RID (2009) as well as additional data from this study,

at least six fault events of the KMF zone were detected while four fault events were reported by the DMR (2007). However, the DMR reported that the four earthquake events have the approximate ages of occurrences of 2,000, 3,000, 4,700 and 9,400 years ago that are comparable to the fault event E1, E2, E3 and E5 in this study. The mean recurrence interval should be computed from all fault events. Based on the recurrence interval calculation proposed by Martel (2002), in this study, six fault events give the mean recurrence interval of approximately 2,200 years with the standard deviation of 830 years. The DMR estimated the recurrence interval from the time span between the last two events. It is approximately 1,000 years. In fact, if the mean recurrence interval was re-calculated from the mentioned four ages of tectonic movements, it is approximately 2,500 years with the high standard deviation of 2,000 years. The mean recurrence interval derived from this study is shorter than that (127,398 years) obtained from Wong et al. (2005)'s study. Moreover, the mean recurrence interval of the KMF zone in this study is almost similar to those of the active fault in northern, western and eastern Thailand. The recurrence intervals of the Thoen, Mae Yom, Three Pagoda and Nakhornnayok/Onkaruk faults which are approximately 1,000 years (Fenton et al., 1997), 1,300 years (Charusiri et al., 2006), 2,100 years (Kosuwan et al., 2006) and 1,500 years (RID, 2007), respectively, lie in the same range of the recurrence interval in this study.

The slip rates of the KMF that were re-estimated in this study are in the similar range with those calculated by the DMR (2007). Additionally, the lower limit of the slip rate (0.08-0.1 mm/yr) of this study is consistent with the slip rates for active faults bounding Tertiary basins in Thailand with recognizable tectonic geomorphology that are approximately 0.1 mm/yr (Fenton et al, 2003).

6.1.2 RNF

Results of the DEM interpretation show that the RNF zone occupies the mountainous areas starting from Thap Sakae district of Prachuab Khirikhun province southwest toward Chumphon and Ranong province, and ending at Takua Pa district of Phang Nga province. Geomorphologically, it can be divided into two segments, i.e. north and south segments as mentioned by Wong et al. (2005) and RID (2006, 2008). The RID (2009) reported that the RNF consists of three segments—north, central and south segments. The north segment cannot be traced in the DEM in this study. The rupture lengths of the north and south segments interpreted from this study are approximately 180 km and 160 km, respectively, while those reported by Wong et al. (2005) and RID (2006) are 200 km and 130 km, respectively. However, the total length of the RNF reported by this study and others is equivalent.

Four fault events were encountered in this study whereas three fault events were found in the DMR (2007)'s study. The mean recurrence interval calculated in this study is approximately 8,300 years which is almost equal to that estimated by Wong et al. (2005 as mentioned in Petersen et al., 2007), 8,473 years, and DMR (2007), 2,000 years. Wong et al. (2005)'s and DMR (2007)'s reports cannot be searched how they computed the recurrence interval. The slip rate of this study is 0.04-0.17 mm/yr which is less than that of DMR (2007)'s report (0.27-0.7 mm/yr) but is equivalent to Petersen et al. (2007)'s application (0.1 mm/yr). For the calculation of the slip rate, the author used the real age derived from the age dating while DMR (2007) adopted approximate age. This is a reason why the slip rate value is unequal.

6.2. Seismicity Sources

6.2.1 Comparison between with and without KMF Areal Source

In this study two more areal sources, the Ratchaprapha reservoir and the KMF zone areas, were included in the analysis but excluded in previous studies. The reasons for application of these two areal sources are:

- (1) Epicenters that occurred in the Ratchaprapha reservoir were proved to be the reservoir-triggered seismicity by the EGAT.
- (2) Four earthquakes, not related to any faults were detected in the KMF zone. So, they were defined as the background earthquakes. This areal source was bounded by epicenters of these earthquakes covering Surat Thani and Krabi provinces

In this study, the KMF zone was divided into line and areal sources for the hazard analysis. The total weights of contribution of these two sources are equal one, i.e. the weights of line and area sources are 0.1 and 0.9, respectively. If the KMF areal source is excluded in the analysis (give the weight of the line source equal 1 and that of the areal source equal 0), it can be seen that the ground motion level is not changed significantly. For example, at the site with the longitude of 98.82°E and latitude of 9.21°N to which the KMF areal source highly contribute, the results of calculation of the peak ground acceleration without the KMF areal source is given in Table 6.1 and shown as the hazard curve in Figure 6.1. It can be summarized that the acceleration decreases 1%, 5%, 9% and 19% for the return period of 10,000, 2,500, 1,000 and 500 years, respectively. It means that the areal source influences the ground motion for the shorter return period more than the longer period.

Table 6.1 Ground acceleration at the site with longitude of 98.82°E and latitude of 9.21°N contributed by with and without KMF areal source.

Contribution Weight		Acceleration (g)			
Area	Line	500 yr	1,000 yr	2,500 yr	10000 yr
0.9	0.1	0.085	0.214	0.274	0.362
0	1	0.069	0.195	0.26	0.357
% difference		19	9	5	1

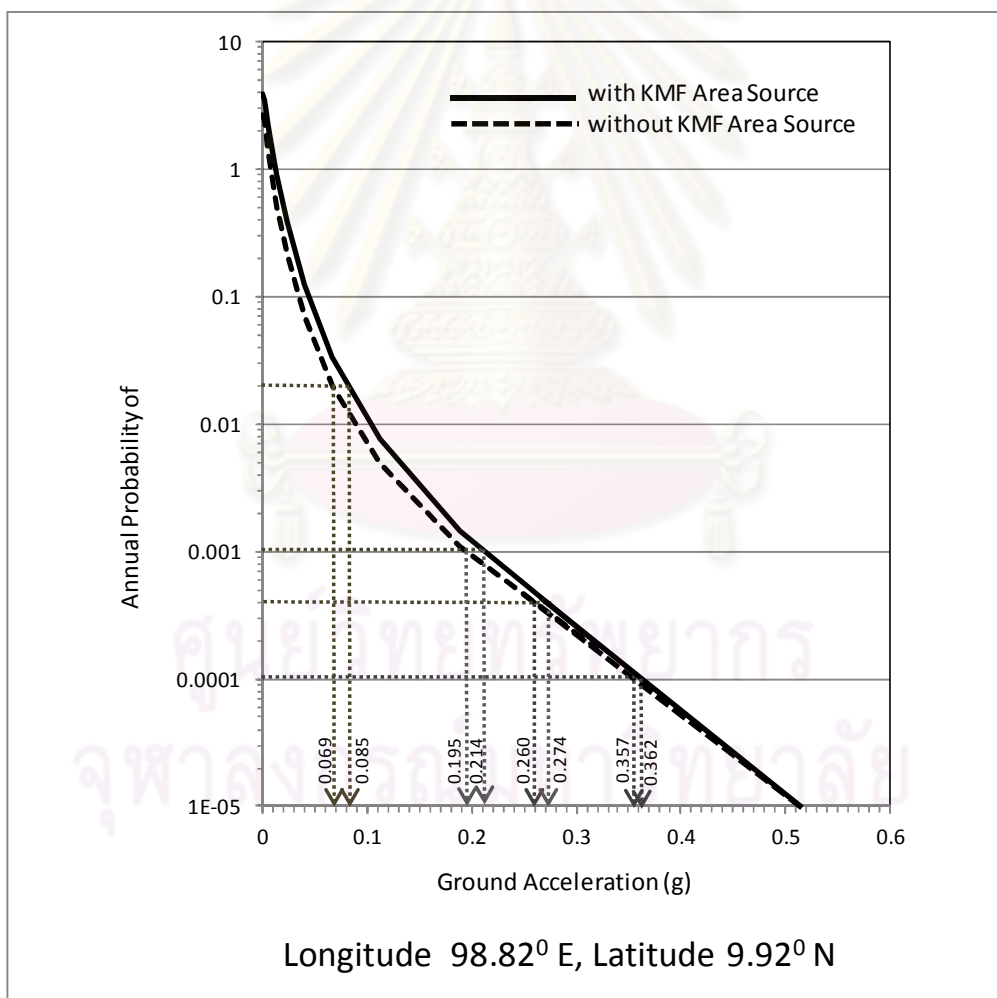


Figure 6.1 Hazard curve at longitude of 98.82°E and latitude of 9.21°N contributed by with and without KMF areal source.

6.2.2 Seismogenic Depth and Fault Plane Inclination

The distances between the earthquake sources and calculated sites are the important parameter effecting the ground motion at the site, and dependent upon the seismogenic depth and dip angle of fault plain. In previous works, except Petersen et al. (2007)'s works, normally mentioned only two-dimensional areal and fault sources. They did not discuss about the third dimension of the areal source which is the depth of seismicity occurrence and the dip angle of the fault sources. Only Petersen et al. (2007) adopted average 15-km seismogenic depth for the areal source as well as the KMF and RNF. In this study, the seismogenic thicknesses of 10, 15 and 20 km for all fault sources, 15 km for Khlong Marui Fault areal source and 8, 10 and 15 km for Ratchprapha Dam RTS were applied.. Besides the depths of seismogenic occurrence, the dip angles of all active faults were included in this research analysis. Due to either poorly understood or unknown fault geometry, the dip angle of all fault source surfaces were assumed to be 90° similar to Petersen et al. (2007)' assumption used for the KMF and RNF surfaces. It can be concluded that the different intensity of acceleration shown in the seismic hazard maps prepared in this study and by Petersen et al. (2007) do not concern the seismogenic depth and the dip angle of the fault plane. This conclusion cannot report between this study and other studies.

6.2.3 Effect of b-value on Calculated Ground Motion

The b-values calculated and adopted in this study, are approximately equal to the global b-value of 1. Petersen et al. (2007) also applied the b-value of 1 for the sources in southern Thailand and adjacent area. Pailoplee (2009) adopted very low b-values for the line and areal sources that influence the ground motion in southern Thailand. He specified the b-values for the KMF, RNF, TNF and KYF as 0.25 and for TVF and TPF as 0.79 and 0.51, respectively. Furthermore, he also defined the b-values for

the areal sources that effect the ground shaking in southern Thailand—Zone O:western Thailand, Zone R:Malaysia-Malacca and Zone T:Tenasserim—equal to 0.6. In general, the lower b-value, the lower ground acceleration. This remark can be proved. For example, the results of computation of the acceleration for the site at longitude of 98.82°E and latitude of 9.21°N with varying the b-value are shown in Figure 6.2 and given in Table 6.2. It can be stated that decrease in the b-value and increase in the return period, increase in the acceleration. From the Table 6.2, if the b-values decrease 25% (0.75 b-value), 50% (0.5 b-value) and 75% (0.25 b-value) from the b-value of 1, the accelerations increase approximately 11-15%, 26-38%, and 45-67%, respectively.

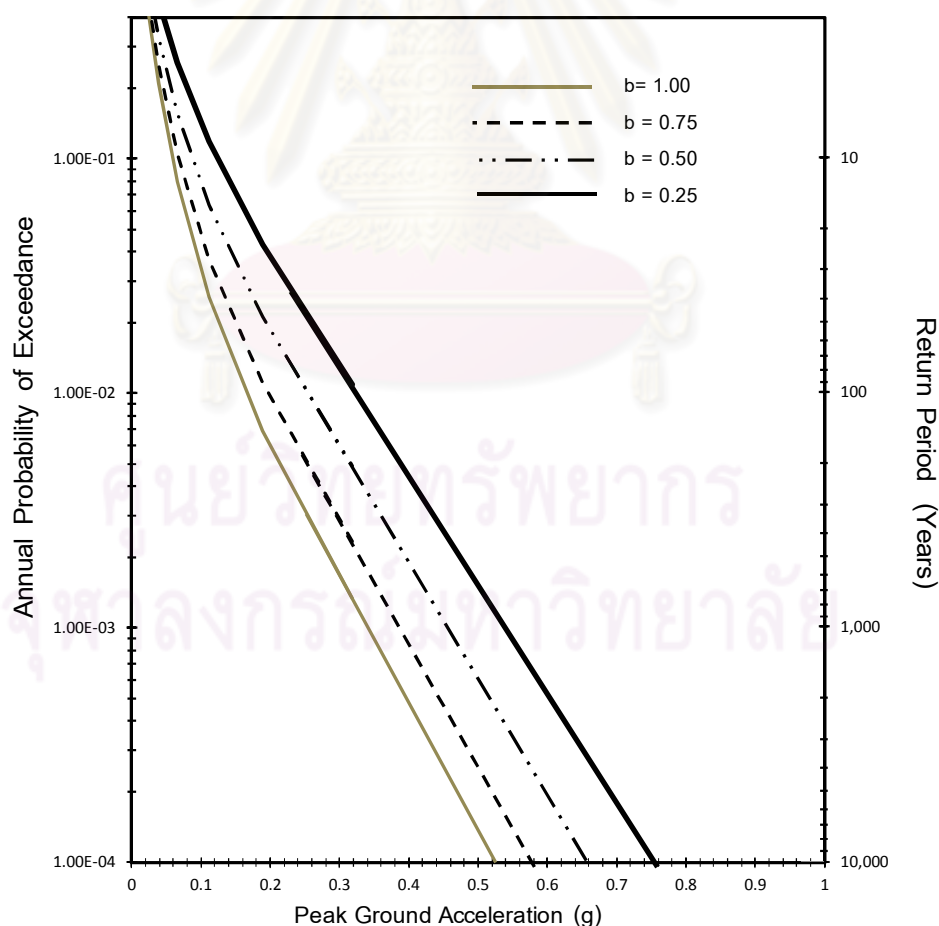


Figure 6.2 Hazard curve showing the influence of b-value on the ground motion

Table 6.2 Effect of b-value on the acceleration.

Return Period	b- value						
	1	0.75		0.5		0.25	
(year)	g	g	%increase	g	%increase	g	%increase
500	0.29	0.33	15	0.40	38	0.48	67
1,000	0.34	0.39	15	0.46	35	0.54	59
2,500	0.44	0.49	12	0.56	28	0.66	50
10,000	0.52	0.58	11	0.66	26	0.76	45

Based on the sensitivity of the b-value to the acceleration, it can be used to describe why the seismic hazard maps produced by Pailoplee (2009) give the higher acceleration values than those obtained from this study.

6.3 Effect of Attenuation Relationships on Ground Motion

The attenuation models play the important factor on what calculated acceleration of the ground will be. In this section, the author try to compare the influence of different attenuation models for the crustal earthquakes applied by this study (Boore et al., 1997, Abrahamson and Silva, 1997, Campbell and Bozorgnia, 2003, and Sadigh et al., 1997), by Pailoplee (Idiss, 1993) and by Palasri and Ruangrussamee (Idriss, 1993, and Sadgn et al., 1997). The graphs showing the relation between the distance and the acceleration of each attenuation model for the magnitude of M_w5 and M_w7 can be presented in Figure 5.3 and 5.4, respectively. The four relations used in this study were given the same weight for calculation. So, the average value is shown as the red line in the figures. For the magnitude of M_w5 , the Idriss's model gives insignificantly higher acceleration than the average acceleration from four models applied in this study when the source-to-site distance is less than 20 km but significantly lower acceleration when

the source-to-site distance is more than 50 km (Figure 6.3). In case of the magnitude $M_w 7$, It is not so much different acceleration derived from the Idriss's model and the average of Boore et al.'s, Abrahamson and Silva's, Campbell and Bozorgnia's, and Sadigh et al.'s models (Figure 6.4). It can be said that the low and high ground acceleration illustrated in Palasri and Rungrussamee's, and Pailoplee's seismic hazard maps, respectively are not significantly dependent upon the applied attenuation model.

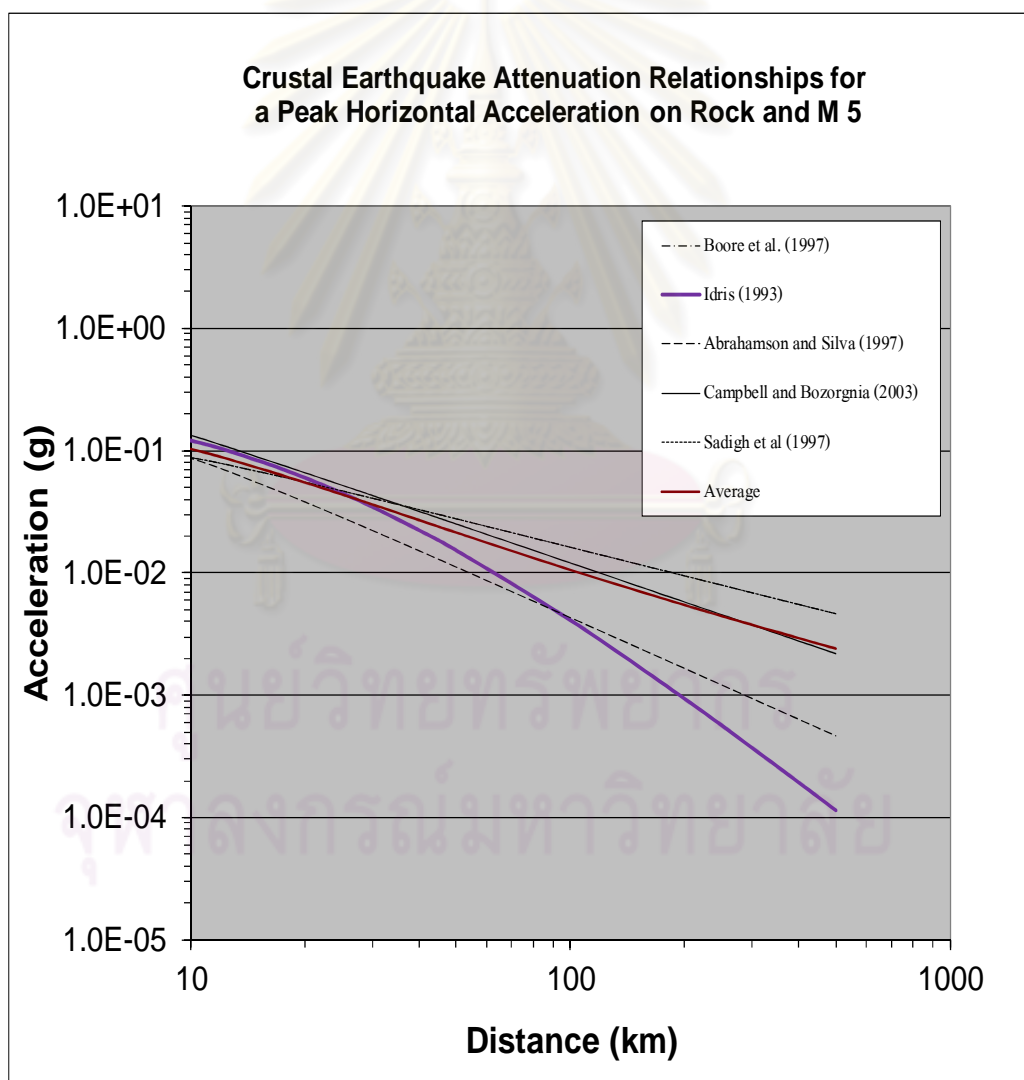


Figure 6.3 Peak horizontal acceleration-attenuation relationships for the magnitude $M_w 5$.

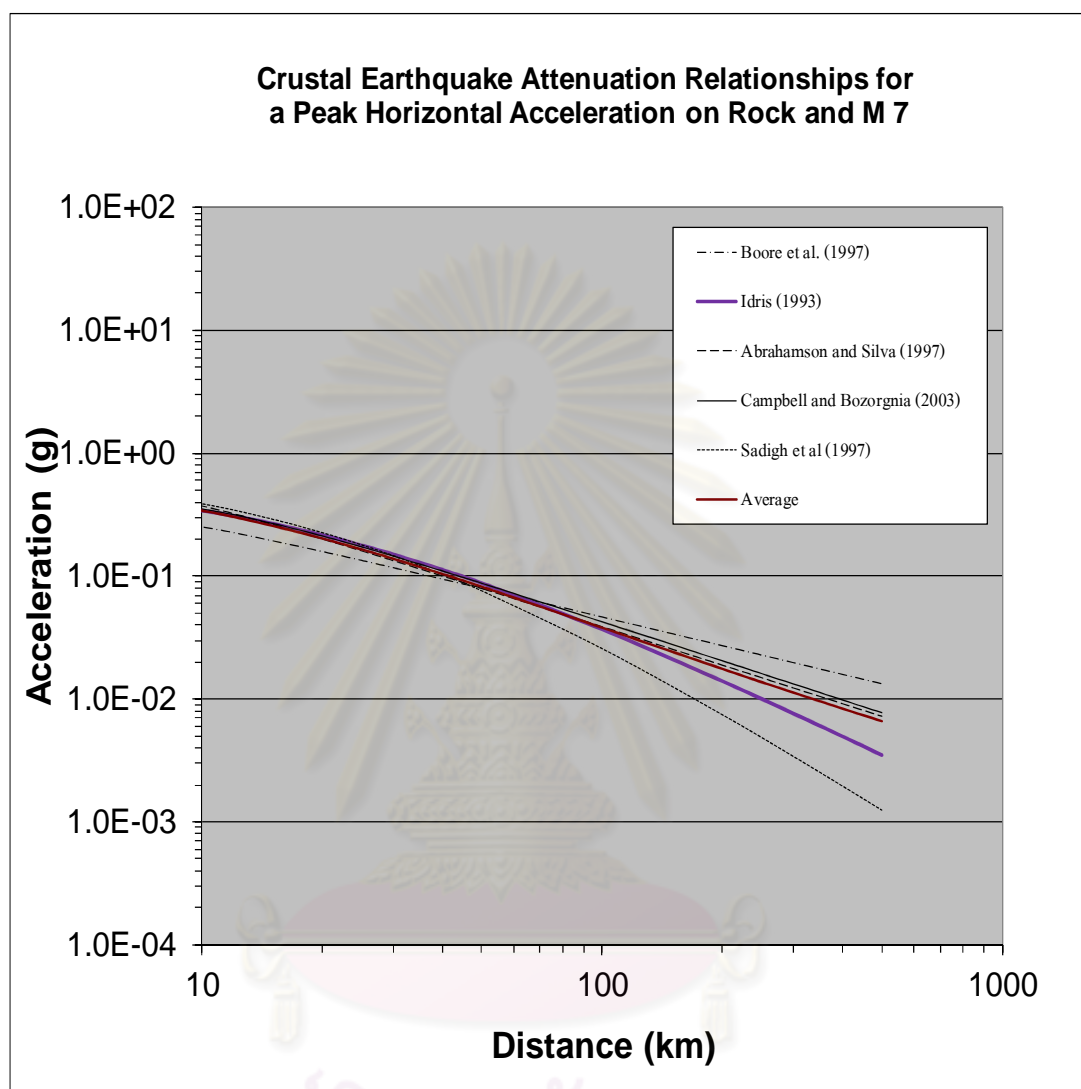


Figure 6.4 Peak horizontal acceleration-attenuation relationships for the magnitude M_w 7.

6.4 Usefulness of Hazard Curves

The hazard curves attached in Appendix F, can be used preliminary to determine the return period of the earthquakes at any site when the ground acceleration or intensity is known. For example, two earthquakes with the magnitude of M_w 4.7 and

M_w 5.0 (USGS website) occurred in the Gulf of Thailand nearby Prachuab Khirikhun province on 28 September 2006 and 8 October 2006 produce ground shaking as shown by seismic intensity maps (DMR, 2006) in Figure 6.5 and 6.6, respectively, as well as an earthquake with the magnitude of M_L 2.7 triggered at Krabi province on 4 May 2008 as shown by the seismic intensity map (done in this study) in Figure 6.7. As a result, the maximum seismic intensities caused by these earthquakes are VI MM scale. If the seismic intensity-peak ground acceleration relationships proposed by Wald et al. (1999) is applied, the maximum peak ground acceleration related to VI MM scale is approximately 0.09g-0.18g. Based on the hazard curve at Plai Phraya district of Krabi province and Muang district of Prachuab Khirikhun province as shown in Figure 6.8 and 6.9, respectively, It can be seen that the return periods of the earthquakes generating the seismic intensity of VI MM scale at Plai Phraya district of Krabi province and Muang district of Prachuab Khirikhun province are about 170-800 years and 850-6,000 years, respectively or the probabilities of exceedance in 50-year hazard level are approximately 48%-96% and 5%-40%, respectively.

6.5 Earthquake Source Contribution

Seismic hazard in southern Thailand is controlled by inland faults, namely KMF, RMF, TNF, TVF, KYF, TPF, KMF areal zone, and the reservoir of Ratchaprapha Dam. The Sumatra-Andaman subduction zone is not a significant contributor to hazard in southern Thailand. This statement can be confirmed by an example of a hazard curve of a nearest site to the Sumatra-Andaman subduction zone as shown in Figure 6.10. This site is located at longitude of 98.16°E and latitude of 7.89°N on the west of Phuket Island. It can be seen that the main contributor is the KMF.

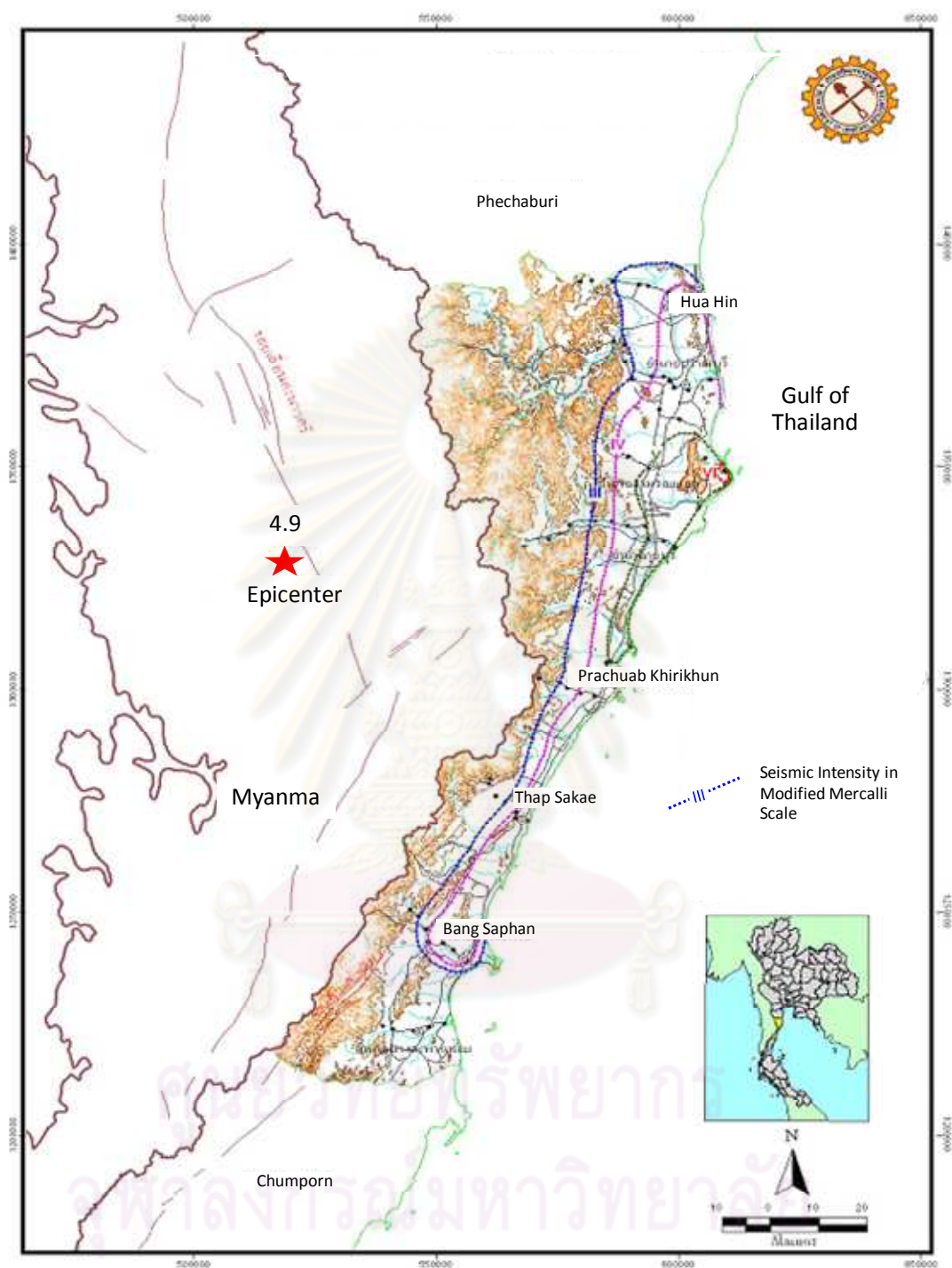
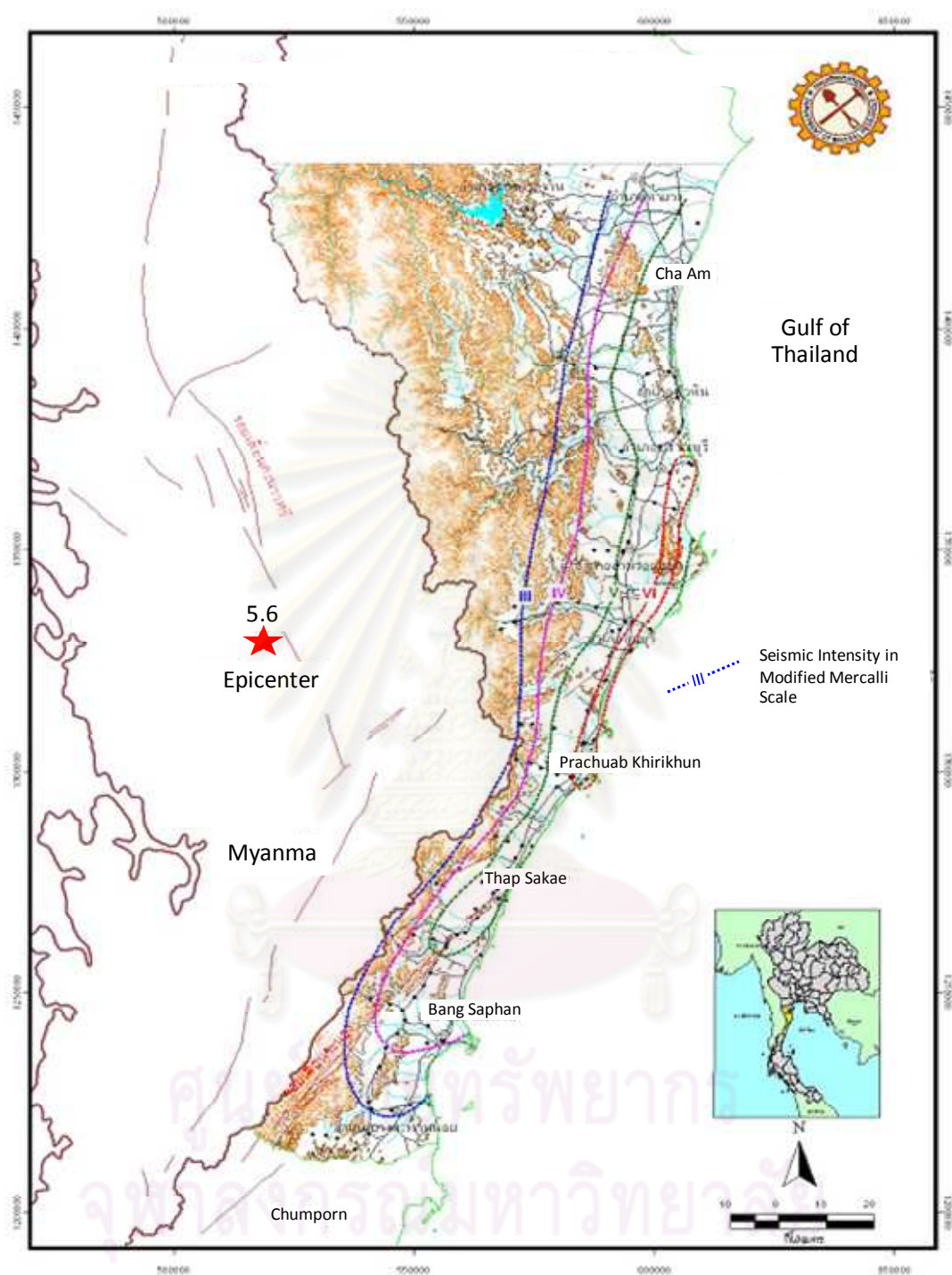
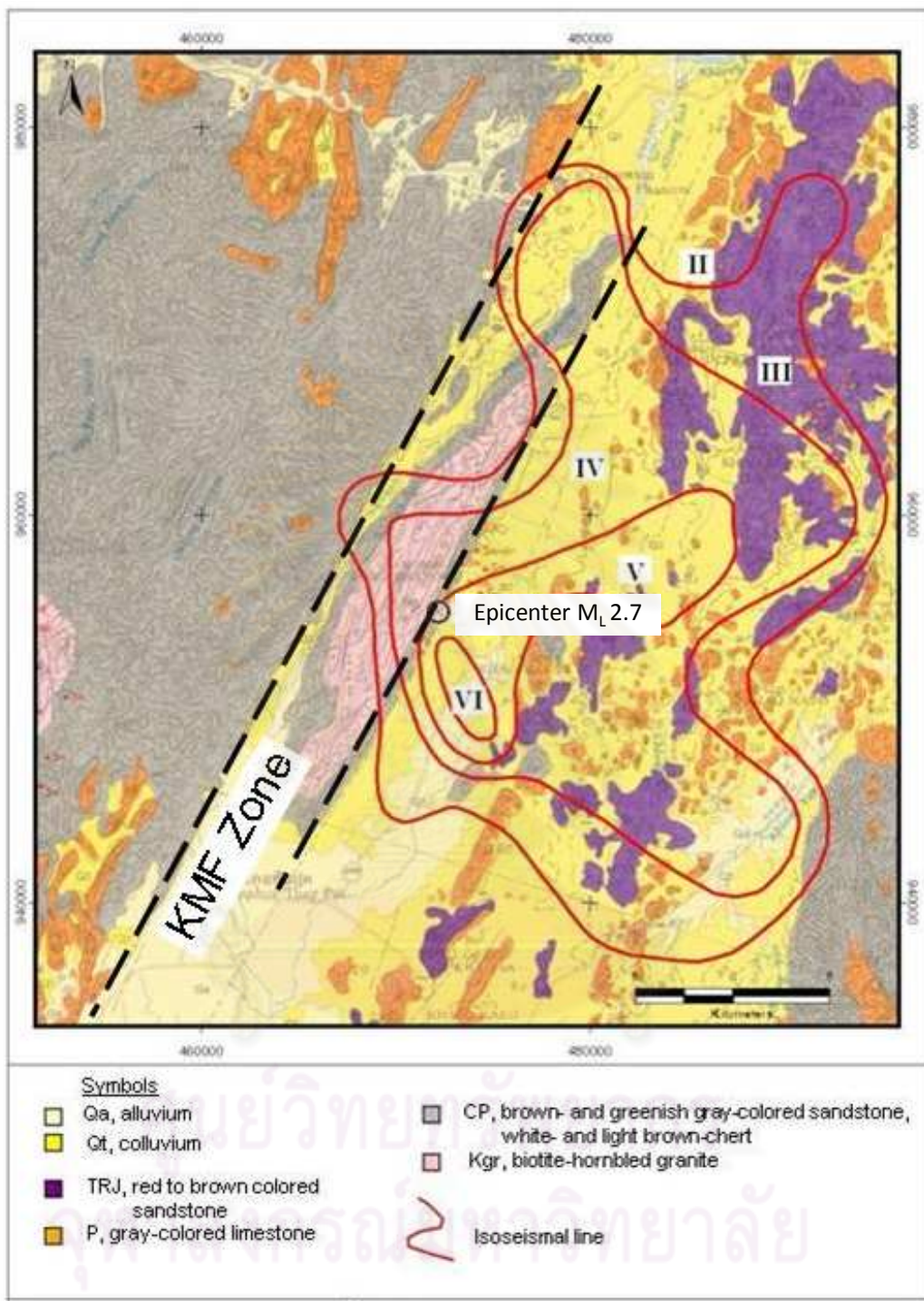


Figure 6.5 Seismic intensity map of the earthquake occurred in the Gulf of Thailand nearby Prachuab Khirikhun province on 28 September 2006 (Department of Mineral Resources, 2006).



Fig

Figure 6.6 Seismic intensity map of the earthquake occurred in the Gulf of Thailand nearby Prachuab Khirikhun province on 8 October 2006 (Department of Mineral Resources, 2006).



Fi

Figure 6.7 Seismic intensity map of the earthquake occurred at Plai Phraya district, Krabi province on 4 May 2008 investigated by this study.

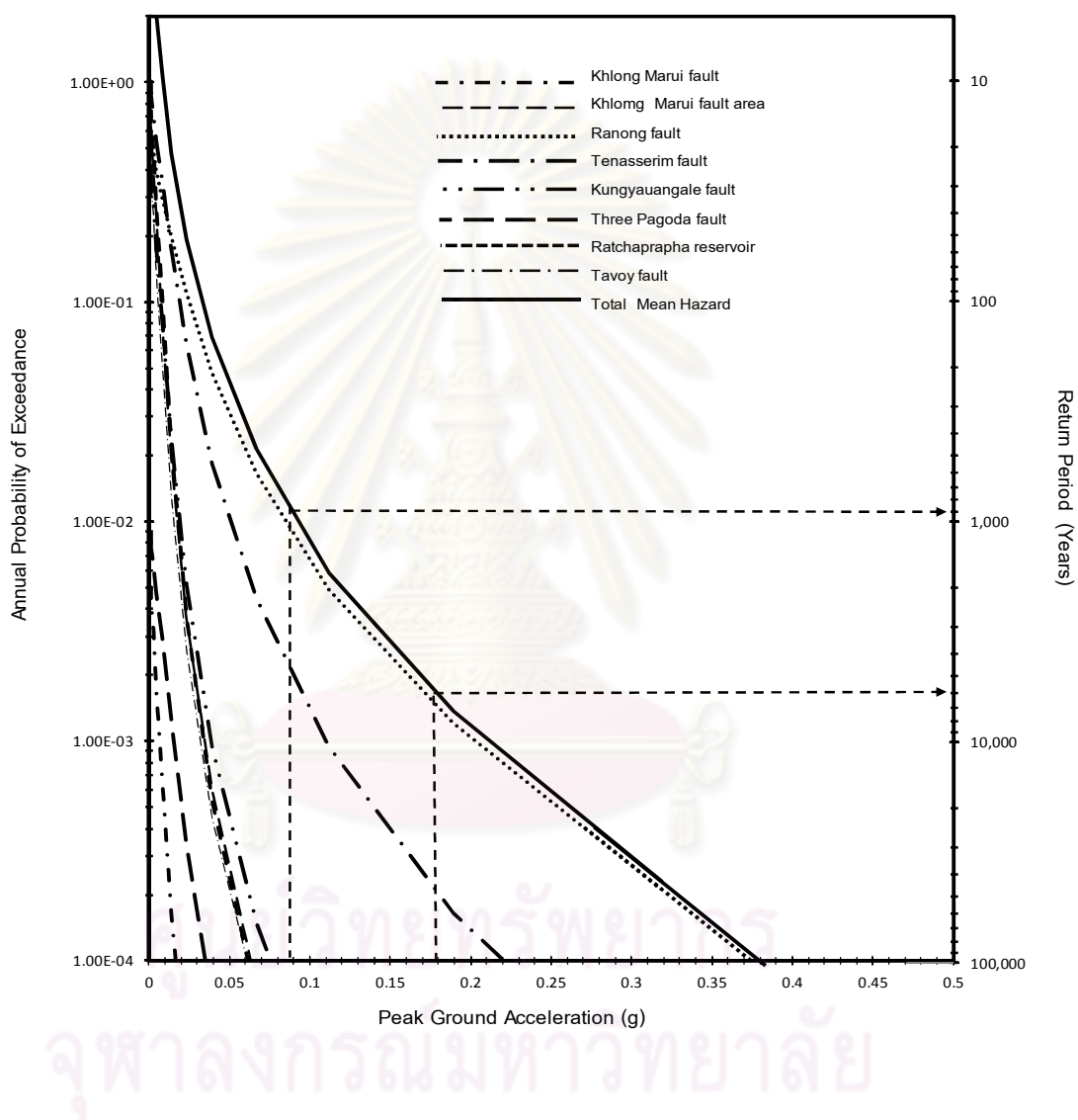


Figure 6.8 Hazard curves for mean peak horizontal acceleration at the site with longitude of 99.81°E and latitude of 11.85°N at Prachaub Khirikhun province.

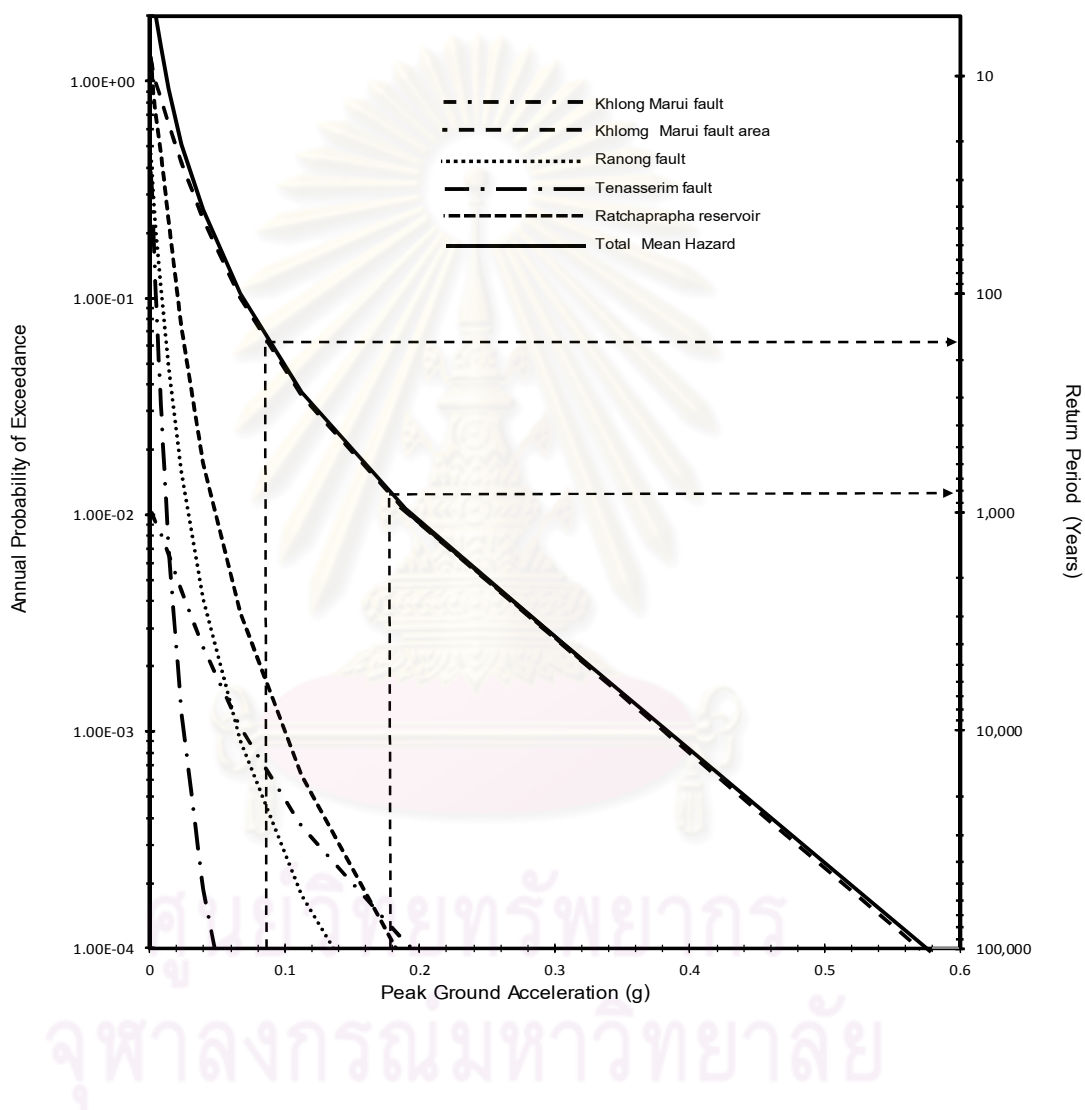


Figure 6.9 Hazard curves for mean peak horizontal acceleration at the site with longitude of 98.82°E and latitude of 8.55°N at Prai Phraya district of Krabi province.

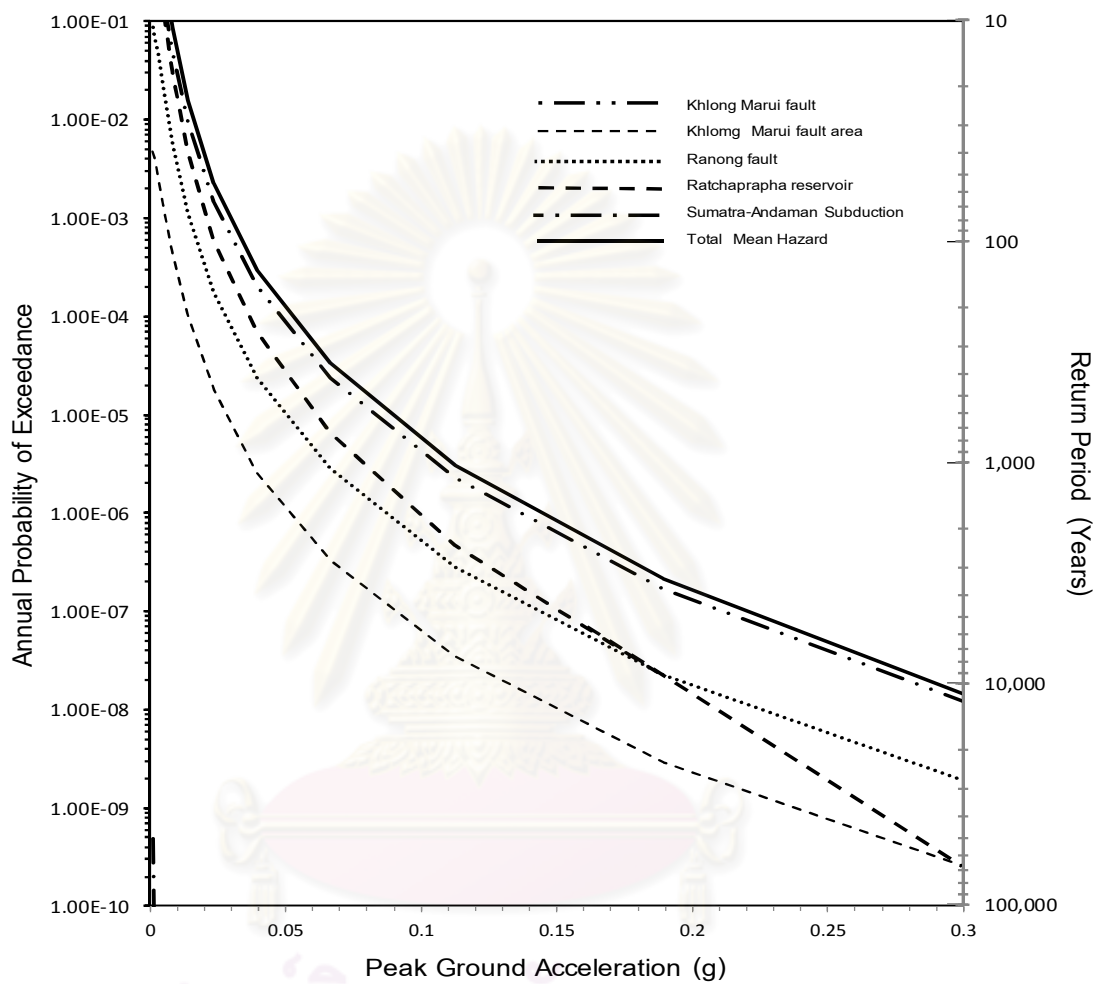


Figure 6.10 Hazard curves for mean peak horizontal acceleration at the site with longitude of 98.16°E and latitude of 7.89°N on the west of Phuket Island.

CHAPTER VII

CONCLUSION AND RECOMMENDATION

7.1 Conclusion

1. The KMF and RNF are both active faults. At least six and four possible large earthquake events of these active KMF and RNF, respectively, are recognized. The ages of these events obtained from TL- and ^{14}C -age dating methods are 1,640-2340 cal yr B.P., 2,580–4,040 cal yr B.P., 4,140-6,140 cal yr B.P., 6,240-7,440 cal yr B.P., 8,640-10,393 cal yr B.P., and 11,640-14,140 cal yr B.P. for the KMF, and 8,230-8,330 cal yr B.P., 9,220-9,340 cal yr B.P., 20,840-21,040 cal yr B.P., and 26,540-41,540 cal yr B.P. for the RNF.

2. Both the KMF (115 km long) and RNF (340 km long) are capable generating the earthquakes with the maximum moment magnitude of M_w 7.2 and M_w 7.9, respectively.

3. The mean recurrence intervals and slip rates of the KMF are approximately $2,200 \pm 830$ years and 0.08-0.5 mm/yr, and those of the RNF are $8,300 \pm 5,544$ years and 0.04-0.17 mm/yr.

4. The probabilities of the KMF's large earthquake occurrence that do not depend on how much time elapsed from the last earthquake can be calculated by supposing the earthquakes distribute randomly (Poisson distribution). The maximum probability of the large earthquake occurrence with the mean recurrence interval is 37%.

5. Active earthquake sources influencing the ground motion in southern Thailand are mainly local line sources as the KMF, RNF, TPF, TNF, TV, and KYF and

6. local areal sources as the reservoir area of Ratchaprapha Dam and the KMF zone. Minor effect is from the Sumatra-Andaman subduction zone.

7. Based on the background earthquakes, the applied b-values of earthquake sources in southern Thailand and western Thailand are 1.03 ± 0.04 and 0.94 ± 0.16 . The evaluated b-value of the Sumatra-Andaman subduction zone is 0.91 ± 0.05 .

8. Due to limitation of strong ground motion data in Thailand, the suitable attenuation relationship has not been developed. In accordance with similar geology and seismotectonic setting, the attenuation relationships established in western North America—for crustal seismic source, i.e. Boore et al.(1997), Abrahamson and Silva (1997), Campbell and Bozorgnia(2003), and Sadigh et al. (1997); and for the Sumatra-Andaman subduction zone, namely Youngs et al. (1997) and Atkinson and Boore (2003)—are applied.

9. Resolving uncertainties of earthquake source characteristics and attenuation relationships, the logic tree approach is adopted in this seismic hazard analysis.

10. Sixteen seismic hazard maps obtained from this study are mean horizontal peak ground, mean 0.2-, 0.3- and 1.0-sec horizontal spectral accelerations with 10%, 5%, 2% and 0.5% probability of exceedance in 50 years for rock site condition. The maximum mean horizontal peak and spectral accelerations are located along the KMF zone at Thap Put district of Phang Nga province, Muang, Phanom and Viphavadi districts of Surat Thani province, and Plai Phraya district of Krabi province.

11. The peak ground and spectral accelerations obtained from this study are higher than those derived from previous studies carried out by Shrestha (1986), Lukkunaprasit and Kuhatasanadeeku (1993), Lisantono (1994), Warnitchai and Lisantono (1997), Warnitchai (1998), Petersen et al. (2007), and Palasri and Ruangrassameen (2010) but lower than the study performed by Pailoplee (2009) at site by site.

12. The b-value is significant parameter in the seismic hazard analysis, i.e. it has more effects on the ground motion for the lower return period than for the higher return period and if the b-value decreases about 75%, the ground acceleration can increase up to almost 70% at the return period of 500 years or 45% at the return period of 10,000 years.

7.2 Recommendation

1. Paleoseismic investigations should be studied further, particularly age-dating data, to determine the characteristics (recurrence interval and slip rate) of the fault sources influencing the ground motion in southern Thailand.

2. Strong ground motion data in Thailand should be collected continuously and systematically from all earthquake-monitoring stations owned by the TMD, RID, EGAT, the Hydrographic Department of Royal Thai Navy and others. If sufficient strong ground motion data are available, the attenuation relationship should be developed for Thailand region.

3. If new data on types and characteristics of seismic sources that effect the ground shaking in southern Thailand are obtained, the seismic hazard map of southern Thailand should be revised.

4. The seismic hazard maps derived from this research are useful as a guideline for preliminary design of buildings and high hazard structures located on the rocks to resist the earthquake force. If any high hazard structures such as high dams will be designed in details, the suitable peak ground acceleration at specified return periods should be studied and evaluated repeatedly.

5. For any structures to be founded on soils, the peak ground or spectral accelerations from this research's seismic hazard maps cannot be adopted directly to the design. The earthquake amplification and liquefaction phenomena should be considered.

REFERENCE

- Abrahamson, N.A. and Silva, W.J. 1997. Empirical response spectral attenuation relations for shallow crustal earthquakes. Seismological Research Letters 68 (1), pp. 94-109.
- Aitken, M.J. 1985. Thermoluminescence dating. London. Academic Press.
- Allen, C.R., et al. 1984. Red River and associated faults, Yunnan province, China—Quaternary geology, slip rates and seismic hazard. Geological Society of America Bulletin 95: pp. 686-700.
- Atkinson, G.M., and Boore, D.M. 2003. Empirical ground-motion relations for subduction zone earthquakes and their applications to Cascadia and other regions. Bulletin of the Seismological Society of America 93: pp. 1703-1729.
- Atkinson, G.M., and Boore, D.M. 2007. Erratum—Earthquake ground-motion prediction equations for eastern North America. Bulletin of the Seismological Society of America 97: pp. 1032.
- Bilham, R. 2005. A flying start, then a slow slip. *Science* 308: pp.1126-1127.
- Boore, D., and Atkinson, G. 2007. Next generation attenuation relations to be published in *Earthquake Spectra* (referred by Petersen et al., 2007).
- Boore, D.M., Joyner, W.B., and Fumal, T.E. 1997. Equations for estimating horizontal response spectra and peak acceleration from western North American earthquakes: A summary of recent work. Seismological Research Letters 68(1): pp. 128–153.
- Bott, J., et al. 1997. Contemporary seismicity in northern Thailand and its tectonic implications. Proceedings of the International Conference on Stratigraphy and Tectonic Evolution of Southeast Asia and the South Pacific, *Geothai* 97, P. Dheeradilok and others (eds.): Thai Department of Mineral Resources 1: pp. 453-464.
- Braun, E. V., et al. 1976. Radiometric age determinations of granites in northern Thailand. Geologischen Jahrbuch B 2: pp.171-204.

- Bunopas, S., and Vella, P. 1992. Geotectonics and geologic evolution of Thailand. Proceedings of a National Conference on Geologic Resources of Thailand: Potential for Future Development, C. Piancharoen (ed.): Thai Department of Mineral Resources, pp. 209-228.
- Campbell, K. W. 1985. Strong motion attenuation relations: a ten year perspective. Earthquake Spectra 1: pp.759-804.
- Campbell, K.W., and Bozorgnia, Y. 2003. Updated near-source ground motion (attenuation) relations for the horizontal and vertical components of peak ground acceleration and acceleration response spectra. Bulletin of Seismological Society of America 93, pp. 314-331.
- Campbell, K., and Bozorgnia, Y. 2007. Next generation attenuation relations to be published in Earthquake Spectra (referred by Petersen et al., 2007).
- Charles, J.A., Abbiss, C.P., Gosschalk, E.M., and Hinks J.L. 1991. An engineering guide to seismic risk to dams in the United Kingdom. Building Research Establishment Report.
- Charusiri, P. 2005. Active fault study in Ongkalak Fault Zone, Ongkalak, Nakhon Nayok, Central Thailand. Technical report, Department of Geology, Faculty of Science, Chulalongkorn University, Bangkok, Thailand. 185p. (in Thai with English abstract).
- Charusiri, P., Doarerk, V., Archibald, D., Hisada, K., and Ampaiwan, T. 2002. Geotectonic evolution of Thailand: A new synthesis. Journal of the Geological Society of Thailand 1: pp.1-20.
- Charusiri, P., Kosuwan, S., Daoroek, V., Vechbunthoeng, B., and Khuthranon, S. 2000. Earthquake in Thailand and Southeast Asia. Technical report, National Research Council of Thailand, Bangkok, Thailand: 171p. (in Thai).
- Charusiri, P., Kosuwan, S., and Imsamut, S. 1997. Tectonic evolution of Thailand: from Bunopas (1981)'s to a new scenario. Proceedings of the International Conference on Stratigraphy and Tectonic Evolution of Southeast Asia and the South Pacific, Department of Mineral Resources, Bangkok, Thailand: pp.414-420.

- Charusiri, P., Pananon, P., Wan-in, K., Pailoplee, S., and Danphaiboonphol, V. 2006. Trenching and study of Mae Yom fault at Kaeng Sua Ten dam, Song district of Phrae province. Final report submitted to the Royal Irrigation Department (in Thai).
- Charusiri, P., et al. 2007. Regional tectonic setting and seismicity of Thailand with reference to reservoir construction. Proceeding of GEOTHAI'07 International Conference on Geology of Thailand: Toward Sustainable Development and Sufficiency Economy, Bangkok, Thailand: pp.274-287.
- Chen, W., and Molnar, P. 1983. Focal depths of intracontinental and intraplate earthquakes and its implications for the thermal and mechanical properties of the lithosphere. Journal of Geophysical Research 88, pp. 4183-4214.
- Chintanapakdee, C., Naguit, M.E., and Charoenyuth, M. 2008. Suitable attenuation model for Thailand. The 14th World Conference on Earthquake Engineering, October 12-17, 2008, Beijing, China.
- Chiou, B., and Youngs, R. 2007. Next generation attenuation relations to be published in Earthquake Spectra (referred by Petersen et al., 2007).
- Chlieh, M., et al. 2006. Coseismic slip and afterslip of the great (Mw9.15) Sumatra-Andaman earthquake of 2004. Bulletin of the Seismological Society of America 97, no. 1A: pp. S152–S173.
- Chuaviroj, S. 1991. Geotectonics of Thailand. Technical report, Geological Survey Division, Department of Mineral Resources, Bangkok, Thailand, p.58. (in Thai)
- Convertito, V., Emolo, A., and Zollo A. 2006. Seismic-hazard assessment for a characteristic earthquake scenario: an integrated probabilistic–deterministic method. Bulletin of the Seismological Society of America 96, no. 2: pp.377-391.
- Cornell, C.A. 1968. Engineering seismic risk analysis. Bulletin of the Seismological Society of America 58: pp. 1583-1606.
- Cornell, C. A., and Van Marke, E.H. 1969. The major influences on seismic risk. Proceeding Third World Conference on Earthquake Engineering, Santiago, Chile, A-1: pp.69–93.

- Coppersmith, K. J., and Youngs, R. R. 1986. Capturing uncertainty in probabilistic seismic hazard assessments within intraplate tectonic environments. *Proceedings of the Third U.S. National Conference on Earthquake Engineering 1*: pp.301–312.
- Crouse, C.B. (1991). Ground motion attenuation equation for earthquakes on Cascadia subduction zones. *Earthquake Spectra* 7(2): pp. 201-236.
- Das, S., Gupta, I.D., and Gupta, V.K. 2006. A probabilistic seismic hazard analysis of Northeast India. *Earthquake Spectra* 22(1): pp. 1-27.
- dePolo, C.M., and Slemmons, D.B. 1990. Estimation of earthquake size for seismic hazards. *Geological Society of America Reviews in Engineering Geology VII*, pp. 1-27.
- DMR (Department of Mineral Resources) 1976. Geological map of Phangnga province sheet, 1:250,000 scale.
- DMR (Department of Mineral Resources) 2002. Preliminary active fault map of Thailand.
- DMR (Department of Mineral Resources) 2005. Seismic intensity map of Thailand.
- DMR (Department of Mineral Resources) [Online] 2006. Active Fault Map of Thailand. Available from: <http://www.dmr.go.th>. [2006, May 5].
- DMR (Department of Mineral Resources) 2007. Study on recurrence interval of faults in Prachub Khirikhun, Chumporn, Ranong, Surat Thani, Krabi, Phangnga and Phuket provinces (Ranong and Khlong Marui faults) carried out by the Department of Geology, Faculty of Science, Chulalongkorn University Final Report (in Thai).
- DMR (Department of Mineral Resources) [Online] 2008. Seismic intensity map of Thailand. Available from: <http://www.dmr.go.th>. [2008, May 22].
- Douglas, J. 2001. A comprehensive worldwide summary of strong-motion attenuation relationships for peak ground acceleration and spectral ordinates (1969 to 2000). Technical report, Engineering Seismology and Earthquake Engineering (ESEE) 01-1, 144p.

- Ducrocq, S., et al. 1992. Tertiary continental basins of Thailand as a result of strike-slip motions induced by the India-Asia collision. Journal of Southeast Asian Earth Sciences 7: pp. 260.
- Duerrast, H., Dangmuan, S., and Lohawijarn, W. 2007. Khlong Marui and Ranong fault zones in southern Thailand re-activated by the 26 December 2004 Mw 9.3 Sumatra-Andaman Earthquake. Proceeding of the 2007 International Conference on Geology of Thailand: Towards Sustainable Development and Sufficiency Economy, GEOTHAI'07, 21-22 NOVEMBER 2007, Bangkok, pp.141-144.
- Esteva, L., and Villaverde, R. 1973. Seismic risk, design spectra and structural reliability. Proceeding of 5th World Conference on Earthquake Engineering, Rome, Italy: pp. 2586-2597.
- Fenton, C.H., Charusiri P., Hinthong C., Lumjuan A., and Mangkonkarn B. 1997. Late Quaternary faulting in northern Thailand. Proceeding of the International Conference on Stratigraphy and Tectonic Evolution of Southeast Asia and South Pacific. Department of Mineral Resources. Bangkok, pp. 436-452.
- Fenton, C.H., Charusiri, P., and Wood, S.H. 2003. Recent paleoseismic investigations in Northern and Western Thailand. Annals of Geophysics 46(5): pp.957-981.
- Gardner, J.K., and Knopoff, L. 1974. Is the sequence of earthquakes in Southern California, with aftershocks removed, Poissonian?. Bulletin of the Seismological Society of America 64(1): pp.363-367.
- Garson, M.S. 1970. Transform faulting in the Thai peninsula. Nature 220: pp.45-47.
- Geological Department, Science Faculty, Chulalongkorn University, and Physical Department, Science Faculty, Mahidol University 2006. Trenching and Mae Nam Yom fault investigation at Kaeng Sua Ten dam, Song district, Phrae province, Thailand (in Thai).
- Geyh, A.A., and Schleicher H. 1990. Absolute age determination. Springer-Verlag, Berlin
- Golonka J. 2002. Plate-tectonic maps of the Phanerozoic. In: W. Kiessling, E. Flügel, & J. Golonka (Editors), Phanerozoic reef patterns. SEPM Spec. Publ. 72: pp.21-75.

- Gregor, N., Silva, W., Wong, I., and Youngs, R. 2002. Ground motion attenuation relationships for Cascadia subduction zone megathrust earthquakes based on a stochastic finite-fault model. Bulletin of the Seismological Society of America 92: pp. 1923-1932.
- Gutenberg, B., and Richter, C.F. 1954. Seismicity of the Earth and Associated Phenomena. Princeton University Press, Princeton, New Jersey.
- Hanks, T.C., and Kanamori, H. 1979. A moment-magnitude scale. Journal of Geophysical Research 84: pp.2348–2350.
- Harnpattanapanich, T. 2010. Thin-skinned fold-and-thrust belt of Khorat Plateau. RGJ Seminar Series LXVII on Geohazards: Incoming Disasters for Thailand? Abstract. Bangkok Center Hotel, Bangkok, Thailand (unpublished).
- Hattori, S. 1980. Seismic risk map in the Asian countries (maximum acceleration and maximum particle velocity)—China, India, Pakistan, Burma, Thailand, Philippines, Indonesia and Others. International Conference on Engineering for Protection from Natural Disasters, Asian Institute of Technology, Bangkok, pp. 491-504.
- Hinthong, C. 1991. Role of Tectonic Setting in Earthquake Events in Thailand. In the proceedings of Asean-EC Workshop on Geology and Geophysics, Jakarta, Indonesia, 7-11 October 1997, pp. 236-242.
- Hinthong, C. 1995. The study of active fault in Thailand. In the proceedings of the technical conference on the progression and vision of mineral resources development, Department of Mineral Resources, Bangkok, pp.129-40.
- Hoke, L., and Campbell, H.J., 1995, Active mantle melting beneath Thailand? Proceedings of the International Conference of Geology, Geotechnology, and Mineral Resources of Indochina, Khon Kaen, Thailand, W. Youngme, C. Buaphan, K. Srisuk, and R. Lertsirivorakul (eds.). Department of Geotechnology, Khon Kaen University, pp. 13-22.

- Idriss, I.M. 1985. Evaluating seismic risk in engineering practice. Proceeding of the 11th International Conference on Soil Mechanics and Foundation Engineering, San Francisco 1: pp. 255-320.
- Idriss, I.M. 1993. Procedures for selecting earthquake ground motions at rock sites. Technical report NIST GCR 93-625, U.S. Department of Commerce, National Institute of Standards and Technology, Gaithersburg, Maryland.
- International Committee on Large Dams, 1989. Guidelines for selecting seismic parameters for dams, Bulletin 72.
- Ishii, M., Shearer, P.M., Houston, H., and Vidale, J.E. 2005. Rupture extent, duration, and speed of the 2004 Sumatra-Andaman earthquake imaged by the Hi-Net array. *Nature* 999: pp. 1-4.
- Iwakuni, M., Kato, T., Takiguchi, H., Nakaegawa, T., and Satomura, M. 2004. Crustal deformation in Thailand and tectonics of Indochina peninsula as seen from GPS observations. Geophysical Research Letters 31, 4 p.
- Kosuwan, S., Saithong, P., and Wiwegwin, W. 2006. Paleoearthquake on the Three Pagoda and Sri Sawat fault zones, Kanchanaburi, western Thailand. Report of Geological Hazard Division, Department of Mineral resources, (in Thai with English abstract).
- Kramer, S.L. 1996. Geotechnical Earthquake Engineering. Prentice Hall, Inc., Upper Saddle River, New Jersey. 563 p.
- Krinitzsky, E.L. 1995. Deterministic versus probabilistic seismic hazard analysis for critical structures. Engineering Geology 40: pp.1-7.
- Kulkarni, R. B., Youngs R. R., and Coppersmith K. J. 1984. Assessment of confidence intervals for results of seismic hazard analysis. Proceedings of the Eighth World Conference on Earthquake Engineering, San Francisco 1: pp.263–270.
- Lee, T.Y., and Lawver, L.A. 1994. Cenozoic plate reconstruction of the South China Sea region. *Tectonophysics* 235: pp.149-180.

- Lisantono, A. 1994. Development of a seismic risk map for the structural design code in Thailand. M.E. thesis, Asian Institute of Technology, Bangkok, Thailand.
- Lukkunaprasit, P., and Kuhatasanadeekul, N. 1993. Seismic zoning and seismic coefficients for Thailand. Proceeding on Annual Meeting of the Engineering Institute of Thailand under H.M. the King's Patronage, November 27-30, pp. 268-285.
- Markirt, T., Laoprapaipan, P., Sanguanlosit, A., Jariyabhumi, O., and Anupandhanant, P. 1984. Lignite exploration at Krabi basin. Proceeding of Conference on Application of Geology and the National Development, Bangkok, pp.9-39.
- Martel, S.J. [Online] 2002. Recurrence intervals and probability (18). Engineering geology lecture notes. Department Geology and Geophysics, School of Ocean and Earth Science and Technology, University of Hawaii at Manoa. Available from: <http://www.soest.hawaii.edu/martel/courses/GG454/GG454 lec 18.pdf> [2010, January 3]
- McCalpin, J. 1996. Paleoseismology. Elsevier Inc., California, USA.
- McCalpin, J. 2009. Paleoseismology. 2nd Edition, Elsevier Inc., California, USA.
- McGuire, R.K. 2001. Deterministic vs. probabilistic earthquake hazards and risks. Soil Dynamics and Earthquake Engineering 21: pp. 377-384
- Metcalf, I. 1996. Pre-Cretaceous evolution of SE Asia terranes. In: Hall, R., Blundell, D.J. (eds). Tectonic Evolution of Southeast Asia. Geological Society, London, Special Publication 106: pp.97-122.
- Metcalf, I 2009. Late Paleozoic and Mesozoic tectonic and paleogeographical evolution of SE Asia. Special Report of the Geological Society of London 315: pp.7-23.
- Morley, C. K. 2001. Combined escape tectonics and subduction rollback-back arc extension, a model for the evolution of Tertiary rift basins in Thailand, Malaysia, and Laos. Journal of the Geological Society of London 158: pp.461-474.
- Morley, C. K. 2004. Nested strike – slip duplexes, and other evidence for Late Cretaceous – Paleogene transpressional tectonics before and during India – Eurasia collision, in Thailand, Myanmar and Malaysia. Journal of the Geological Society of London 161: pp.799 – 812.

- Morley, C.K. 2007. Variations in Late Cenozoic-Recent strike-slip and oblique-extensional geometries, within Indochina: The influence of pre-existing fabrics. Journal of Structural Geology 29: pp.36-58.
- Morley, C. K. 2008. Structural and Tectonic Controls on Cenozoic Petroleum Provinces and Systems in Thailand. Proceedings of International Symposia on Geoscience Resources and Environments of Asian Terranes, Bangkok, Thailand, pp. 54-55.
- Nutalaya, P., Sodsri, S., and Arnold, E.P. 1985. Series on seismology, volume II – Thailand: In E.P Arnold (ed.), Technical report Southeast Asia Association of Seismology and Earthquake Engineering.
- Olinstad, T., Moriarty, T., Harder, S., and McCabe, R. 1989. Cenozoic rifting in Thailand. EOS, Transactions of the American Geophysical Union 70: pp. 1343.
- Ordaz, M., Aguilar A., and Arboleda, J. 2007. CRISIS 2007, Program for computing seismic hazard. Engineering Institute of the National University of Mexico (UNAM).
- Packham, G.H. 1993. Plate tectonic and the development of sedimentary basins of the dextral regimes: revisions and a new peak ground velocity relation. Journal of Southeast Asian Earth Sciences 8: pp.497-511.
- Pailoplee, S. 2004. Thermoluminescence regeneration method. M.S. thesis, Department of Geology, Chulalongkorn University, Bangkok, Thailand.
- Pailoplee, S. 2009. Seismic hazard assessment in Thailand using probabilistic and deterministic methods, Master 's thesis, Department of Geology, Faculty of Science, Chulalongkorn University, Bangkok, Thailand. 163 p.
- Palasri, C., and Ruangrassamee, A. 2010. Probabilistic seismic hazard map of Thailand, Journal of Earthquake and Tsunami 4: pp. 369-389.
- Pananon, P. 2009. Earthquake Hazard Risk Study in Prachuabkirikhan Province and adjacent Area. Final Report (in Thai).
- Pankow, K.L., and Pechmann, J.C. 2004. The SEA99 ground-motion predictive relations for extensional regimes: Revisions and a new peak ground velocity relation. Bulletin of Seismological Society of America 94, pp. 341-348.

- Park, J., et al. 2005. Earth's free oscillations excited by the 26 December 2004 Sumatra-Andaman earthquake. Science 308: pp.1139-1144.
- Peltzer, G., and Tapponnier, P. 1988. Formation and evolution of strike-slip faults, rifts, and basins during the India-Asia collision: an experimental approach. Journal of Geophysical Research 93: pp. 15,085-15,177.
- Petersen, M., et al. 2004. Probabilistic seismic hazard analysis for Sumatra, Indonesia and across the Southern Malaysian Peninsula. Tectonophysics 390: pp. 141–158.
- Petersen M., et al. 2007. Documentation for the Southeast Asia seismic hazard map. Administrative Report, September 30, 2007, U.S. Department of the Interior and U.S. Geological Survey.
- Promthong C., Simons, W. J. F., and Satirapod, C. 2006. Deformation of Thailand measured by GPS due to the December 2004 mega-thrust earthquake. Proceedings of the 17th United Nations Regional Cartographic Conference for Asia and the Pacific, Bangkok, 18-22 September 2006.
- Phromthong, C., Yusamran, S., Sathiraphoj, C., Simon W.J.F., and Ambrosius, B. A. C. 2005. Deformation of the reference network after 26 December 2004 large earthquake, 7 p. (in Thai).
- Poolachan, S. 1988. Summary of the structural evolution of the Mergui Basin, S.E. Andaman Sea and the development of Tertiary basins in Thailand. Newsletter, Chiangmai Univeraity, 1 p. (unpublished).
- Power M.S., Coppersmith, K.J., Youngs, R.R., Schwartz, D.P. and Swan, R.H. 1981. Seismic exposure analysis for the WNP-2 and WNP-1/4 site: Appendix 2.5K to Amandment No.18 Final Safety Analysis Report for WNP-2, Woodward-Clyde Consultants, San Francisco, 63 p. (referred in Kramer,1996).
- Polachan, S., et al. 1991. Development of Cenozoic basins in Thailand. Marine and Petroleum Geology 8: pp.84-97.

- Rajendran, C.P., et al. 2007. Crustal deformation and seismic history associated with the 2004 Indian Ocean earthquake—A perspective from the Andaman-Nicobar Islands. Bulletin of the Seismological Society of America 97: pp. S174–S191.
- Reid, H.F. 1910. The Mechanics of the Earthquake, The California Earthquake of April 18, 1906. Report of the State Investigation Commission 2, Carnegie Institution of Washington, Washington, D.C.
- Reiter, L. 1990. Earthquake hazard analysis: issues and insight. Columbia University Press, New York.
- Rhodes, B.P., Perez, R., Lamjuan, A., and Kosuwan, S. 2004. Kinematics and tectonic implications of the Mae Kuang Fault, northern Thailand. Journal of Asian Earth Sciences 24(1): pp.79-89.
- Richter, C.F. 1958. Elementary Seismology. W.H. Freeman, San Francisco
- RID (The Royal Irrigation Department), 2006. Environmental development and mitigation on Tha Sae Dam project, Chumporn province, Thailand. Final report prepared by Panya Consultants Co., Ltd. and P & C Management Co., Ltd. (in Thai).
- RID (The Royal Irrigation Department), 2007, Dam break study for Khlong Madue Dam, Nakhorn Nayok province, Thailand. Final report prepared by Panya Consultants Co., Ltd., Kasetsart University and Phisut Technology Co., Ltd. (in Thai).
- RID (The Royal Irrigation Department), 2008. Feasibility study and detailed design of dams and water distribution network in Phangnga province: Khlong Tham Dam project, Muang district, Phang Nga province, Thailand. Final report prepared by Panya Consultants Co., Ltd., Phisut Technology Co., Ltd., and Megatech Consultant Co., Ltd. (in Thai).
- RID (The Royal Irrigation Department), 2009. Active fault investigation for Lam Rooyai dam in Thaiy Muang district, Phang Nga province. Final report prepared by Panya Consultants Co., Ltd. (in Thai).
- Sadigh, K., Chang, C.Y., Egan, J.A., Makdisi, F., and Youngs, R.R. 1997. Attenuation relationships for shallow crustal earthquakes based on California strong motion data. Seismological Research Letters 68(1): pp. 180–189.

- Santoso, D. 1981. Natural hazard of Bangkok area (earthquake and flooding). M.S. thesis, No. GT-81-22, Asian Institute of Technology, Bangkok, Thailand.
- Schwartz, D.P., and Coppersmith, K. J. 1984. Fault behavior and characteristic earthquakes--examples from the Wasatch and San Andreas fault zones. Journal of Geophysical Research 89: pp. 5681-5698.
- Searle, M. P., et al. 1987. The closing of Tethys and the tectonics of Himalaya. Geological Society of America Bulletin 98, pp. 678-701.
- Shrestha, P.M. 1986. Investigation of active faults in Kanchanaburi province, Thailand. M.S. thesis, No. GT-86-30, Asian Institute of Technology, Bangkok, Thailand.
- Simons, W. J. F, et al. [Online] 2005. GPS measurements in S.E. Asia: Sundaland motion and deformation before and after the December 26th, 2004 magnitude 9.0 earthquake. Available from www.deos.tudelft.nl/seamerges/docs/seminarsimon.pdf. [2005, December 4].
- Siribhakdi, K. 1986. Seismogenic of Thailand and periphery. 1st Workshop on Earthquake Engineering and Hazard Mitigation, Bangkok, Thailand, P. Lukkunaprasit, K., Chandrangsu, S. Poobrasert, and M. Mahasuverachai (eds.): Southeast Asia Association of Seismology and Earthquake Engineering (SEASEE) and National Earthquake Committee of Thailand, pp. 151-158.
- Socquet, A., et al. 2006. India and Sunda plates motion and deformation along their boundary in Myanmar determined by GPS. Journal of Geophysical Research 111, B05406, doi: 10.1029/2005JB003877, 11 p.
- Stein, S., and Okal, E.A. 2005. Speed and size of the Sumatra earthquake. Nature 434: pp.581-582.
- Suensilpong, S., Putthapiban, P., and Mantajit, N. 1981. Some aspects of tin granites and its relationship to tectonic setting. Geological Society of America Bulletin, Special volume 1981, 9 p.
- Sutiwanich, C., Hanpatanapanich, T., Charusiri, P., and Trinetra, K. 2008. Seismic hazard analysis of the Khlong Tham dam project in Thailand. Proceeding of the International Symposia on Geoscience Resources and Environments of Asian

- Terrains (GREAT 2008), 4th IGCP 516 and 5th APSEG, Bangkok, Thailand: pp. 416-420.
- Takashima, I., and Honda S. 1989. Comparison between K-Ar and TI dating results of pyroclastic flow deposits in the Aizutajima area, northeast Japan. Journal of Geological Society, Japan 95: pp.807-816.
- Tapponier, P., Peltzer, G., and Armijo, R. 1988. On the mechanics of the collision between India and Asia. In M. P. Coward and A. C. Ries (eds.), Collision Tectonics. Geological Society of America Bulletin, Special Publication, No. 19: pp. 115-157.
- TEAM (Team Consulting Engineers Co., Ltd. and Quality Team Consultants Co., Ltd.) 1995. Final report (Annex), Feasibility study and environmental impact assessment of Tha Sae-Rub Ro reservoirs project, Chumporn Province, Thailand.
- Toro, G.R. 2002. Modification of the Toro et al. (1997) attenuation equations for large magnitudes and short distances. Risk Engineering, pp.4-1 to 4-10.
- Tuniz, C., Bird, J. R., Fink, D., and Herzog, G. F. 1998. Accelerator mass spectrometry: ultrasensitive analysis for global science. CRC Press LLC.
- US Army Corps of Engineers 1999. Response spectra and seismic analysis for concrete hydraulic structures. Engineering Manual:EM 1110-2-6050.
- USCOLD (U.S. Committee of Large Dam 1985. Guidelines for selecting seismic parameters for dam projects, October.
- USCOLD (U.S. Committee on Large Dams) 1998. Updated guidelines for selecting parameters for dam project, 50 p.
- USGS (U.S. Geological Survey) [Online] 2005a. Magnitude 9.0 –Northern Sumatra, Indonesia, December 26 ,2004. Available from:<http://earthquake.usgs.gov/earthquakes/equithenews/2005/usweax/> [2011, January 6].
- USGS (U.S. Geological Survey) [Online] 2005b, Magnitude 8.6 –Northern Sumatra, Indonesia, March28, 2005. Available from:<http://earthquake.usgs.gov/earthquakes/equithenews/2005/usweax/> [2011, January 6].

- Vigny, C., et al. 2003. Present-day crustal deformation around Sagaing Fault, Myanmar. Journal of Geophysical Research 108: pp.6-1- 6-10.
- Vigny, C., et al. 2005. Insight into the 2004 Sumatra – Andaman earthquake from GPS measurement in southeast Asia. Nature 436: pp.201 – 206.
- Wald, D.J., Quitoriano, V., Heaton T.H., and Kanamori H. 1999. Relationships between peak ground acceleration, peak ground velocity, and modified Mercalli intensity in California. Earthquake Spectra 15: pp.557-564.
- Warnitchai, P. 1998. Potential earthquake disaster in Thailand and its mitigation. Proceeding of International Seminar on Earthquake Resistant Design of Structures, Chiang Mai, Thailand, pp.108-126.
- Warnitchai, P., and Lisantoso, A. 1997. Probabilistic seismic risk mapping for Thailand. Proceeding of the Second Workshop on Building Design Resisting Seismicity, Asia Hotel, Bangkok, Thailand, pp.135-143.
- Watkinson I., Elders C., and Hall R. 2008. The kinematic history of the Khlong Marui and Ranong faults, southern Thailand. Journal of Structural Geology 30: pp.1554-1571.
- WCFS (Woodward-Clyde Federal Services), 1996, Seismic hazards evaluation, environmental impact assessment: geological aspect, Kaeng Sua Ten Dam Project, Changwat Phrae: unpublished report prepared by GMT Corporation and others for the Department of Mineral Resources.
- WCFS (Woodward-Clyde Federal Services), 1998, Seismic hazard evaluation of Khao Laem and Srinagarind Dams, Thailand: unpublished report prepared for Electricity Generation Authority of Thailand, Bangkok, Nonthaburi 11000.
- Weichert, D.H. 1990. Estimation of the earthquake recurrence parameters for unequal observation period for different magnitudes. Bulletin of the Seismological Society of America 84: pp. 1,337-1,346.
- Well, D.L., and Coppersmith, K.J. 1994. New empirical relationships among magnitude, rupture length, rupture width, rupture area, and surface displacement. Bulletin of the Seismological Society of America 91: pp.12,587-12,631.

- Wichagul, P. 1986. Krabi coal deposit. Geological report, volume 1, Electricity Generating Authority of Thailand's report no.211-01-2914.
- Wieland, M. and Brenner, R.P. [Online] 2011. Current seismic safety requirements for large dam and their omplication on existing dams. Available from: http://www.poyry.ch/linked/en/aboutus/Current_seismic_safety_requirements_for_large_dams_0408.pdf [2011, April 22].
- Woessner, J., and Wiemer, S. 2005. Assessing the quality of earthquake catalogues: Estimating the magnitude of completeness and its uncertainty. Bulletin of the Seismological Society of America 95: pp.684-698.
- Wong, I., Fenton, C., Dober, M., Zachariassen, J., and Terra, F. 2005. Seismic hazard evaluation of the Tha Sae project, Thailand. Final report submitted to the Royal Irrigation Department, Bangkok, Thailand, 118 p.
- Youngs, R.R., Chiou, S.J., Silva, W.J., and Humphrey, J.R. 1997. Strong ground motion attenuation relationships for subduction zone earthquakes. Seismological Research Letters 68: pp. 58–73.
- Youngs, R.R., and Coppersmith, K.J. 1985. Implications of fault slip rates and earthquake recurrence models to probabilistic seismic hazard estimates. Bulletin of the Seismological Society of America 75: pp. 939-964.
- Zimmermann, D.W. 1971. TL dating using fine grains from pottery. Archaeometry 13: pp.29-59.
- Zhao, J., et al. 1997. Attenuation relations of strong motion in Japan using site classification based on predominant period. Bulletin of the Seismological Society of America 96: pp. 898.



APPENDICES

ศูนย์วิทยทรัพยากร
จุฬาลงกรณ์มหาวิทยาลัย



APPENDIX A

CONSTANT VALUES OF ATTENUATION RELATIONSHIPS

ศูนย์วิทยทรัพยากร
จุฬาลงกรณ์มหาวิทยาลัย

Table A.1 Constant values for Abrahamson and Silva (1997) attenuation relationships.

Period(s)	c_4	a_1	a_2	a_3	a_4	a_5	a_6	a_9	a_{10}	a_{11}	a_{12}	a_{13}	c_1	c_5	n
PGA	5.6	1.64	0.512	-1.145	-0.144	0.61	0.26	0.37	-0.417	-0.23	0	0.17	6.4	0.03	2
0.02	5.6	1.64	0.512	-1.145	-0.144	0.61	0.26	0.37	-0.417	-0.23	0	0.17	6.4	0.03	2
0.03	5.6	1.69	0.512	-1.145	-0.144	0.61	0.26	0.37	-0.47	-0.23	0.014	0.17	6.4	0.03	2
0.04	5.6	1.78	0.512	-1.145	-0.144	0.61	0.26	0.37	-0.555	-0.251	0.025	0.17	6.4	0.03	2
0.05	5.6	1.87	0.512	-1.145	-0.144	0.61	0.26	0.37	-0.62	-0.267	0.028	0.17	6.4	0.03	2
0.06	5.6	1.94	0.512	-1.145	-0.144	0.61	0.26	0.37	-0.665	-0.28	0.03	0.17	6.4	0.03	2
0.075	5.58	2.037	0.512	-1.145	-0.144	0.61	0.26	0.37	-0.628	-0.28	0.03	0.17	6.4	0.03	2
0.09	5.54	2.1	0.512	-1.145	-0.144	0.61	0.26	0.37	-0.609	-0.28	0.03	0.17	6.4	0.03	2
0.1	5.5	2.16	0.512	-1.145	-0.144	0.61	0.26	0.37	-0.598	-0.28	0.028	0.17	6.4	0.03	2
0.12	5.39	2.272	0.512	-1.145	-0.144	0.61	0.26	0.37	-0.591	-0.28	0.018	0.17	6.4	0.03	2
0.15	5.27	2.407	0.512	-1.145	-0.144	0.61	0.26	0.37	-0.577	-0.28	0.005	0.17	6.4	0.03	2
0.17	5.19	2.43	0.512	-1.135	-0.144	0.61	0.26	0.37	-0.522	-0.265	-0.004	0.17	6.4	0.03	2
0.2	5.1	2.406	0.512	-1.115	-0.144	0.61	0.26	0.37	-0.445	-0.245	-0.014	0.17	6.4	0.03	2
0.24	4.97	2.293	0.512	-1.079	-0.144	0.61	0.232	0.37	-0.35	-0.223	-0.024	0.17	6.4	0.03	2
0.3	4.8	2.114	0.512	-1.035	-0.144	0.61	0.198	0.37	-0.219	-0.195	-0.036	0.17	6.4	0.03	2
0.36	4.62	1.955	0.512	-1.005	-0.144	0.61	0.17	0.37	-0.123	-0.173	-0.046	0.17	6.4	0.03	2
0.4	4.52	1.86	0.512	-0.988	-0.144	0.61	0.154	0.37	-0.065	-0.16	-0.052	0.17	6.4	0.03	2
0.46	4.38	1.717	0.512	-0.965	-0.144	0.592	0.132	0.37	0.02	-0.136	-0.059	0.17	6.4	0.03	2
0.5	4.3	1.615	0.512	-0.952	-0.144	0.581	0.119	0.37	0.085	-0.121	-0.064	0.17	6.4	0.03	2
0.6	4.12	1.428	0.512	-0.922	-0.144	0.557	0.091	0.37	0.194	-0.089	-0.074	0.17	6.4	0.03	2
0.75	3.9	1.16	0.512	-0.885	-0.144	0.528	0.057	0.331	0.32	-0.05	-0.086	0.17	6.4	0.03	2
0.85	3.81	1.02	0.512	-0.865	-0.144	0.512	0.038	0.309	0.37	-0.028	-0.093	0.17	6.4	0.03	2
1	3.7	0.828	0.512	-0.838	-0.144	0.49	0.013	0.281	0.423	0	-0.102	0.17	6.4	0.03	2
1.5	3.55	0.26	0.512	-0.772	-0.144	0.438	-0.05	0.21	0.6	0.04	-0.12	0.17	6.4	0.03	2
2	3.5	-0.15	0.512	-0.725	-0.144	0.4	-0.09	0.16	0.61	0.04	-0.14	0.17	6.4	0.03	2
3	3.5	-0.69	0.512	-0.725	-0.144	0.4	-0.16	0.089	0.63	0.04	-0.173	0.17	6.4	0.03	2
4	3.5	-1.13	0.512	-0.725	-0.144	0.4	-0.2	0.039	0.64	0.04	-0.196	0.17	6.4	0.03	2
5	3.5	-1.46	0.512	-0.725	-0.144	0.4	-0.2	0	0.664	0.04	-0.215	0.17	6.4	0.03	2

Table A.2 Constant values for Boore *et al.* (1997) attenuation relationships.

Period(s)	B_{SS}	B_2	B_3	B_5	B_V	V_A	h
PGA	-0.313	0.527	0.000	-0.778	-0.371	1396	5.57
0.10	1.006	0.753	-0.226	-0.934	-0.212	1112	6.27
0.11	1.072	0.732	-0.230	-0.937	-0.211	1291	6.65
0.12	1.109	0.721	-0.233	-0.939	-0.215	1452	6.91
0.13	1.128	0.711	-0.233	-0.939	-0.221	1596	7.08
0.14	1.135	0.707	-0.230	-0.938	-0.228	1718	7.18
0.15	1.128	0.702	-0.228	-0.937	-0.238	1820	7.23
0.16	1.112	0.702	-0.226	-0.935	-0.248	1910	7.24
0.17	1.090	0.702	-0.221	-0.933	-0.258	1977	7.21
0.18	1.063	0.705	-0.216	-0.930	-0.270	2037	7.16
0.19	1.032	0.709	-0.212	-0.927	-0.281	2080	7.10
0.20	0.999	0.711	-0.207	-0.924	-0.292	2118	7.02
0.22	0.925	0.721	-0.198	-0.918	-0.315	2158	6.83
0.24	0.847	0.732	-0.189	-0.912	-0.338	2178	6.62
0.26	0.764	0.744	-0.180	-0.906	-0.360	2173	6.39
0.28	0.681	0.758	-0.168	-0.899	-0.381	2158	6.17
0.30	0.598	0.769	-0.161	-0.893	-0.401	2133	5.94
0.32	0.518	0.783	-0.152	-0.888	-0.420	2104	5.72
0.34	0.439	0.794	-0.143	-0.882	-0.438	2070	5.50
0.36	0.361	0.806	-0.136	-0.877	-0.456	2032	5.30
0.38	0.286	0.820	-0.127	-0.872	-0.472	1995	5.10
0.40	0.212	0.831	-0.120	-0.867	-0.487	1954	4.91
0.42	0.140	0.840	-0.113	-0.862	-0.502	1919	4.74
0.44	0.073	0.852	-0.108	-0.858	-0.516	1884	4.57
0.46	0.005	0.863	-0.101	-0.854	-0.529	1849	4.41
0.48	-0.058	0.873	-0.097	-0.850	-0.541	1816	4.26
0.50	-0.122	0.884	-0.090	-0.846	-0.553	1782	4.13
0.55	-0.268	0.907	-0.078	-0.837	-0.579	1710	3.82
0.60	-0.401	0.928	-0.069	-0.830	-0.602	1644	3.57
0.65	-0.523	0.946	-0.060	-0.823	-0.622	1592	3.36
0.70	-0.634	0.962	-0.053	-0.818	-0.639	1545	3.20
0.75	-0.737	0.979	-0.046	-0.813	-0.653	1507	3.07
0.80	-0.829	0.992	-0.041	-0.809	-0.666	1476	2.98
0.85	-0.915	1.006	-0.037	-0.805	-0.676	1452	2.92
0.90	-0.993	1.018	-0.035	-0.802	-0.685	1432	2.89
0.95	-1.066	1.027	-0.032	-0.800	-0.692	1416	2.88
1.00	-1.133	1.036	-0.032	-0.798	-0.698	1406	2.90
1.10	-1.249	1.052	-0.030	-0.795	-0.706	1396	2.99
1.20	-1.345	1.064	-0.032	-0.794	-0.710	1400	3.14
1.30	-1.428	1.073	-0.035	-0.793	-0.711	1416	3.36
1.40	-1.495	1.08	-0.039	-0.794	-0.709	1442	3.62
1.50	-1.552	1.085	-0.044	-0.796	-0.704	1479	3.92
1.60	-1.598	1.087	-0.051	-0.798	-0.697	1524	4.26
1.70	-1.634	1.089	-0.058	-0.801	-0.689	1581	4.62
1.80	-1.663	1.087	-0.067	-0.804	-0.679	1644	5.01
1.90	-1.685	1.087	-0.074	-0.808	-0.667	1714	5.42
2.00	-1.699	1.085	-0.085	-0.812	-0.655	1795	5.85

Table A.3 Constant values for Campbell and Bozorgnia (2003) attenuation relationships.

Period(s)	c_1	c_2	c_3	c_4	c_5	c_6	c_7	c_8	c_9	c_{10}	c_{11}
PGA	-4.033	0.812	0.036	-1.061	0.041	-0.005	-0.018	0.766	0.034	0.343	0.351
0.05	-3.74	0.812	0.036	-1.121	0.058	-0.004	-0.028	0.724	0.032	0.302	0.362
0.075	-3.076	0.812	0.05	-1.252	0.121	-0.005	-0.051	0.648	0.04	0.243	0.333
0.1	-2.661	0.812	0.06	-1.308	0.166	-0.009	-0.068	0.621	0.046	0.224	0.313
0.15	-2.27	0.812	0.041	-1.324	0.212	-0.033	-0.081	0.613	0.031	0.318	0.344
0.2	-2.771	0.812	0.03	-1.153	0.098	-0.014	-0.038	0.704	0.026	0.296	0.342
0.3	-2.999	0.812	0.007	-1.08	0.059	-0.007	-0.022	0.752	0.007	0.359	0.385
0.4	-3.511	0.812	-0.015	-0.964	0.024	-0.002	-0.005	0.842	-0.016	0.379	0.438
0.5	-3.556	0.812	-0.035	-0.964	0.023	-0.002	-0.004	0.842	-0.036	0.406	0.479
0.75	-3.709	0.812	-0.071	-0.964	0.021	-0.002	-0.002	0.842	-0.074	0.347	0.419
1	-3.867	0.812	-0.101	-0.964	0.019	0	0	0.842	-0.105	0.329	0.338
1.5	-4.093	0.812	-0.15	-0.964	0.019	0	0	0.842	-0.155	0.217	0.188
2	-4.311	0.812	-0.18	-0.964	0.019	0	0	0.842	-0.187	0.06	0.064
3	-4.817	0.812	-0.193	-0.964	0.019	0	0	0.842	-0.2	-0.079	0.021
4	-5.211	0.812	-0.202	-0.964	0.019	0	0	0.842	-0.209	-0.061	0.057

Table A.4 Constant values for Sadigh *et al.* (1997) attenuation relationships.

Period(s)	C_1	C_2	C_3	C_4	C_5	C_6	C_7
PGA	-1.274	1.1	0.000	-2.100	-0.48451	0.524	0.0
0.07	-0.540	1.1	0.006	-2.128	-0.48451	0.524	-0.082
0.10	-0.375	1.1	0.006	-2.148	-0.48451	0.524	-0.041
0.20	-0.497	1.1	-0.004	-2.080	-0.48451	0.524	0.0
0.30	-0.707	1.1	-0.017	-2.028	-0.48451	0.524	0.0
0.40	-0.948	1.1	-0.028	-1.990	-0.48451	0.524	0.0
0.50	-1.238	1.1	-0.040	-1.945	-0.48451	0.524	0.0
0.75	-1.858	1.1	-0.050	-1.865	-0.48451	0.524	0.0
1.00	-2.355	1.1	-0.055	-1.800	-0.48451	0.524	0.0
1.50	-3.057	1.1	-0.065	-1.725	-0.48451	0.524	0.0
2.00	-3.595	1.1	-0.070	-1.670	-0.48451	0.524	0.0
3.00	-4.350	1.1	-0.080	-1.610	-0.48451	0.524	0.0
4.00	-4.880	1.1	-0.100	-1.570	-0.48451	0.524	0.0

Table A.5 Constant values for Atkinson and Boore (2003) attenuation relationships.

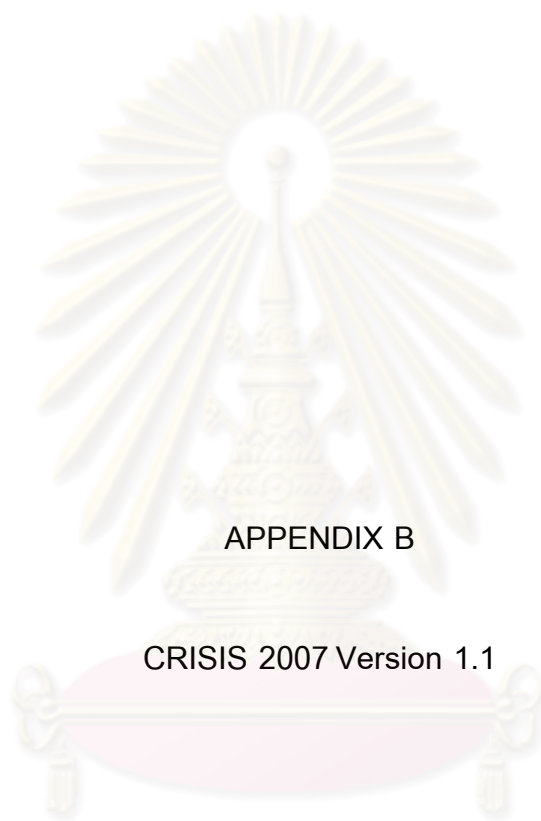
Freq	c_1	c_2	c_3	c_4	c_5	c_6	c_7	σ	σ_1	σ_2
0.33	2.301	0.02237	0.00012	0.000	0.10	0.25	0.36	0.36	0.31	0.18
0.5	2.1907	0.07148	0.00224	0.000	0.10	0.25	0.40	0.34	0.29	0.18
1	2.1442	0.1345	0.00521	- 0.00110	0.10	0.30	0.55	0.34	0.28	0.19
2.5	2.5249	0.1477	0.00728	- 0.00235	0.13	0.37	0.38	0.29	0.25	0.15
5	2.6638	0.12386	0.00884	- 0.00280	0.15	0.27	0.25	0.28	0.25	0.13
10	2.7789	0.09841	0.00974	- 0.00287	0.15	0.23	0.20	0.27	0.25	0.10
25	2.8753	0.07052	0.01004	- 0.00278	0.15	0.20	0.20	0.26	0.22	0.14
PGA	2.991	0.03525	0.00759	- 0.00206	0.19	0.24	0.29	0.23	0.20	0.11

Table A.6 Constant values for Youngs *et al.* (1997) attenuation relationships.

Period(s)	C_1	C_2	C_3	C_4^*	C_5^*
PGA	0.0	0.0	-2.552	1.45	-0.1
0.075	1.275	0.0	-2.707	1.45	-0.1
0.1	1.188	-0.0011	-2.655	1.45	-0.1
0.2	0.722	-0.0027	-2.528	1.45	-0.1
0.3	0.246	-0.0036	-2.454	1.45	-0.1
0.4	-0.115	-0.0043	-2.401	1.45	-0.1
0.5	-0.400	-0.0048	-2.360	1.45	-0.1
0.75	-1.149	-0.0057	-2.286	1.45	-0.1
1.0	-1.736	-0.0064	-2.234	1.45	-0.1
1.5	-2.634	-0.0073	-2.160	1.50	-0.1
2.0	-3.328	-0.0080	-2.107	1.55	-0.1
3.0	-4.511	-0.0089	-2.033	1.65	-0.1

* Standard deviation for magnitudes greater than M 8 set equal to the value for M 8.

ศูนย์วิทยทรัพยากร
จุฬาลงกรณ์มหาวิทยาลัย



APPENDIX B

CRISIS 2007 Version 1.1

ศูนย์วิทยทรัพยากร
จุฬาลงกรณ์มหาวิทยาลัย

Seismic Hazard Analysis
Probabilistic Seismic Hazard Analysis

CRISIS 2007 VERSION 1.1



Seismic Hazard Analysis
Probabilistic Seismic Hazard Analysis

CRISIS 2007 VERSION 1.1



Seismic Hazard Analysis
Probabilistic Seismic Hazard Analysis

CRISIS 2007 VERSION 1.1



Seismic Hazard Analysis
Probabilistic Seismic Hazard Analysis

CRISIS 2007 VERSION 1.1



Seismic Hazard Analysis
Probabilistic Seismic Hazard Analysis

CRISIS 2007 VERSION 1.1



Seismic Hazard Analysis
Probabilistic Seismic Hazard Analysis

CRISIS 2007 VERSION 1.1



CRISIS 2007 VERSION 1.1

**Seismic Hazard Analysis
Probabilistic Seismic Hazard Analysis**

Input → Maps

Site Name	Longitude	Latitude
1 SOUTH OF THAILAND	98.0	10.5
4	98.0	7.5
	100.5	07.5
	100.5	10.5
6 Surat Thani, Krabi, Krabi, Phangnga, Phuket, Phuket, Nakhon Si Thammarat, Lumiyai dam, Phangnga,	98.92, 8.06, 98.39, 7.89, 99.96, 8.46, 98.30, 8.64	99.33, 9.14, 98.52, 8.44

CRISIS 2007 VERSION 1.1



**Seismic Hazard Analysis
Probabilistic Seismic Hazard Analysis**

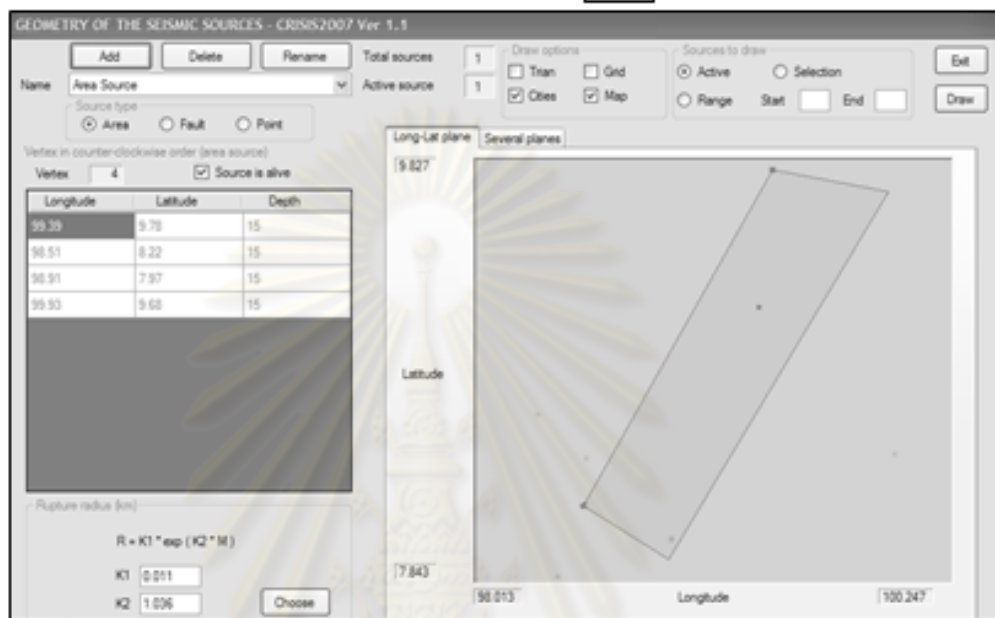
Input → Sites of computation of hazard

Number of grid size = 3-3



Location of Dam

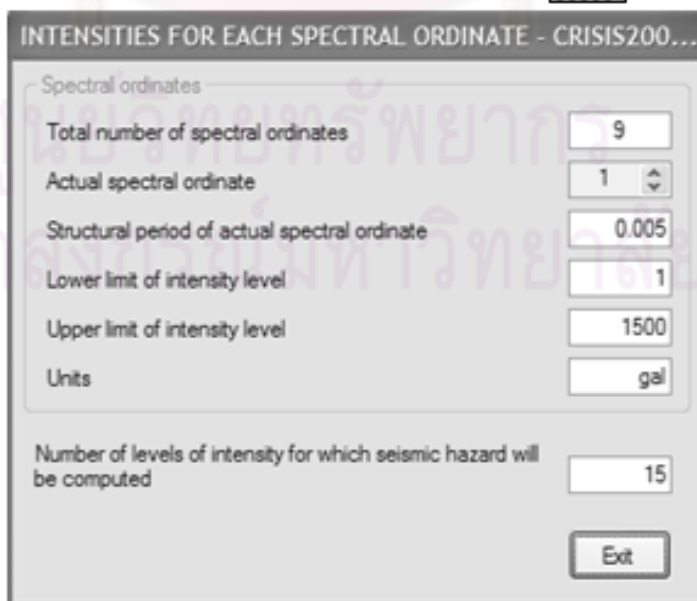
CRISIS 2007 VERSION 1.1

Input  **Geometry of the seismic sources** 



CRISIS 2007 VERSION 1.1

Input  **Intensities for each spectral ordinate** 



Seismic Hazard Analysis
Probabilistic Seismic Hazard Analysis

CRISIS 2007 VERSION 1.1

Input \Rightarrow Seismicity  \Rightarrow Poisson Model

Seismic Hazard Analysis
Probabilistic Seismic Hazard Analysis

CRISIS 2007 VERSION 1.1

Input \Rightarrow Seismicity  \Rightarrow Poisson Model

CRISIS 2007 VERSION 1.1

Input ⇒ **Attenuation Data**



ATTENUATION DATA - CRISIS2007 Ver 1.1

Number of spectral ordinates: 9 Attenuation tables: 1

Attenuation table: 1 D:\KMR HAZRD\ATTENUATION\01ABSS50.atn

Buttons: Add user model, Add built-in model, Delete model

Attenuation relation: Source

Magnitude: 7 Attenuation properties: Truncation parameter= 500

Depth (Km): 0 Coefficient of H= 0

No. spect. ord: 1 Sigma_0= 0.7

Intensity in gal for T=0.005

Draw

General model | Particular models

General attenuation model assigned to active source: 1

D:\KMR HAZRD\ATTENUATION\01ABSS50.atn

The attenuation equations for Crustal Earthquake.
Abrahamson and Silva (1997),
Boore et al., (1997),
Campbell and Bozorgnia (2003),
Sadigh et al. (1997)

The attenuation equations for subduction zone.
Young et al. (1997)

Exit

CRISIS 2007 VERSION 1.1

Input ⇒ **Global Parameters**



GLOBAL PARAMETERS - CRISIS2007 Ver 1.1

Integration parameters

Maximum integration distance: 500 km

Minimum triangle size: 100 km

Minimum Distance/Triangle Size ratio: 10

Fixed return periods

First return period: 500 years

Second return period: 1000 years

Third return period: 3000 years

Fourth return period: 5000 years

Fifth return period: 10000 years

Distance for deaggregation

Focal

Epicentral

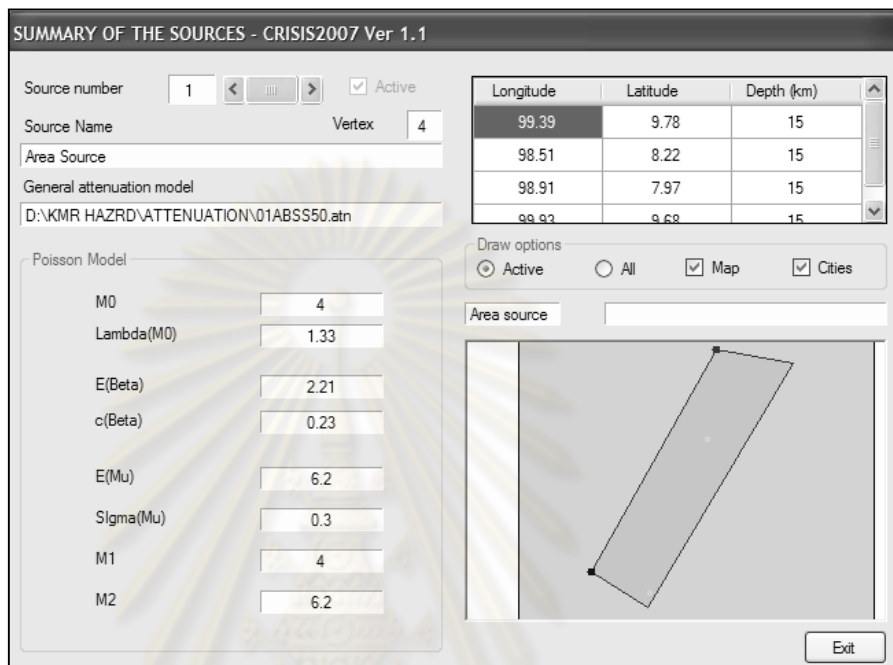
Joyner and Boore

Closest to rupture area

Exit

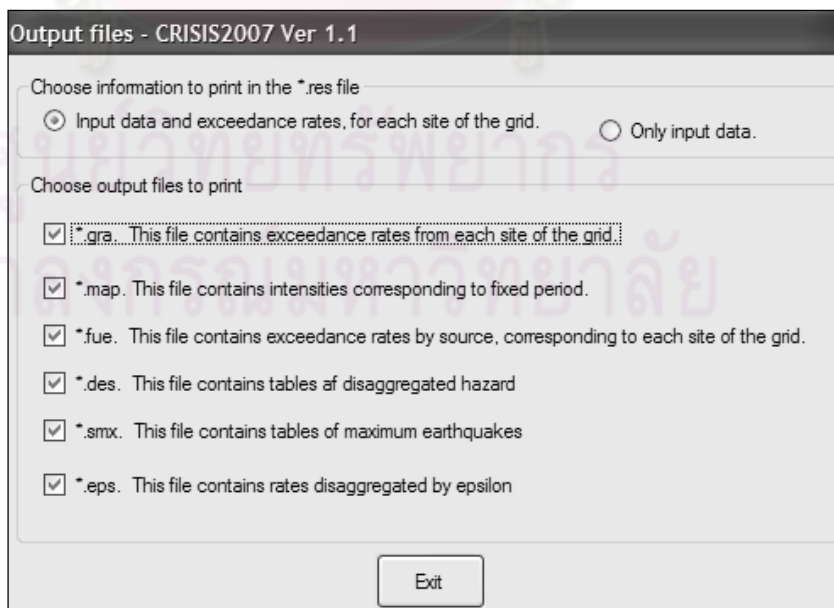
CRISIS 2007 VERSION 1.1

Input \Rightarrow Summary of the source 



CRISIS 2007 VERSION 1.1

Out put of Crisis 2007



CRISIS 2007 VERSION 1.1

Out put of Crisis 2007: *RES

```

*****
Program CRISIS2007 Version 1.1.0
Run Title:Klongmarui Dam
Date:28/6/2552
File:*RES
*****
Longitude and latitude of this site: 98.3 8.64
Number of site:5

SUMMARY OF COMPUTATIONS FOR THIS SITE
Considered Points used to Occurrence Time elapsed Attenuation model
Region integrate Model (sec)
      1         2 Poisson 0.078      1

INTENSITY versus EXPECTED EXCEEDANCE RATE

Intensity 1          Intensity 2          Intensity 3
1.00E+00    9.82E-01    1.00E+00    1.27E+00    1.00E+00    1.20E+00
1.69E+00    7.10E-01    1.69E+00    1.16E+00    1.69E+00    1.03E+00
2.84E+00    4.30E-01    2.84E+00    9.57E-01    2.84E+00    7.86E-01
4.79E+00    2.10E-01    4.79E+00    6.82E-01    4.79E+00    5.16E-01
8.08E+00    8.06E-02    8.08E+00    4.05E-01    8.08E+00    2.83E-01
1.36E+01    2.48E-02    1.36E+01    1.93E-01    1.36E+01    1.28E-01
2.30E+01    6.49E-03    2.30E+01    7.13E-02    2.30E+01    4.73E-02
3.87E+01    1.51E-03    3.87E+01    2.04E-02    3.87E+01    1.48E-02
6.53E+01    2.86E-04    6.53E+01    4.69E-03    6.53E+01    4.11E-03
1.10E+02    3.84E-05    1.10E+02    8.99E-04    1.10E+02    1.00E-03
1.86E+02    3.29E-06    1.86E+02    1.39E-04    1.86E+02    1.98E-04
3.13E+02    1.64E-07    3.13E+02    1.48E-05    3.13E+02    2.60E-05
5.28E+02    0.00E+00    5.28E+02    0.00E+00    5.28E+02    0.00E+00
8.90E+02    0.00E+00    8.90E+02    0.00E+00    8.90E+02    0.00E+00
1.50E+03    0.00E+00    1.50E+03    0.00E+00    1.50E+03    0.00E+00

```

ศูนย์วิทยทรัพยากร
จุฬาลงกรณ์มหาวิทยาลัย

Seismic Hazard Analysis
Probabilistic Seismic Hazard Analysis

CRISIS 2007 VERSION 1.1

Out put of Crisis 2007: *FUE

```

.....
Program CRISIS2007 Version 1.1.0
Run Title:Klongmarui Dam
Date:28/6/2552
File:*Fue
.....

```

98.3 8.64					
SOURCES:1					
INTENSITY 1		INTENSITY 2		INTENSITY 3	
1.00E+00	9.82E-01	1.00E+00	1.27E+00	1.00E+00	1.20E+00
1.69E+00	7.10E-01	1.69E+00	1.16E+00	1.69E+00	1.03E+00
2.04E+00	4.30E-01	2.04E+00	9.57E-01	2.04E+00	7.66E-01
4.79E+00	2.10E-01	4.79E+00	6.82E-01	4.79E+00	5.16E-01
8.08E+00	8.08E-02	8.08E+00	4.05E-01	8.08E+00	2.83E-01
1.36E+01	2.48E-02	1.36E+01	1.93E-01	1.36E+01	1.28E-01
2.30E+01	6.49E-03	2.30E+01	7.13E-02	2.30E+01	4.73E-02
3.87E+01	1.51E-03	3.87E+01	2.04E-02	3.87E+01	1.48E-02
6.53E+01	2.88E-04	6.53E+01	4.89E-03	6.53E+01	4.11E-03
1.10E+02	3.84E-05	1.10E+02	8.99E-04	1.10E+02	1.00E-03
1.86E+02	3.29E-06	1.86E+02	1.39E-04	1.86E+02	1.98E-04
3.13E+02	1.64E-07	3.13E+02	1.48E-05	3.13E+02	2.60E-05
5.28E+02	0.00E+00	5.28E+02	0.00E+00	5.28E+02	0.00E+00
8.90E+02	0.00E+00	8.90E+02	0.00E+00	8.90E+02	0.00E+00
1.50E+03	0.00E+00	1.50E+03	0.00E+00	1.50E+03	0.00E+00

Seismic Hazard Analysis
Probabilistic Seismic Hazard Analysis

CRISIS 2007 VERSION 1.1

Out put of Crisis 2007: *SMX

```

.....
Program CRISIS2007 Version 1.1.0
Run Title:Klongmarui Dam
Date:28/6/2552
.....

```

Longitude	Latitude	N	M=0				M=0.5				M=1.0				M=1.5			
			Intensity	Mag	Dist	Src	Intensity	Mag	Dist	Src	Intensity	Mag	Dist	Src	Intensity	Mag	Dist	Src
98.3	8.64	1	3.948E+01	5.95	45.33	1	5.60E+01	5.95	45.33	1	7.99E+01	5.95	45.33	1	1.13E+02	5.95	45.33	1
98.3	8.64	2	7.987E+01	5.95	45.33	1	1.16E+02	5.95	45.33	1	1.67E+02	5.95	45.33	1	2.42E+02	5.95	45.33	1
98.3	8.64	3	8.713E+01	5.95	45.33	1	1.28E+02	5.95	45.33	1	1.88E+02	5.95	45.33	1	2.77E+02	5.95	45.33	1
98.3	8.64	4	7.642E+01	5.95	45.33	1	1.12E+02	5.95	45.33	1	1.67E+02	5.95	45.33	1	2.46E+02	5.95	45.33	1
98.3	8.64	5	5.335E+01	5.95	45.33	1	7.99E+01	5.95	45.33	1	1.19E+02	5.95	45.33	1	1.77E+02	5.95	45.33	1
98.3	8.64	6	3.790E+01	5.95	45.33	1	5.64E+01	5.95	45.33	1	8.49E+01	5.95	45.33	1	1.27E+02	5.95	45.33	1
98.3	8.64	7	2.910E+01	5.95	45.33	1	4.41E+01	5.95	45.33	1	6.67E+01	5.95	45.33	1	1.01E+02	5.95	45.33	1
98.3	8.64	8	1.887E+01	5.95	45.33	1	2.87E+01	5.95	45.33	1	4.37E+01	5.95	45.33	1	6.68E+01	5.95	45.33	1
98.3	8.64	9	1.314E+01	5.95	45.33	1	2.01E+01	5.95	45.33	1	3.00E+01	5.95	45.33	1	4.79E+01	5.95	45.33	1
Longitude	Latitude	N	M=2.0															
			Intensity	Mag	Dist	Src												
98.3	8.64	1	1.60E+02	5.95	45.33	1												
98.3	8.64	2	3.51E+02	5.95	45.33	1												
98.3	8.64	3	4.06E+02	5.95	45.33	1												
98.3	8.64	4	3.64E+02	5.95	45.33	1												
98.3	8.64	5	2.64E+02	5.95	45.33	1												
98.3	8.64	6	1.90E+02	5.95	45.33	1												
98.3	8.64	7	1.53E+02	5.95	45.33	1												
98.3	8.64	8	1.01E+02	5.95	45.33	1												
98.3	8.64	9	7.20E+01	5.95	45.33	1												

CRISIS 2007 VERSION 1.1

Out put of Crisis 2007: *MAP

```

*****
Program CRISIS2007 Version 1.1.0
Run Title:klongmarui Dam
File:*Map
Date:      28/6/2552
*****
INTENSITY LEVELS FOR FIXED RETURN PERIODS

NNP=Flag to show the kind of operation executed.
If NNP=0 then interpolation was executed
NNP=1 then extrapolation was executed
NNP=2 then value was impossible to calculate

FIXED RETURN PERIODS
Long.  Lat.  NT  5.00E+02  1.00E+03  3.00E+03  5.00E+03  1.00E+04  NNP
98.3   8.64   1   3.50E+01  4.41E+01  6.22E+01  7.17E+01  8.58E+01  0
98.3   8.64   2   8.55E+01  1.06E+02  1.45E+02  1.68E+02  2.01E+02  0
98.3   8.64   3   8.53E+01  1.10E+02  1.57E+02  1.85E+02  2.21E+02  0
98.3   8.64   4   7.46E+01  9.73E+01  1.42E+02  1.67E+02  2.04E+02  0
98.3   8.64   5   5.30E+01  7.05E+01  1.05E+02  1.24E+02  1.52E+02  0
98.3   8.64   6   3.82E+01  5.06E+01  7.61E+01  9.01E+01  1.13E+02  0
98.3   8.64   7   3.03E+01  4.11E+01  6.25E+01  7.39E+01  9.18E+01  0
98.3   8.64   8   2.03E+01  2.75E+01  4.21E+01  4.99E+01  6.28E+01  0
98.3   8.64   9   1.45E+01  1.97E+01  3.01E+01  3.62E+01  4.50E+01  0

```

ศูนย์วิทยทรัพยากร
จุฬาลงกรณ์มหาวิทยาลัย



APPENDIX C

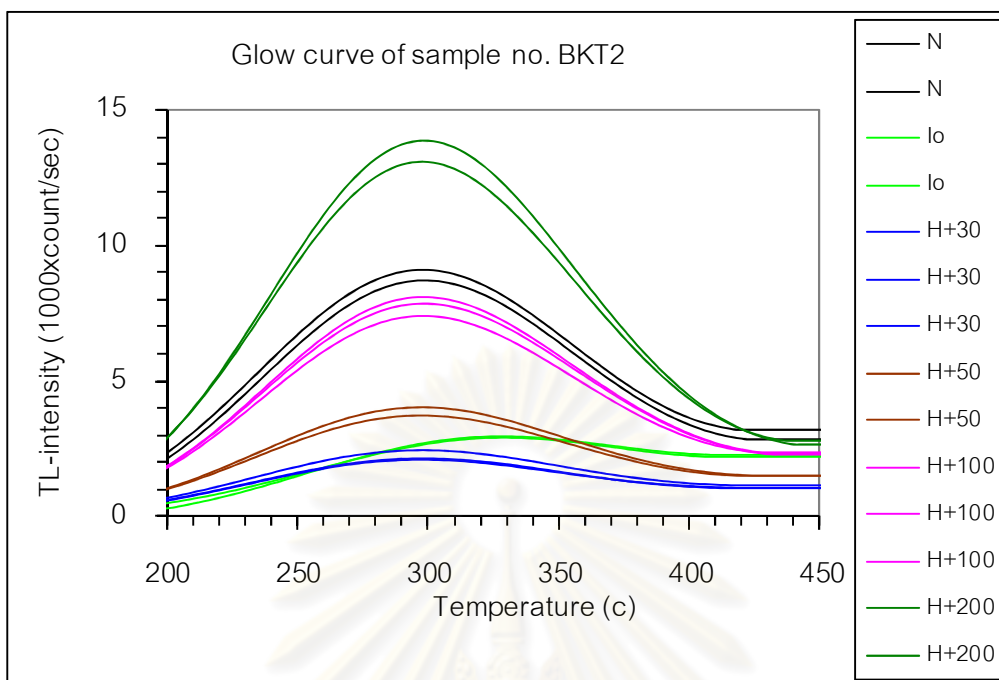
Thermoluminescence (TL) Dating Results

ศูนย์วิจัยทรัพยากร
จุฬาลงกรณ์มหาวิทยาลัย

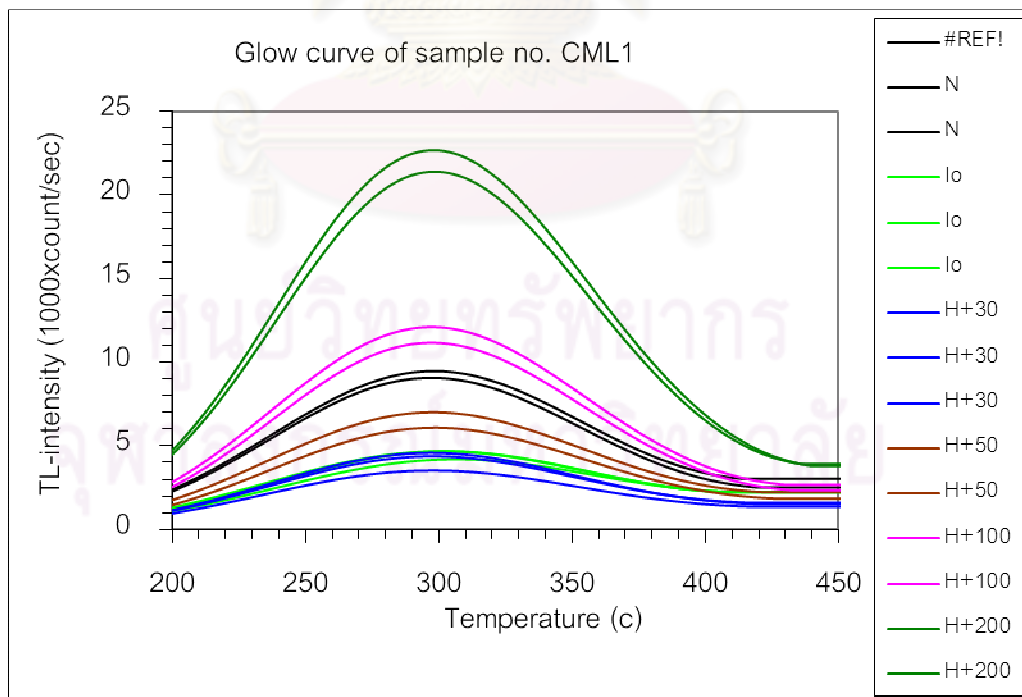
Table C.1 Summary of TL-age dating results carried out in this study

Sample No.	Grain size (μm)	U (ppm)	U (Error)	Th (ppm)	Th (Error)	K (%)	K (Error)	Sample No.	W (%)	AD (Gy/ka)	AD (Error)	ED (Gy)	ED (Error)	Age (Yr)	Error (Yr)
BKT2	120.00	3.04	0.08	16.79	0.62	1.83	0.07	BKT2	10	6.64	0.61	88.19	0.07	13200	1200
CML1	120.00	2.10	0.07	25.21	0.57	1.42	0.06	CML1	12	6.96	0.77	38.54	0.09	5500	600
CML2	120.00	2.70	0.09	25.65	0.79	2.79	0.09	CML2	14	8.61	1.13	470.55	0.30	54600	7100
CML3	120.00	2.38	0.09	24.90	0.90	2.51	0.09	CML3	15	7.99	1.21	241.87	0.18	30200	4500
SHP5	120.00	2.70	0.06	10.55	0.47	0.21	0.05	SHP5	7	3.85	0.28	22.07	0.07	5700	400
SHP6	120.00	2.80	0.06	10.90	0.44	0.74	0.05	SHP6	12	4.33	0.28	26.71	0.02	6100	300
SHP8	120.00	2.39	0.07	12.21	0.54	0.52	0.05	SHP8	11	4.11	0.36	23.40	0.05	5600	400
TSG3	120.00	2.54	0.09	27.21	0.80	1.33	0.07	TSG3	9	7.62	1.18	40.00	0.10	5200	800
TSG6	120.00	1.82	0.07	27.34	0.77	1.24	0.06	TSG6	13	6.86	1.08	135.43	0.07	19700	3100
WNP4	120.00	2.43	0.05	10.30	0.50	0.26	0.05	WNP4	6	3.74	0.29	49.03	0.12	13100	1000

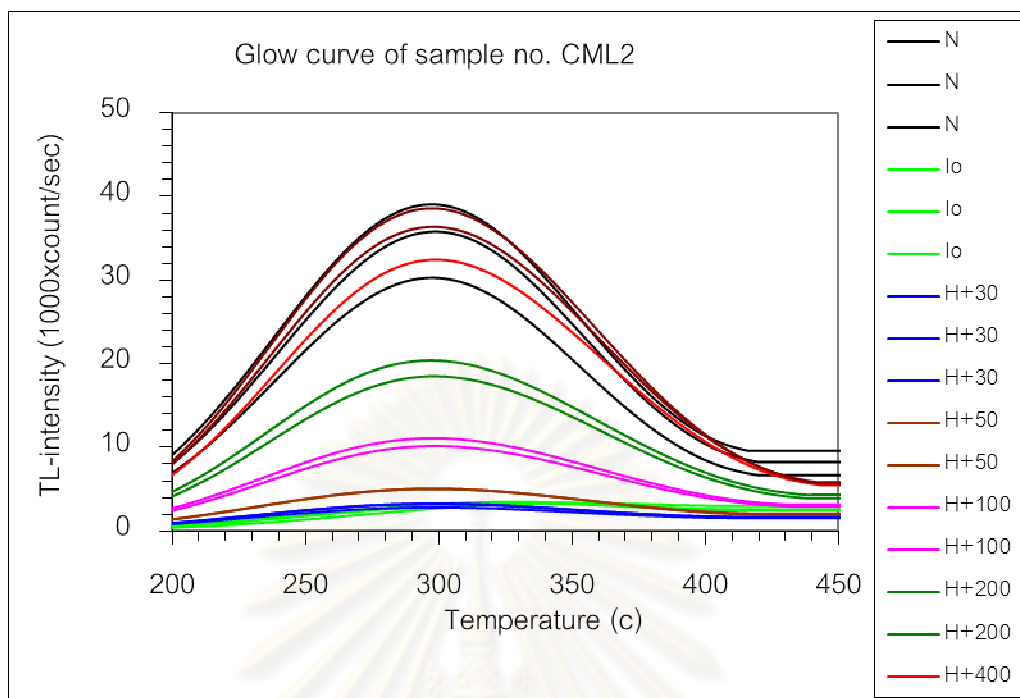
ศูนย์วิทยทรัพยากร
จุฬาลงกรณ์มหาวิทยาลัย



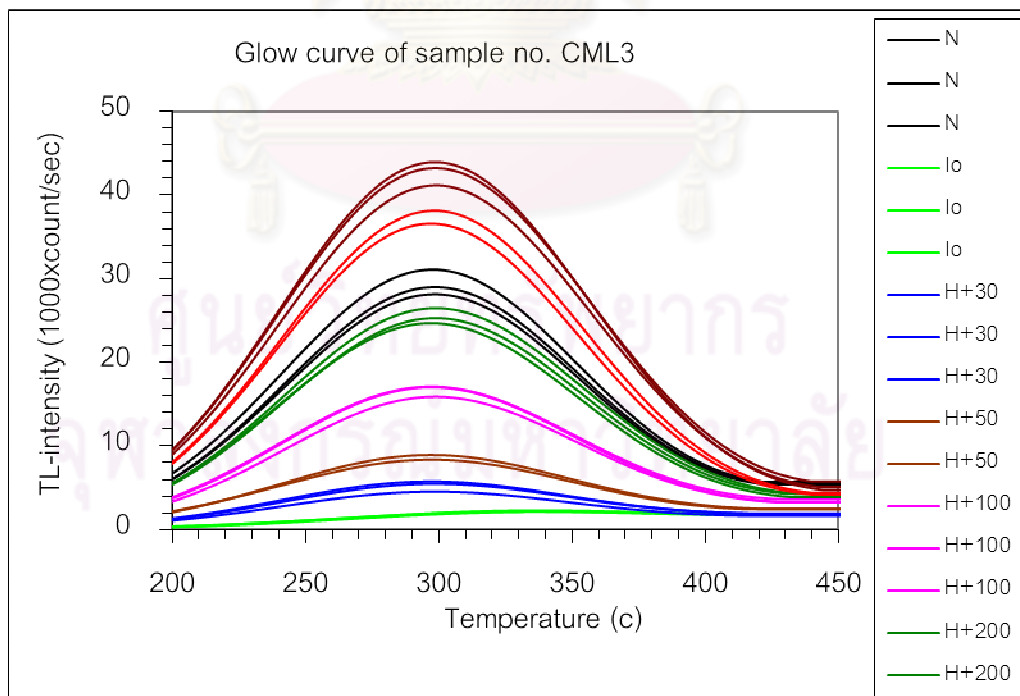
Sample No. BKT2



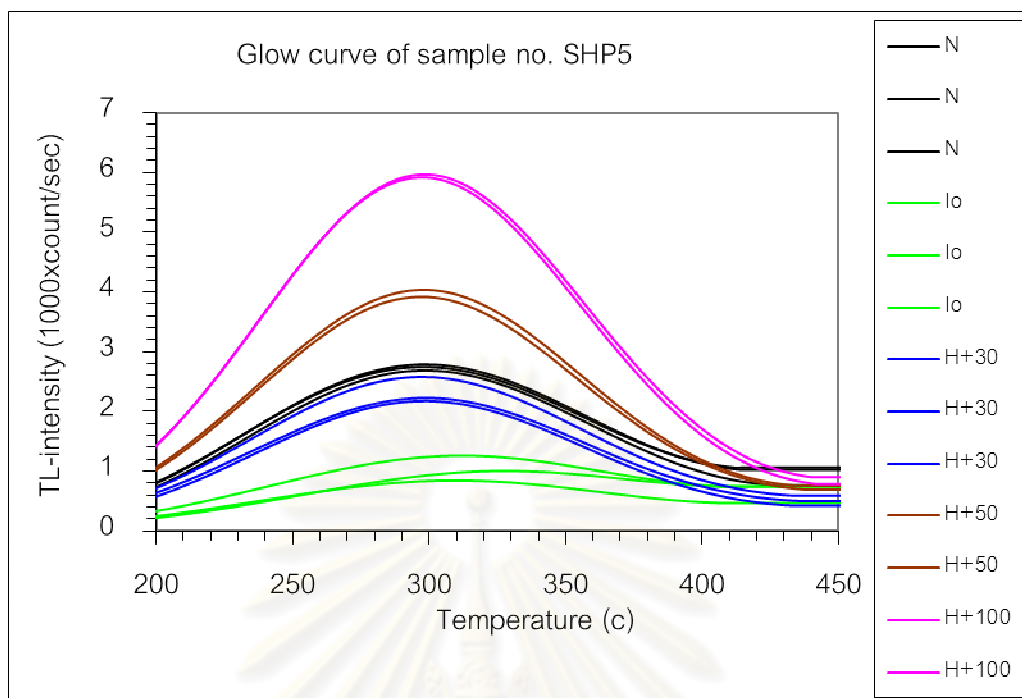
Sample No.CML1



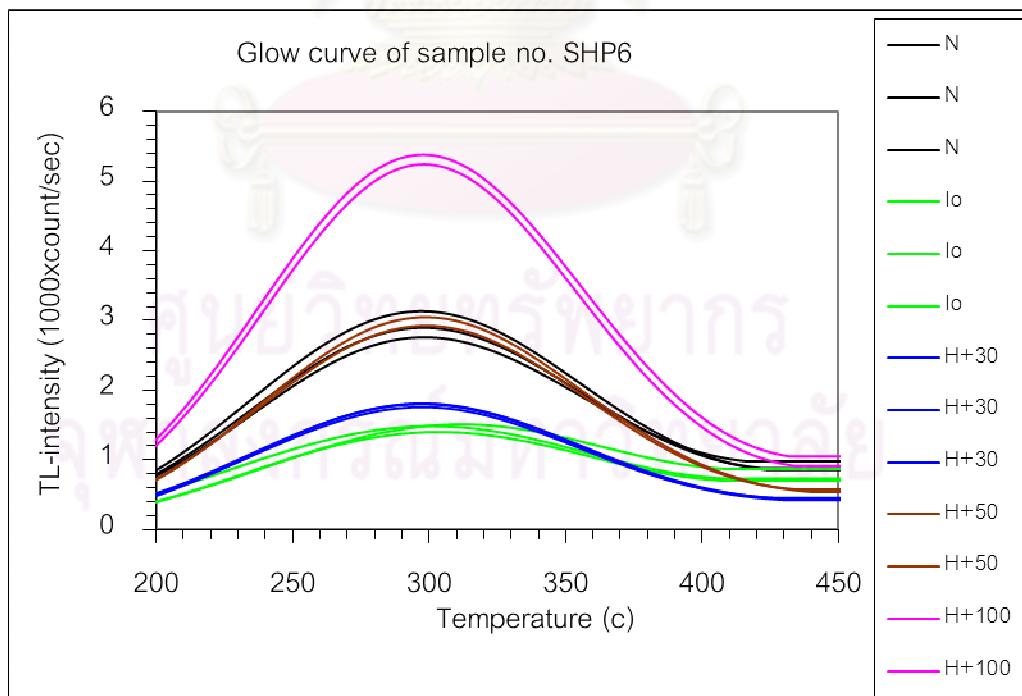
Sample No.CML2



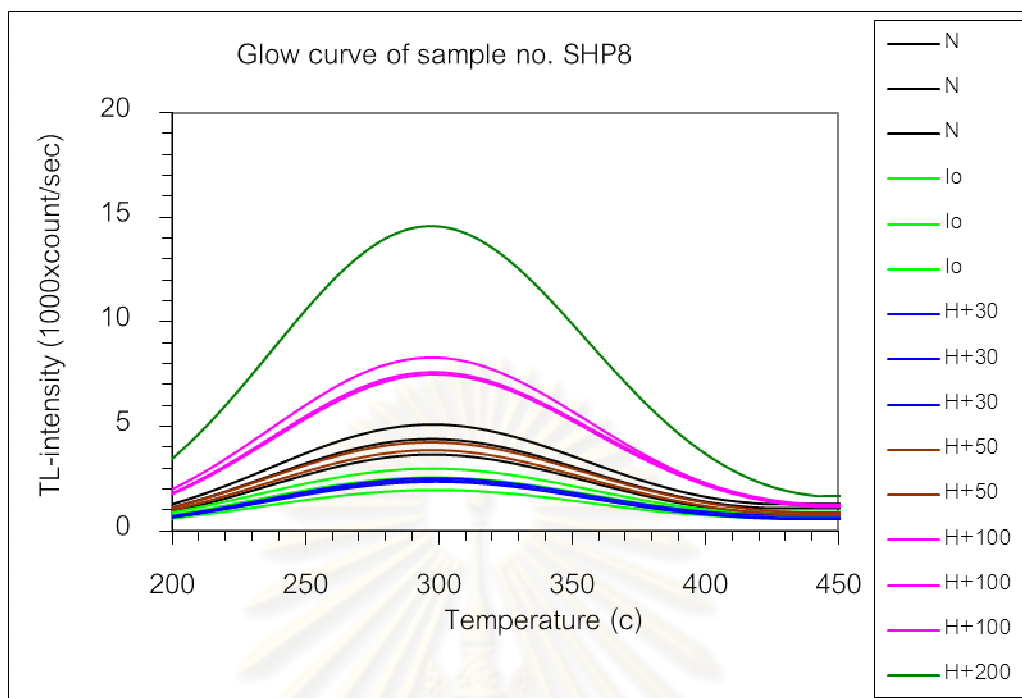
Sample No.CML3



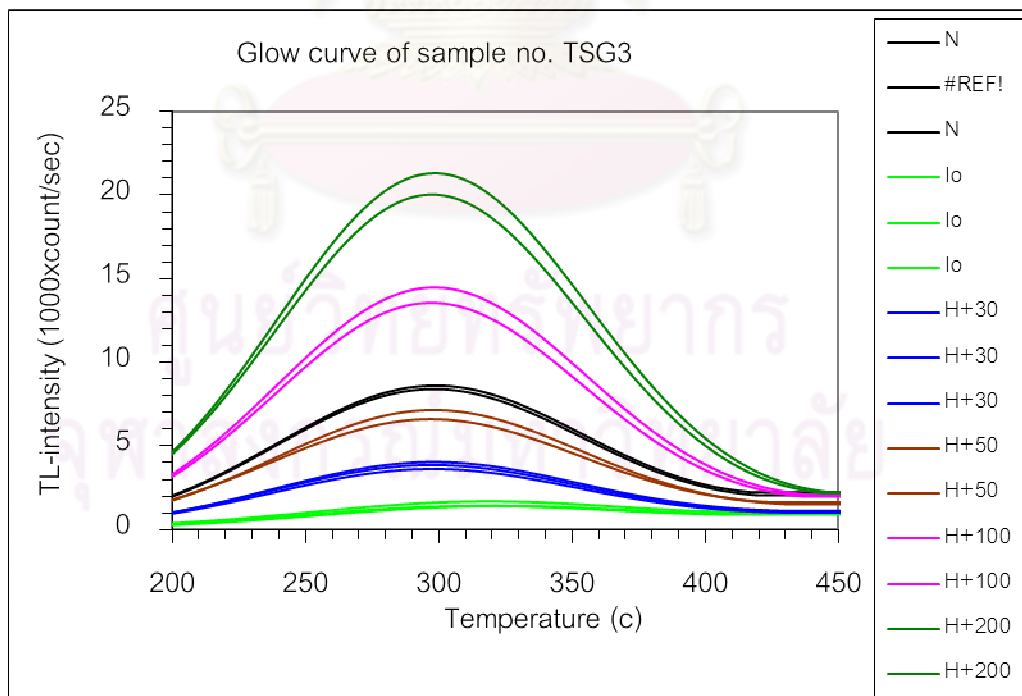
Sample No.SHP5



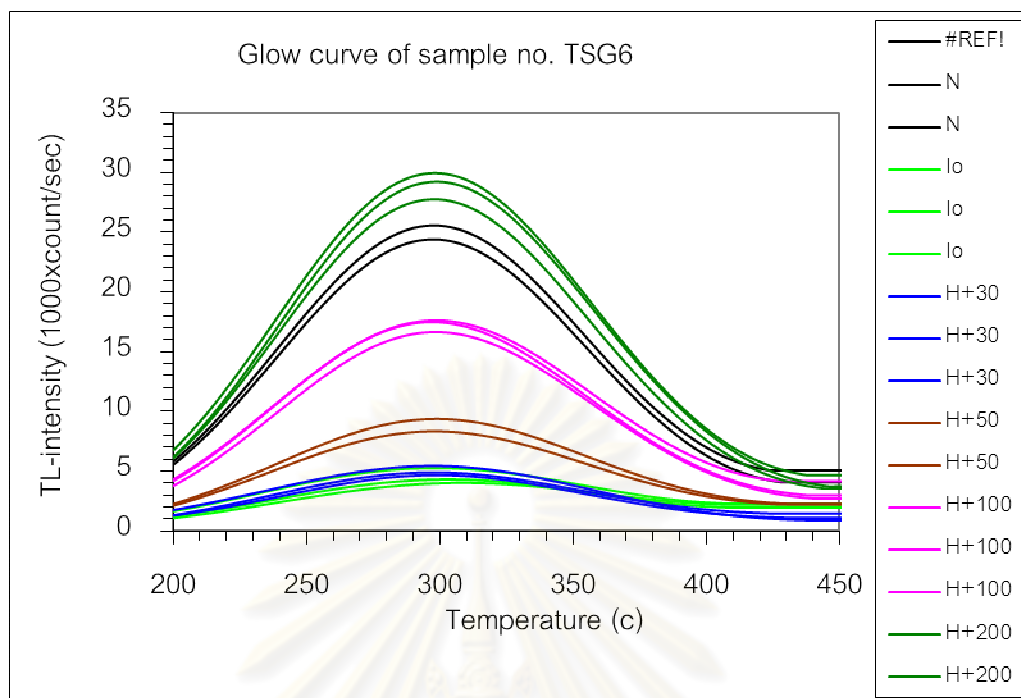
Sample No.SHP6



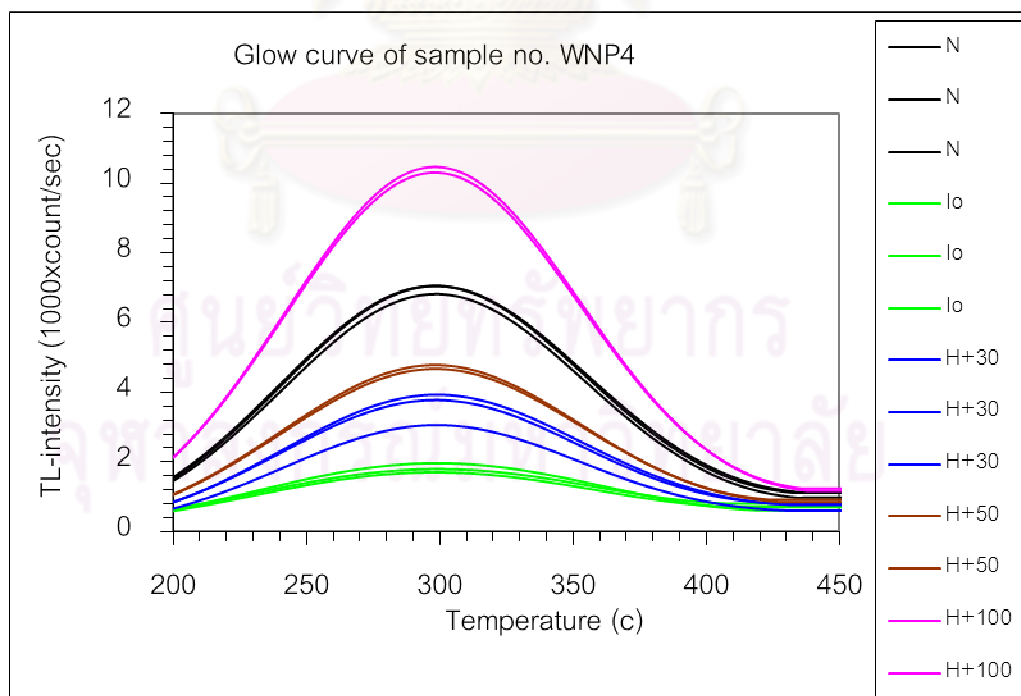
Sample No.SHP8



Sample No.TSG3



Sample No.TSG6



Sample No.WNP4



APPENDIX D

RID's Trench Logs (2009)

ศูนย์วิทยทรัพยากร
จุฬาลงกรณ์มหาวิทยาลัย

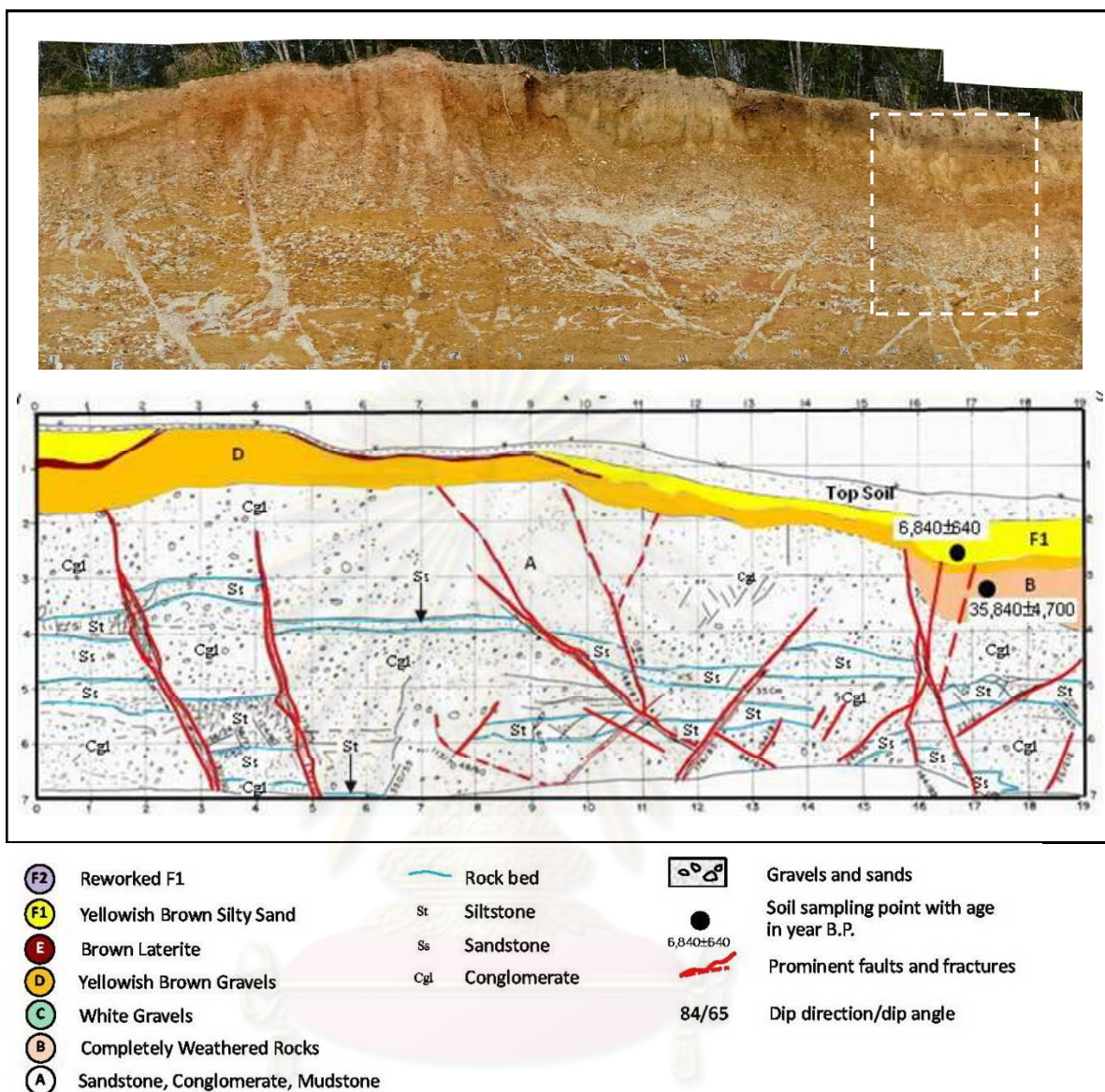
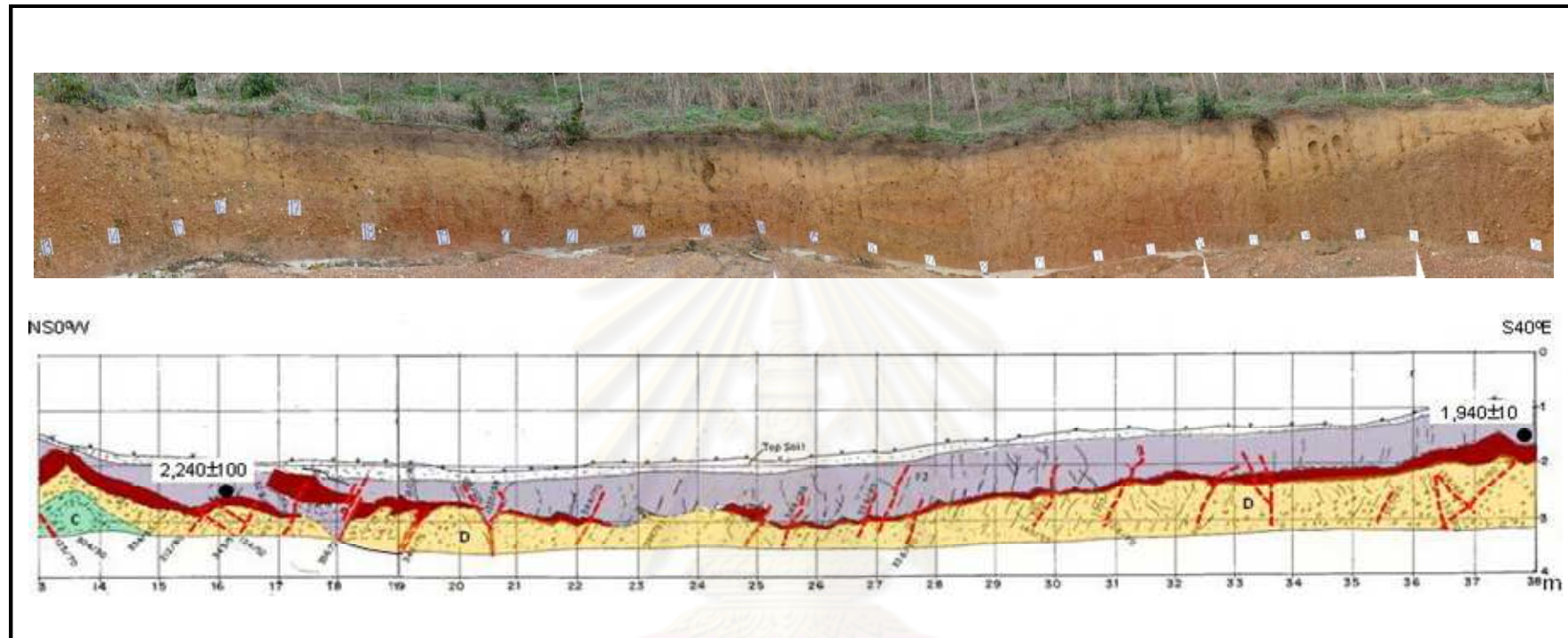


Figure D.1 Log of the exposure no.1 at Ban Phophana, Vibavadi district of Surat Thani province, the white gravel (Unit C) and reworked F1 (Unit F2) disappear in this section. The photograph in a white rectangular area is shown in Figure D.2.



- | | | |
|---------------------------------------|------------------|---|
| (F2) Reworked F1 | Rock bed | Gravels and sands |
| (F1) Yellowish Brown Silty Sand | St Siltstone | Soil sampling point with age in year B.P. |
| (E) Brown Laterite | Ss Sandstone | Prominent faults and fractures |
| (D) Yellowish Brown Gravels | Cgl Conglomerate | Dip direction/dip angle |
| (C) White Gravels | | |
| (B) Completely Weathered Rocks | | |
| (A) Sandstone, Conglomerate, Mudstone | | |

Figure D.2 Log of the exposure no.2 at Ban Phophana, Vibavadi district of Surat Thani province, the Unit A, Unit B, and Unit F1 disappear in this section.

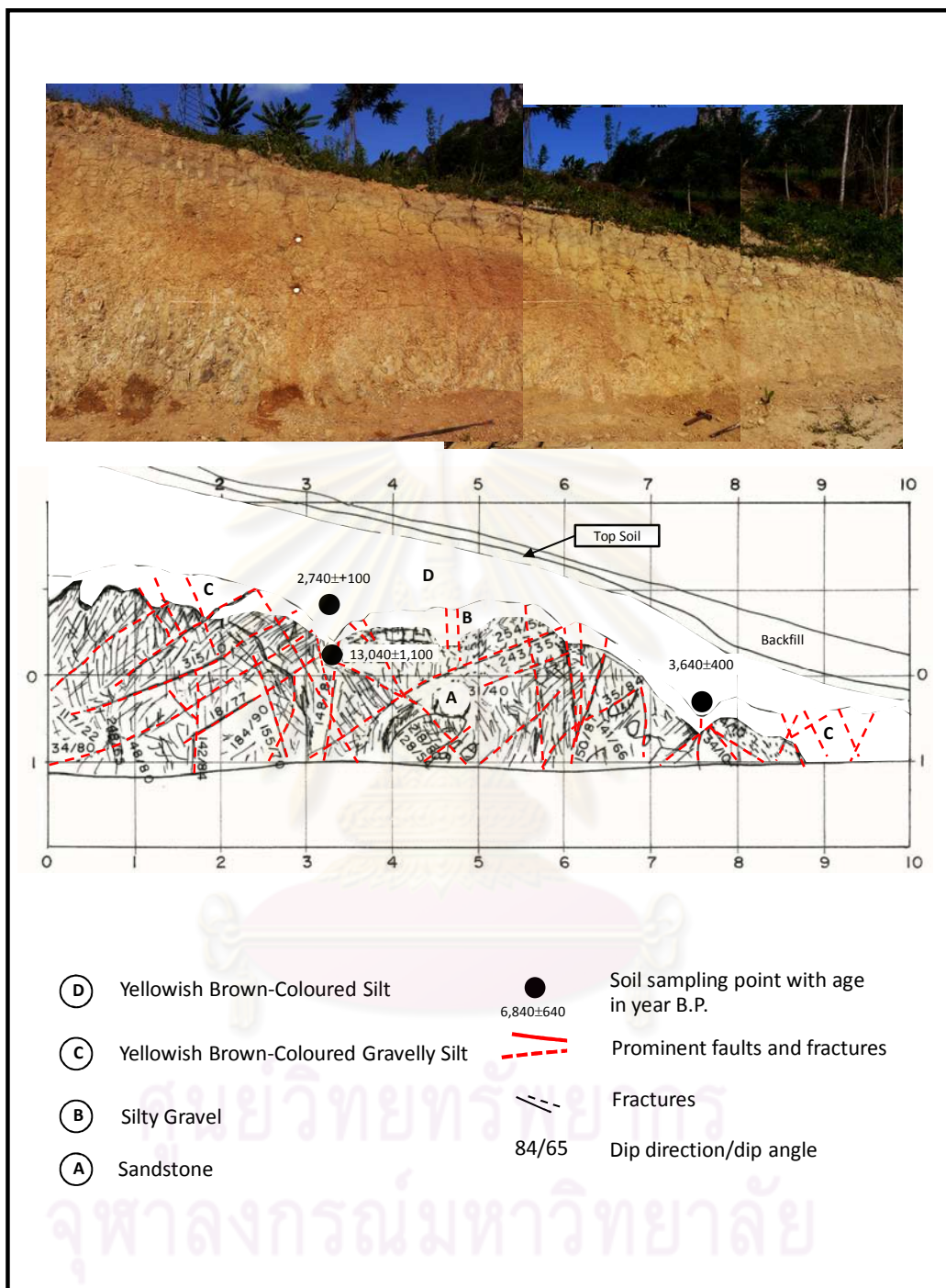


Figure D.3 Log of the cleaned exposure at Ban Song Phinong, , Phanom subdistrict, Phanom district, Surat Thani province

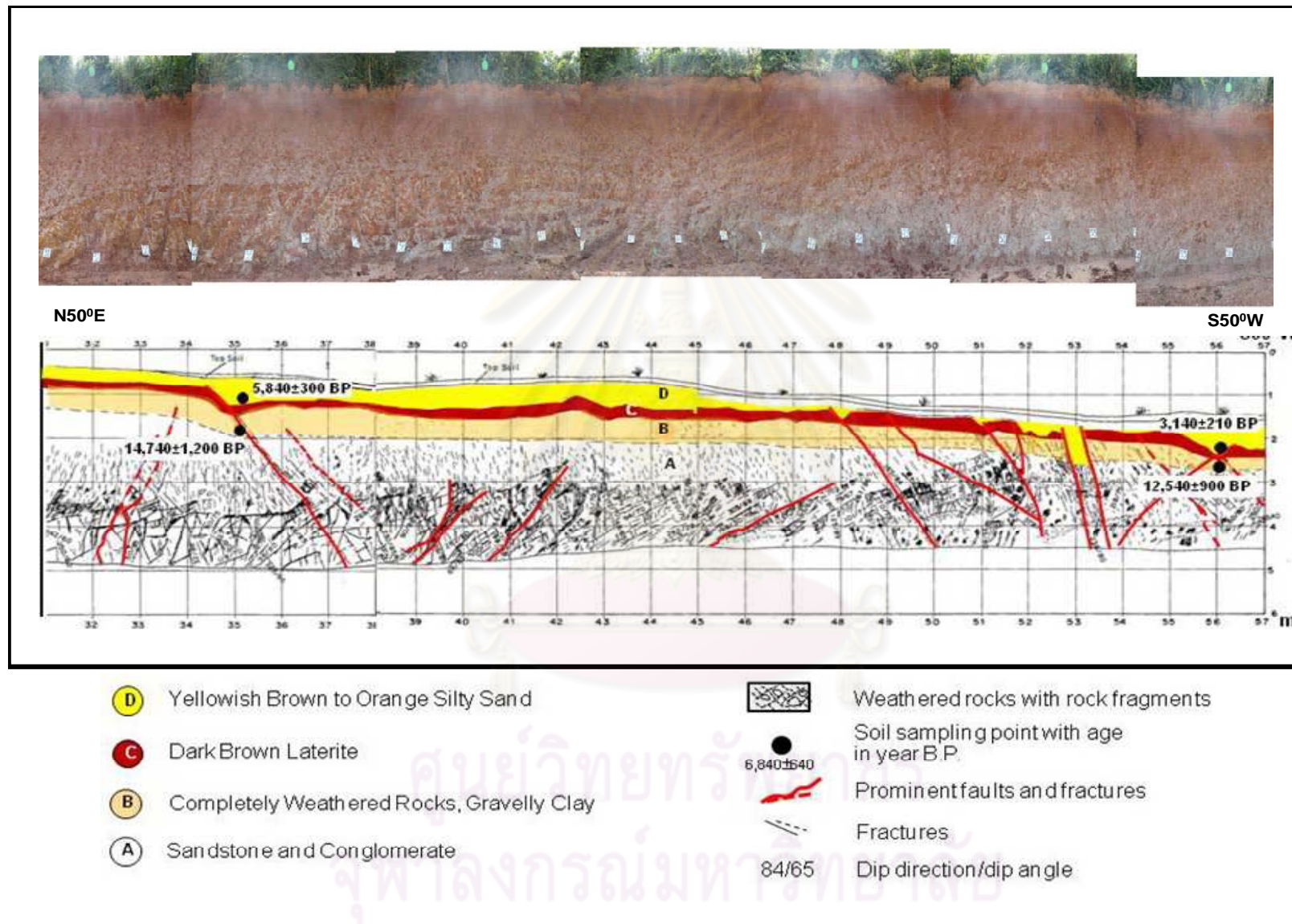


Figure D.4 Log of the exposure no.1 at Ban Chong Maliew, Phanom subdistrict, Phanom district, Surat Thani province.

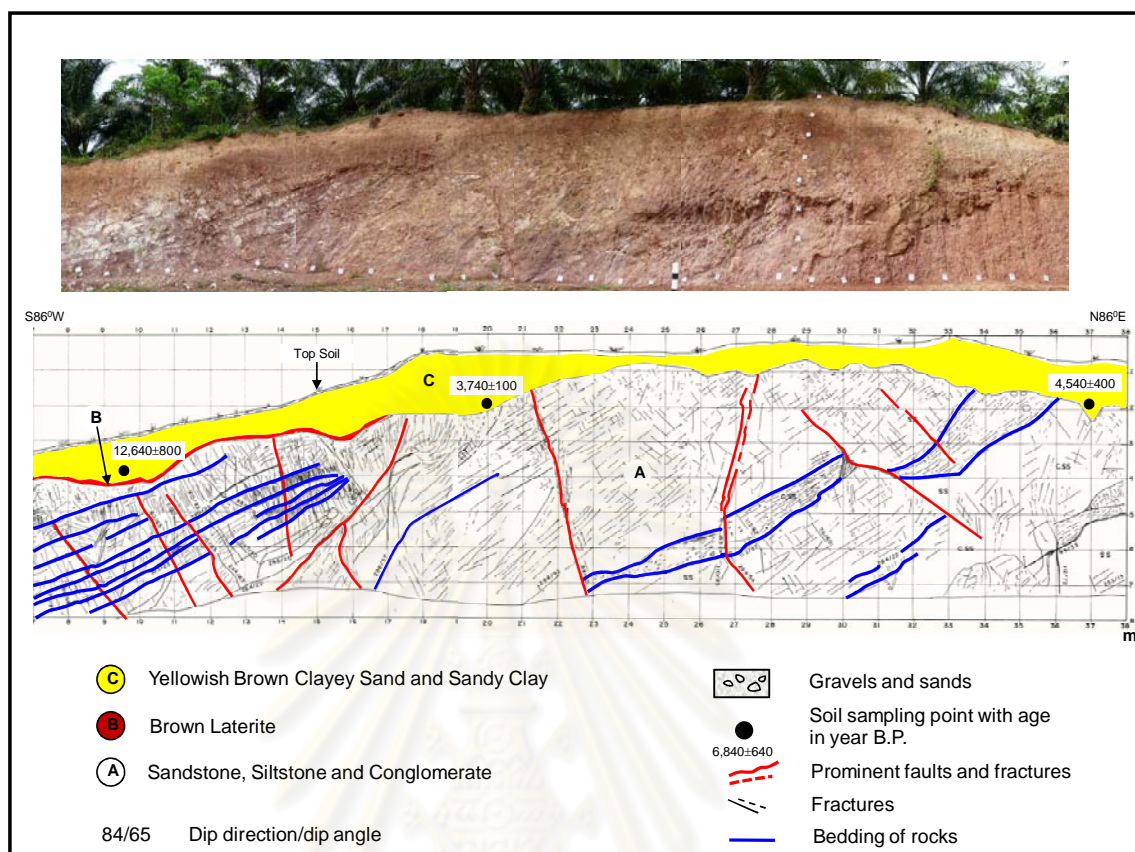


Figure D.5 Log of exposure at Ban Nongtao, Ao Luek Tai subdistrict, Ao Luek district, Krabi province

ศูนย์วิทยทรัพยากร
จุฬาลงกรณ์มหาวิทยาลัย

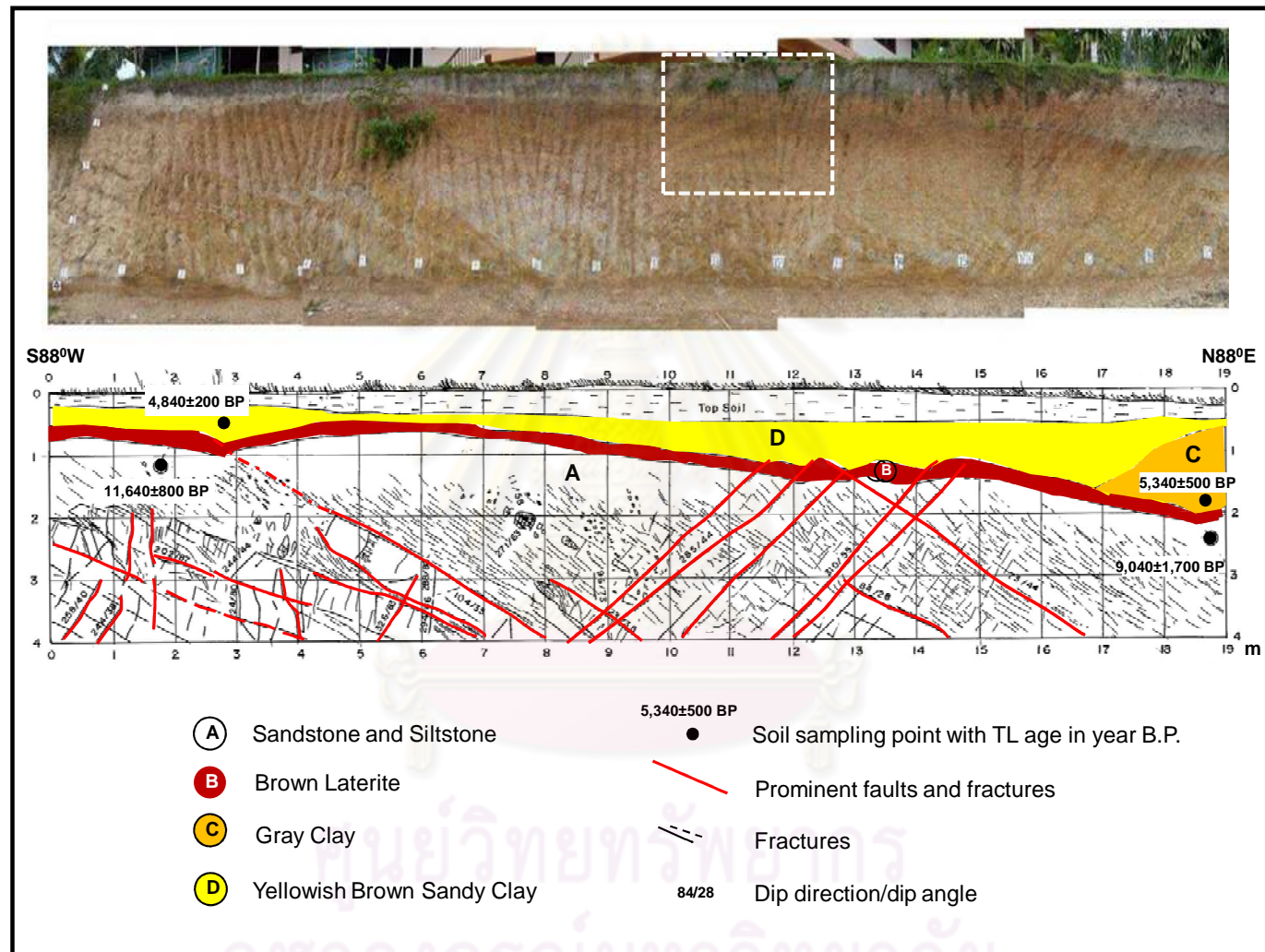


Figure D.6 Log of exposure at Ban Bangsai, Thap Put subdistrict, Thap Put district, Phang Nga province.

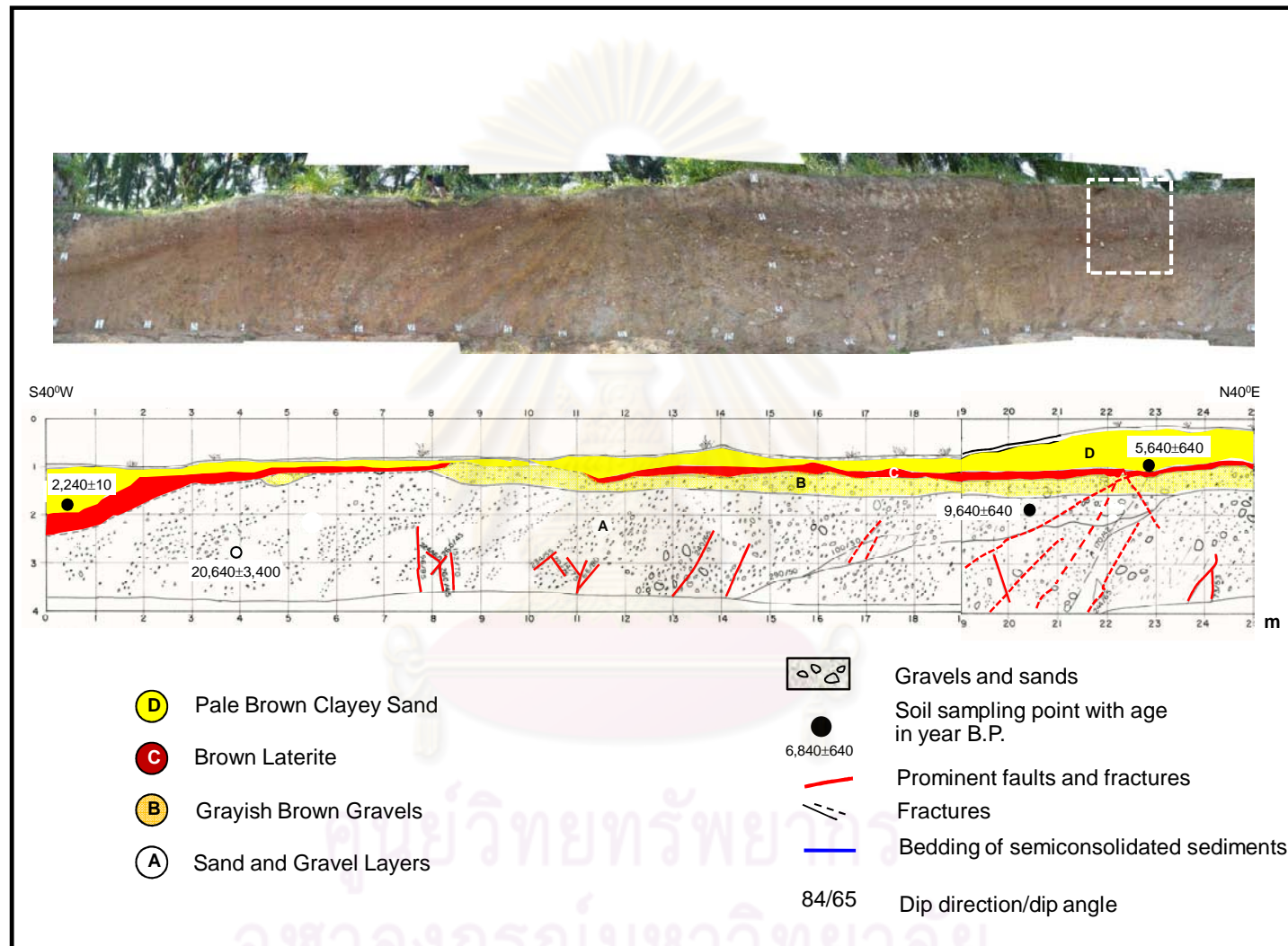


Figure D.7 Log of exposure in the borrow pit at Ban Khao To, Khao Khane subdistrict, Plai Phraya district, Krabi province.



Figure D.8 Log of exposure at Naiprab temple, Tha Sadej subdistrict, Khian Sa district, Surat Thani province

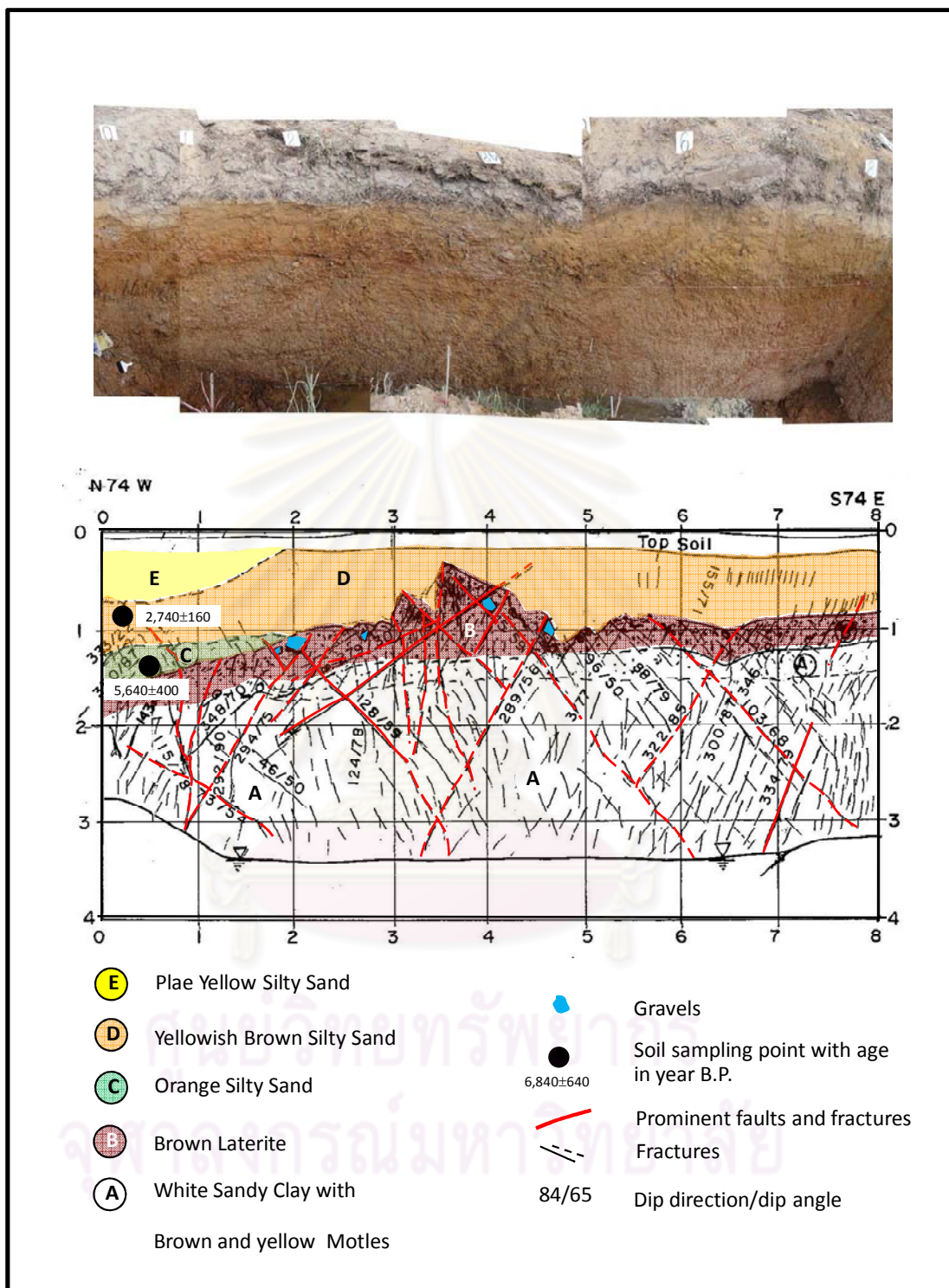


Figure D.9 Log of trench lying in the direction of N74°W-S74°E at palm field, Krabi Noi sub-district, Muang district, Krabi province

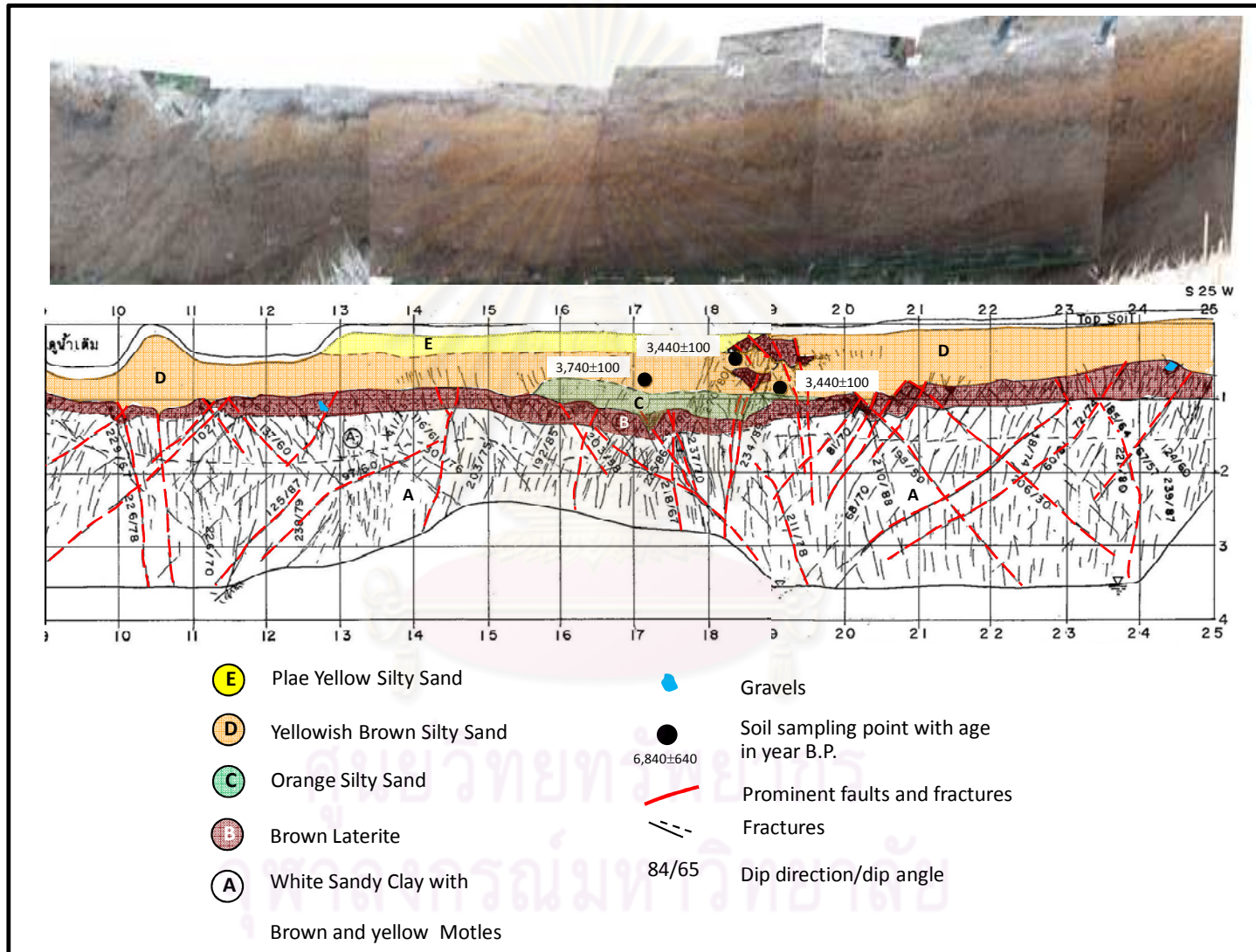


Figure D. 10 Log of trench no. 2 in the direction of N25°E-S25°W at palm field, Krabi Noi sub-district, Muang district, Krabi province

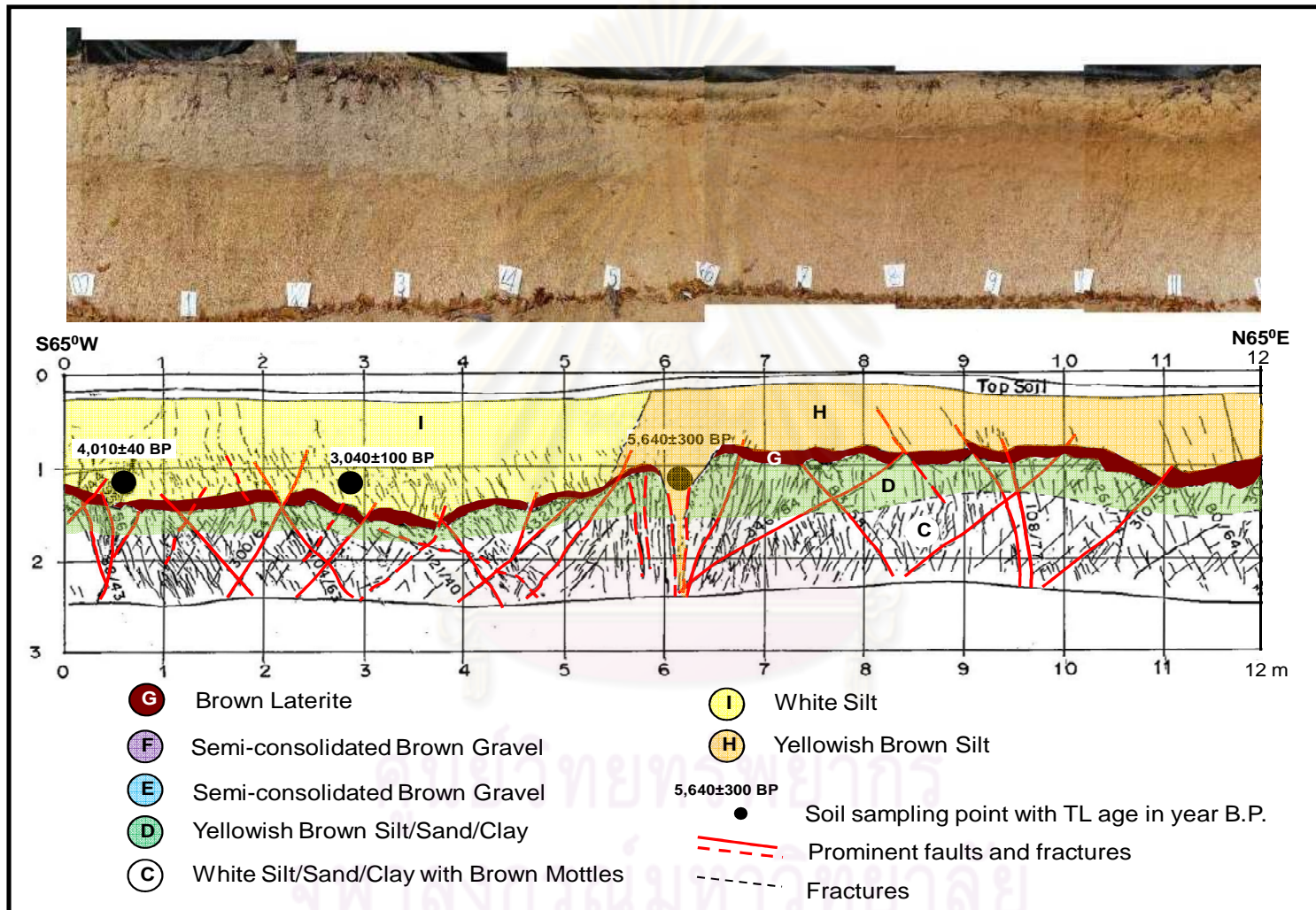


Figure D.11 Log of exposure at Thung Saingam school, Thap Put district, Phang Nga province from stations 0-12 m.

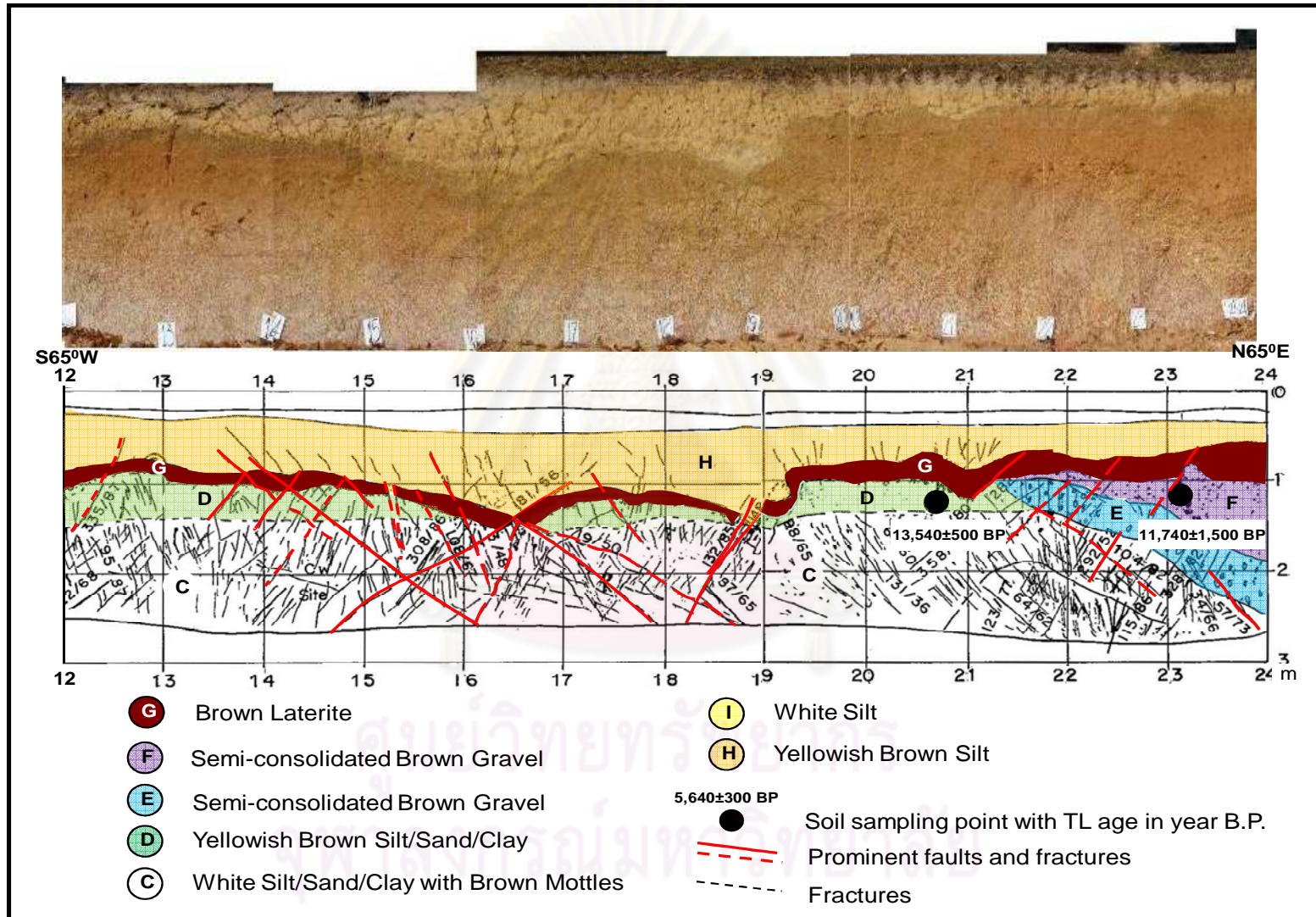


Figure D.12 Log of exposure at Thung Saingam school, Thap Put district, Phang Nga province from stations 12-24 m.

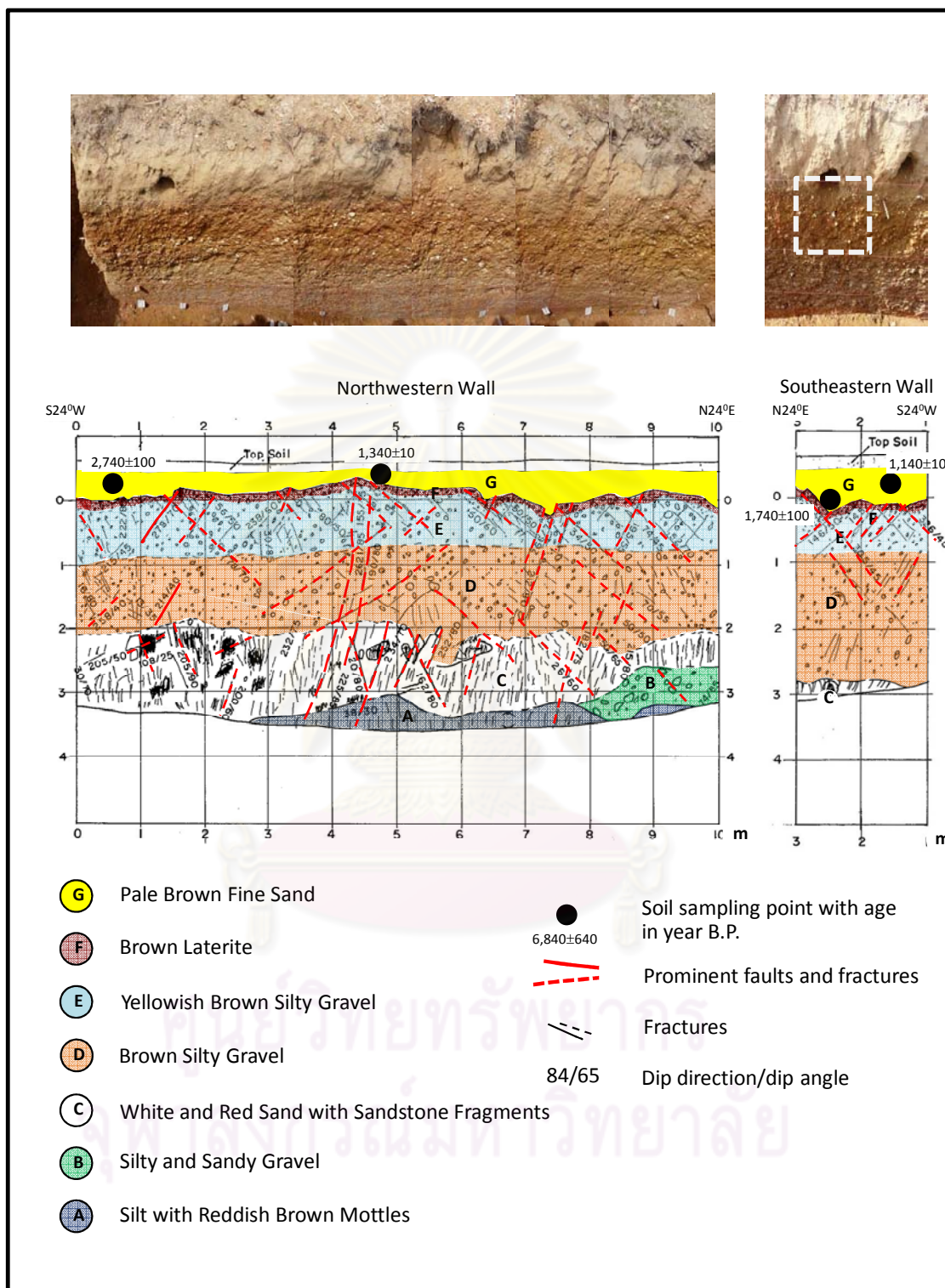


Figure D.13 Log of trench wall at Ban Lum Kriab, Thap Put sub-district, Thap Put district, Phang Nga province.

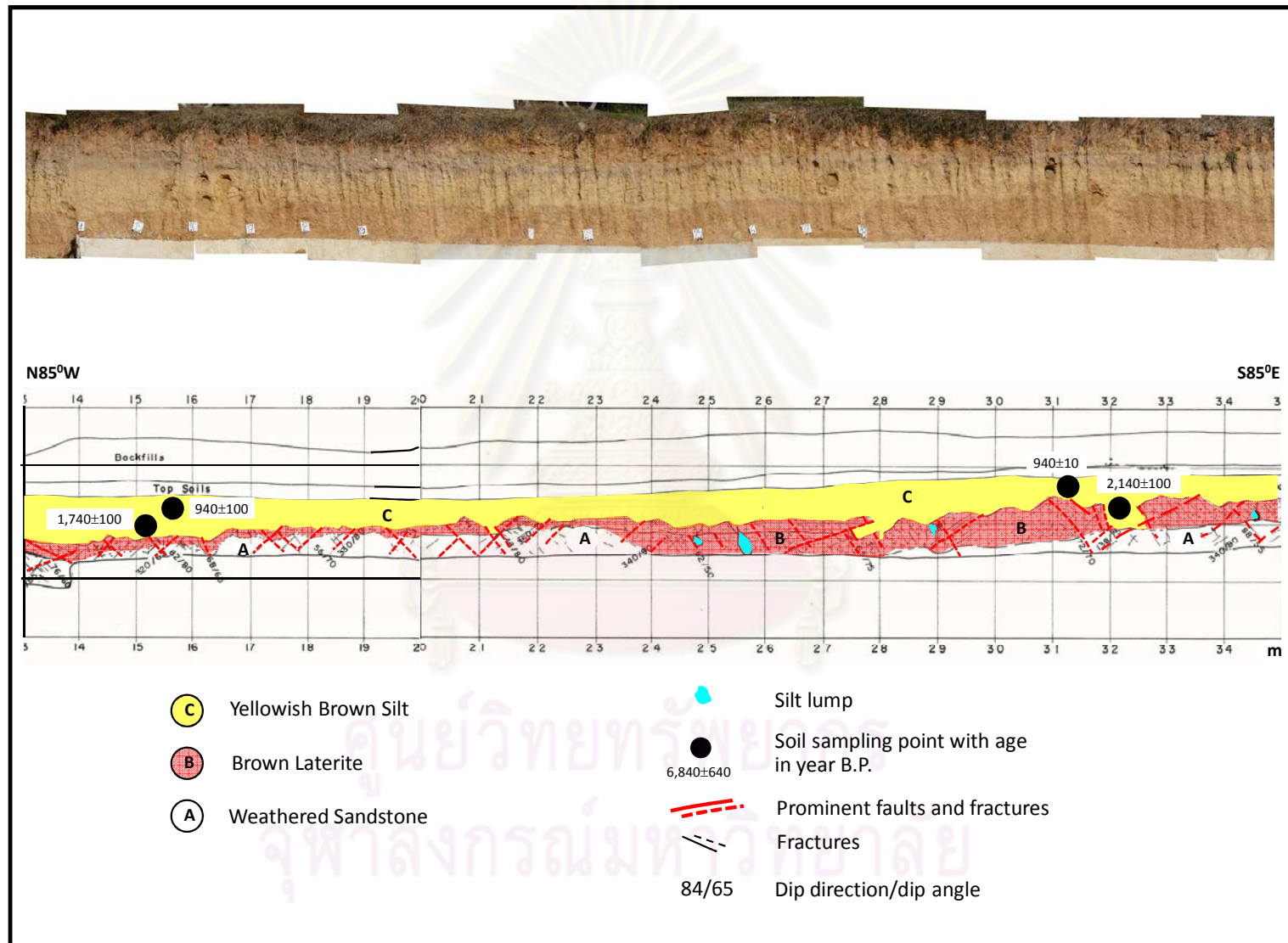
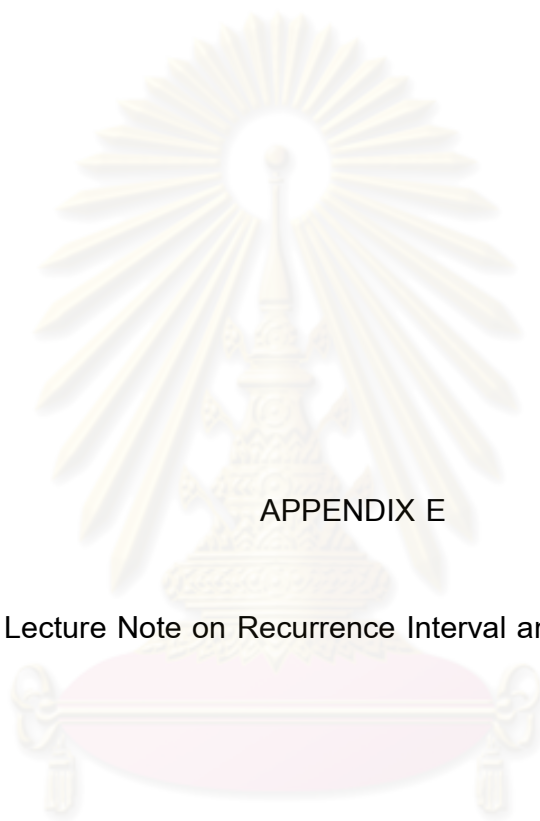


Figure D.14 Log of exposure along the highway from Thup Put district, Phang Nga Province to Muang district, Krabi province



APPENDIX E

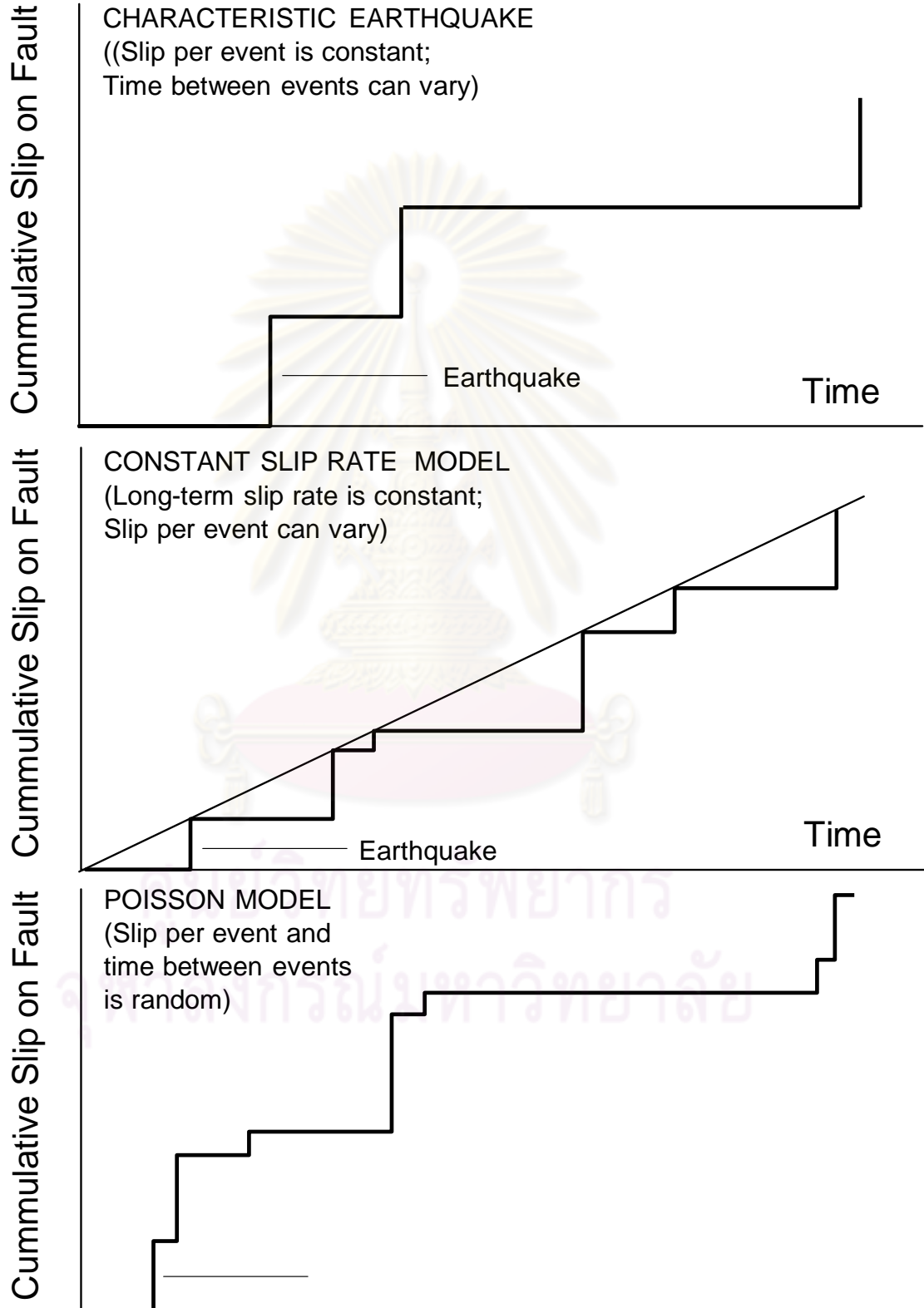
Martel's Lecture Note on Recurrence Interval and Probability (2002)

ศูนย์วิทยทรัพยากร
จุฬาลงกรณ์มหาวิทยาลัย

RECURRENCE INTERVALS AND PROBABILITY (18)

- I Main Topics
 - A Recurrence intervals
 - B Simple empirical earthquake recurrence models
 - C Seismic gaps
 - D Probability distributions
 - http://www.seismo.berkeley.edu/seismo/hayward/probabilities_new.html
 - <http://quake.usgs.gov/prepare/ncep/>
 - E Exercise on probability of "The Big One" in So. Cal. in next 30 years
 - F Recognition, Characterization, Risk Evaluation, Risk Assessment
- II Recurrence interval:
 - A Used to evaluate when an earthquake is likely to occur
 - B Recurrence interval = time between consecutive earthquakes (usually with reference to earthquakes of a given magnitude)
 - C Can be determined by geologic means
 - 1 Dating of individual events (e.g. data from trench study)
 - 2 Average recurrence int. = Average slip per event/average slip rate
- III Simple empirical earthquake recurrence models
 - A Characteristic Earthquake Model
 - 1 Same rupture length and slip distribution (and seismic moment)
 - 2 Recurrence interval can vary through time
 - B Constant slip rate (time-predictable) Earthquake Model
 - 1 Slip rate across fault is constant
 - 2 Recurrence interval depends on slip during earthquake
 - C Random (Poisson) Model
 - 1 Historical record too short to separate any patterns from "noise"
 - 2 Earthquakes might best be considered as random events in time
 - D Problems with resolving dates of events
- IV Seismic gaps
 - A Used to evaluate where an earthquake is likely to occur
 - B Along an active fault, the probability of an earthquake occurring is ~highest where the most time has elapsed since the last rupture

COMPARISON OF THREE EARTHQUAKE MODELS

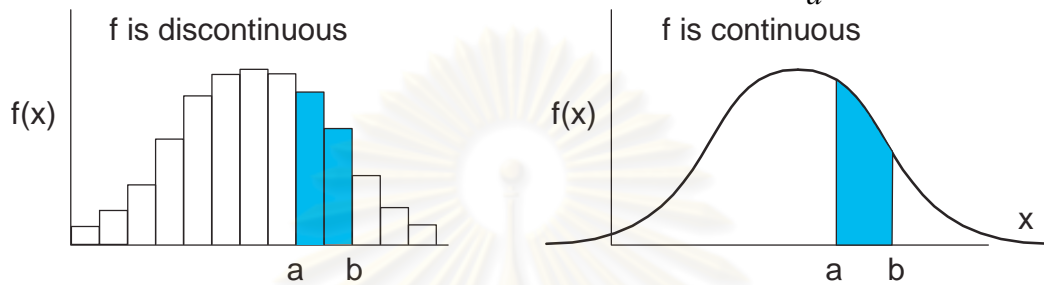


V Probability distributions

A Probability density functions [PDF = $f(x)$]: general comments

1 Probability ($a < X < b$) = probability of an outcome between a and b

$$= P(a < X < b) = \text{area under } f(x) \text{ from } a \text{ to } b = \int_a^b f(x) dx$$



a Example 1: Probability of Micheal Jordan scoring 25-35 points

b Example 2: Probability of quake ($M_W = 7.5$) in next 25-35 years

2 ($P(-\infty < X < \infty)$) = area under $f(x)$ from $-\infty$ to $\infty = \int_{-\infty}^{\infty} f(x) dx = 1 = 100\%$

3 For continuous distributions, $P(x=a)$ = area under $f(x)$ from a to a
 $= \int_a^a f(x) dx = \underline{0}$

B The normal distribution ("The bell-shaped curve"): one kind of PDF

1 Described by mean μ and standard deviation σ

$$\mu = \frac{\sum_{i=1}^n x_i}{n} = \frac{\sum_{i=1}^n f_i x_i}{\sum_{i=1}^n f_i}$$

$$\sigma = \frac{\sum_{i=1}^n (x_i - \mu)^2}{n-1}$$

2 $P(\mu - \sigma < X < \mu + \sigma) \approx 2/3$; $P(\mu - 2\sigma < X < \mu + 2\sigma) \approx 95\%$ $P(\mu - 3\sigma < X < \mu + 3\sigma) \approx 99\%$

VI Exercise on probability of "The Big One" in So. Cal. in next 30 years

VII Recognition, Characterization, Risk Evaluation, Risk Assessment

A Probabilistic assessment allows the likelihood of given effects (e.g. intensities), and hence potential damages, to be estimated for a given area for a given time frame. **This is what is meant by evaluating the level of risk.**

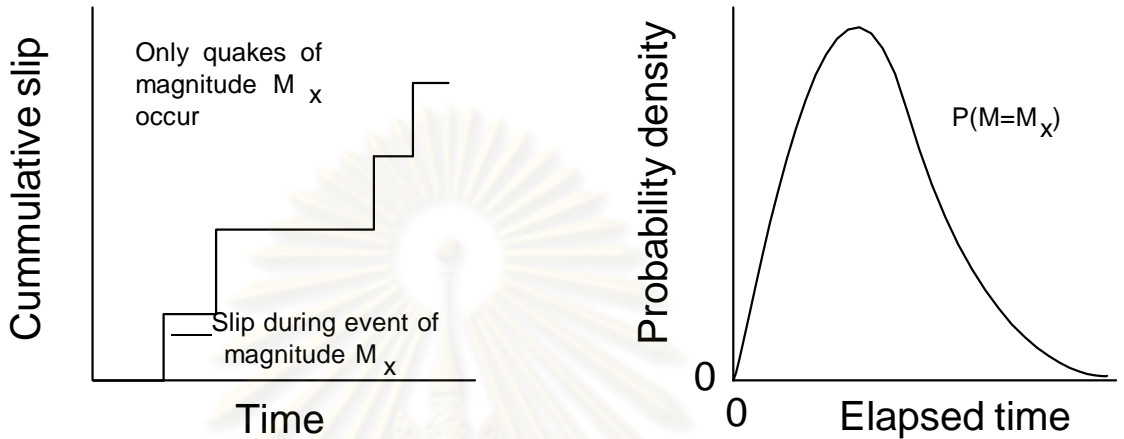
B Steps 1 and 2 must be done in order to get to step 3 (and then 4)

C Outcome probabilities are sensitive to the model one chooses

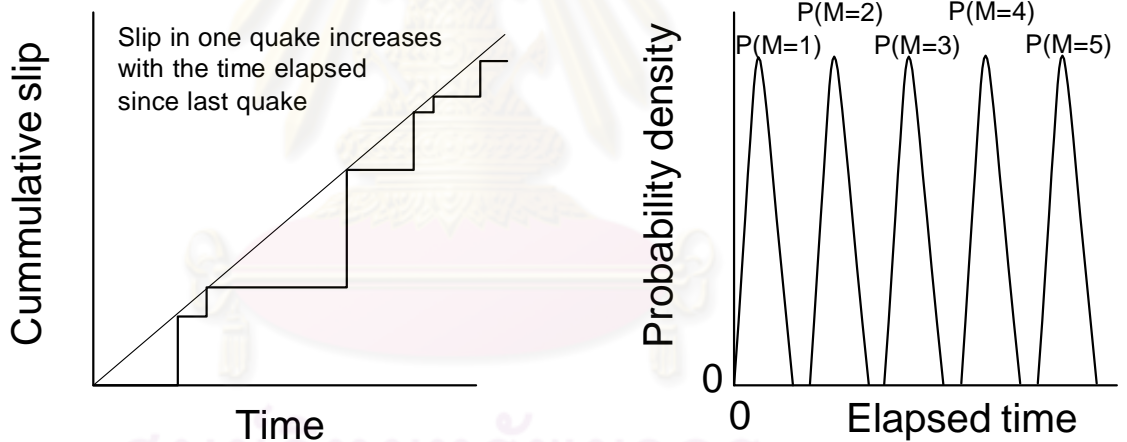
D This approach can be (and has been) applied to many phenomena

Probability distribution curves for three earthquake models

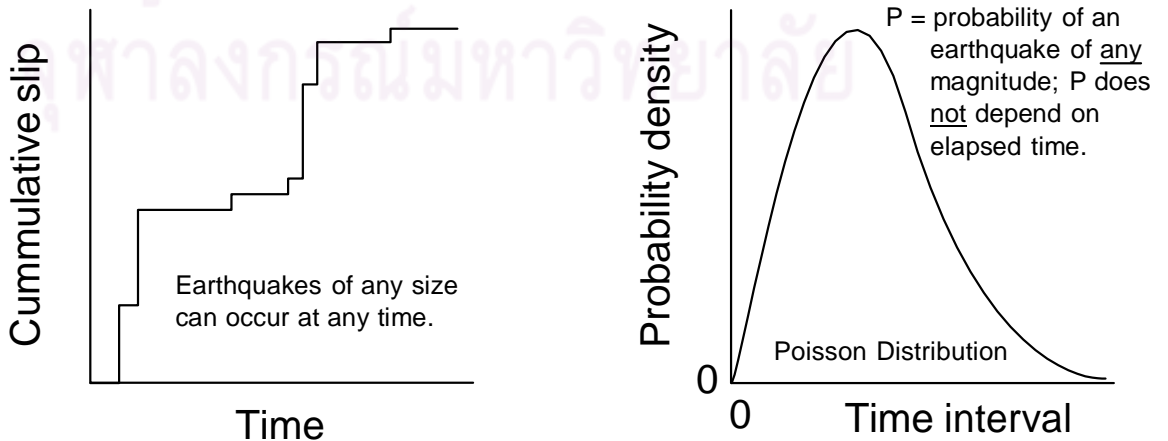
Characteristic Earthquake model



Time-predictable model



Random model



Method for Predicting the Annual Likelihood of "The Big One" at Pallet Creek

Kerry Sieh, a professor at Cal Tech, has done more than any other single person to document the hazard presented by recurring large earthquakes on the San Andreas fault in Southern California. We will use some of Kerry's results to estimate the probability of a large earthquake on the San Andreas fault in Southern California.

Here are Kerry's estimates (from his 1984 JGR paper) on the time of the last 12 large earthquakes at Pallet Creek (the uncertainties associated with these events are dropped):

1857, 1720, 1550, 1350, 1080, 1015, 935, 845, 735, 590, 350, 260

- 1 Based on the time between the oldest event listed above and the 1857 quake, calculate the average (mean) recurrence interval for large earthquakes at Pallet Creek.

Mean Recurrence Interval = (1857-260)years/11 intervals = 1597 yr/11 = 145 years

- 2 The earthquakes are not occurring at a perfectly regular pace. Calculate the recurrence times between each successive pair of earthquakes.

137, 170, 200, 270, 65, 80, 90, 110, 145, 240, 90

- 3 Calculate the standard deviation of the 11 recurrence intervals associated with the 12 quakes. The equation to use is:

$$\sigma = \sqrt{\frac{\sum_{i=1}^n (R_i - R^*)^2}{n-1}}$$

where σ is the standard deviation, R_i is the recurrence time between a given pair of events, R^* is the mean recurrence interval, and n is the number of recurrence intervals (not the # of quakes!).

68 years

- 4a Assuming the year is 1993, how many years have elapsed since the last large San Andreas earthquake in southern California?

$$1993-1857 = 136 \text{ years}$$

- 4b How many years shy of the mean recurrence interval would we be?

$$145-136 = 9 \text{ years}$$

- 4c How many standard deviations shy of the mean recurrence interval would we be?

$$9 \text{ years}/68 \text{ years} = 0.13 \text{ standard deviations}$$

- 5 We will now suppose the distribution of recurrence intervals is normally distributed about the mean recurrence interval. On the supplied paper, plot the equation

$$f(t) = \frac{1}{\sigma\sqrt{2\pi}} \exp\left[-\frac{(t - t^*)^2}{2\sigma^2}\right]$$

where $f(t)$ is the normal distribution, t is time, t^* is the mean, and σ is the standard deviation.

Plot this for $0 \leq t \leq 250$ years.

- 6 What is the probability of an earthquake on the San Andreas fault at Pallet Creek in the next 30 years from 1993 given our model? This probability is the area under the curve from 1993 to 30 years hence divided by the area from 1993 to infinity.

Suppose the year is 1993 - 9 years (0.13 standard deviations) shy of the mean recurrence interval. In 30 years we would be 21 years (or $21/68 = 0.31$ standard deviations) past the mean recurrence interval. The area under the probability density curve from the mean to 0.13 standard deviations shy of the mean is 0.0517. The area under the probability density curve from the mean to 0.31 standard deviations past the mean is 0.1217. The area under the probability density curve from 0.13 standard deviations shy of the mean to ∞ is $0.5 + 0.0517$. So:

$$P = (0.0517 + 0.1217) / (0.5 + 0.0517) = 0.1734/0.5517 = 31\%$$

Even though Kerry doesn't think he missed a quake, suppose there were circumstantial evidence (e.g. Indian legends) for one large quake in the year 490 and another in 1215.

- 7 What would the new mean recurrence interval and standard deviation be?

New mean recurrence interval = 1597 years/13 intervals = 122.8 years = 123 years
 New standard deviation = 38 years (larger % change in standard deviation than in mean!)

- 8 Assuming the year is 1993, what would the recalculated probability be for a large quake at Pallet Creek in the next 30 years?

The year 1993 would be 13 years (or $13/38 = 0.34$ standard deviations) past the mean recurrence interval. In 30 years we would be 43 years (or $43/38 = 1.13$ standard deviations) past the mean recurrence interval. The area under the probability density curve from the mean to 0.34 standard deviations from the mean is 0.1331. The area under the probability density curve from the mean to 1.13 standard deviations past the mean is 0.3708. The area under the probability density curve from 0.34 standard deviations past the mean to ∞ is $(0.5 - 0.1331)$. So:

$$P = (0.3708 - 0.1331) / (0.5 - 0.1331) = 0.2377/0.3669 = 65\%$$

Now suppose we consider the earthquakes to be distributed randomly (i.e. they are characterized by a Poisson distribution). Then the probability of an earthquake occurring does not depend on how much time has elapsed since the last earthquake. The probability of "x" number of earthquakes occurring in a given interval of time t is given by:

$$P(x) = \frac{(vt)^x e^{-vt}}{x!}$$

where "v" is the average rate of occurrence. So if the average recurrence interval is 145 years, the probability of getting 1 event in 145 years is:

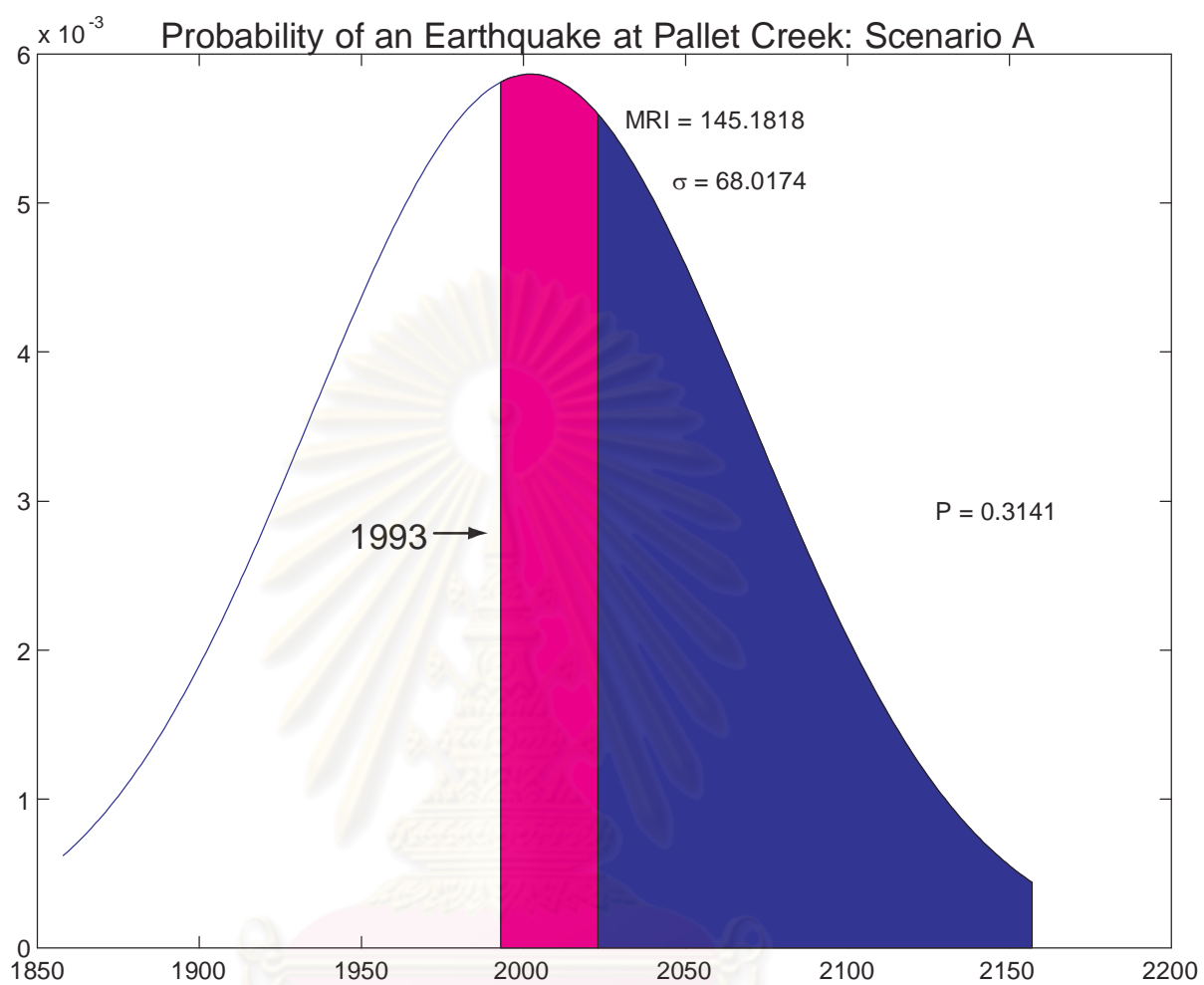
$$P(1) = \frac{\left(\frac{1 \text{ event}}{145 \text{ yrs}} 145 \text{ yrs}\right)^1 e^{-\left(\frac{1 \text{ event}}{145 \text{ yrs}} 145 \text{ yrs}\right)}}{1!} = e^{-1} = 37\%$$

The probability of getting one event in 30 years is:

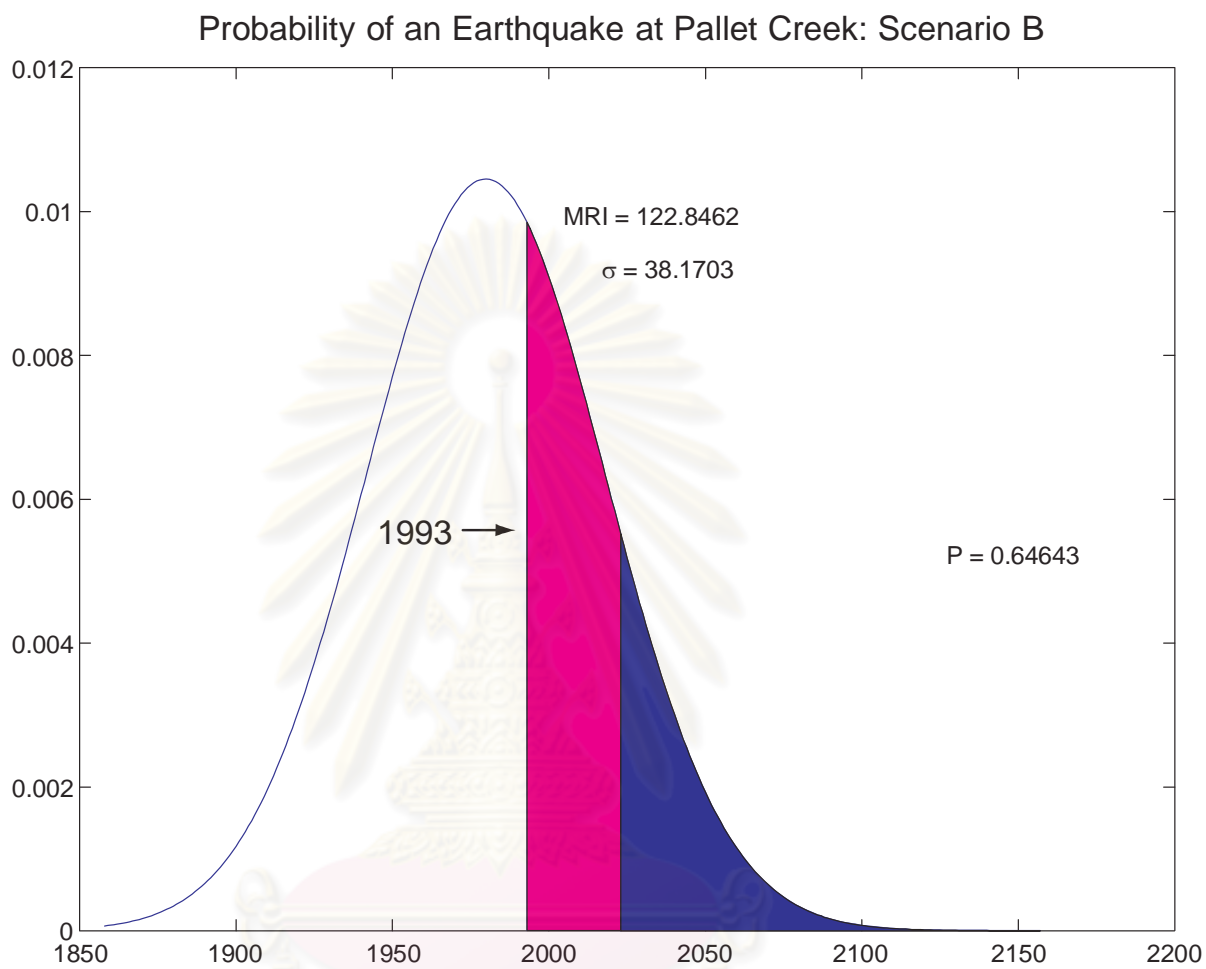
$$P(1) = \frac{\left(\frac{1 \text{ event}}{145 \text{ yrs}} 30 \text{ yrs}\right)^1 e^{-\left(\frac{1 \text{ event}}{145 \text{ yrs}} 30 \text{ yrs}\right)}}{1!} = (30/145)(e^{-30/145}) = 17\%$$

The probability of getting no event in 30 years is:

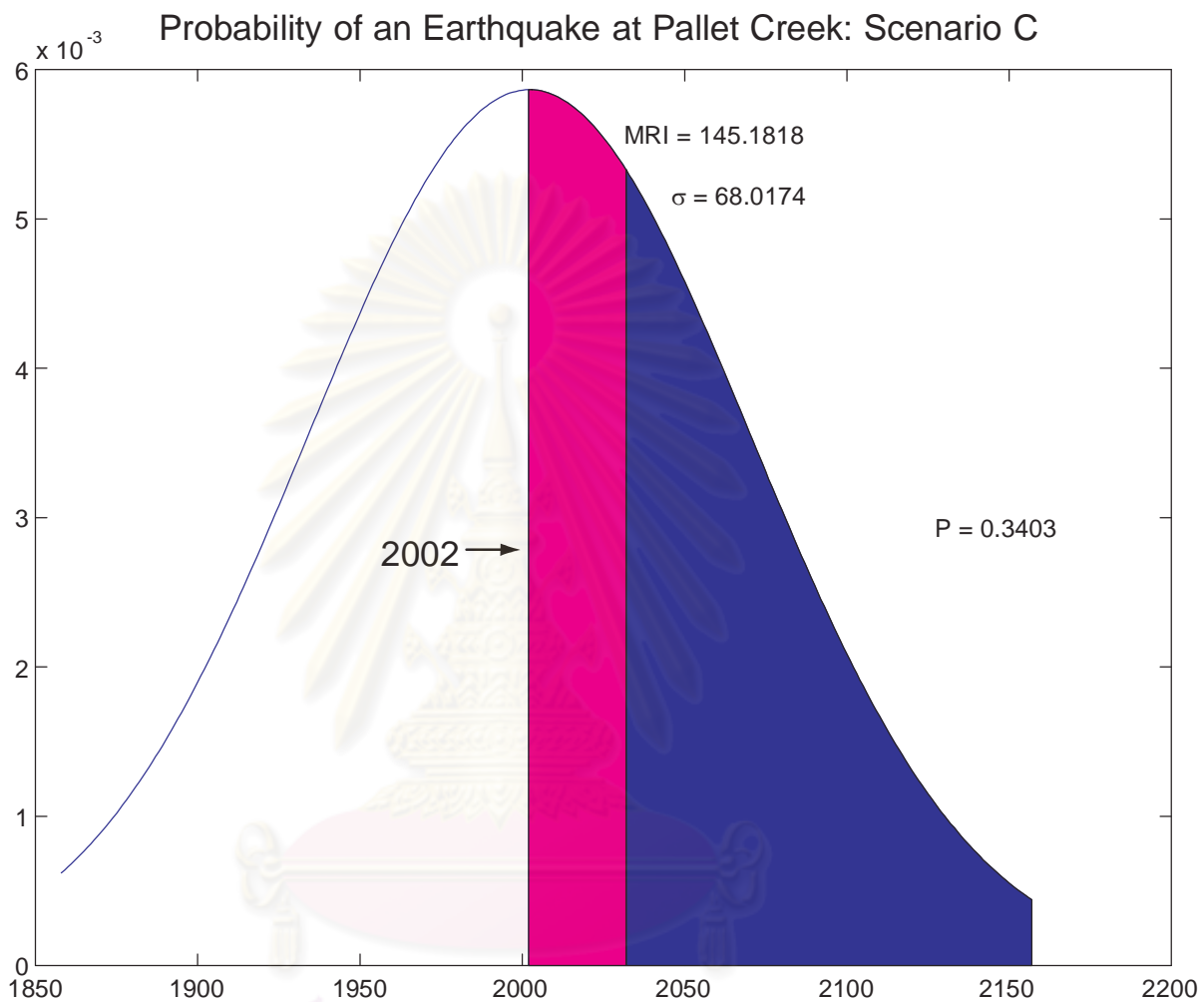
$$P(1) = \frac{\left(\frac{1 \text{ event}}{145 \text{ yrs}} 30 \text{ yrs}\right)^0 e^{-\left(\frac{1 \text{ event}}{145 \text{ yrs}} 30 \text{ yrs}\right)}}{0!} =$$



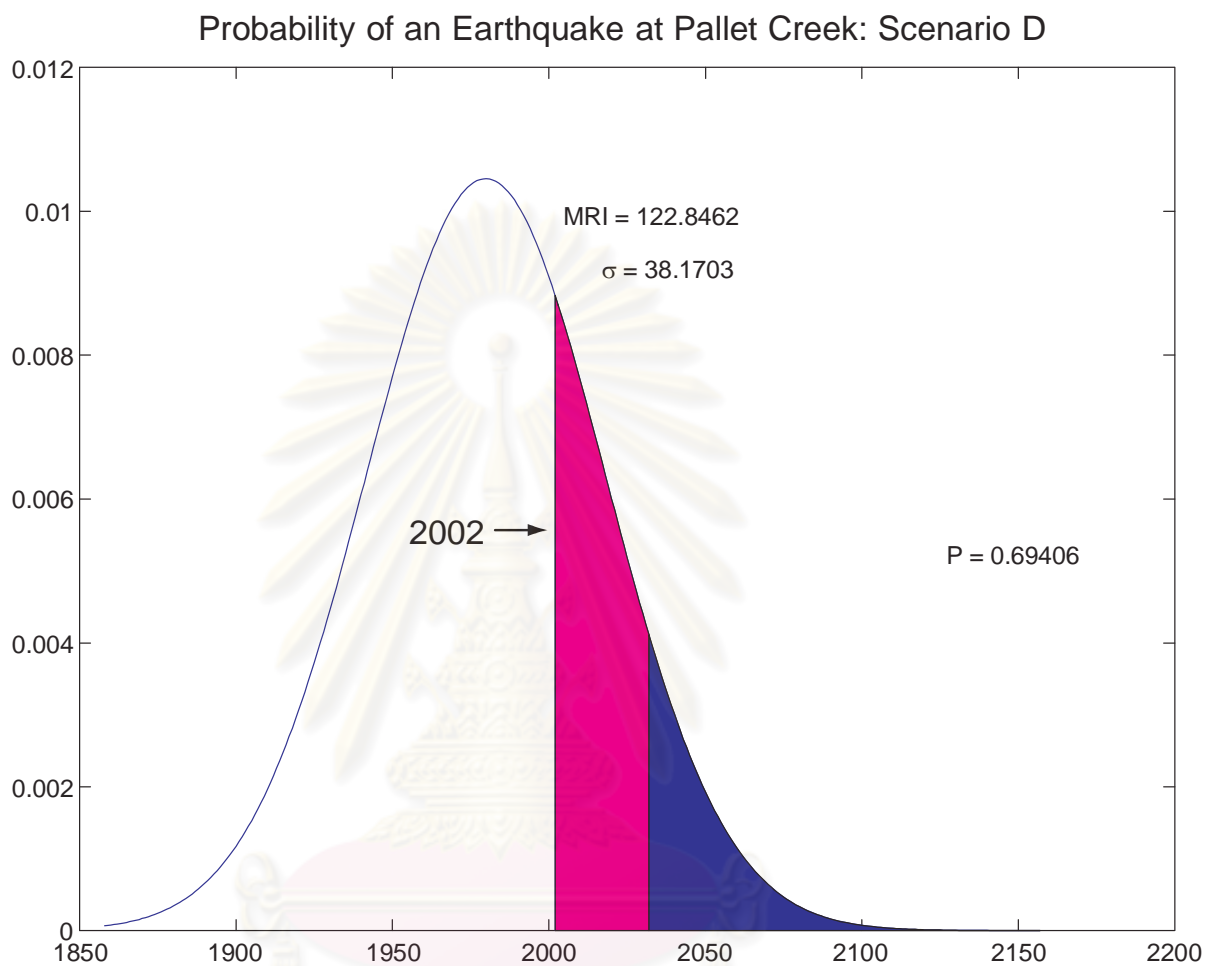
ศูนย์วิทยทรัพยากร
จุฬาลงกรณ์มหาวิทยาลัย



ศูนย์วิทยทรัพยากร
จุฬาลงกรณ์มหาวิทยาลัย



ศูนย์วิทยทรัพยากร
จุฬาลงกรณ์มหาวิทยาลัย



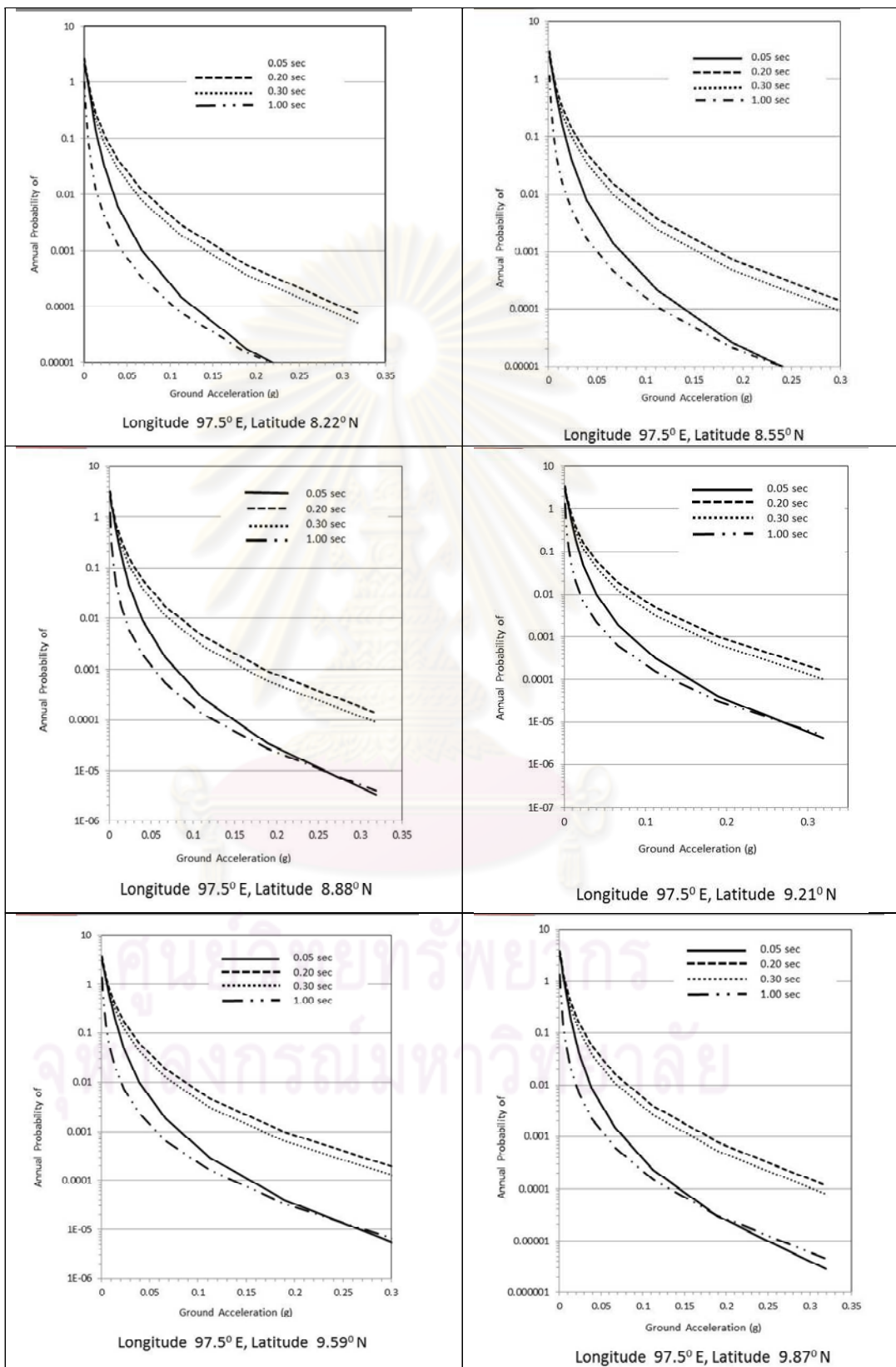
ศูนย์วิทยทรัพยากร
จุฬาลงกรณ์มหาวิทยาลัย

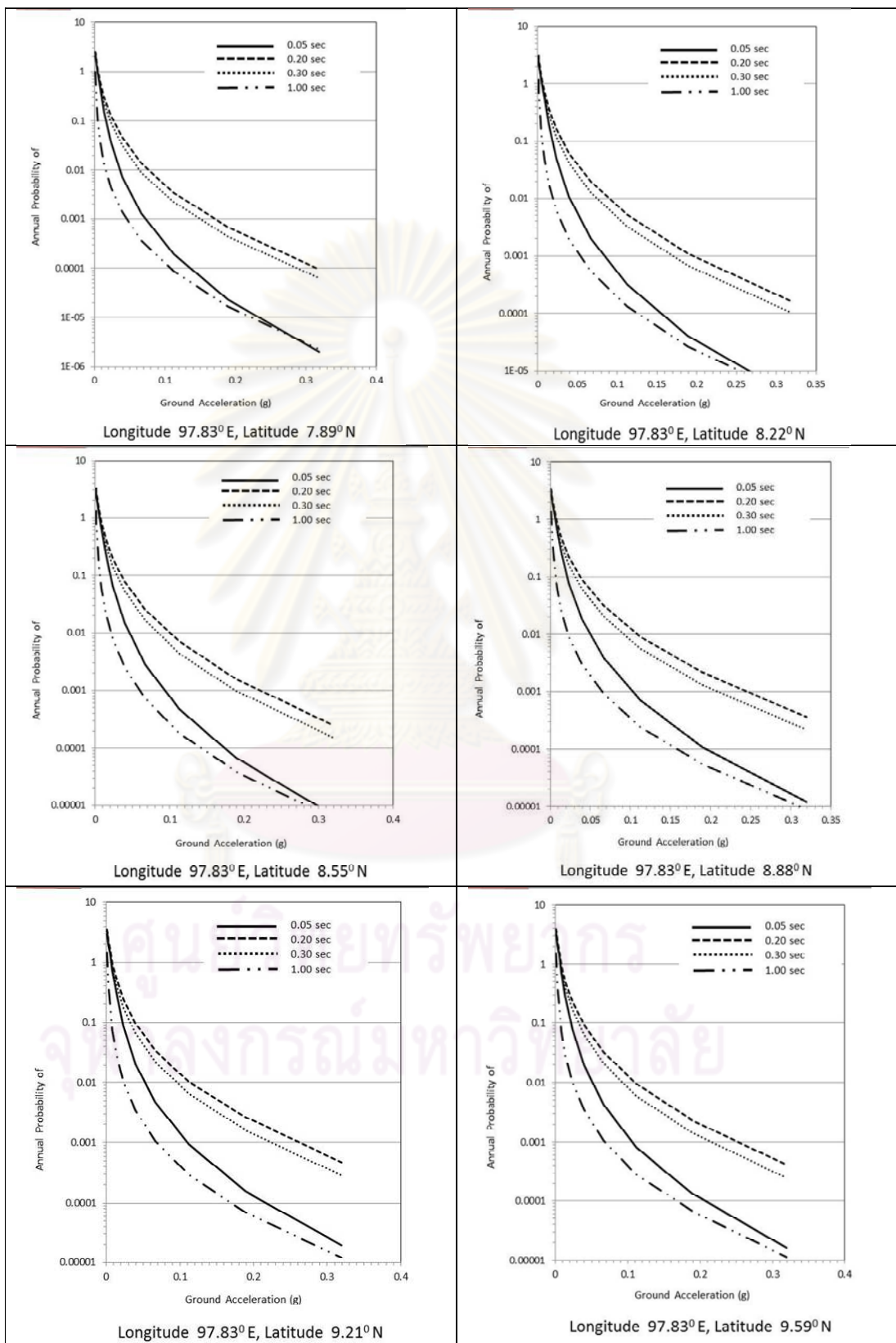


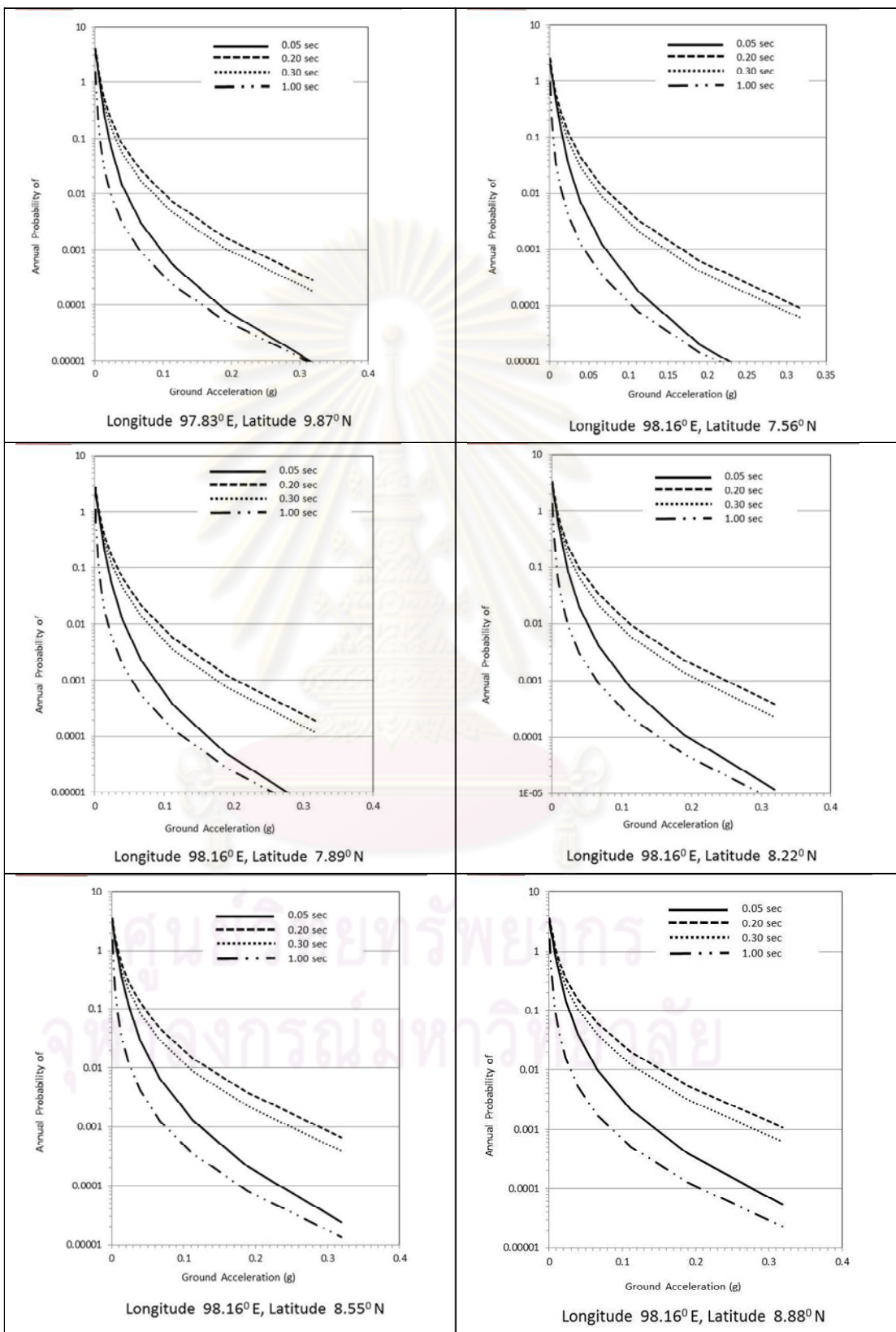
APPENDIX F

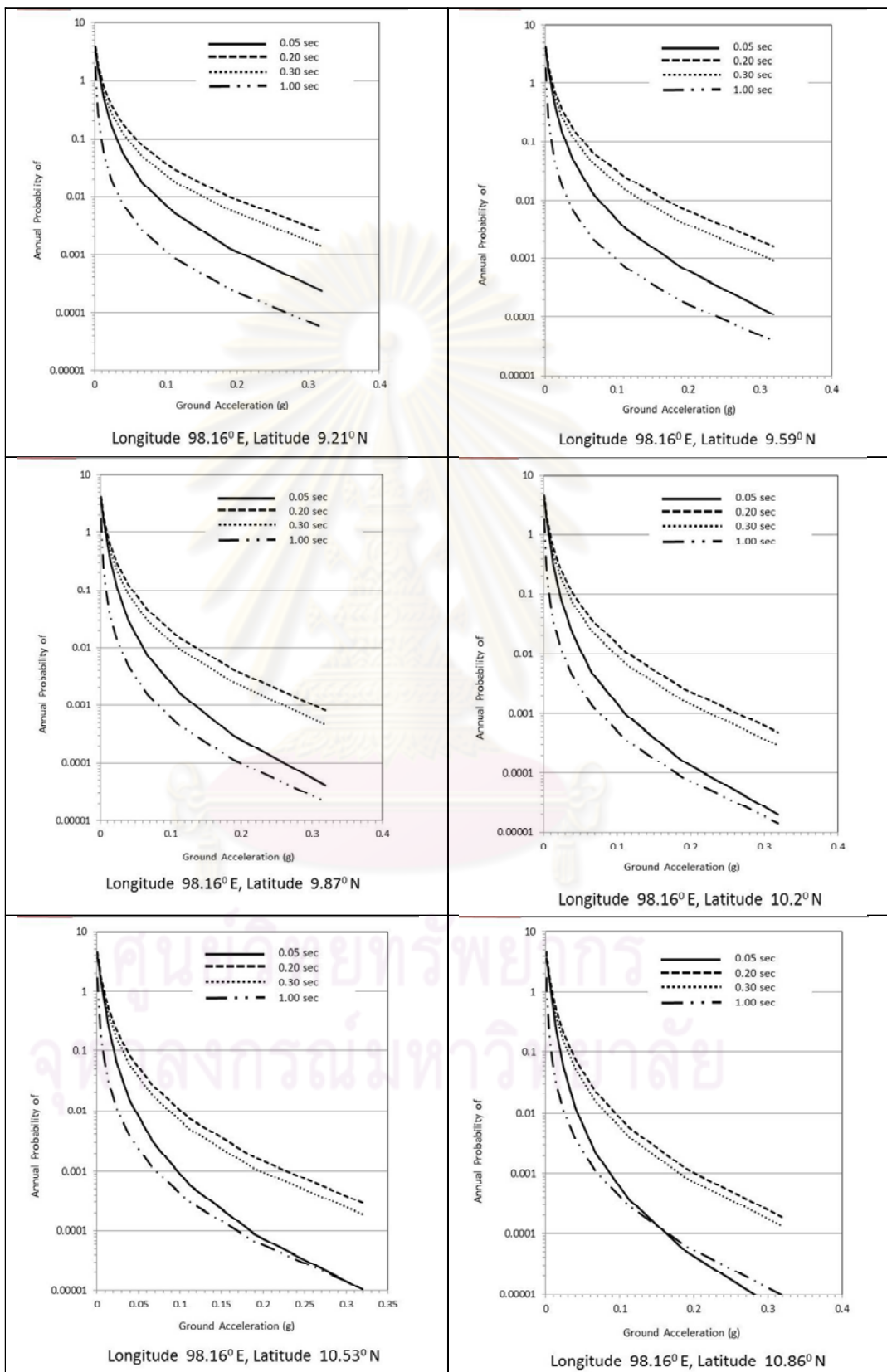
Hazard Curves

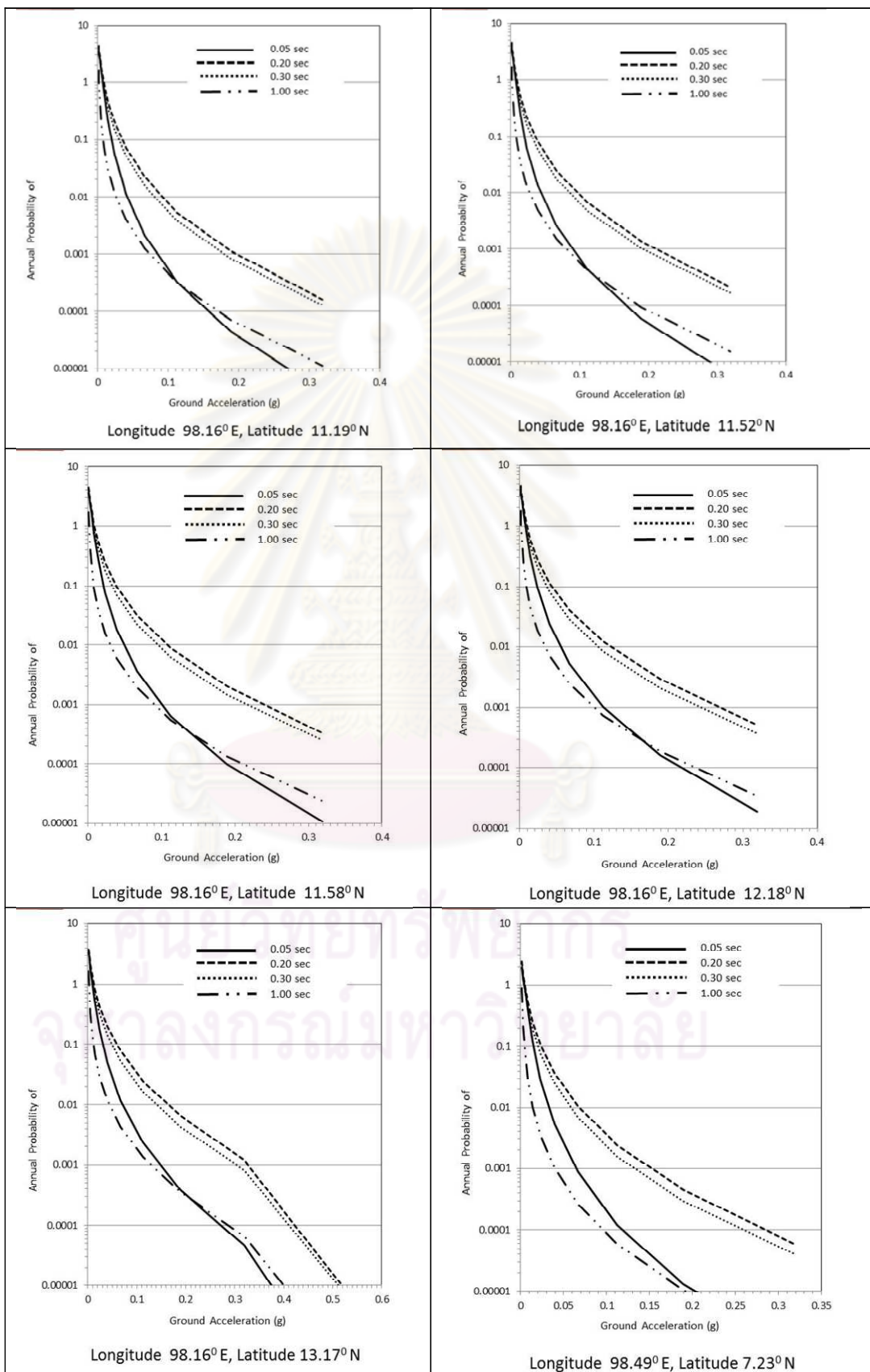
ศูนย์วิทยทรัพยากร
จุฬาลงกรณ์มหาวิทยาลัย

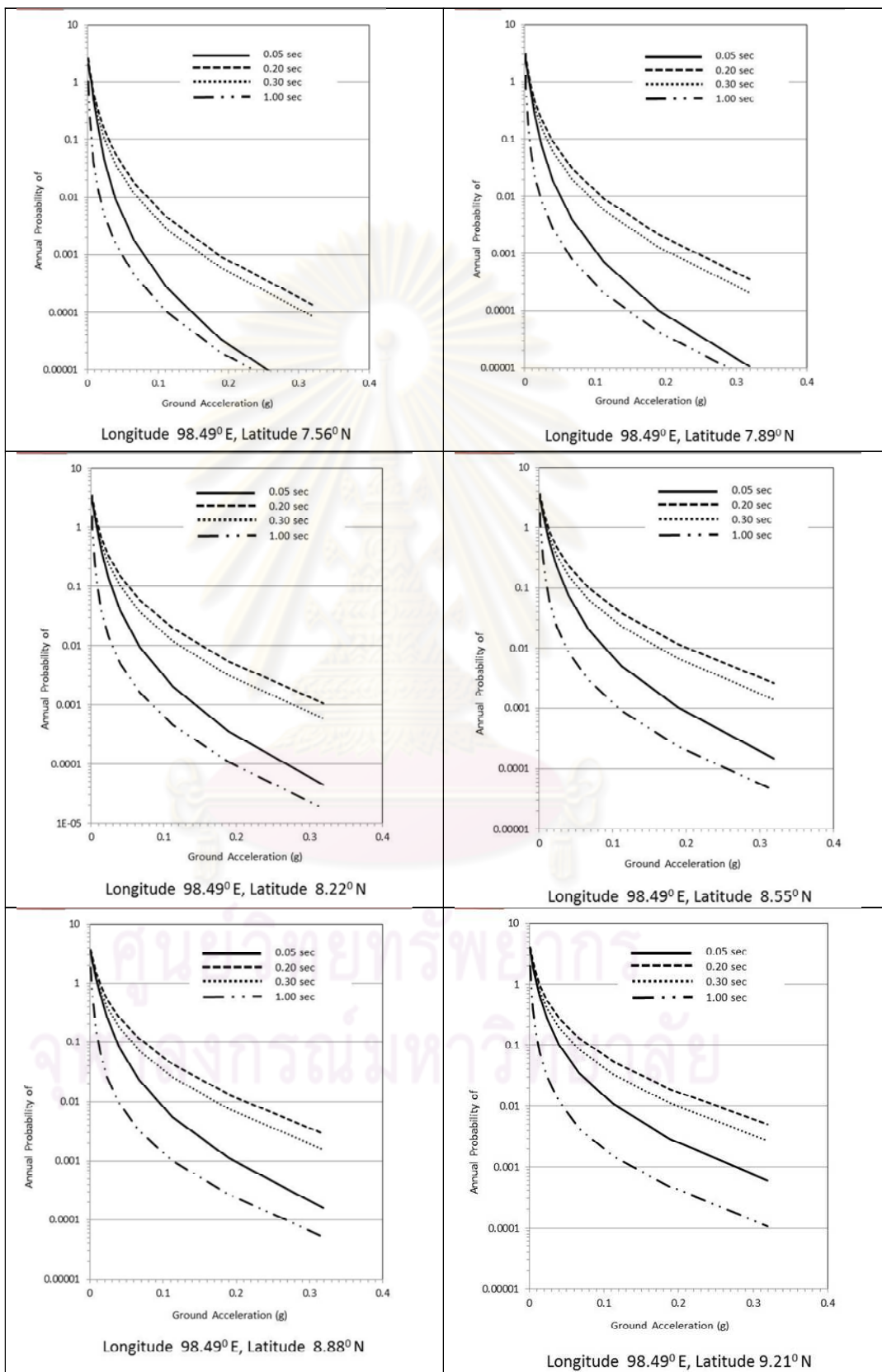


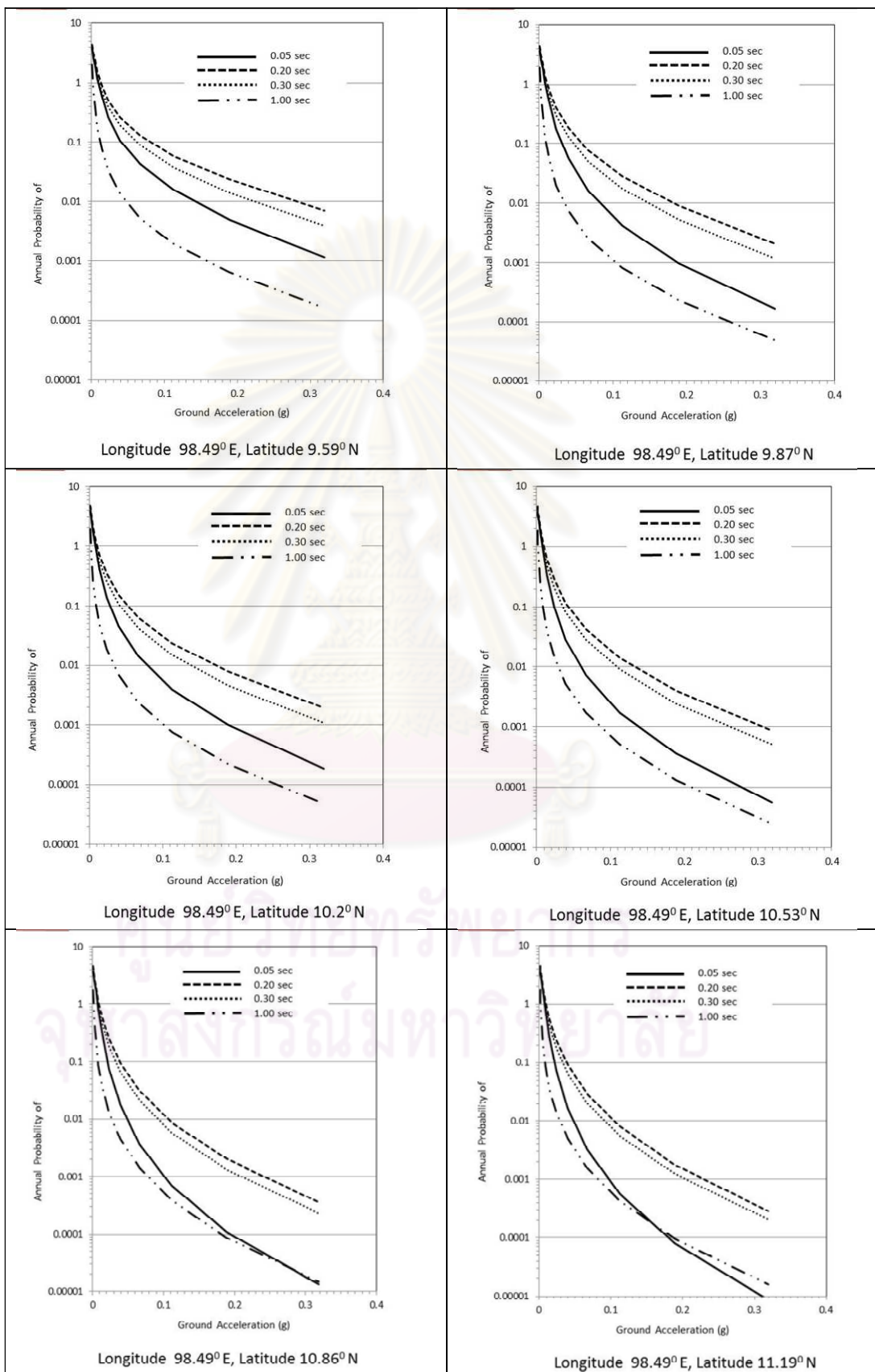


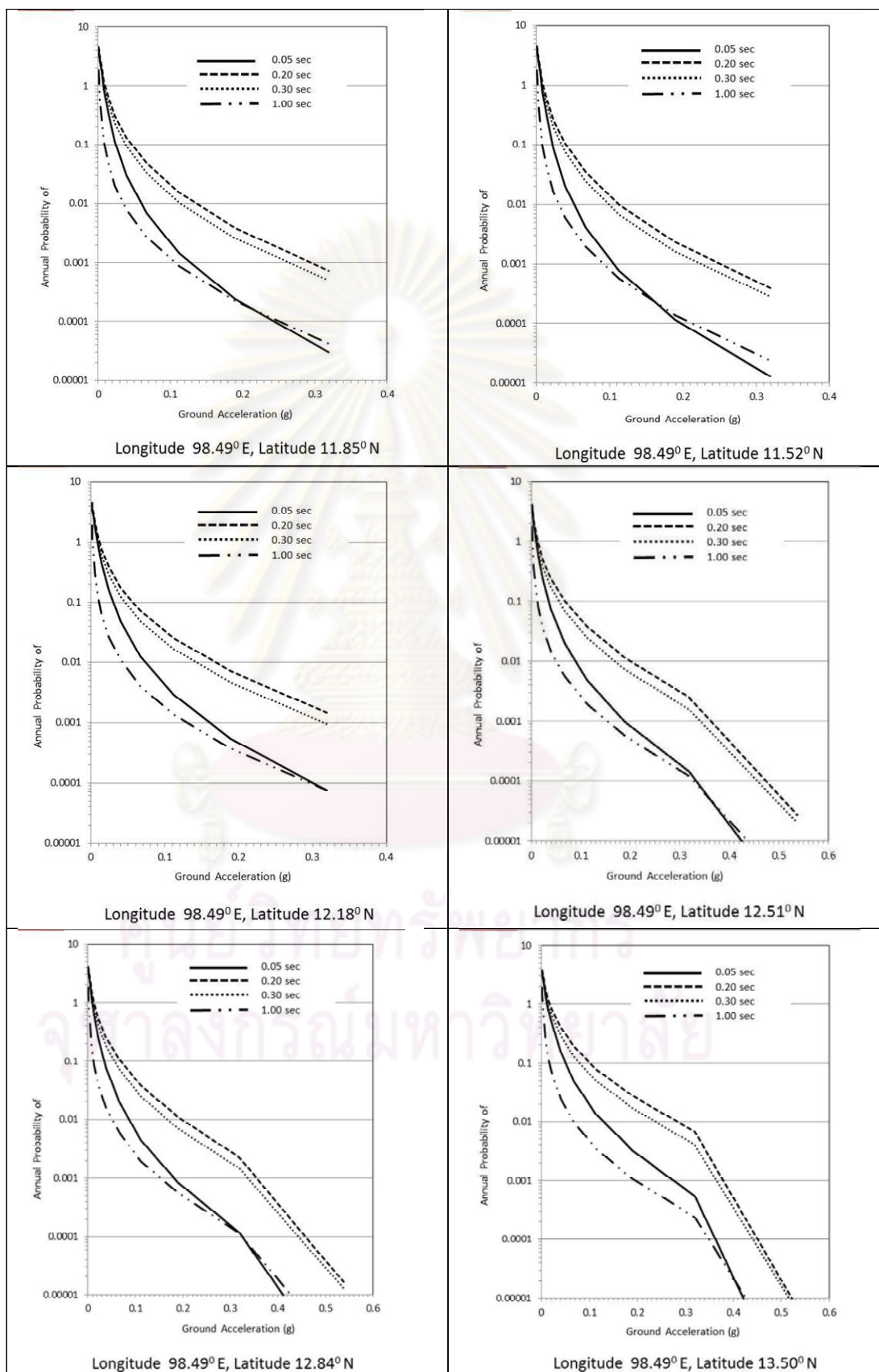


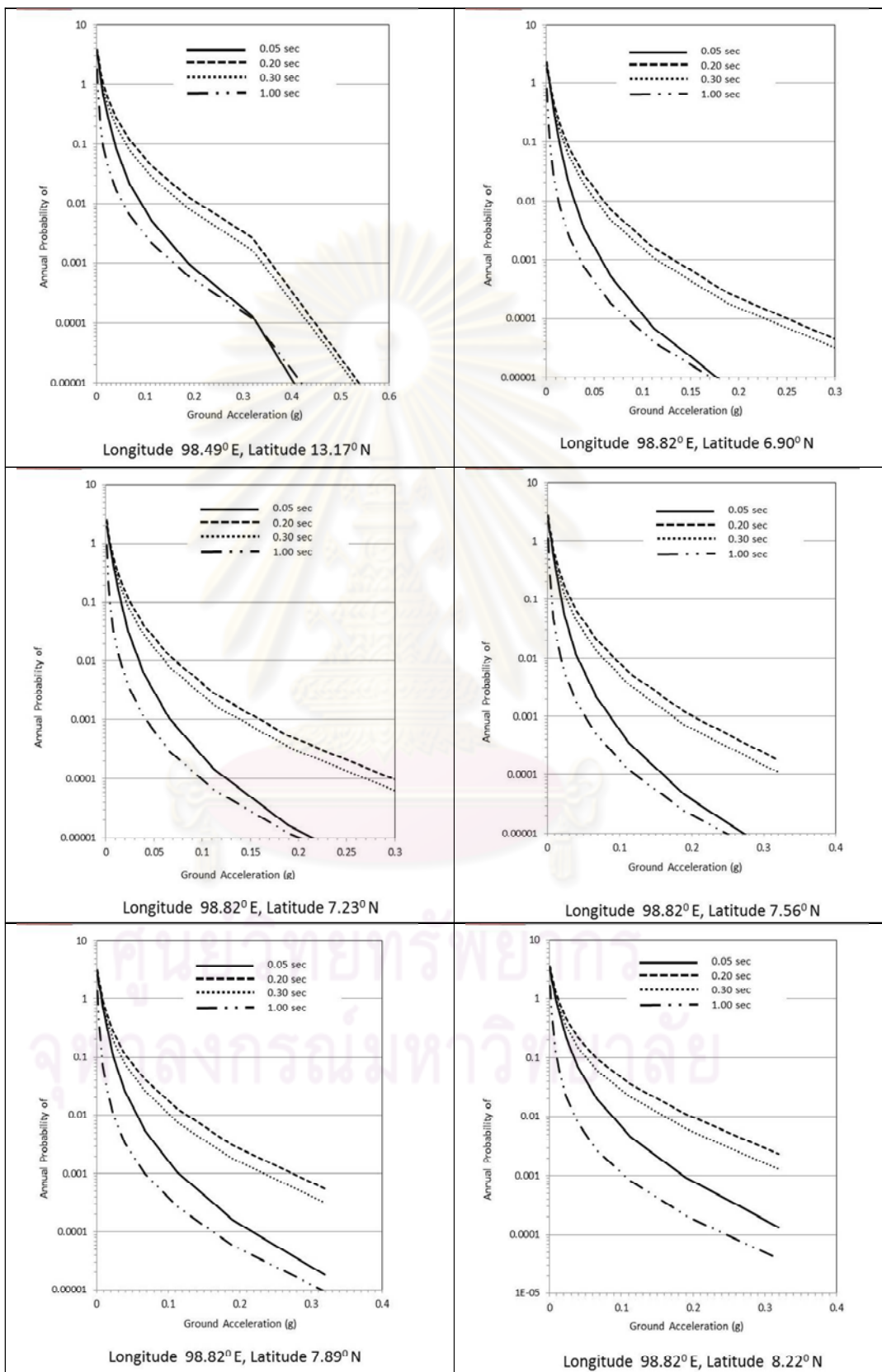


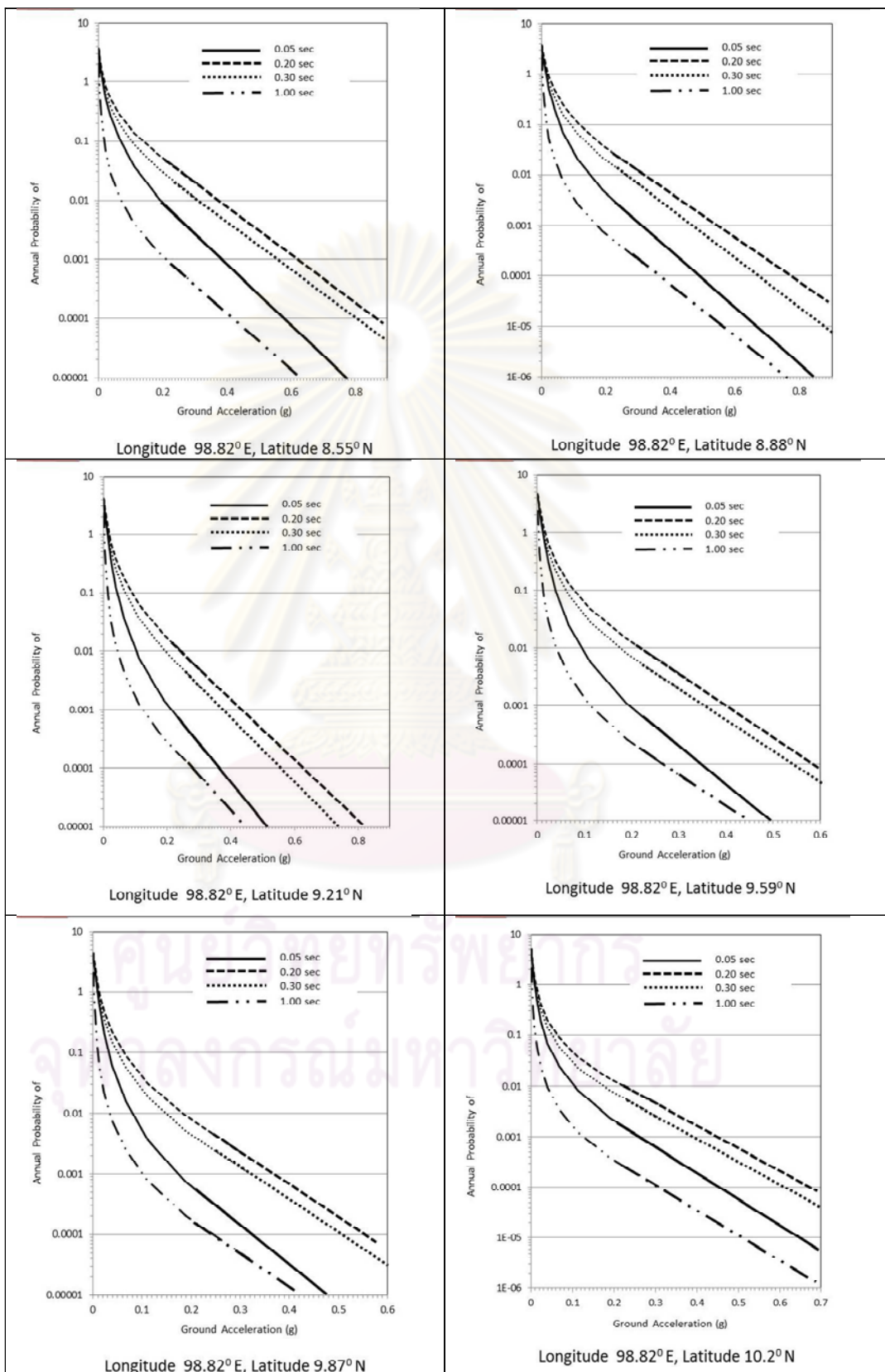


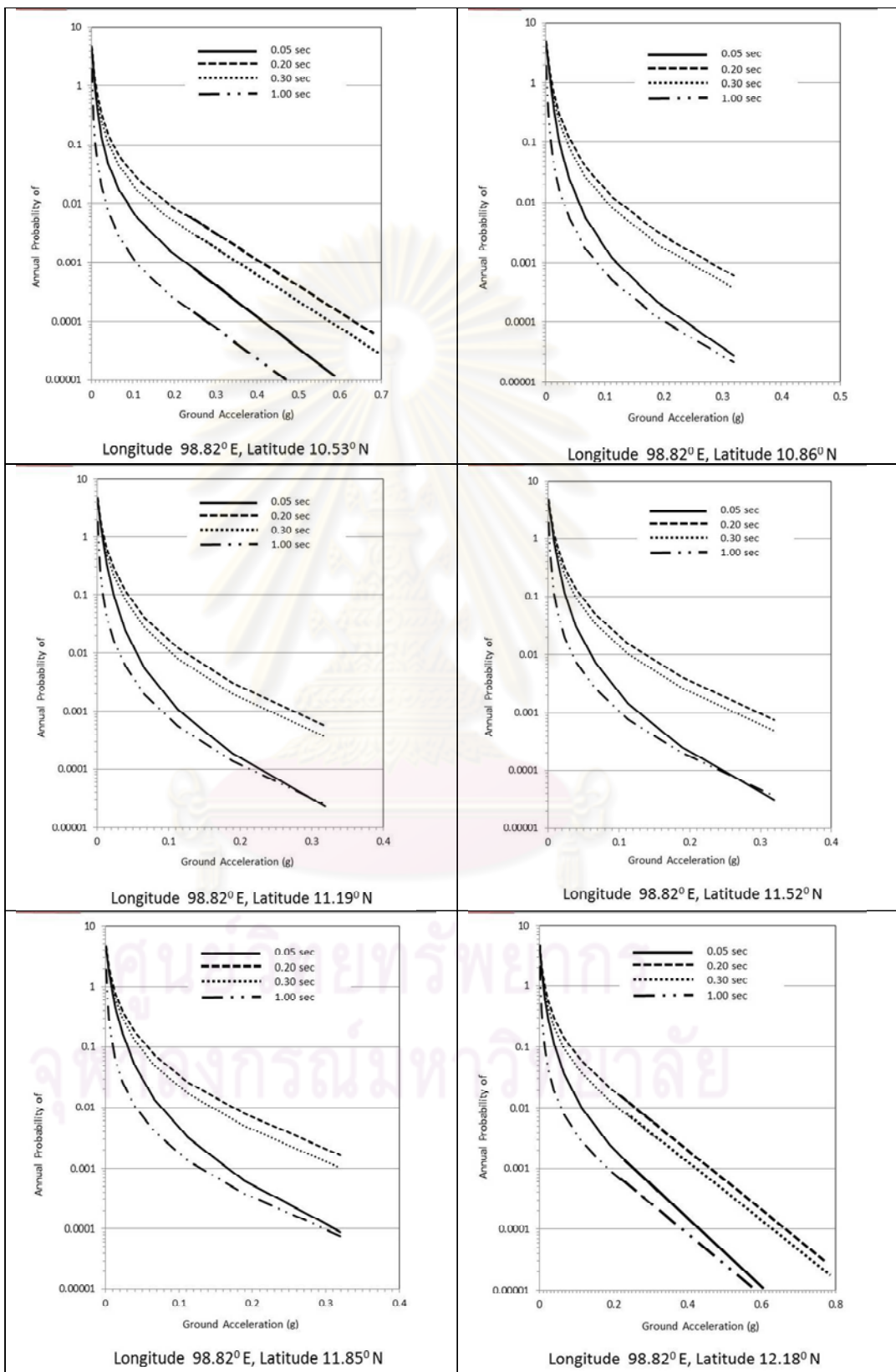


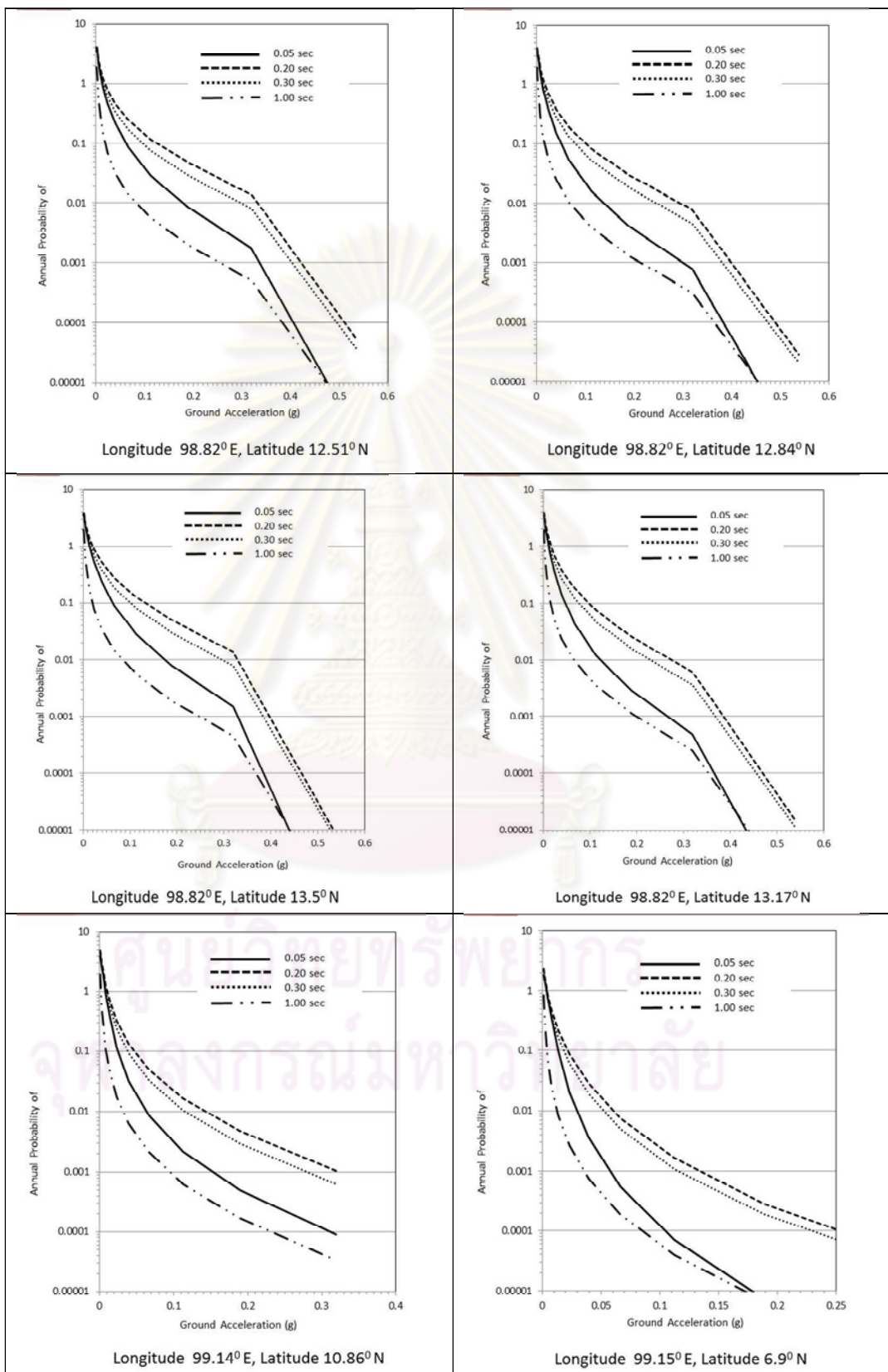


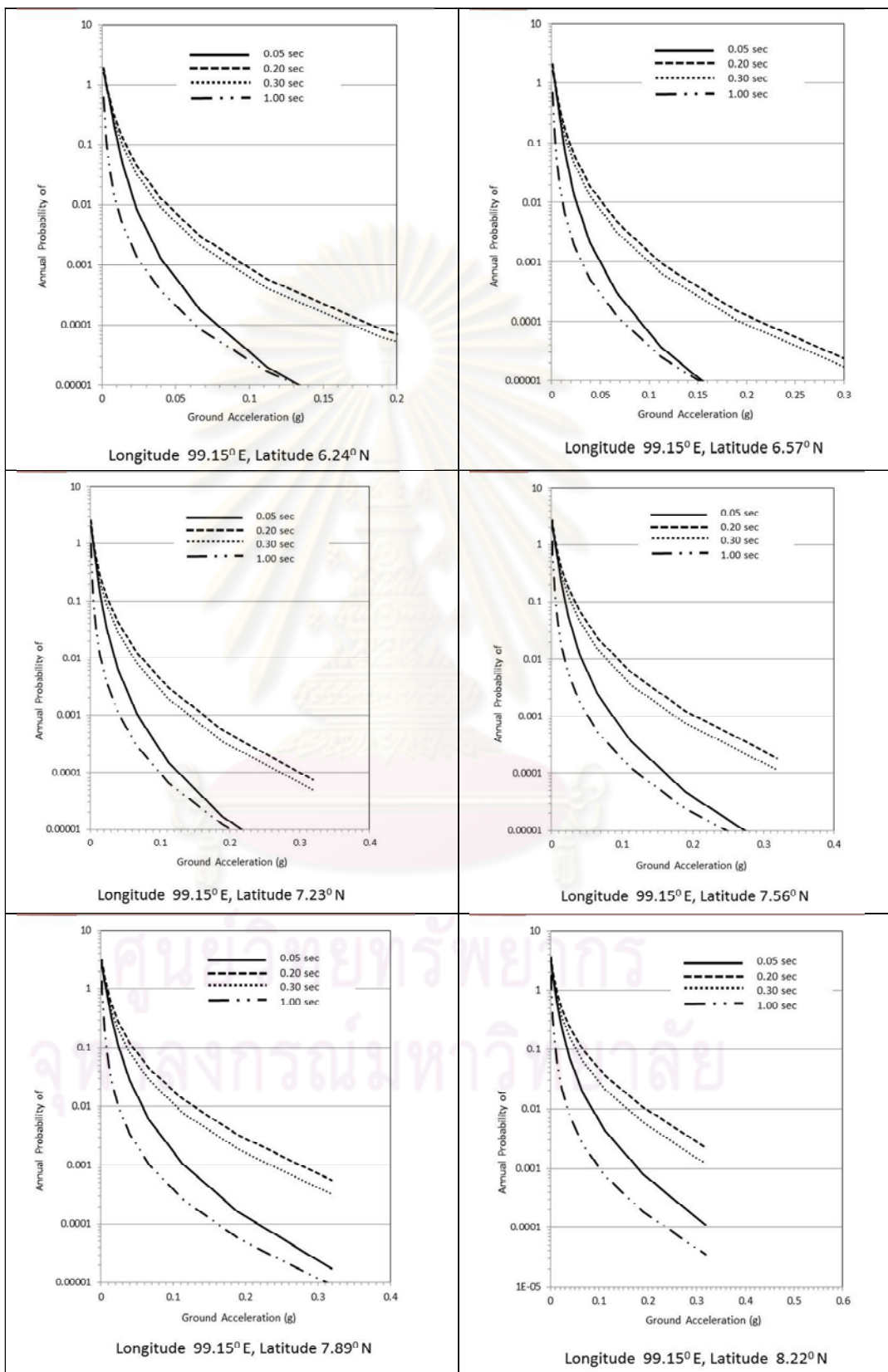


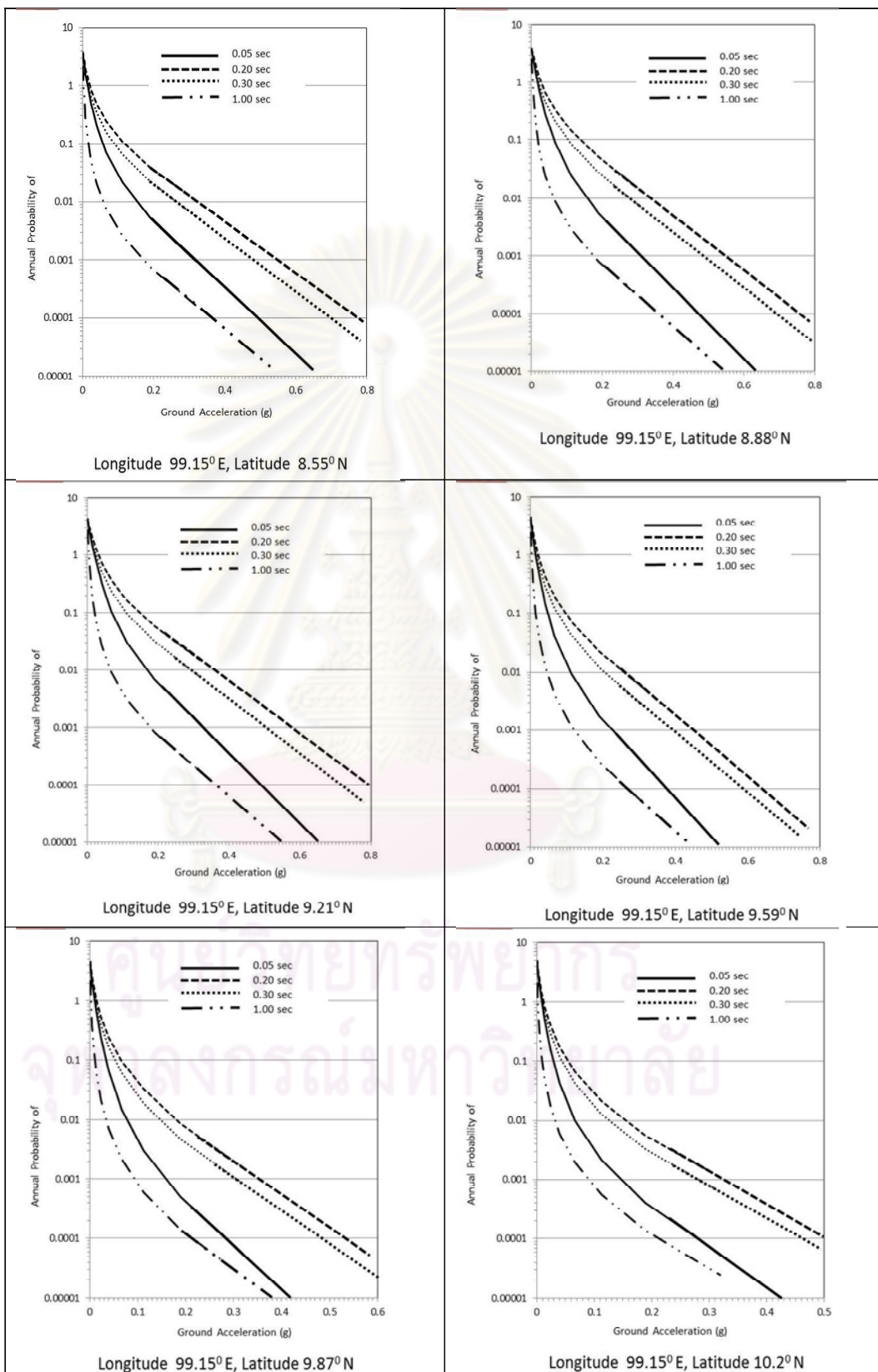


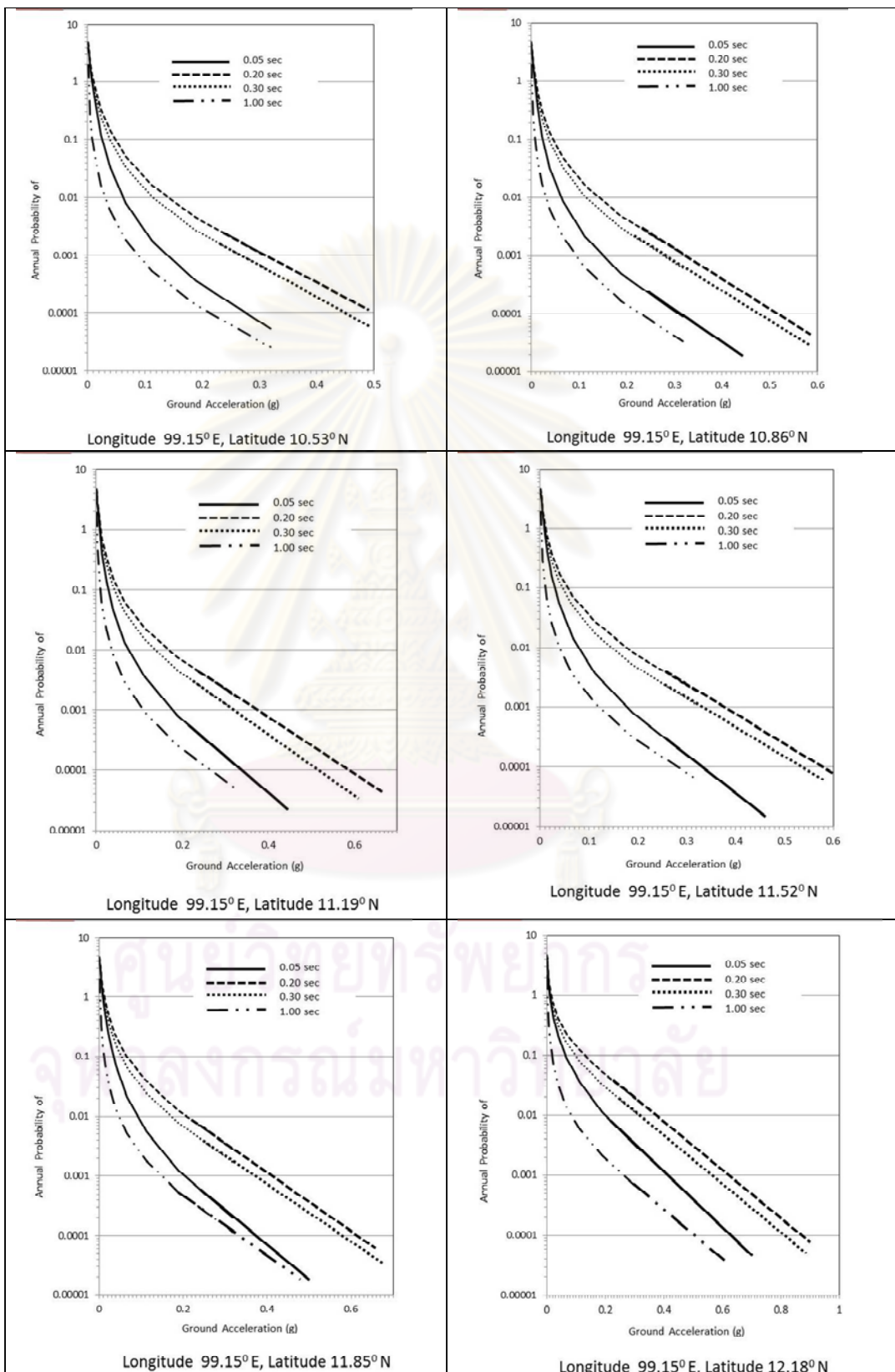


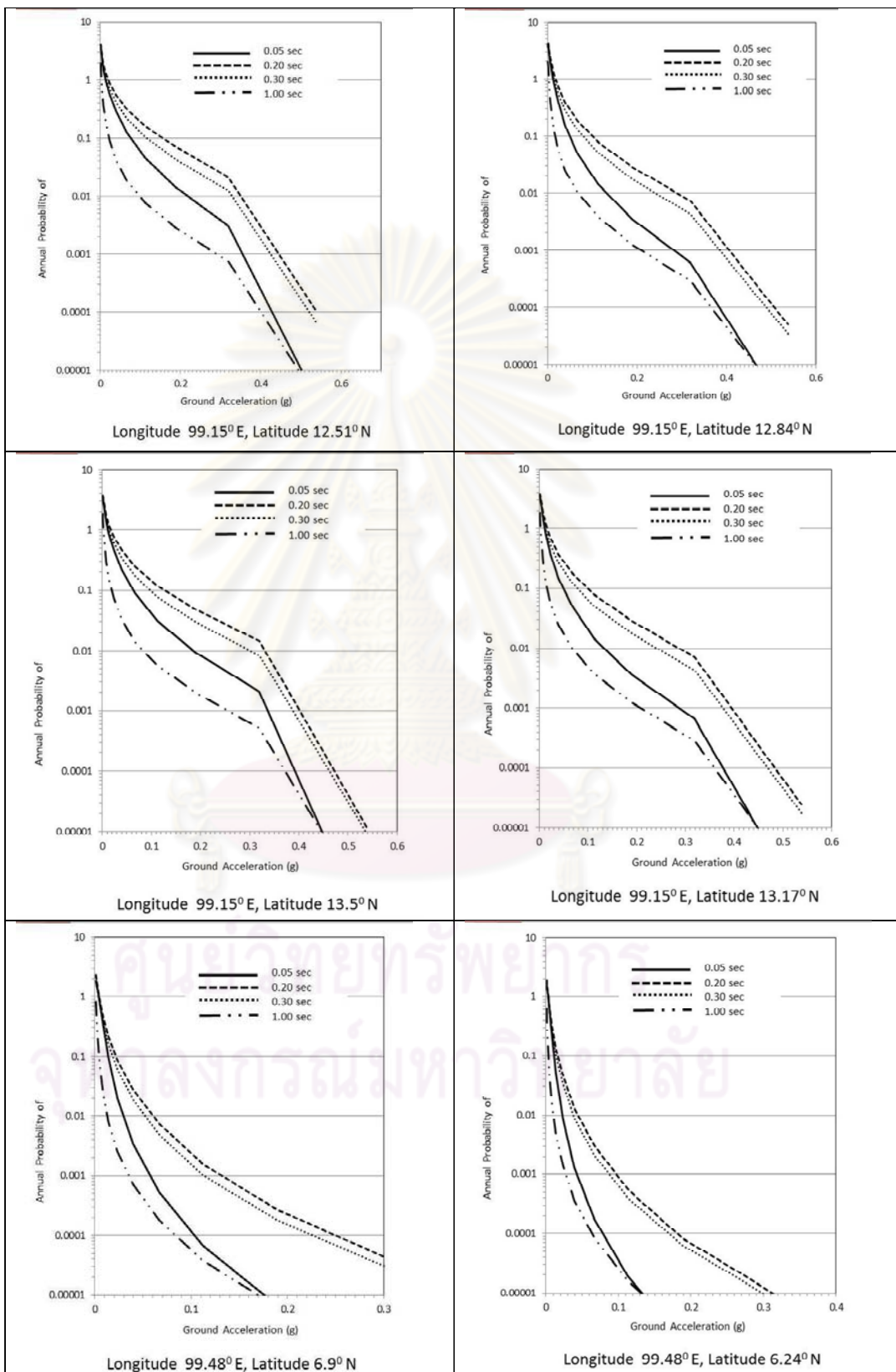


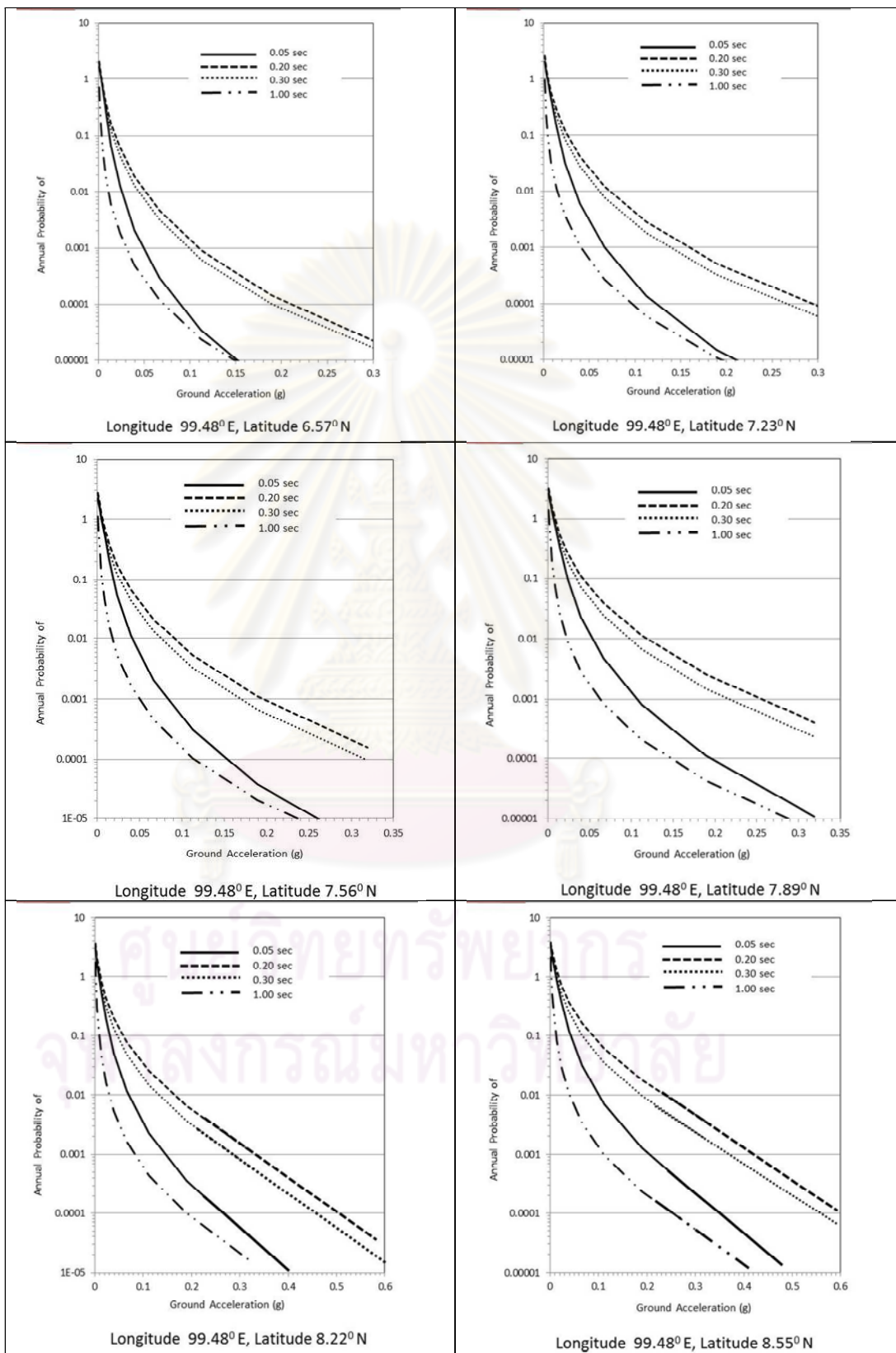


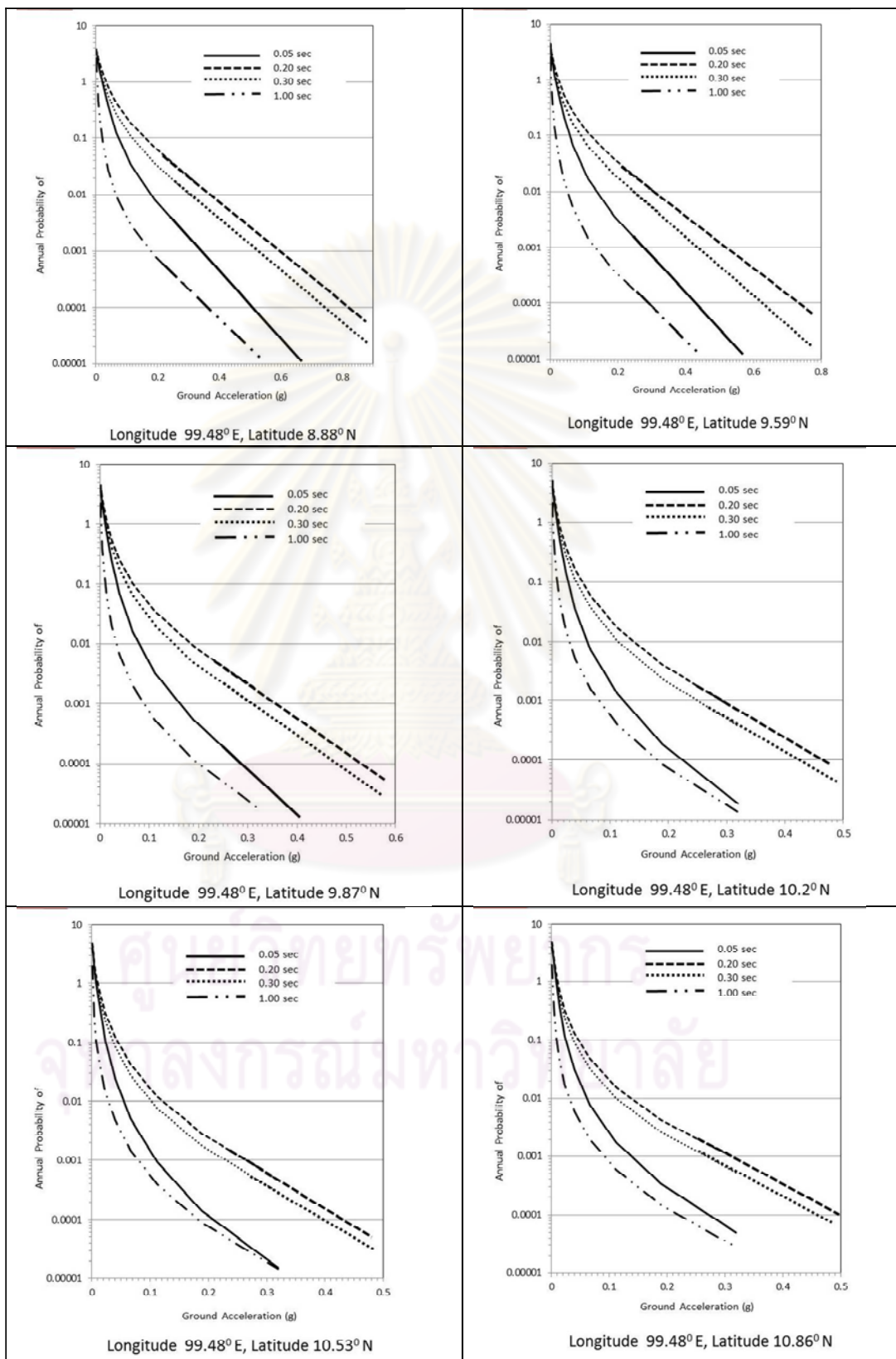


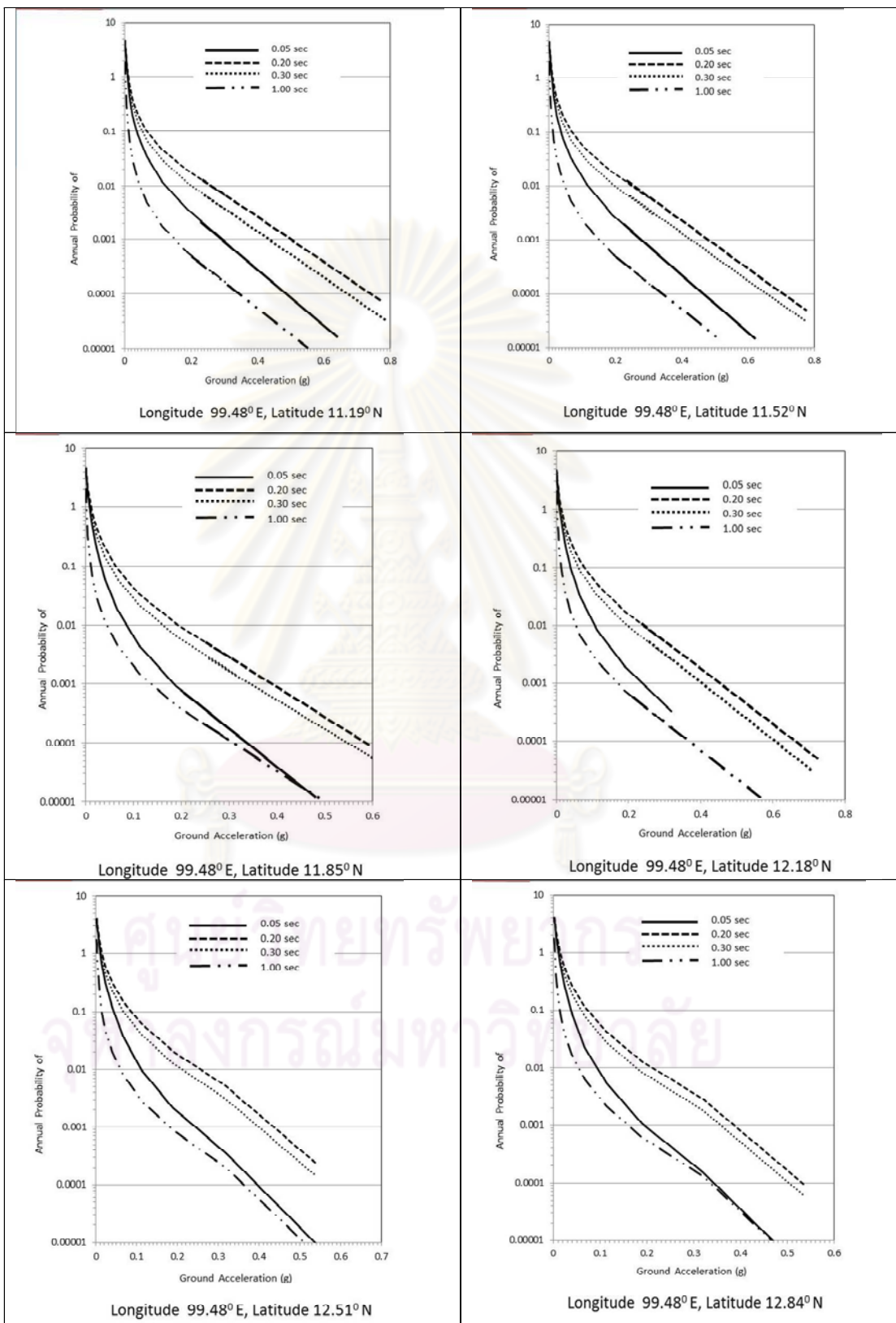


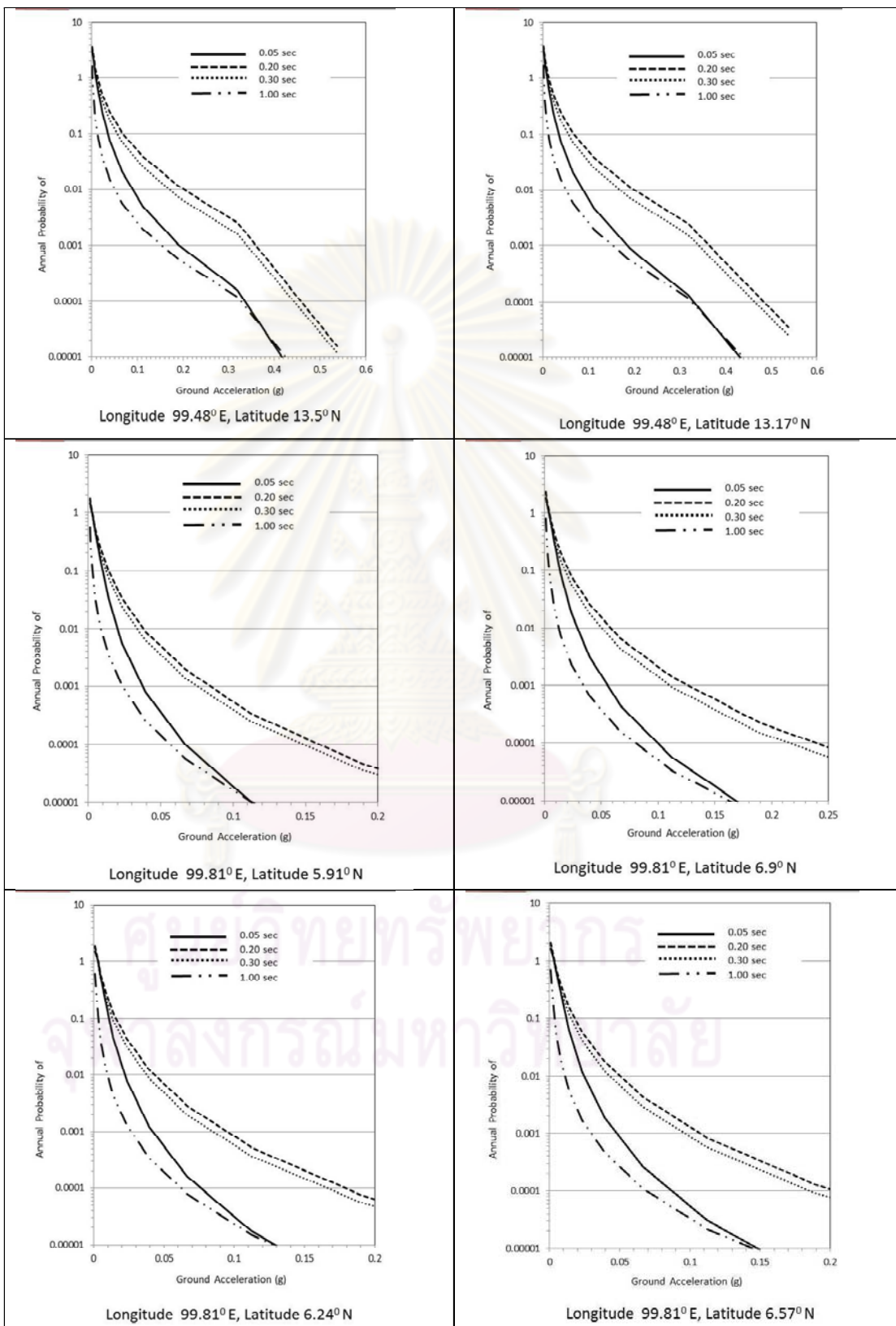


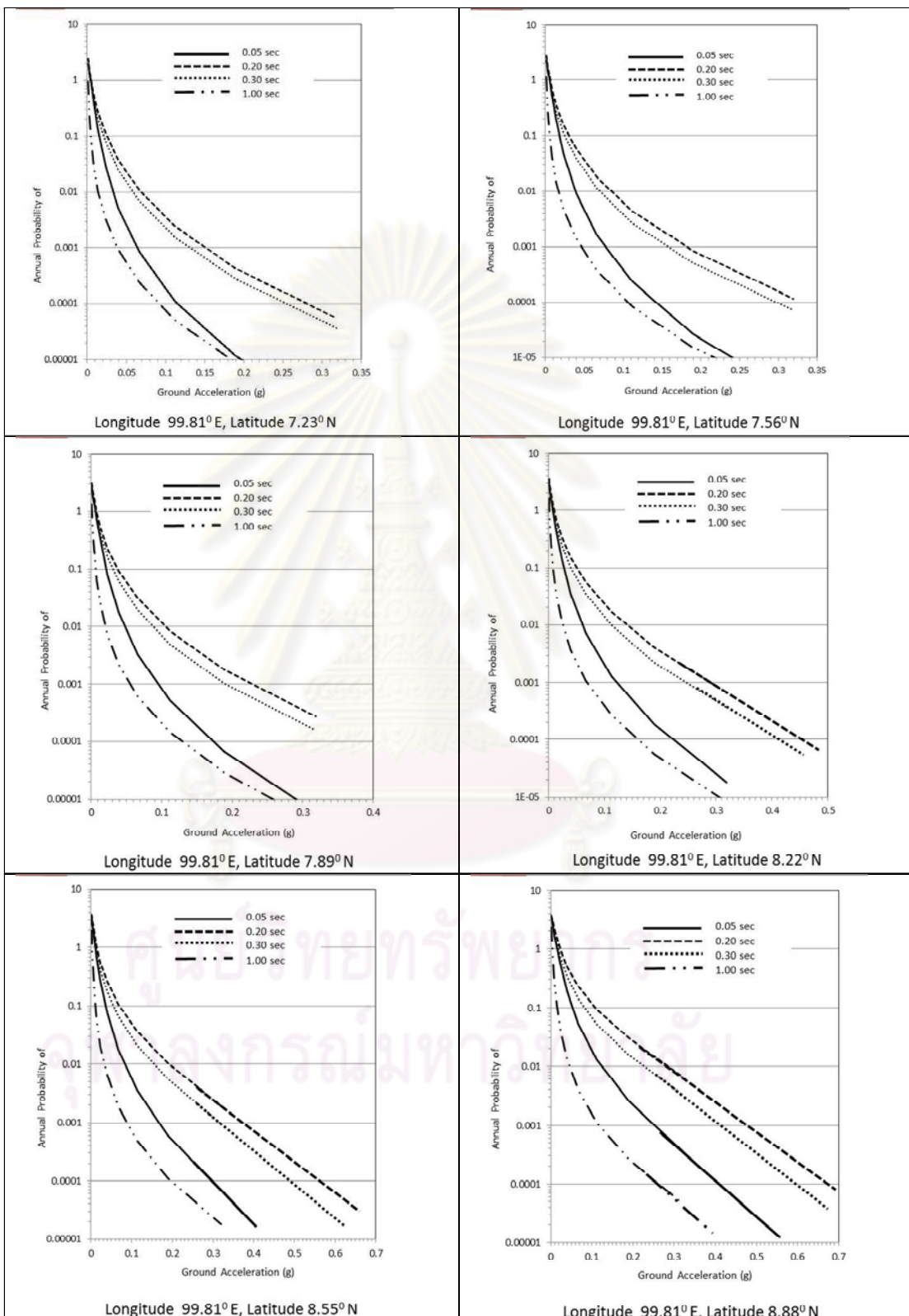


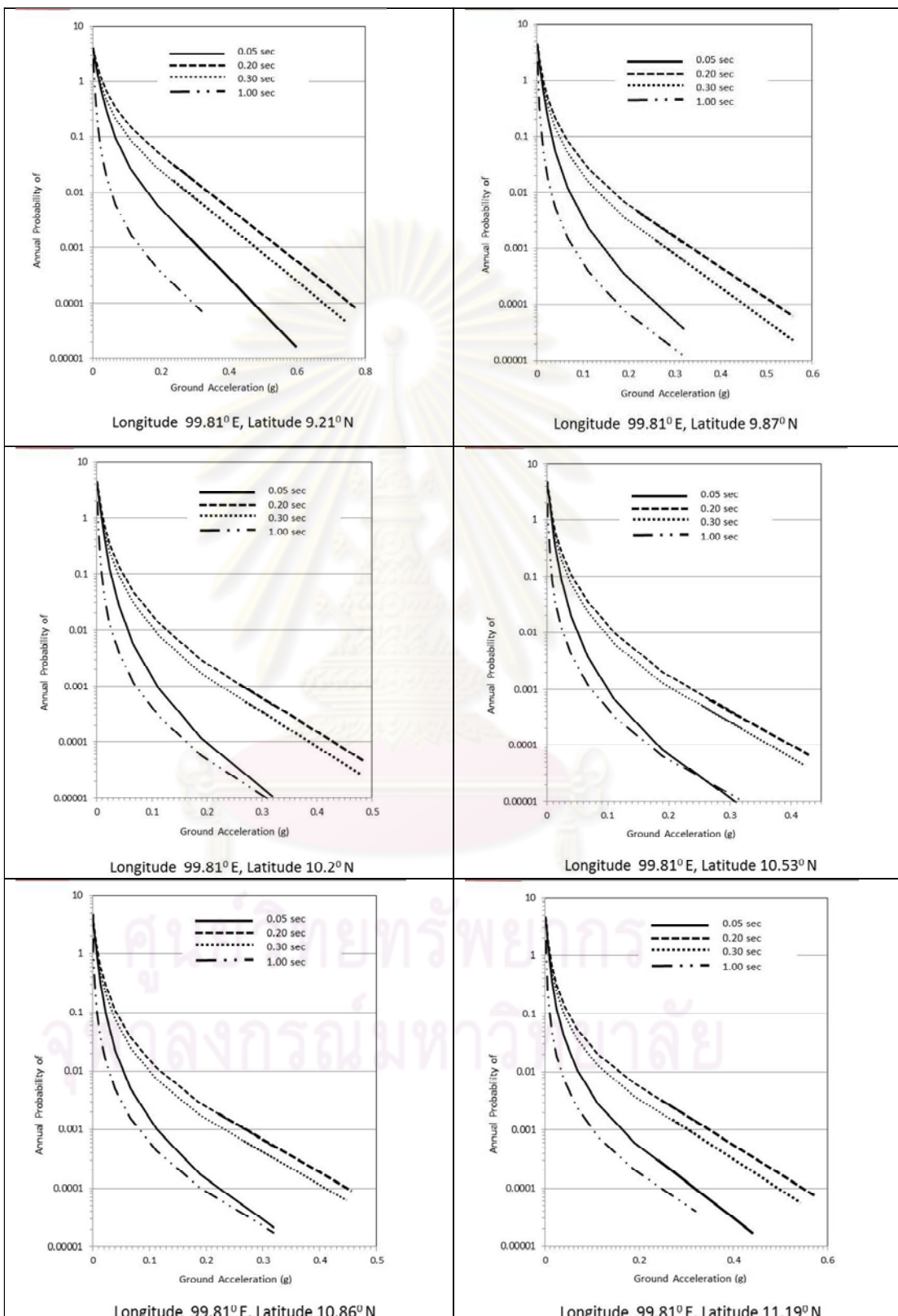


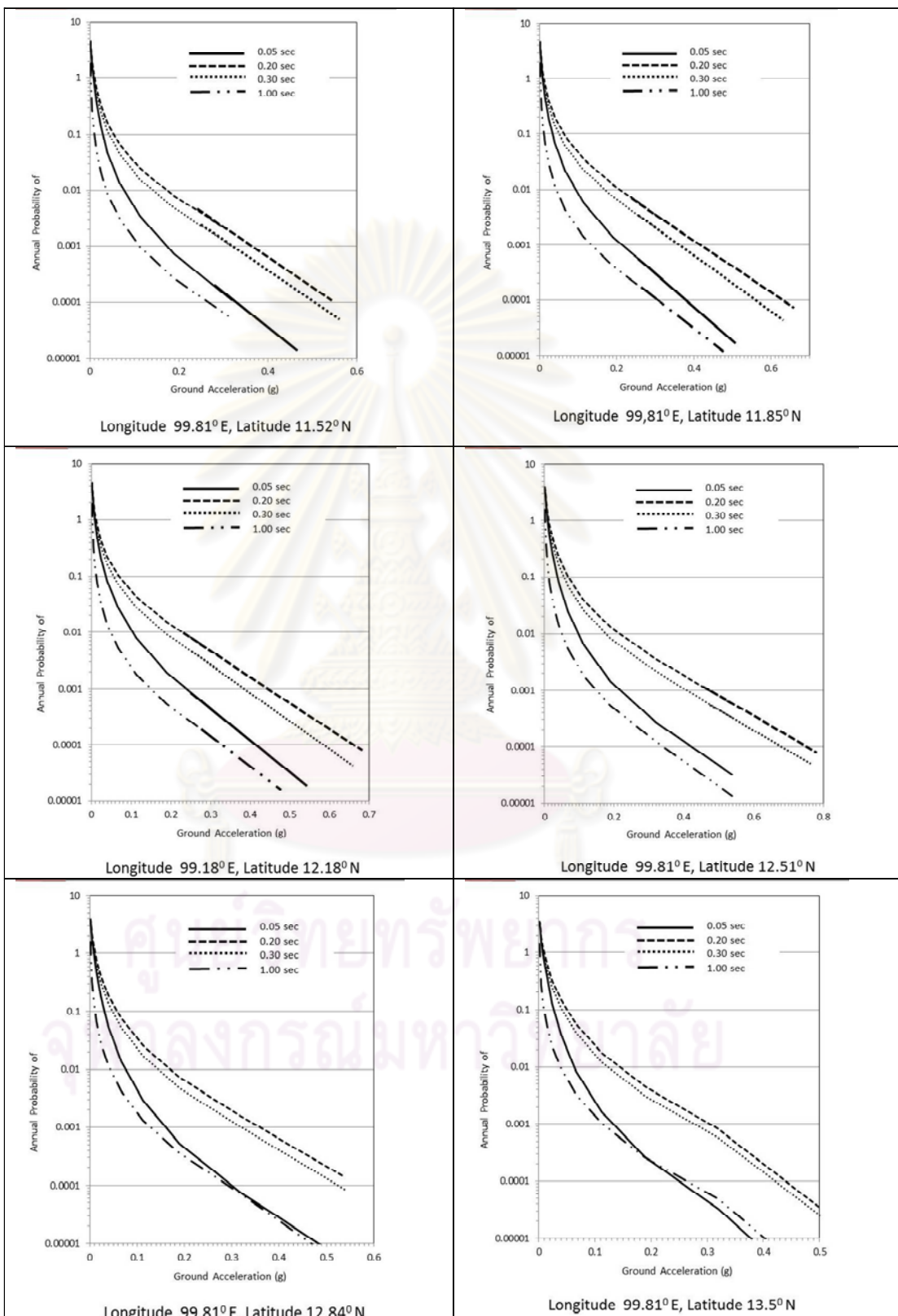


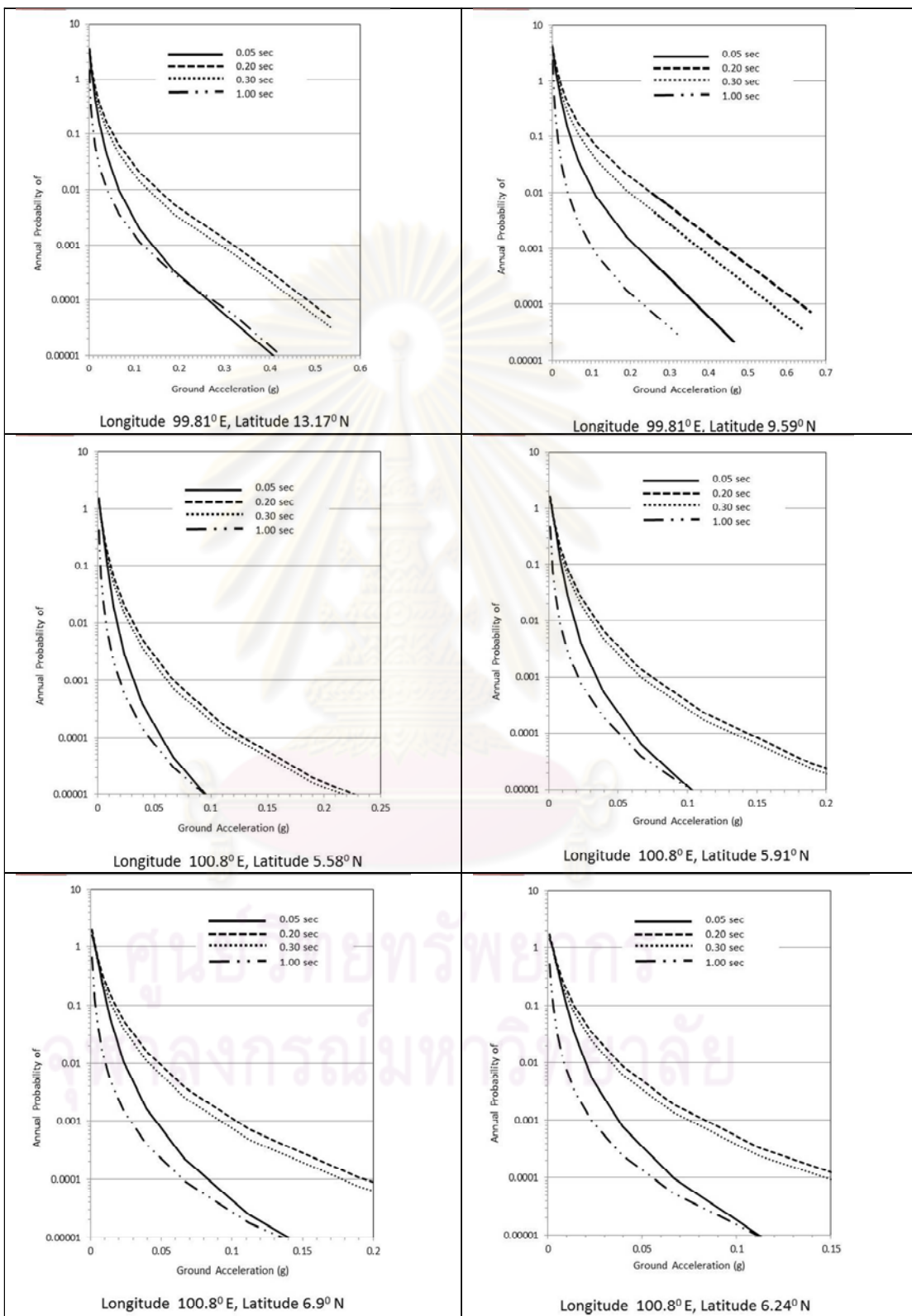


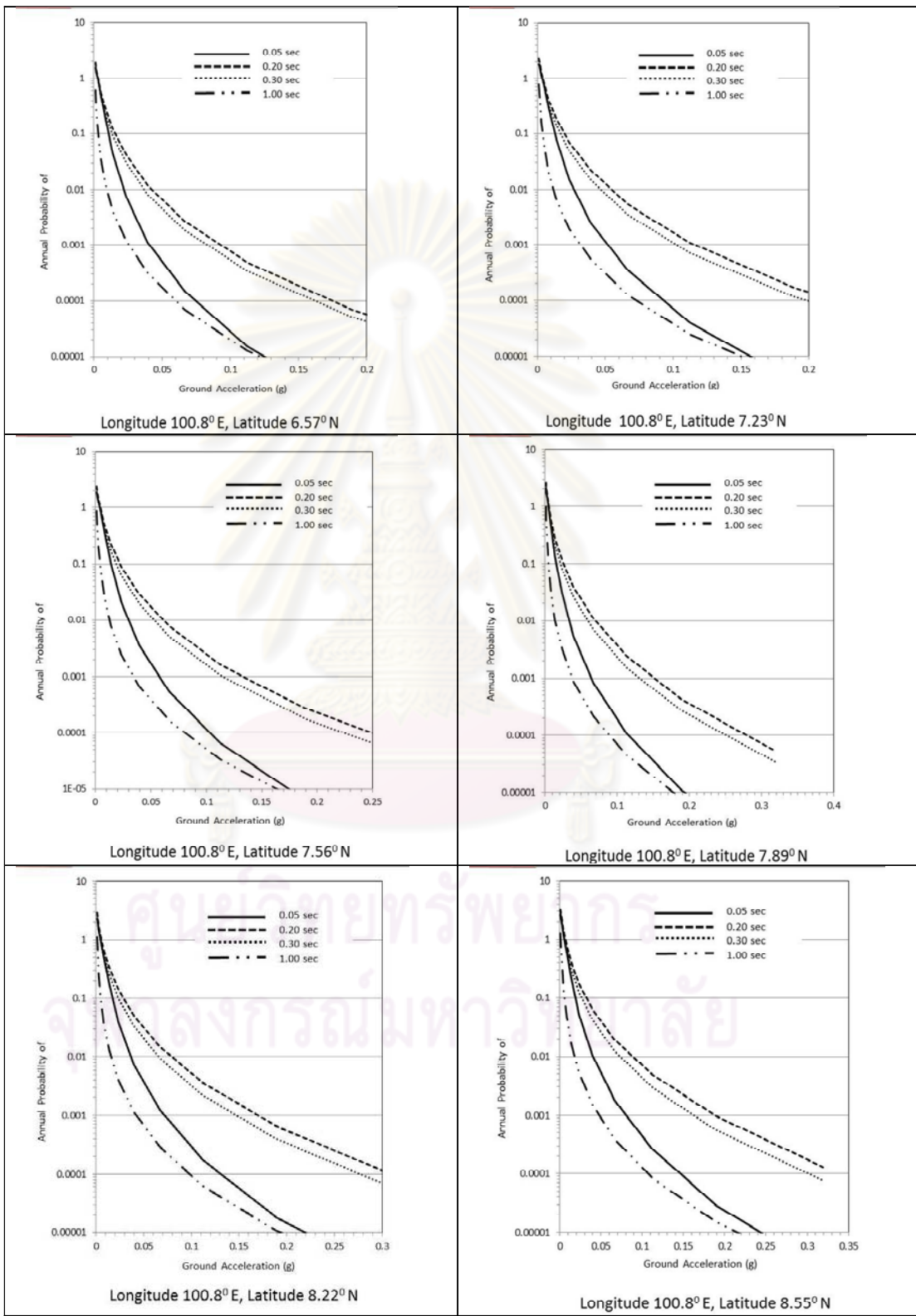


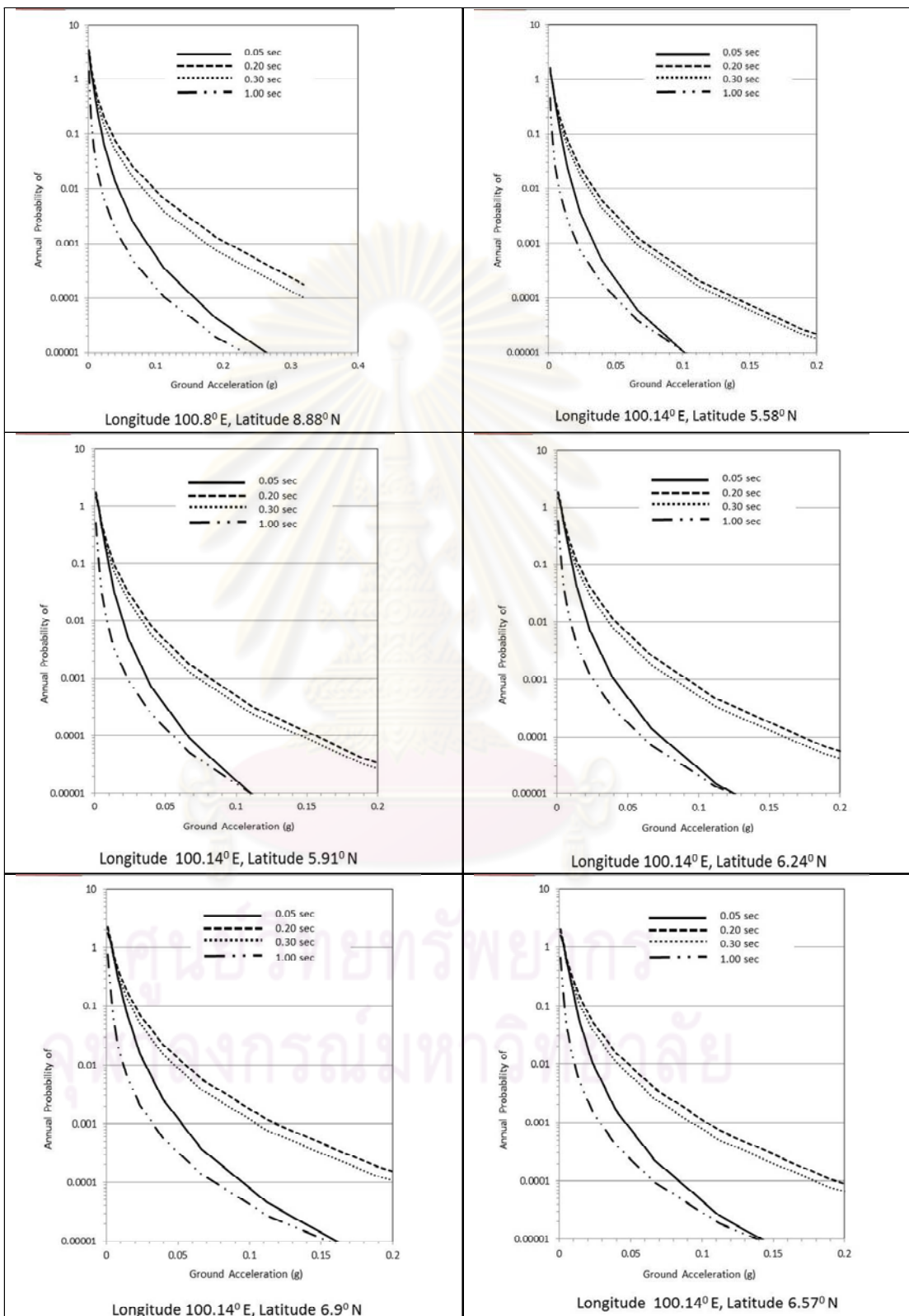


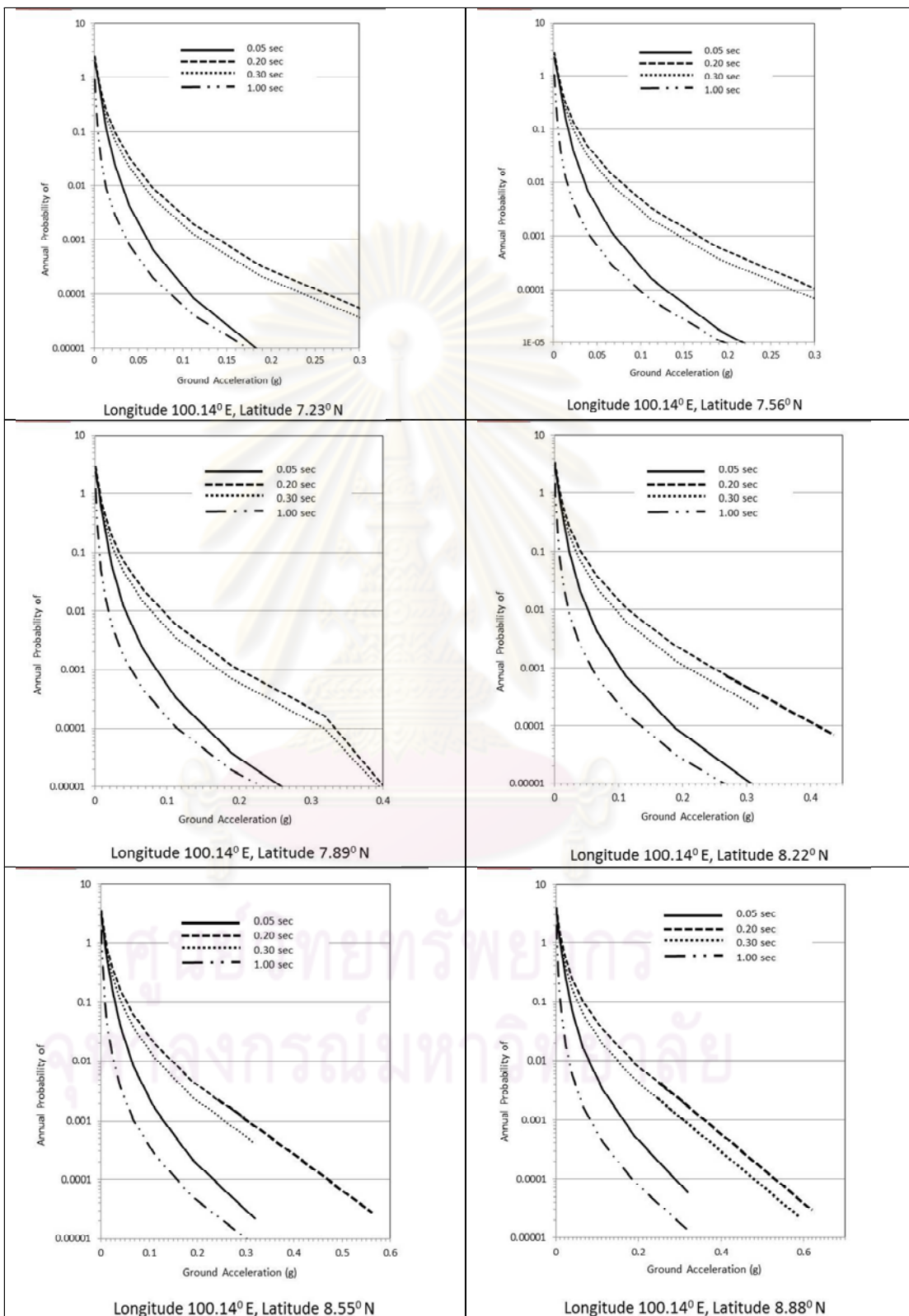


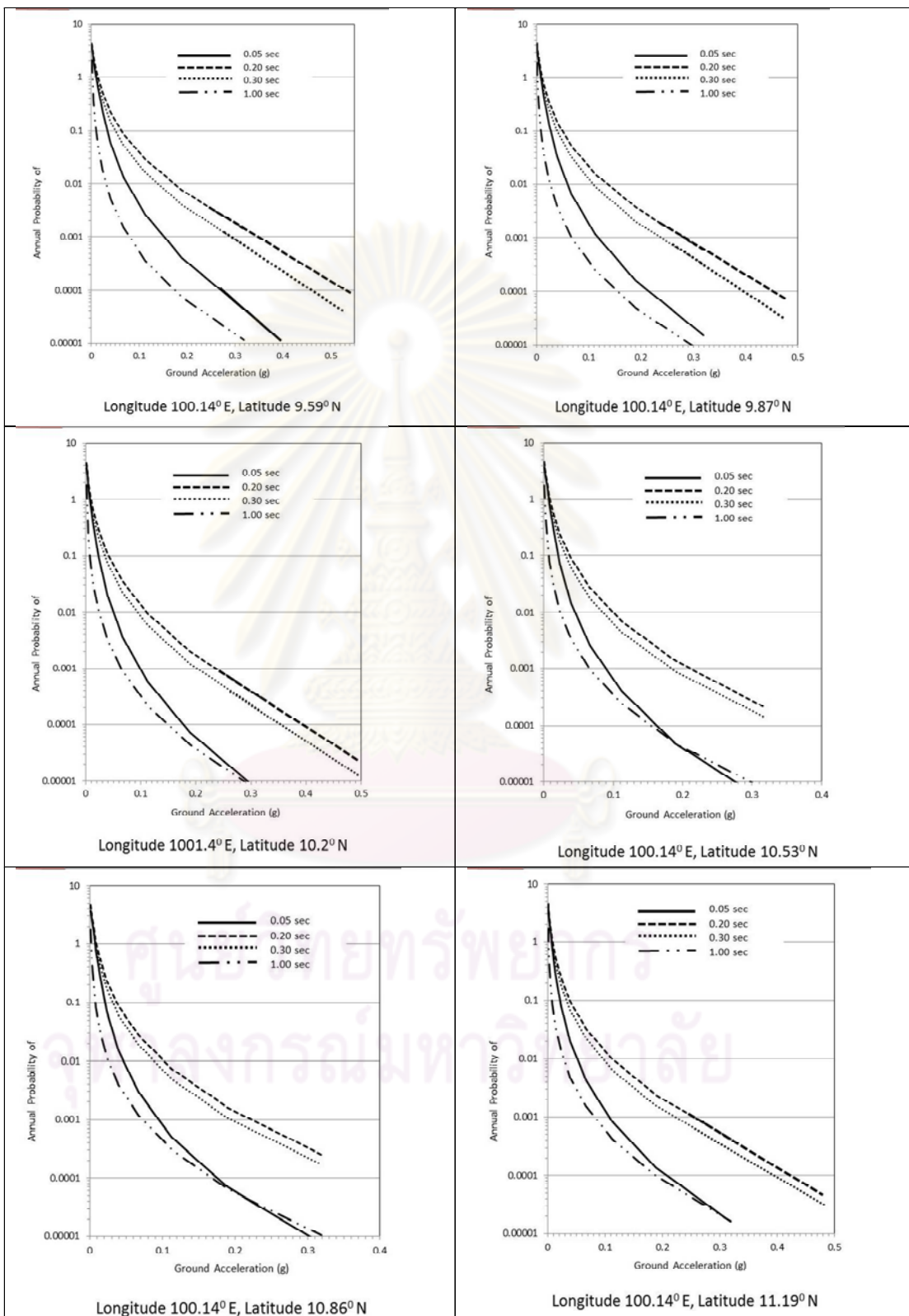


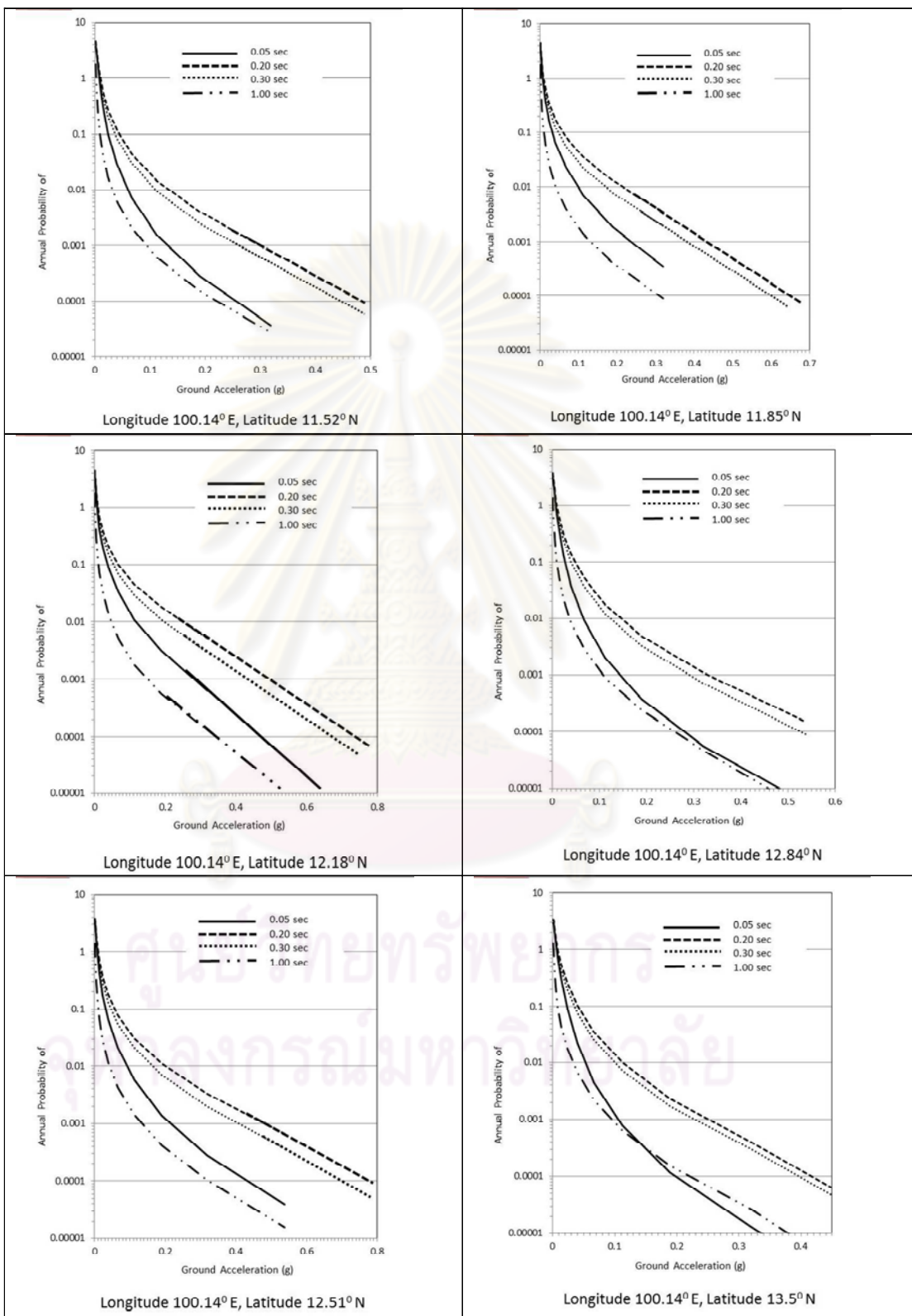


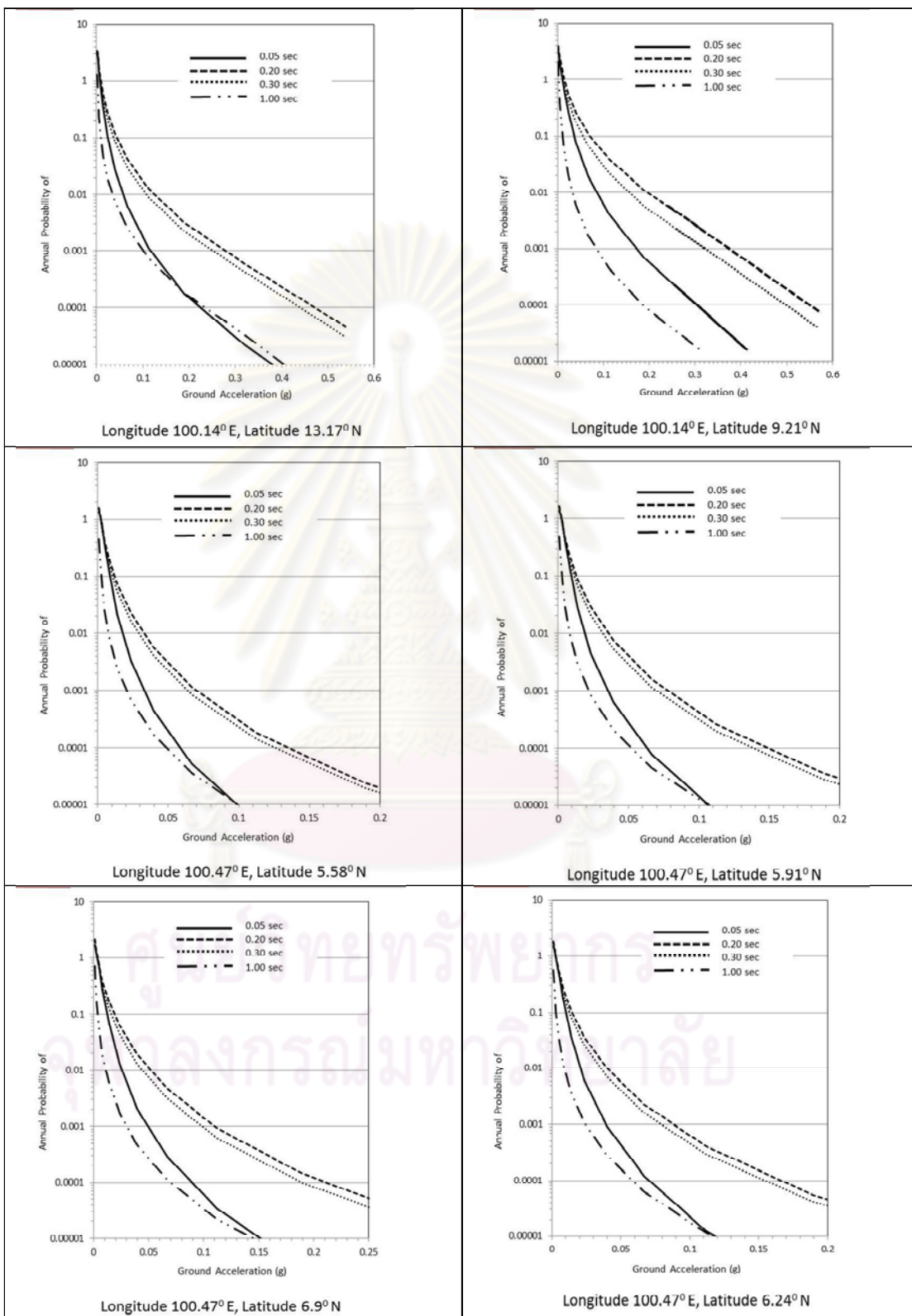


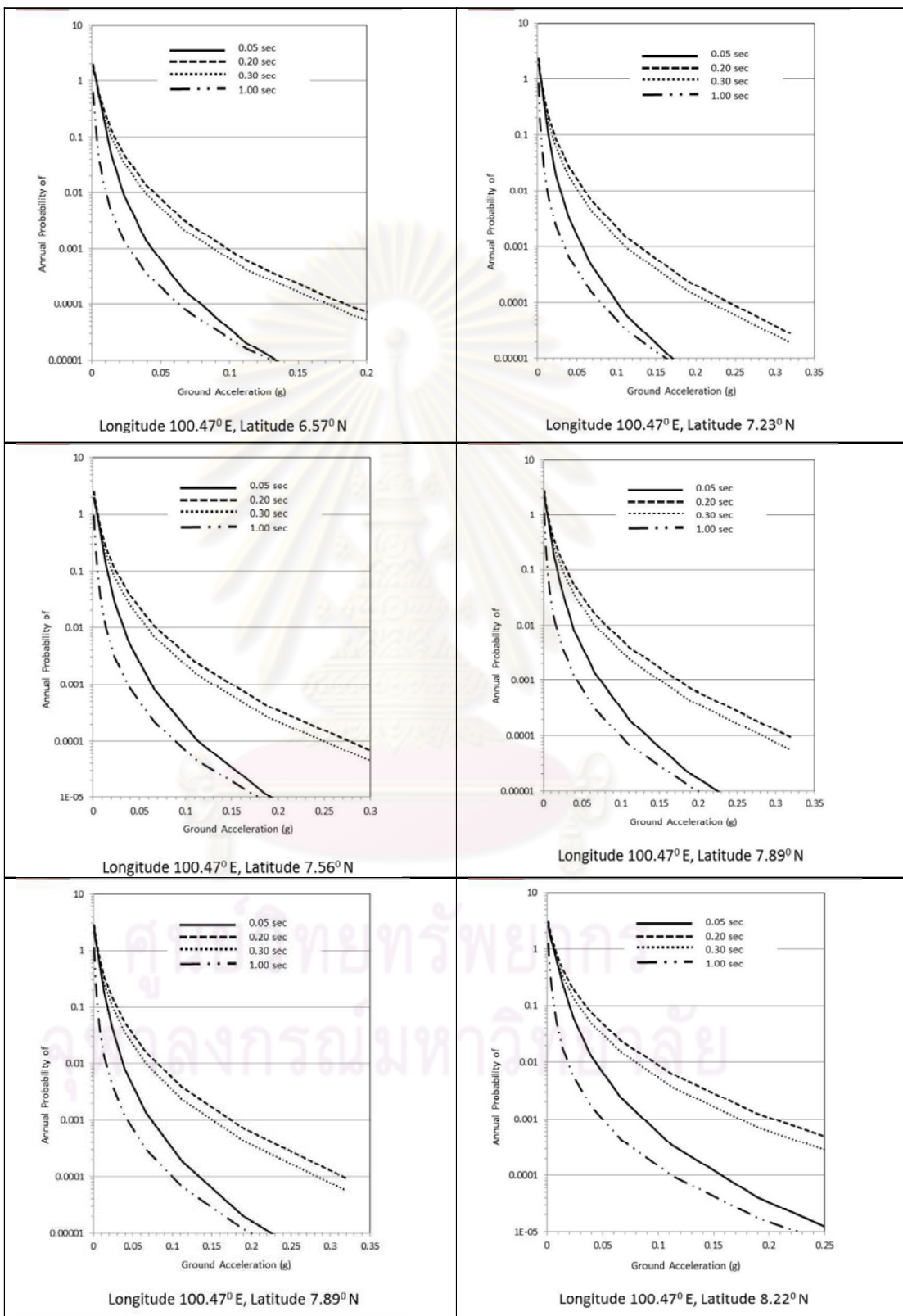


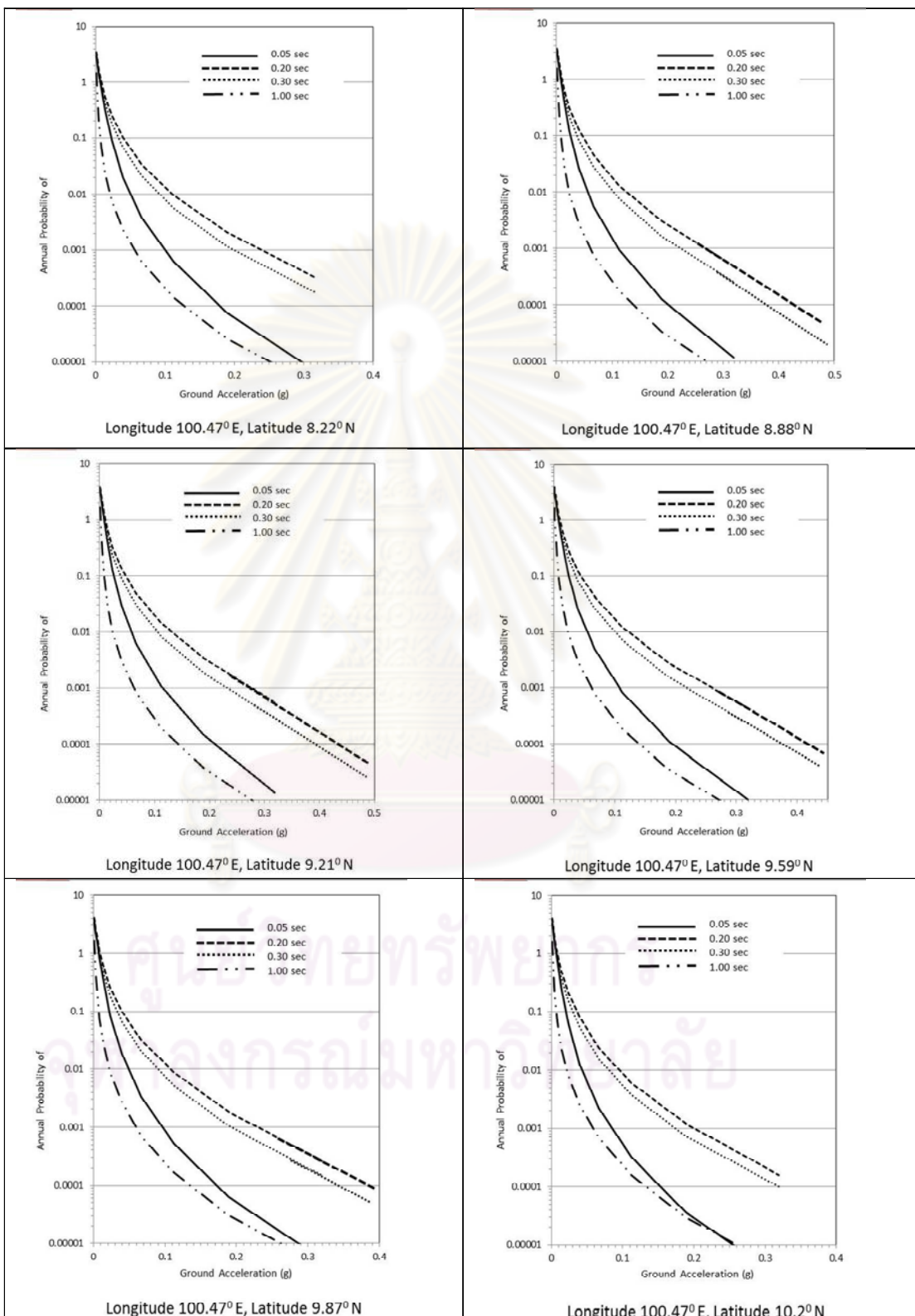


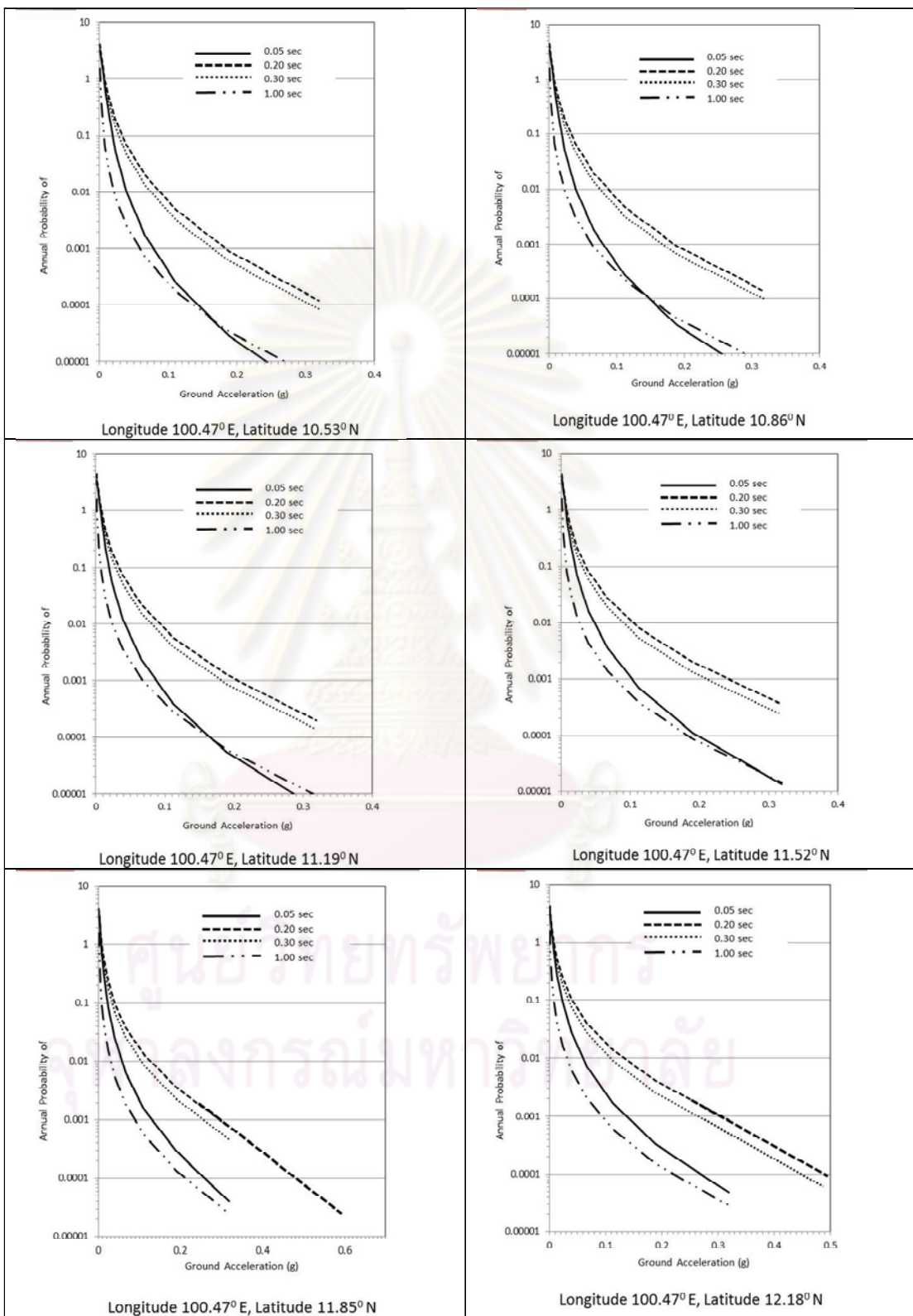












Longitude 100.47° E, Latitude 10.53° N

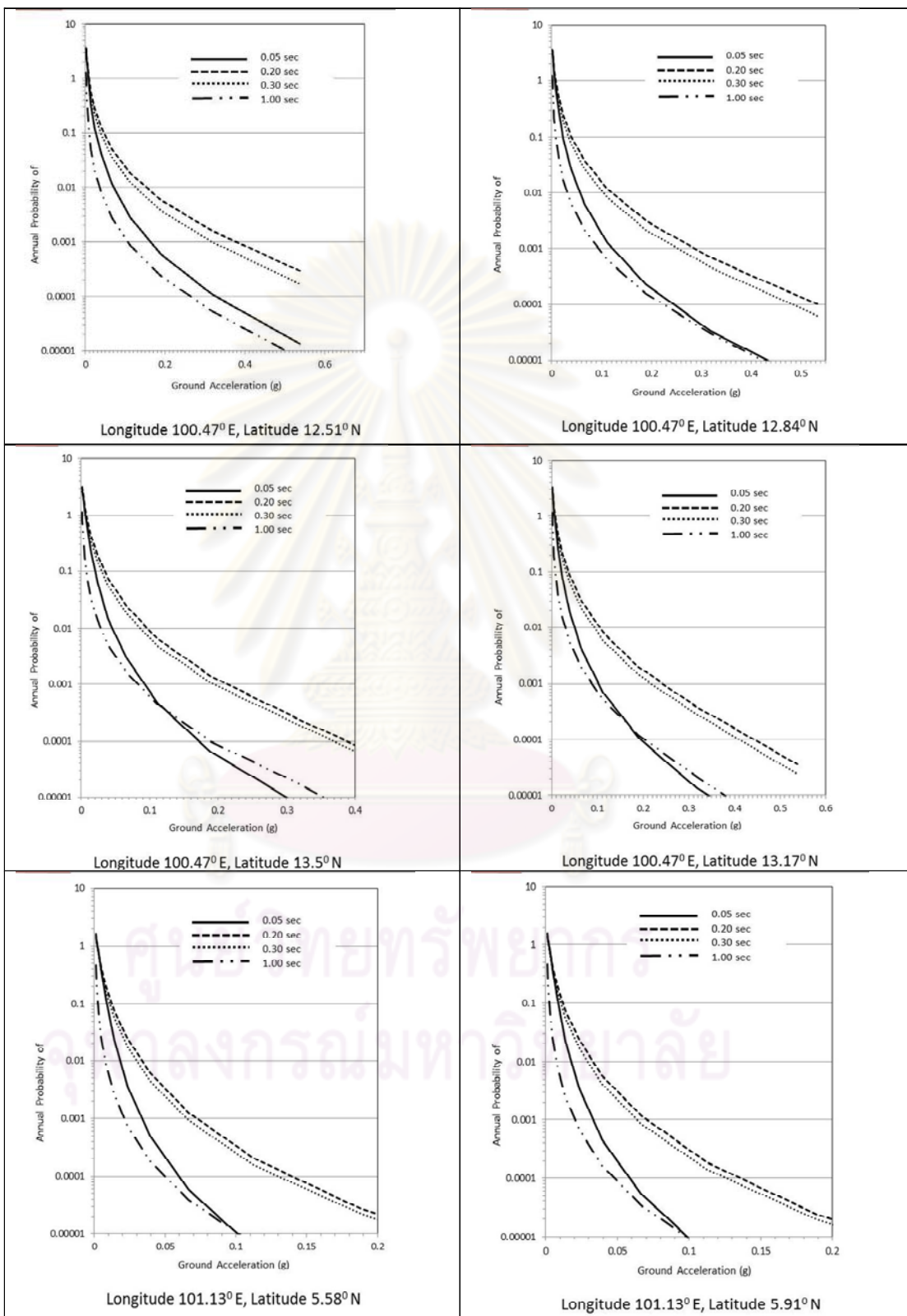
Longitude 100.47° E, Latitude 10.86° N

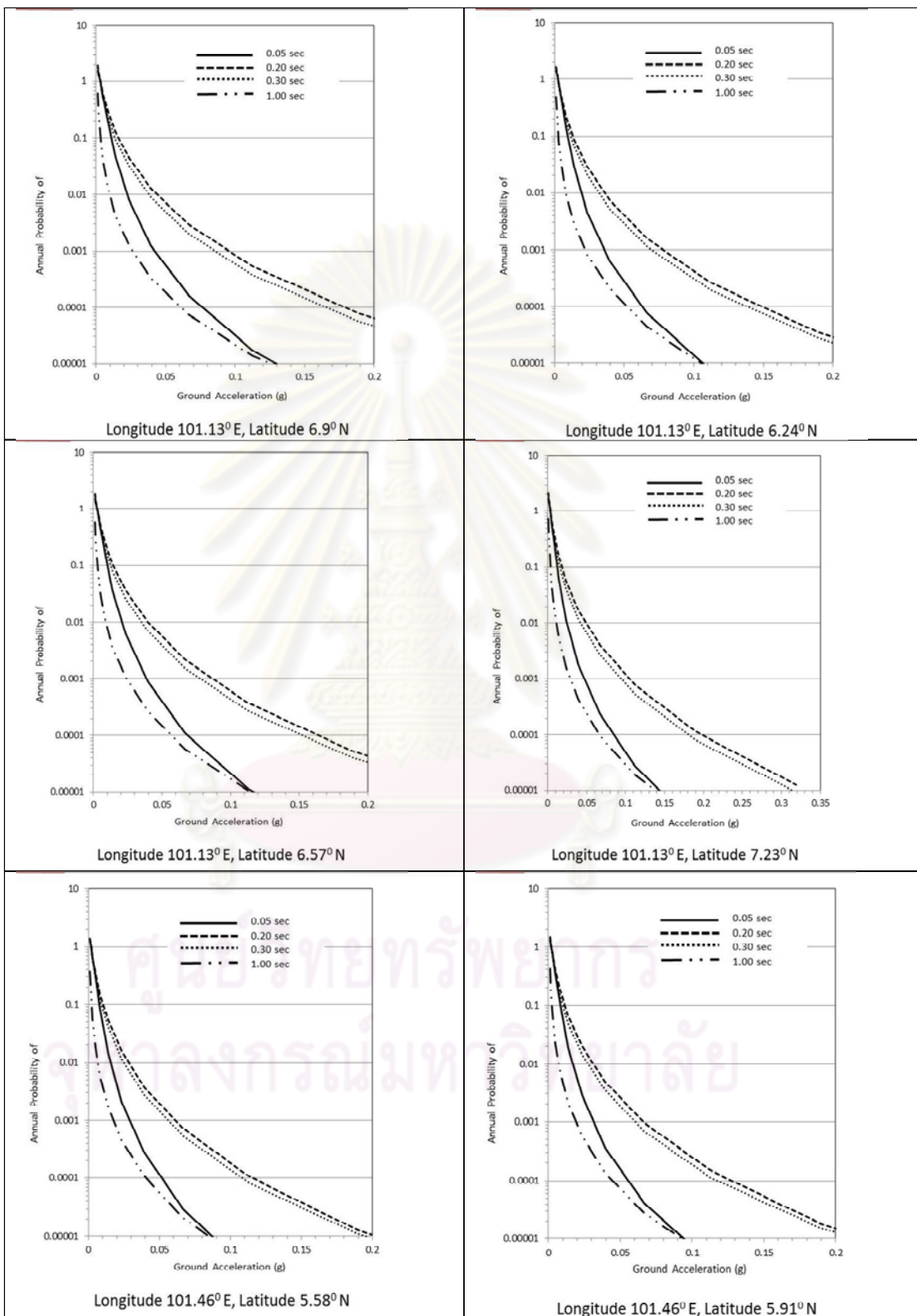
Longitude 100.47° E, Latitude 11.19° N

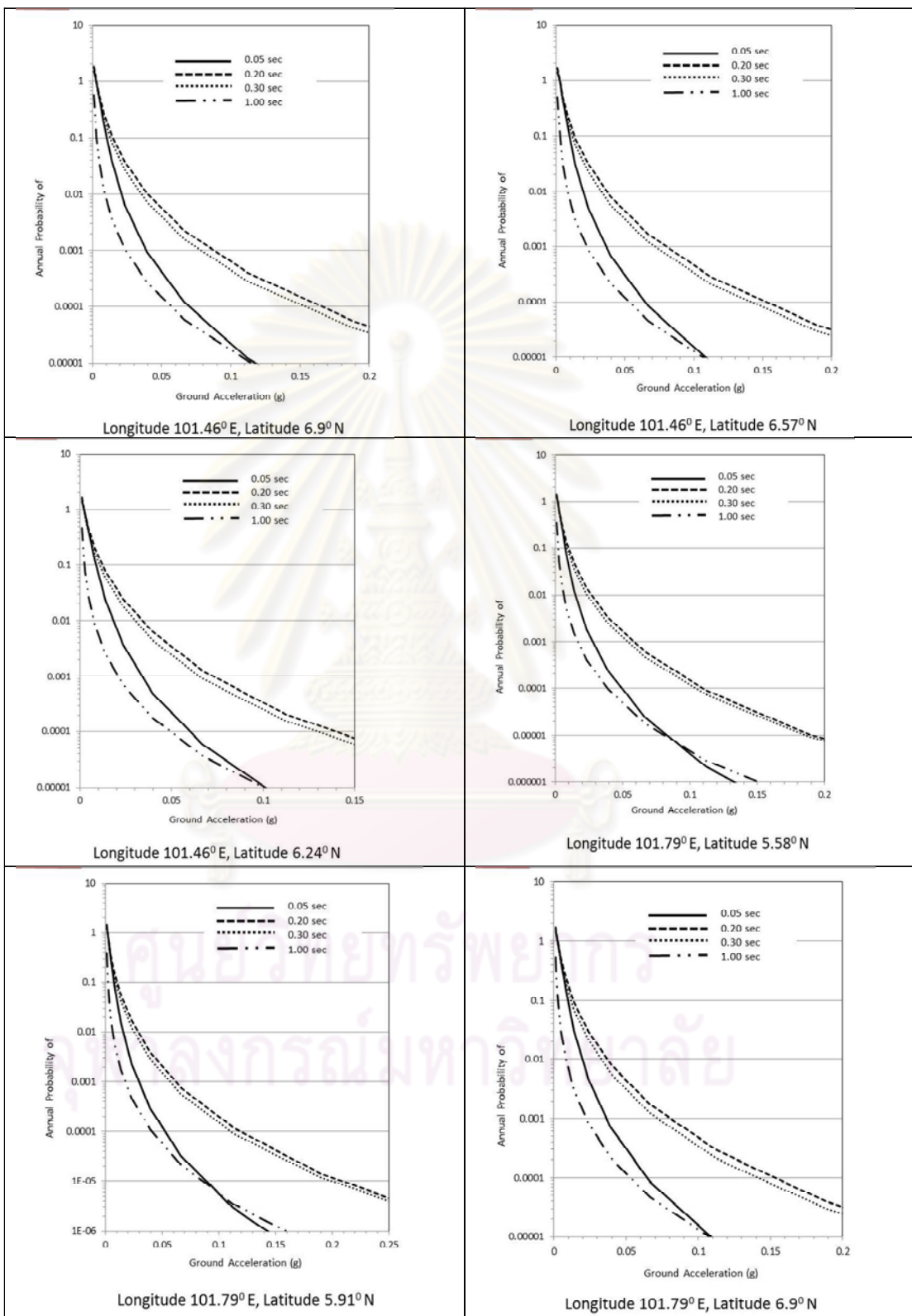
Longitude 100.47° E, Latitude 11.52° N

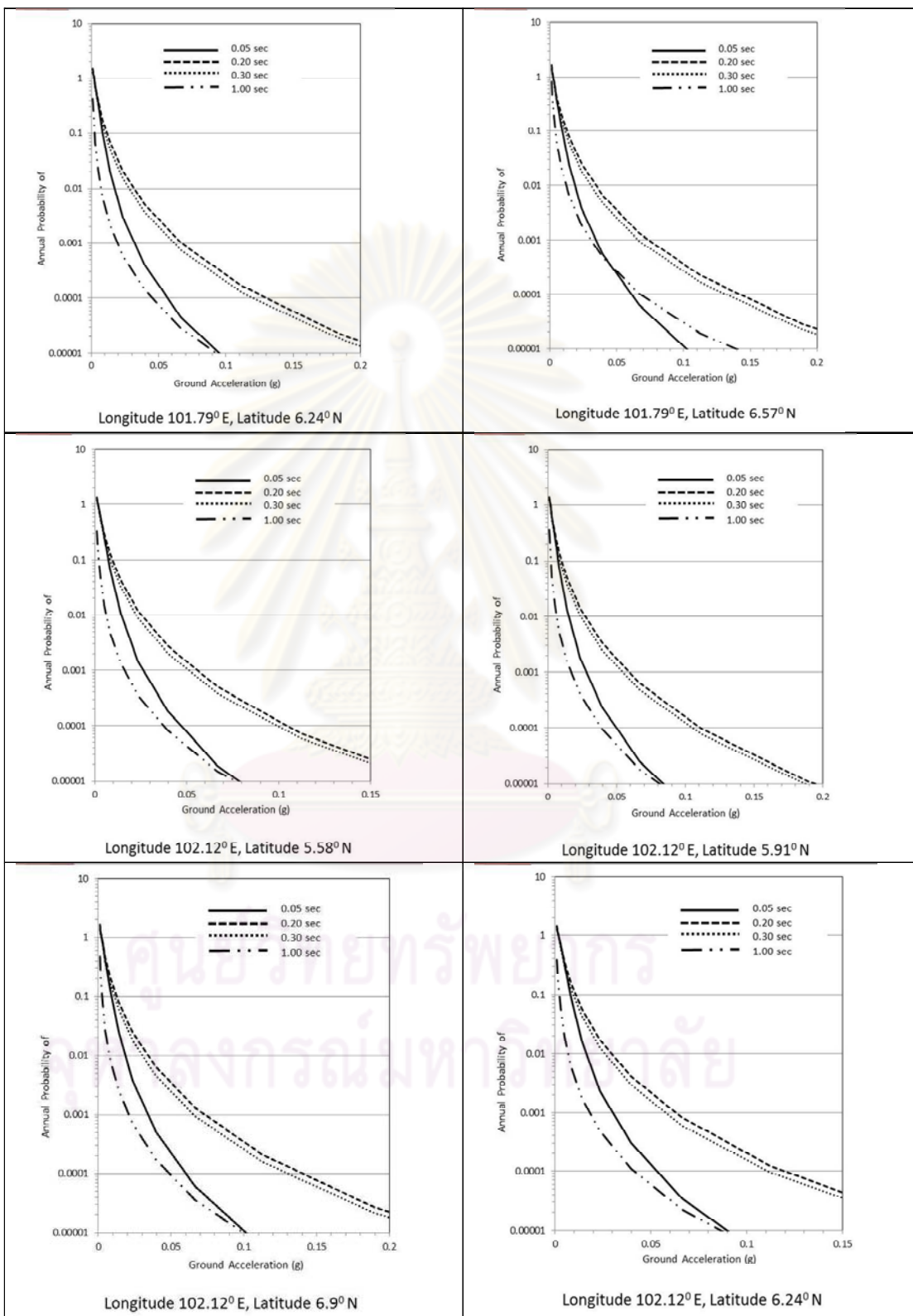
Longitude 100.47° E, Latitude 11.85° N

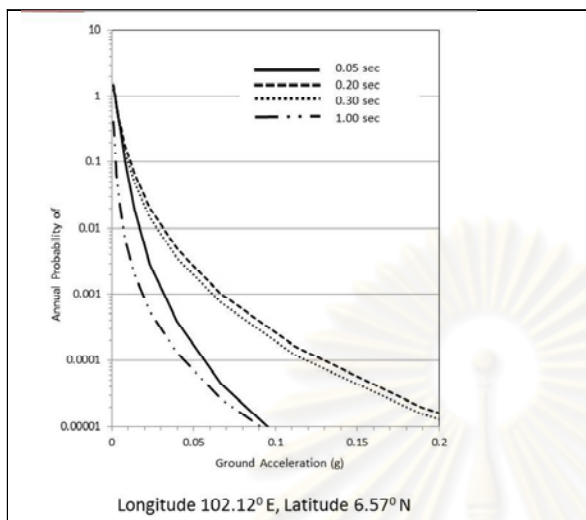
Longitude 100.47° E, Latitude 12.18° N











ศูนย์วิทยทรัพยากร
จุฬาลงกรณ์มหาวิทยาลัย

BIOGRAPHY

Mr. Chinda Sutiwanich was born in Muang district, Uthaithani province in 1959. He studied in a local primary and secondary schools in Uthaithani province for 12 years during 1966 to 1977. He graduated with the bachelor degree of Science (B.SC.) in the field of geology from Chiang Mai University in 1981. Before he further studied he worked as the field geologist of the Geothermal Project in Sankamphaeng district of Chiang Mai province for the Electricity General Authority of Thailand (EGAT). He attended the Asian Institute of Technology (AIT) at Rangsit district of Prathumthani province for his master degree study and obtained the master degree (engineering geology) in 1984. He tough in the Department of Mining and Metallurgical Engineering, Faculty of Engineering of the Prince of Songkhla University at Had Yai district of Songkhla province about two years. Between 1986 and 2010, he joined various companies, namely TEAM Consulting Engineers Co., Ltd., Geotechnical Engineering and Mineral Exploration and Testing Co., Ltd. (GMT), Geotechnical and Foundation Engineering Co., Ltd. (GFE), Panya Consultants Co., Ltd. and Asia Thai Mining Co., Ltd. During he worked he also studied and received the bachelor degrees of general management and business economic from Sukhothai Thammathirat University in 1998 and 2002, respectively. At present he is working at Ch. Karnchang (Laos) Co., Ltd. for the Xayaburi Hydroelectric Power Project at Xayaburi province, Lao PDR.

He attended the doctoral program of the Department of Geology, Faculty of Science of Chulalongkorn University in 2006. His Ph.D.'s thesis mainly involves in re-evaluation of paleo-seismic investigation along the Khlong Marui and Ranong fault zones and probabilistic seismic hazard analysis so as to establish the probabilistic seismic hazard maps of southern Thailand.